Second Series *June 15, 1932* *Vol. 40, No. 6*

THE

PHYSICAL REVIEW

The Relative Abundance of Hydrogen Isotopes in Natural Hydrogen

By CHARLES A. BRADLEY, JR. AND HAROLD C. UREY

Department of Chemistry, Columbia University

(Received April 30, 1932)

The relative abundances of isotopes have been investigated extensively in recent years, but few researches of such ratios when one isotope is very rare have been reported. We have investigated a number of samples of hydrogen from various sources, water from the crater of Mt. Kilauea, an obsidian, Devonian water, and hydrogen from helium bearing natural gases. The spectrographic method used for detection is not free from objections, but the results show that there is no appreciable variation of abundance of H^2 in the samples investigated.

THE question as to whether the relative abundances of isotopes vary in different samples of elements has interested many investigators in recent years, because any variation would give evidence that transmutation reactions are progressing on the earth or that the elements as found on earth have not been thoroughly mixed.[1] These researches have shown no such variation with the possible exceptions of boron and lithium. It seems probable that the variations reported in the case of lithium are due to the different methods used and also that the observed differences in the atomic weights of boron may possibly be due to systematic errors due, for example, to variations in impurities. At least there exists no certain evidence for any variation in relative abundances of isotopes.

In spite of these negative results, it seemed worth while to investigate natural hydrogens to see whether any source of hydrogen containing appreciably larger amounts of H^2 than that contained in meteoric water could be found. The probable disintegration of nuclei by cosmic rays might produce small amounts of certain nuclei and if these are rare relative to other isotopes,

[1] O. Hönigschmid and Birckenbach, Ber. **56,** (B) 1467 (1923); H. V. A. Briscoe and P. L. Robinson, J. Chem. Soc. **127,** 696 (1925); and Stephenson, ibid., 70 (1927); ibid., 150 (1925); and Smith, ibid., 282 (1927); Cousens and Turner, ibid., 2654 (1928); G. P. Baxter and T. Thorvaldson, J. Am. Chem. Soc. **33,** 337 (1911); Baxter and C. R. Hoover, ibid. **34,** 1657 (1912); and L. W. Parsons, ibid. **43,** 507 (1921); and Hilton, ibid. **45,** 694 (1923); and M. J. Dorcas, ibid. **46,** 357 (1924); Mlle. I. Curie, Compt. Rend. **172,** 1025 (1921); Mlle. E. Gleditsch and B. Samdahl, ibid. **174,** 746 (1922); W. D. Harkins and S. B. Stone, J. Am. Chem. Soc. **37,** 1367 (1926); J. N. Brönsted and Hevesy, Nature **109,** 813 (1922); Jaeger and Dijkstra, Proc. K. Akad. Wetensch. Amsterdam **27,** 393 (1924); A. D. Munro, J. Chem. Soc. **121,** 986 (1922); Muzaffar, J. Am. Chem. Soc. **45,** 2009 (1923); Willard and McAlpine, ibid. **43,** 797 (1924); Weatherill, ibid. **46,** 2437 (1924); A. Elliott, Zeits. f. Physik **67,** 75 (1931); Nature **126,** 203, 845 (1930); F. W. Aston, Nature **128,** 149 (1931); van Wijk and v. Koeveringe, Proc. Roy. Acad. **132,** 98 (1931); Morand, Thesis, Paris, (1929); H. Schüler, Die Naturwiss. **19,** 772 (1931); J. L. Hundley, Phys. Rev. **30,** 864 (1927).

a small amount of such a transmutation reaction might give a sufficient change in the isotopic ratios to be detected. Such a case of a rare isotope is furnished by the H^2 isotope reported by Urey, Brickwedde and Murphy.[2] Further Menzel[3] reports that the H^2 isotope must be very rare in the sun and thus it seemed to us well to be certain whether any large variation in abundance of this nuclear species could be detected in terrestrial sources of hydrogen.

Samples and Experimental Method

The samples of hydrogen investigated consisted of water collected by Dr. E. S. Shepherd from the crater of Mt. Kilauea in 1912, an obsidian containing about 0.75 percent of water from Cerro Noagua, New Mexico, a sample of water containing dissolved chlorides of sodium and magnesium trapped in the Devonian rocks of New York State secured by Professor C. P. Berkey in 1920, and hydrogen of helium bearing natural gases from the Cliffside and Panhandle gas fields in Texas. The water from the Kilauea samples was separated from other gases by collecting the water in a CO_2 trap and pumping the other gases out with a Toepler pump. The obsidian water was secured by heating the obsidian under vacuum in a quartz tube at $\sim 1000°$ C. The natural gases were passed over copper oxide to oxidize the hydrocarbons to water and carbon dioxide and the water was collected in a CO_2 trap. The connate water was used without purification.

These samples of water were introduced into the discharge tube used in a previous research[2] which was about 40 cm long, 8 mm inside diameter and carried about one ampere current. The $H\beta$ lines were photographed in the second order of a grating with a dispersion of 1.3A per millimeter. D. C. Ortho Eastman plates were used which gave lines free from excessive irradiation and hallation. The second order symmetrical ghosts in the second order of the grating appear to have about the same intensity as the $H^2\beta$ line from meteoric water. The exposure times used for all samples were ten and twenty minutes.

Visual observation as well as microphotometer curves show that there is no detectable difference between the special samples of water investigated and ordinary laboratory distilled water. The method of investigation is open to objection because of the partial reabsorption of the H^1 lines in the discharge tube.[4] However the conditions of the discharge tube were very nearly constant for all samples investigated and any marked differences in abundances would have been detected although the relative abundance cannot be satisfactorily determined.

We are indebted to Dr. E. S. Shepherd of the Carnegie Institution of Washington for supplying us with the Kilauea water and the sample of obsidian used; to Professor C. P. Berkey for the connate water and to Mr. R. A. Cattell of the United States Bureau of Mines for the helium bearing natural gases.

[2] H. C. Urey, F. G. Brickwedde, and G. M. Murphy, Phys. Rev. **40**, 1 (1932).
[3] D. H. Menzel, Publ. Ast. Soc. Pacific **44**, 41 (1932).
[4] H. C. Urey, F. G. Brickwedde, and G. M. Murphy, Phys. Rev. **40**, 464 (1932).

Equivalent Chemical Bonds Formed by s, p, and d Eigenfunctions*

By RALPH HULTGREN
California Institute of Technology

(Received April 25, 1932)

1. The work of Pauling on the linear combinations of eigenfunctions to form bond functions has been extended.

2. A theorem concerning the maximum strength in a given direction of a bond function orthogonal to existing bond functions has been derived. It is found that the strongest bond functions must lie at such angles to one another that the maximum of each coincides with a node of each of the others.

3. A general expression for equivalent Pauling bond functions formed from linear combinations of *s*, *p*, and *d* eigenfunctions has been derived.

4. By assuming the bond functions to have cylindrical symmetry, like the best possible bond functions, the equations can be readily solved. It is found that equivalent cylindrical bond functions will be orthogonal if the angles between every pair have no more than two values. The angles must be greater than 54°44′ and their sum must be greater than 180°; otherwise they are unrestricted. No more than six such bond functions may be formed. Solutions for six and less equivalent bond functions are given.

5. There are only four possible configurations for six equivalent cylindrical bond functions. Two of these are much weaker than the other two and so are improbable. The configurations for the stronger bond functions are in striking agreement with the only two structures, the octahedron and the trigonal prism, which are found experimentally.

6. A discussion of the factors influencing bond energies is made and examples of chemical compounds cited. It is predicted that the structure of P_4 is that of a tetrahedron with a *P* atom at each corner.

I. INTRODUCTION

IN THE theory of directed bonds of Pauling and Slater the bonds formed by a given atom tend to assume certain directions relative to one another; namely, those in which the single electron eigenfunctions of the atom have their maximum concentration, permitting maximum "overlapping" with the eigenfunctions of the other atoms with which bonds are formed. The prediction of bond angles is reduced by this theory to the determination of these directions; moreover, some information regarding the strength of a bond can be obtained from the consideration of the amount of concentration of the bond eigenfunction in the bond direction.

In the simple approximate treatment given by Pauling,[1] it is assumed that the bond eigenfunctions are formed by linear combination of a set of eigenfunctions

$$\Psi_{nlm}(r, \theta, \phi) = R_{nl}(r) P_l^{|m|}(\cos\theta) \{A \cos m\phi + B \sin m\phi\}$$

($P_l^m(\cos\theta)$ is Ferrer's associated Legendre polynomial)

* (Contribution from Gates Chemical Laboratory, California Institute of Technology, No. 317.)

[1] Linus Pauling, J. Am. Chem. Soc. **53**, 1367 (1931).

which have approximately the same energy. The coefficients in the linear combinations are determined by a consideration of the θ, ϕ parts of the functions only, it being assumed that the r parts are similar (though not identical) in all of the functions. Neglecting the r part, the eigenfunctions with $l=0$, 1, and 2, $\cdots$ normalized to 4π, are:

$$
\begin{aligned}
s &= P_0^0(\cos\theta) && = 1 \\
p_z &= (3)^{1/2}P_1^0(\cos\theta) && = (3)^{1/2}\cos\theta \\
p_x &= (3)^{1/2}P_1^1(\cos\theta)\cos\phi && = (3)^{1/2}\sin\theta\cos\phi \\
p_y &= (3)^{1/2}P_1^1(\cos\theta)\sin\phi && = (3)^{1/2}\sin\theta\sin\phi \\
d_z &= (5)^{1/2}P_2^0(\cos\theta) && = \tfrac{1}{2}(5)^{1/2}(3\cos^2\theta-1) \\
d_{x+z} &= [(15)^{1/2}/3]P_2^1(\cos\theta)\cos\phi && = (15)^{1/2}\sin\theta\cos\theta\cos\phi \\
d_{y+z} &= [(15)^{1/2}/3]P_2^1(\cos\theta)\sin\phi && = (15)^{1/2}\sin\theta\cos\theta\sin\phi \\
d_x &= [(15)^{1/2}/12]P_2^2(\cos\theta)\cos 2\phi && = \tfrac{1}{2}(15)^{1/2}\sin^2\theta\cos 2\phi \\
d_{x+y} &= [(15)^{1/2}/12]P_2^2(\cos\theta)\sin 2\phi && = \tfrac{1}{2}(15)^{1/2}\sin^2\theta\sin 2\phi
\end{aligned}
$$

The maximum values of these eigenfunctions are 1.000 for s, 1.732 for p_x, p_y, and p_z, 2.236 for d_z, and 1.936 for the other d eigenfunctions. For polar graphs of these see reference 1. (More bond functions of the same shape and strength as the d_z function can be formed by linear combinations of the other d functions.) These values are called the "strengths" of the bond functions, inasmuch as they indicate the amount of concentration of the functions in particular directions and hence give a rough measure of the bond-forming power of the functions. The meaning of the *strength* in terms of energy units has not been determined, but the resonance energy undoubtedly increases rapidly with the strength.

In certain cases, as in C ($1s^2 2s 2p 2p 2p$), the s-p quantization may be broken and stronger bond functions can then be formed using linear combinations of s and p eigenfunctions. The strongest possible s-p bond functions have a strength of 2.000 and are directed to the four corners of a tetrahedron, in agreement with the tetrahedral carbon atom long known to organic chemists and accounting for many other bond angles of about 109°28′.[1]

For elements of the long periods, the d eigenfunctions probably play an important part in bond formation, since, for example, the $3d$ term value for elements of the first long period has probably not a greatly different energy from that of the $4s$ level. Just as in the case of s and p eigenfunctions the quantization may be broken and s-p-d, s-d, or p-d combinations may be formed.

In this paper a method for finding the best equivalent s-p-d bond functions will be developed. The equations prove to be too complex to be solved in the general case, but by making the reasonable assumption that the bond functions have cylindrical symmetry (the best possible bond functions do have cylindrical symmetry), solutions are obtained which cannot be far from the best.

II. The Maximum Strength of Bond Functions

It has been shown by Pauling (reference 1) that the strongest bond function $\Psi_j=\sum_{k=1}^{m}a_{jk}\psi_k(\theta,\phi)$ which can be formed in the direction θ_0, ϕ_0 has a

strength in that direction $\Psi_j(\theta_0,\phi_0) = \{\sum_{k=1}^{m}[\psi_k(\theta_0, \phi_0)]^2\}^{1/2}$. If it be required that this bond function be orthogonal to n pre-existing bond functions $\Psi_i(\theta, \phi) = \sum_{k=1}^{m} a_{ik}\psi_k(\theta, \phi)$, it can be shown (See appendix I) that the maximum strength is reduced to

$$\Psi_j(\theta_0, \phi_0) = \left\{ \sum_{k=1}^{m}[\psi_k(\theta_0, \phi_0)]^2 - \sum_{i=1}^{n}[\Psi_i(\theta_0, \phi_0)]^2 \right\}^{1/2}.$$

When the range of summation m comprises only completed subgroups, the first term is equal to m, and the formula becomes

$$\Psi_j(\theta_0, \phi_0) = \left\{ m - \sum_{i=1}^{n}[\Psi_i(\theta_0, \phi_0)]^2 \right\}^{1/2}.$$

If some of the eigenfunctions of the subgroups are excluded from bond formation, as is the case when they are occupied by an unshared pair of electrons, the formula still holds, providing these excluded eigenfunctions are treated as pre-existing bond functions.

This theorem gives us several important conclusions at once. *The strongest bond functions lie at such angles to one another that the maximum of each coincides with a node of each of the others.* In general, only three such bond functions are geometrically possible. For *s-p* bond functions, however, as we have seen, the nodal angle of 109°28′ allows the construction of four.

The best *s-p-d* bond function (reference 1) (with the maximum along the z axis) is

$$\Psi = \frac{1}{3}s + \frac{1}{(3)^{1/2}}p_z + \frac{(5)^{1/2}}{3}d_z.$$

It has a strength of $(9)^{1/2}$ and has nodes at 73°09′ and 133°37′. We may conclude that *s-p-d bonds tend to form at angles of 73°09′ and 133°37′. The closer the bond angles approach these values, the greater will be the resonance energy of the bond.* Only three of these bonds are geometrically possible and, as will be shown later, these angles may be modified considerably in the case of larger coordination numbers by orthogonality conditions.

In the same way it may be seen that the best *p* bond functions have a strength of $(3)^{1/2}$ and are formed at angles of 90°; the best *d* bond functions have a strength of $(5)^{1/2}$ and angles 54°44′ and 125°16′; the best *p-d* bond functions have a strength $(8)^{1/2}$ and angles 65°44′ and 144°12′; and the best *s-d* bond functions have a strength $(6)^{1/2}$ and angles 63°26′ and 116°34′.

III. Equivalent Bond Functions

Two bond functions may be defined as equivalent when they differ from one another by a rotation only. A method of finding equivalent bonds is to set up the most general *s-p-d* eigenfunction containing shape parameters and orientation parameters. Two eigenfunctions with the same values of the shape parameters will be equivalent.

Denoting the generalized eigenfunctions by capital letters, we have:

$$P = ap_z + bp_x + cp_y = \frac{(3)^{1/2}}{r}(ax + by + cz).$$

But by a rotation transformation P can be expressed as $a'z'/r$, with z' measured along an axis with direction cosines $a:b:c$. Hence a, b, and c are orientation and not shape parameters, and the most general shape of P is $P = p_z$. It may also be shown (See appendix II) that the most general D eigenfunction has the shape of a linear combination of d_z and d_x.

We can now express the most general *s-p-d* bond function as a linear combination of arbitrarily oriented S, P, and D eigenfunctions. The most general shape of the function, that is, the shape of the polar graph of strength against direction, will be determined by five parameters; three of them determine the relative amounts of s, p_z, d_z, and d_x which are in the bond (there are not four because of the normalization condition), and two the relative orientation of P to D. The orientation parameters may be determined by carrying out a rotation transformation on these eigenfunctions. This may be most conveniently done by rotating the axes as follows: Rotate through an angle ϕ_d' about the z axis, then through θ_d about the y axis, then through ϕ_d about the z axis. The behavior of our functions under these transformations is discussed in appendix III, in which the following expression for an *s-p-d* bond function of arbitrary shape and orientation is obtained:

$$\begin{aligned}
\Psi = {} & \sin\alpha \sin\beta\, s + \sin\alpha \cos\beta \{ [\cos\theta_p \cos\theta_d - \sin\theta_p \sin\theta_d \cos(\phi_p + \phi_d')] p_z \\
& + [\cos\theta_p \sin\theta_d \cos\phi_d + \sin\theta_p \cos\theta_d \cos(\phi_p + \phi_d') \cos\phi_d \\
& - \sin\theta_p \sin(\phi_p + \phi_d') \sin\phi_d] p_x + [\cos\theta_p \sin\theta_d \sin\phi_d \\
& + \sin\theta_p \cos\theta_d \cos(\phi_p + \phi_d') \sin\phi_d + \sin\theta_p \sin(\phi_p + \phi_d') \cos\phi_d] p_y \} \\
& + \cos\alpha \{ [(3/2)\cos\gamma \cos^2\theta_d - \tfrac{1}{2}\cos\gamma + \tfrac{1}{2}(3)^{1/2} \sin\gamma \sin^2\theta_d \cos 2\phi_d'] d_z \\
& + [\tfrac{1}{2}(3)^{1/2} \cos\gamma \sin^2\theta_d \cos 2\phi_d + \sin\gamma \cos 2\phi_d \cos 2\phi_d' \\
& - \tfrac{1}{2}\sin\gamma \sin^2\theta_d \cos 2\phi_d \cos 2\phi_d' - \sin\gamma \cos\theta_d \sin 2\phi_d \sin 2\phi_d'] d_x \\
& + \tfrac{1}{2}(3)^{1/2} \cos\gamma \sin^2\theta_d \sin 2\phi_d + \sin\gamma \sin 2\phi_d \cos 2\phi_d' \\
& - \tfrac{1}{2}\sin\gamma \sin^2\theta_d \sin 2\phi_d \cos 2\phi_d' + \sin\gamma \cos\theta_d \cos 2\phi_d \sin 2\phi_d'] d_{x+y} \\
& + [\tfrac{1}{2}(3)^{1/2} \cos\gamma \sin 2\theta_d \cos\phi_d + \sin\gamma \sin\theta_d \sin\phi_d \sin 2\phi_d' \\
& - \tfrac{1}{2}\sin\gamma \sin 2\theta_d \cos\phi_d \cos 2\phi_d'] d_{x+z} + [\tfrac{1}{2}(3)^{1/2} \cos\gamma \sin 2\theta_d \sin\phi_d \\
& - \sin\gamma \sin\theta_d \cos\phi_d \sin 2\phi_d' - \tfrac{1}{2}\sin\gamma \sin 2\theta_d \sin\phi_d \cos 2\phi_d'] d_{y+z}.
\end{aligned}$$

α, β = shape parameters determining relative amounts of S, P, and D used; γ = shape parameter determining relative amounts of d_z and d_x used; θ_p, ϕ_p = shape parameters determining relative orientation of P to D; θ_d, ϕ_d = direction of z axis after rotation; ϕ_d' = rotation of bond function about new z axis.

The eigenfunction is normalized as written and the only restrictions on the values of the coefficients are the orthogonality conditions. For n bond functions these give $\frac{1}{2}n(n-1)$ equations containing 5 shape parameters and $3n-3$ arbitrary orientation parameters (three may be arbitrarily chosen without loss of generality). The equations are not necessarily independent. If the number of independent equations exceeds the number of unknowns, they are said to be over-determined, and there is no solution. If the numbers are equal, there will be one or more single points in the hyper space which satisfy the equation; while if the number of equations is less, there will be sets of continuous solutions. For certain values of some of the parameters the number of independent equations may be reduced.

From other considerations it seems probable that nine equivalent bond functions (36 equations, 29 unknowns) cannot be formed. The existence of solutions for eight bond functions, having 28 equations and 26 unknowns, is doubtful; but for seven or less bond functions there probably should be continuous solutions.

Unfortunately the orthogonality equations are extremely complicated, each equation containing 46 terms and involving 11 parameters. But by making certain reasonable approximations, we can reduce the equations to a readily soluble form. The best possible *s-p-d* bond function is symmetrical about the direction where it has its maximum value and has the following values of the shape parameters:

$$\theta_p = 0 \text{ (then } \phi_p \text{ may be arbitrary)}, \qquad \alpha = \cos^{-1}(5)^{1/2}/3,$$
$$\gamma = 0, \qquad \beta = \cos^{-1}\tfrac{1}{2}(3)^{1/2}.$$

An increase in γ will quickly reduce the possible bond strength by scattering the d eigenfunction, so any really strong bond function must have γ nearly equal to zero. We may therefore set $\gamma = 0$ with a feeling of considerable confidence that this arbitrary restriction has not eliminated any important bond eigenfunctions which are not rather closely approximated by one of those remaining. The same argument applies to θ_p except that the decrease in strength is not rapid. We shall assume that the p part of the bond function has its maximum in the same direction as the d part ($\theta_p = 0$).

These assumptions enormously simplify the orthogonality equations; the number of terms is reduced from 46 to 9 and the number of parameters from 11 to 6. Furthermore the direction of the maximum value of the bond functions is easy to find; it is θ, $\phi = \theta_d$, ϕ_d. These are the only *s-p-d* combinations with cylindrical symmetry, and will be referred to as *cylindrical bond functions*.

IV. Cylindrical Bond Functions

The above treatment gives us the following expression for the general cylindrical bond function

$$\begin{aligned}\Psi = {} & \sin\alpha \sin\beta\, s + \sin\alpha \cos\beta[\cos\theta_d p_z + \sin\theta_d \cos\phi_d p_x + \sin\theta_d \sin\phi_d p_y] \\ & + \tfrac{1}{2}\cos\alpha[(3\cos^2\theta_d - 1)d_z + (3)^{1/2}\sin^2\theta_d \cos 2\phi_d d_x + (3)^{1/2}\sin^2\theta_d \sin 2\phi_d d_{x+y} \\ & + (3)^{1/2}\sin 2\theta_d \cos\phi_d d_{x+z} + (3)^{1/2}\sin 2\theta_d \sin\phi_d d_{y+z}].\end{aligned}$$

If we place one bond function with its maximum along the z axis, all bond functions orthogonal to it must obey the equation:

$$\sin^2\alpha \sin^2\beta + \sin^2\alpha \cos^2\beta \cos\theta_d + \tfrac{1}{2}\cos^2\alpha(3\cos^2\theta_d - 1) = 0.$$

This is a quadratic in $\cos\theta_d$ and so has two solutions in terms of α and β. Hence the equivalent cylindrical bond functions orthogonal to a function of a given shape must have the loci of their maxima in two cones, which are determined by the shape parameters. Conversely, any two angles will determine the shape parameters.

$$\sin\alpha = \left(\frac{(1-\cos\theta)(1-\cos\theta') - \frac{2}{3}}{(1-\cos\theta)(1-\cos\theta')}\right)^{1/2}$$

$$\sin\beta = \left(\frac{\cos\theta\cos\theta' + \frac{1}{3}}{(1-\cos\theta)(1-\cos\theta') - \frac{2}{3}}\right)^{1/2}.$$

In order to have real solutions, the angles must be restricted as follows:

$$\theta, \theta' \geqq 54°44' \quad \theta + \theta' \geqq 180°.$$

Then all bond functions having their maxima at angles θ or θ' to the maximum of the given bond function will be orthogonal to it, providing the shape parameters are chosen correctly. This can easily be extended by symmetry to include all bond functions of the set, giving the general theorem: *The necessary and sufficient condition for a set of equivalent s-p-d cylindrical bond functions to be orthogonal is that there be no more than two different values for the angles between the direction of the maximum of any given bond function and the direction of the maxima of all the other bond functions.* The shape parameters must be chosen and the angles restricted as given above.

This theorem reduces our problem to the purely geometrical one of finding the ways that n vectors may be oriented such that the angles between all pairs obey the above restriction. It can be easily shown that no more than six vectors may be so placed: *No more than six equivalent cylindrical bond functions can be orthogonal to one another.*

For any values of the angles which satisfy the orthogonality conditions, the strength will be found to be

$$\text{Strength} = \frac{(\cos\theta\cos\theta' + \frac{1}{3})^{1/2} + (-3(\cos\theta + \cos\theta'))^{1/2} + (10/3)^{1/2}}{((1-\cos\theta)(1-\cos\theta'))^{1/2}}.$$

Six equivalent cylindrical bond functions

If we place one vector along the z axis, there may be as many as five in the θ cone, if they are evenly spaced; that is, $\Delta\phi = 72°$ or 144°. If we now make the angles between the vectors equal to θ or θ' by use of the distance formula of spherical trigonometry: $\cos\delta = \cos\theta_1 \cos\theta_2 + \sin\theta_1 \sin\theta_2 \cos(\phi_1 - \phi_2)$ where in this case $\delta = \theta$ or θ'; θ_1 and $\theta_2 = \theta$; and $\phi_1 - \phi_2 = 72°$ or 144°, we get two similar solutions. Placing four bonds in the θ cone and one in the θ' gives us another solution, the octahedral configuration discovered by Pauling.[1] There

is only one more solution; in which the vectors point to the corners of an equilateral triangular prism with square sides.

The first two solutions contain no p eigenfunctions. They are the strongest s-d bond functions that can be formed.

The six equivalent octahedral eigenfunctions[1] are:

$$\Psi_1 = \frac{1}{6^{1/2}}s + \frac{1}{2^{1/2}}p_z + \frac{1}{3^{1/2}}d_z,$$

$$\Psi_2 = \frac{1}{6^{1/2}}s - \frac{1}{2^{1/2}}p_z + \frac{1}{3^{1/2}}d_z,$$

$$\Psi_3 = \frac{1}{6^{1/2}}s + \frac{1}{2^{1/2}}p_x - \frac{1}{12^{1/2}}d_z + \tfrac{1}{2}d_x,$$

$$\Psi_4 = \frac{1}{6^{1/2}}s - \frac{1}{2^{1/2}}p_x - \frac{1}{12^{1/2}}d_z + \tfrac{1}{2}d_x,$$

$$\Psi_5 = \frac{1}{6^{1/2}}s + \frac{1}{2^{1/2}}p_y - \frac{1}{12^{1/2}}d_z - \tfrac{1}{2}d_x,$$

$$\Psi_6 = \frac{1}{6^{1/2}}s - \frac{1}{2^{1/2}}p_y - \frac{1}{12^{1/2}}d_z - \tfrac{1}{2}d_x,$$

with three pure d eigenfunctions orthogonal to them

$$\Psi_7 = d_{x+y};\ \Psi_8 = d_{x+z};\ \Psi_9 = d_{y+z}.$$

The trigonal prism eigenfunctions are:

$$\Psi_1 = \frac{51^{1/2}}{18}s + \frac{1}{6^{1/2}}p_z + \tfrac{1}{3}2^{1/2}p_x + \frac{1}{6(3)^{1/2}}d_z + \tfrac{1}{3}d_x + \frac{1}{3^{1/2}}d_{x+z}$$

$$\Psi_2 = \frac{51^{1/2}}{18}s + \frac{1}{6^{1/2}}p_z - \tfrac{1}{6}2^{1/2}p_x + \frac{1}{6^{1/2}}p_y + \frac{1}{6(3)^{1/2}}d_z - \frac{1}{6}d_x - \frac{1}{2(3)^{1/2}}d_{x+y} - \frac{1}{2(3)^{1/2}}d_{x+z} + \tfrac{1}{2}d_{y+z}$$

$$\Psi_3 = \frac{51^{1/2}}{18}s + \frac{1}{6^{1/2}}p_z - \tfrac{1}{6}2^{1/2}p_x - \frac{1}{6^{1/2}}p_y + \frac{1}{6(3)^{1/2}}d_z - \tfrac{1}{6}d_x + \frac{1}{2(3)^{1/2}}d_{x+y} - \frac{1}{2(3)^{1/2}}d_{x+z} - \tfrac{1}{2}d_{y+z}$$

$$\Psi_4 = \frac{51^{1/2}}{18}s - \frac{1}{6^{1/2}}p_z + \tfrac{1}{3}2^{1/2}p_x + \frac{1}{6(3)^{1/2}}d_z + \tfrac{1}{3}d_x - \frac{1}{(3)^{1/2}}d_{x+z}$$

$$\Psi_5 = \frac{51^{1/2}}{18}s - \frac{1}{6^{1/2}}p_z - \tfrac{1}{6}2^{1/2}p_x + \frac{1}{6^{1/2}}p_y + \frac{1}{6(3)^{1/2}}d_z - \tfrac{1}{6}d_x$$
$$- \frac{1}{2(3)^{1/2}}d_{x+y} + \frac{1}{2(3)^{1/2}}d_{x+z} - \tfrac{1}{2}d_{y+z}$$

$$\Psi_6 = \frac{51^{1/2}}{18}s - \frac{1}{6^{1/2}}p_z - \tfrac{1}{6}2^{1/2}p_x - \frac{1}{6^{1/2}}p_y + \frac{1}{6(3)^{1/2}}d_z - \tfrac{1}{6}d_x$$
$$+ \frac{1}{2(3)^{1/2}}d_{x+y} + \frac{1}{2(3)^{1/2}}d_{x+z} + \tfrac{1}{2}d_{y+z}$$

with the following eigenfunctions remaining.

$$\Psi_7 = \frac{1}{18^{1/2}}s - \frac{17^{1/2}}{18^{1/2}}d_z; \quad \Psi_8 = \frac{1}{3^{1/2}}p_z - \frac{2^{1/2}}{3^{1/2}}d_z; \quad \Psi_9 = \frac{1}{3^{1/2}}p_y + \frac{2^{1/2}}{3^{1/2}}d_{x+y}.$$

Five equivalent cylindrical bond functions

Solutions may of course be obtained by leaving out one bond function of our six-bond solutions. There is also a solution obtained by placing four bond

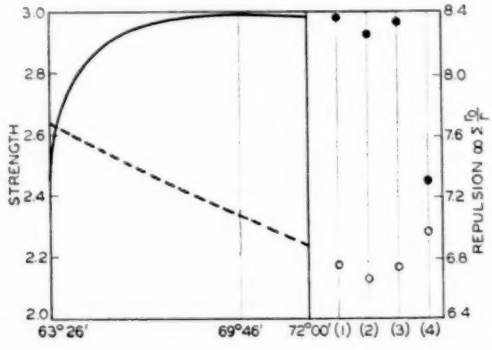

Fig. 1. Strengths of five equivalent cylindrical bonds for all possible configurations. The dotted curve represents a quantity proportional to the energy of possible electrostatic repulsion between the atoms surrounding the central atom. The configuration of maximum strength and minimum repulsion is favored. (1) $\theta = 81°\ 47'$; $\theta' = 135°\ 35'$, (2) $\theta = 90°$; $\theta' = 180°$ (3) $\theta = 120°$; $\theta' = 75°\ 31'$ (4) $\theta = 63°\ 26'$; $\theta' = 116°\ 34'$.

functions equally spaced in a cone 120° from the fifth bond function. These bond functions have a strength of 2.968, with $\theta' = 75°31'$. The conditions are also satisfied by the following relation between θ and θ'.

$$\cos\theta' = \tfrac{1}{2}(3 \pm (5)^{1/2})\cos\theta - \tfrac{1}{2}(1 \pm (5)^{1/2}).$$

In these solutions the five bonds are equally spaced in a cone. The strengths are shown as a function of the angle θ in Fig. 1, the maximum strength being 2.994. The energies of steric repulsion are qualitatively indicated by the dotted line.

Four equivalent cylindrical bond functions

In this case there are six sets of continuous solutions, which include all the previously given solutions for a greater number of bond functions.

$$\cos\theta' = \tfrac{1}{2}(3\cos^2\theta - 1) \tag{1}$$

$$\cos\theta' = \frac{4\cos^2\theta}{1+\cos\theta} - 1 \tag{2}$$

$$\cos\theta' = \cos^2\theta \pm (1-\cos\theta)(\cos^2\theta + (3/2)\cos\theta + \tfrac{1}{2})^{1/2} \tag{3}$$

$$\cos\theta' = \pm\, 2\cos\theta - 1 \tag{4}$$

$$\cos\theta' = \tfrac{1}{2}(3\cos\theta - 1 + (5)^{1/2}(\cos\theta - 1)) \tag{5}$$

$$\cos\theta' = \tfrac{1}{2}[1 - \cos\theta - (5 + 2\cos\theta - 3\cos^2\theta)^{1/2}] \tag{6}$$

The strengths of bond functions for these solutions are shown in Fig. 2. The strongest bond function is obtained from solution (a). It has angles of 136°06′ and 73°49′ and a strength of 2.9992. Single points on two of the curves represent bond functions which contain no *s*, that is, they represent *p-d* bond functions. These are at the largest angles of solutions (a) and (d). The strengths here are respectively 2.828 and 2.817, only slightly weaker than the best *p-d* bond function, which has a strength of 2.8284.

V. Discussion and Application of Results

The configuration assumed by an actual molecule is not, of course, determined solely by the resonance energy but, rather, by the position of minimum potential energy. If the bond is to a considerable extent ionic in character, the resonance energy may become unimportant. In any case forces between the atoms surrounding the central atom, if they are large, will be expected to deform the bond angles from the positions where the bond functions are a maximum. These forces[2] may result from interaction between the dipoles of the bonds (electrostatic forces), from interaction between dipole and bond by induction, or by steric hindrance when atoms or groups are close together. For equivalent bonds, these forces will always tend to make the bond angle larger. The bond energy will also be influenced by the term values of the eigenfunctions used in the bond function and by the term values of the nonbonding electrons. If we neglect the energy of the perturbation caused by bond formation, that set of bond functions will be favored which allows the maximum number of electrons to occupy eigenfunctions of low term values. The energy of eigenfunctions occupied by unshared electron pairs will be more important that the energy of a bond eigenfunction because two electrons are involved compared with one in the bond. Unshared pairs are apt to occupy the eigenfunctions of lowest energy, so that these eigenfunctions cannot be used in the construction of bond functions.

[2] H. A. Stuart, Phys. Rev. **38**, 1372 (1931).

Six equivalent bonds

The first two solutions in Table I have an advantage only in case the p levels lie considerably lower than the others, in which case unshared pairs might occupy them and exclude them from bond formation; or if the p levels

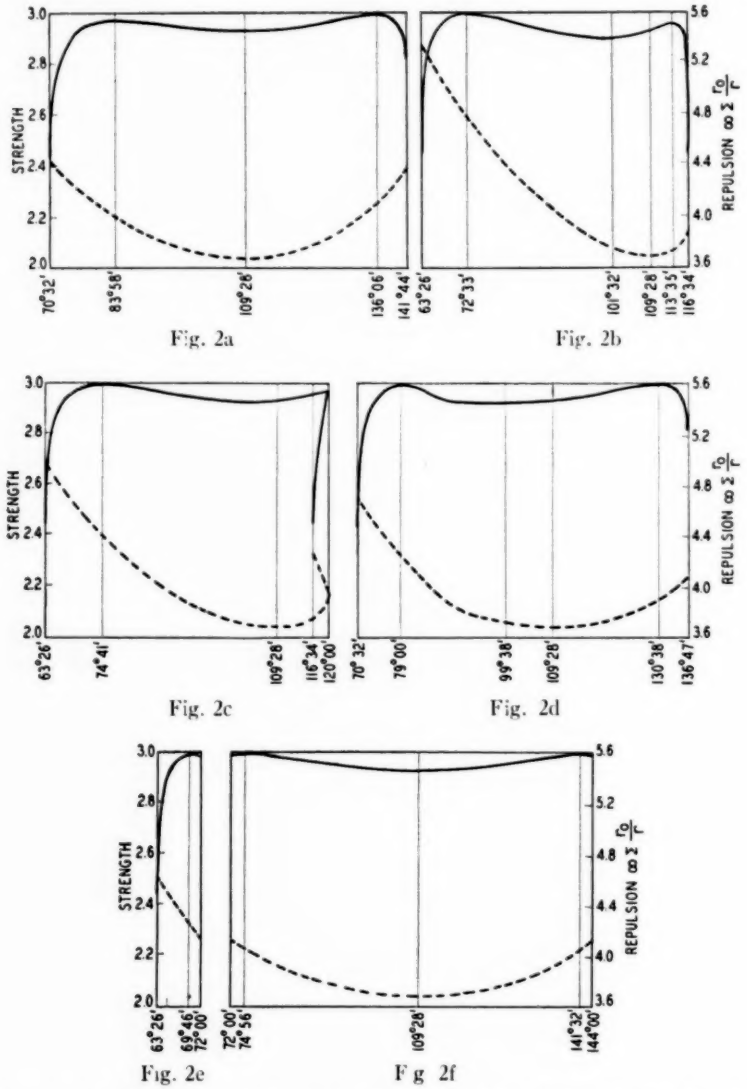

Fig. 2a Fig. 2b

Fig. 2c Fig. 2d

Fig. 2e Fig. 2f

Fig. 2. Strengths and possible electrostatic repulsions of four equivalent cylindrical bonds.

lie considerably higher (with no unshared electron pairs present) so that it would be advantageous not to include them in the bond. There do not seem to be any atoms with large enough separations of energies to compensate for the much weaker bond functions of these solutions.

This leaves for consideration only two configurations, the octahedron and the trigonal prism. As a matter of fact, these are the only two structures

known experimentally, the former being found in the great majority of cases. The trigonal prism is found in molybdenite, MoS_2, and in tungstenite, WS_2. The quantitative experimental data for molybdenite[3] are in striking agreement with the theoretical structure. Each Mo atom is at the center of a trigonal prism whose six corners are occupied by sulfur atoms, the ratio of altitude to base of this regular triangular prism being 1.007 ± 0.039 compared to the theoretical ratio of 1.000.

TABLE I. *Sets of six equivalent cylindrical bond functions.*

	Angles between bonds θ	θ'	No. of angles θ	θ'	Bond strength	Remarks
(1)	63°26′	116°34′	10	5	2.449	Five bonds in cone. *s-d* bond fns.
(2)	116°34′	63°26′	10	5	2.449	Five bonds in cone. *s-d* bond fns.
(3)	90°00′	180°00′	12	3	2.924	Octahedral bonds
(4)	81°47′	135°35′	9	6	2.983	Trigonal prism bonds

The trigonal prism configuration has greater resonance energy per bond, but the octahedron has smaller repulsive forces between the surrounding atoms. The octahedron will be preferred for bonds which are appreciably ionic in character, or for large atoms surrounding the nuclear atom. Since it contains a smaller amount of *d*, it will also be favored where the *d* level lies highest, as in elements of the second period. Where the *d* level lies lowest, the trigonal prism will be favored, unless there are unshared electron pairs. One such pair can be accommodated in the second Ψ_7 eigenfunction given on page 898 which contains 17/18 *d*. But the second pair will have to be excited up to the Ψ_8 level. The fact that molybdenite is diamagnetic[4] indicates that in molybdenum this level is higher than Ψ_7 by an amount greater than the singlet-triplet separation. Hence, where the *d* level lies lowest, two or three unshared electron pairs strongly favor the octahedron, in which the pairs may all be placed in *d* levels.

Five equivalent bonds

The continuous solution gives a slight increase in resonance energy over the trigonal prism solution with one bond left out, but is considerably poorer sterically. The other new solution is poorer than the trigonal prism with one bond missing, both sterically and in bond strength. PCl_5, the structure of which is unknown, would be expected to have *s-p-d* bonds. It is difficult to estimate the magnitude of steric forces, but they are certainly much larger in PCl_5 than in molybdenite. Probably the octahedral configuration with one bond missing (square pyramid) or some sterically more favorable configuration involving non-cylindrical bonds is assumed by this molecule.

Four equivalent bonds

Neglecting a few exceptional regions, where other solutions give slightly better results, the solution shown in Fig. 2a is best both sterically and in bond

[3] Roscoe G. Dickinson and Linus Pauling, J. Am. Chem. Soc. **45**, 1466 (1923).

[4] E. B. Wilson, Jr., private communication.

strength. Bonds of this type will then lie at the configuration for maximum resonance energy, or will be deformed toward the tetrahedral configuration, the most favored sterically, along the curve given. If only one *d* eigenfunction is available, the best bonds are directed to the corners of a square, as shown by Pauling.[1]

As previously mentioned, *three equivalent bonds* of the maximum strength, 3.000, may be formed at angles of 73°09′ and 133°37′. For the configuration most favored sterically, three bonds in a plane at 120°, the strength is 2.881.

Two bonds of strength 3.000 at 133°37′ may be deformed to 180°, reducing the strength slightly to 2.96. This latter configuration will be expected when only one *d* eigenfunction is available. The functions are

$$\Psi_1 = (1/12^{1/2})s + (1/2^{1/2})p_z + (5^{1/2}/12^{1/2})d_z$$
$$\Psi_2 = (1/12^{1/2})s - (1/2^{1/2})p_z + (5^{1/2}/12^{1/2})d_z$$

with the unshared pair of electrons occupying

$$\Psi_3 = (5/6)^{1/2}s - (1/6)^{1/2}d_z$$

These are probably the bonds formed by silver in $Ag(CN)_2^-$ ($4d5s5p$ bonds), which is known to be linear.[5] Here the *s* and *d* levels have nearly the same energy, with the *p* level higher.

Other types of bonds

It may occur that the *s* level, when it lies lowest, will be occupied by an unshared pair of electrons, and *p-d* bonds will be formed. In order for *p-d* bonds to be orthogonal, the angles between them must satisfy the equation:

$$\sin^2\alpha\cos\theta + \tfrac{1}{2}\cos^2\alpha(3\cos^2\theta - 1) = 0.$$

As in the case of the *s-p-d* bond, there are two angles for a given shape of bond. But, since there is only one shape parameter, these angles are not independent. The specification of one angle determines the shape and strength of the bond and also the other possible angle.

Four p-d bonds. No more than four equivalent cylindrical *p-d* bonds may be formed. The two configurations given on page 899, although quite strong, are poor sterically. It is to be expected that SCl_4, which probably has this type of bond, will form a non-cylindrical bond with better steric properties.

Three p-d bonds. Three strongest bonds with a strength 2.828 can be formed at angles 65°44′ and 144°12′. In the molecule P_4 the phosphorus atoms may be bonded by *p* bonds or by *p-d* bonds. In the former case the bond angle would tend to be 90° and the most probable configuration would place the four *P* atoms at the corners of a square, connected by alternate single and double bonds. The single bond functions have a strength of 1.732, while the double bonds have much less than twice the energy of a single bond. Much stronger *p-d* bond functions can be formed if the *P* atoms are placed at the corners of a regular tetrahedron, with bond angles of 60°.

[5] J. L. Hoard, private communication

Bonds may be hindered from their tendency to form in the direction of the maximum of the bond function by steric or geometric factors, with an accompanying decrease in resonance energy. When this occurs, the bond function will rearrange itself so as to give a maximum strength in the new direction. The maxima of the rearranged bond functions will not lie in the directions of the bonds, but will generally assume positions between the bond directions and the directions of the undisturbed maxima. In this case, where the bonds tend to form at 65°44′ but are required by geometry to be at 60°, the maxima of the bond functions will be in directions 64°02′ apart, and their strength in the bond directions is 2.819. The bond functions are then

$$\Psi_1 = 0.4520p_z + 0.3500p_x + 0.3593d_z + 0.2663d_x + 0.6880d_{x+z}$$

$$\Psi_2 = 0.4520p_z - 0.1750p_x + 0.3031p_y + 0.3593d_z - 0.1332d_x - 0.2306d_{x+y} - 0.3440d_{x+z} + 0.5958d_{y+z}$$

$$\Psi_3 = 0.4520p_z - 0.1750p_x - 0.3031p_y + 0.3593d_z - 0.1332d_x + 0.2306d_{x+y} - 0.3440d_{x+z} - 0.5958d_{y+z}.$$

Where the bond directions are (35°16′, 0°), (35°16′, 120°), and (35°16′, 240°). The bonds are composed 32.67 percent of the p eigenfunctions. Bond functions with their maxima at 60° have a strength of only 2.773.

Two p-d bonds. Two bond functions may be formed at 180° with a strength of 2.806 as compared with the strongest bond functions at 144°12′ with a strength 2.828.

I wish to express my appreciation of the assistance of Professor Linus Pauling, at whose suggestion this problem was undertaken. I am also indebted to Dr. Boris Podolsky, now of Kharkov, for some of the rotation transformation formulas.

Appendix I

Problem

To construct the normalized bond function $\Psi_j = \sum_{k=1}^{m} a_{jk}\psi_k$ *with maximum value in the direction* θ_0, ϕ_0 *and orthogonal to n given orthogonal, normalized bond functions of the same type,*

$$\Psi_i = \sum_{k=1}^{m} a_{ik}\psi_k \qquad (i = 1, 2, 3, \cdots, n)(j \neq i). \tag{1}$$

The orthogonality and normalization conditions require

$$\sum_{k=1}^{m} a_{ik}a_{lk} = \delta_{il} \quad (= 0 \text{ where } i \neq l;\ = 1 \text{ where } i = l). \tag{2}$$

Let

$$\Lambda = \sum_{k=1}^{m} a_{jk}\psi_k - \frac{\lambda}{2}\left[\sum_{k=1}^{m} a_{jk}^2 - 1\right] - \sum_{i=1}^{n}\sum_{k=1}^{m} \mu_i a_{ik}a_{jk} = \Psi_j \tag{3}$$

Ψ_j will be a maximum when

$$\frac{\partial \Lambda(\theta_0, \phi_0)}{\partial a_{jk}} = 0 = \psi_k(\theta_0, \phi_0) - \lambda a_{jk} - \sum_{i=1}^{n} \mu_i a_{ik} \qquad k = (1, 2, \cdots, m). \quad (4)$$

Hence

$$a_{jk} = \frac{\psi_k(\theta_0, \phi_0) - \sum_{i=1}^{n} \mu_i a_{ik}}{\lambda}. \quad (5)$$

Multiplying this by a_{lk} $(l \neq j)$ and summing over k it is found that

$$\mu_l = \sum_{k=1}^{m} a_{lk} \psi_k = \Psi_l. \quad (6)$$

By squaring (5) and summing over k we get

$$\lambda = \left[\sum_{k=1}^{m} \psi_k^2 - \sum_{i=1}^{n} \Psi_i^2 \right]^{1/2}. \quad (7)$$

Hence

$$a_{jk} = \frac{\psi_k - \sum_{i=1}^{n} a_{ik} \Psi_i}{\left[\sum_{k=1}^{m} \psi_k^2 - \sum_{i=1}^{n} \Psi_i^2 \right]^{1/2}} \quad (8)$$

$$\Psi_j = \left[\sum_{k=1}^{m} \psi_k^2 - \sum_{i=1}^{n} \Psi_i^2 \right]^{1/2} \quad (9)$$

Corollary

When the m original eigenfunctions comprise only completed subgroups,

$$\sum_{k=1}^{m} \psi_k^2 = m \text{ and } \Psi_j = \left[m - \sum_{i=1}^{n} \Psi_i^2 \right]^{1/2}.$$

Appendix II

Proof that the most general d eigenfunction (arbitrarily oriented) is a linear combination of d_z and d_x. The most general d eigenfunction is

$$\mathcal{D} = Ad_x + Bd_{x+y} + Cd_{x+z} + Dd_{y+z} + Ed_z$$

which in Cartesian coordinates is

$$\mathcal{D} = 1/r^2(a'x^2 + b'y^2 + c'z^2 + d'xy + e'xz + f'yz)$$

that is, the general quadratic. A rotation transformation will change the general quadratic to one containing squares only.

$$\mathcal{D} = 1/r^2(ax^2 + by^2 + cz^2).$$

The coefficients are restricted by the fact that D, to be an eigenfunction, must satisfy Laplace's equation; and also must be normalized, so that

$$a + b + c = 0$$

$$\int_\tau \mathcal{D}^2 d\tau = 4\pi.$$

The normalization equation when evaluated gives the relation

$$3(a^2 + b^2 + c^2) + 2(ab + ac + bc) = 15.$$

From the two relations we get

$$\mathcal{D} = ax^2 - \tfrac{1}{2}(a \pm (15 - 3a^2)^{1/2})y^2 - \tfrac{1}{2}(a \mp (15 - 3a^2)^{1/2})z^2.$$

But this may be obtained from

$$\mathcal{D} = a' d_z - (1 - a'^2)^{1/2} d_z$$

by setting

$$a = \tfrac{1}{2}(15)^{1/2} a' - \tfrac{1}{2}(5)^{1/2}(1 - a'^2)^{1/2}$$

Appendix III

Problem

To determine the behavior of S, P, and D under the general rotation transformation. If the coordinate axes are rotated for an angle ϕ_d' about the z axis, then an angle θ_d about the y axis, then again ϕ_d about the z axis, the coordinates of the point P, θ' and ϕ' appear as shown in Fig. 3, where all lines drawn are arcs of great circles.

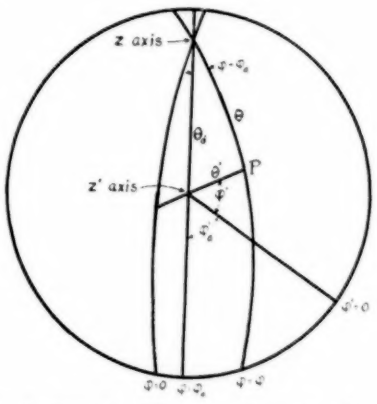

Fig. 3. Rotation of axes on the unit sphere.

By spherical trigonometry we have

$$\cos\theta' = \cos\theta_d \cos\theta + \sin\theta_d \sin\theta \cos(\phi - \phi_d)$$

$$\sin(\phi' + \phi_d') = \frac{\sin\theta \sin(\phi - \phi_d)}{\sin\theta'}$$

$$\cos(\phi' + \phi_d') = \frac{\cos\theta_d \sin\theta \cos(\phi - \phi_d) - \sin\theta_d \cos\theta}{\sin\theta'}.$$

We may easily solve these to get $\sin\phi'$, $\sin 2\phi'$, $\cos\phi'$, $\cos 2\phi'$ in terms of $\theta, \phi, \theta_d, \phi_d, \phi_d'$.

We also wish to evaluate

$$P_l^{|m|}(\cos\theta') = P_l^{|m|}[\cos\theta_d\cos\theta + \sin\theta_d\sin\theta\cos(\phi - \phi_d)].$$

This may be done by use of Gegenbauer C functions.*

$$P_l^{|m|}(\cos\theta') = \frac{(2m)!}{2^m m!}\sin^m\theta' C_{l-m}^{m+1/2}(\cos\theta').$$

But:

$$C_{l-m}^{m+1/2}(\cos\theta_d\cos\theta + \sin\theta_d\sin\theta\cos(\phi - \phi_d)) = \frac{\Gamma(2m)}{[\Gamma(m+\tfrac{1}{2})]^2}\times$$

$$\sum_{\lambda=0}^{l-m}\left\{\frac{(-1)^\lambda 2^{2\lambda}\Gamma(l-m-\lambda+1)}{\Gamma(l+m+\lambda+1)}[\Gamma(m+\lambda+\tfrac{1}{2})]^2\times\right.$$

$$\left.(2m+2\lambda)\sin^\lambda\theta_d\sin^\lambda\theta C_{l-m-\lambda}^{m+\lambda+1/2}(\cos\theta_d)C_{l-m-\lambda}^{m+\lambda+1/2}(\cos\theta)C_\lambda^m(-\cos(\phi-\phi_d))\right\}.$$

Making the following simplifications since l, m, and λ are integers

$$\Gamma(n) = (n-1)!$$

$$\Gamma(n+\tfrac{1}{2}) = \frac{(2n)!}{2^{2n}n!}(\pi)^{1/2}$$

where n is an integer

$$C_{l-m-\lambda}^{m+\lambda+1/2}(\cos x) = \frac{2^{m+\lambda}(m+\lambda)!}{(2m+2\lambda)!\sin^{m+\lambda}x}$$

$$C_\lambda^m(-x) = (-)^\lambda C_\lambda^m(x)$$

we obtain

$$P_l^{|m|}(\cos\theta') = \frac{m!2^m\sin^m\theta'}{\sin^m\theta_d\sin^m\theta}\sum_{\lambda=0}^{l-m}\frac{(l-m-\lambda)!(m+\lambda)}{(l+m+\lambda)!m}$$

$$P_l^{|m|+\lambda}(\cos\theta_d)P_l^{|m|+\lambda}(\cos\theta)C_\lambda^{|m|}(\cos(\phi-\phi_d).$$

Using these formulas we get for our general expressions of eigenfunctions rotated through arbitrary angles

$$s = P_0^0(\cos\theta') = 1$$

$$p_z = 3^{1/2}P_1^0(\cos\theta') = 3^{1/2}(\cos\theta_p\cos\theta + \sin\theta_p\sin\theta\cos(\phi-\phi_p))$$

$$d_z = 5^{1/2}P_2^0(\cos\theta') = \tfrac{1}{4}(5)^{1/2}\{(3\cos^2\theta_d - 1)(3\cos^2\theta - 1)$$

* See Whittaker and Watson, "Modern Analysis", Chap. XV for most of the formulas involving the Gegenbauer function.

$$+ 3 \sin 2\theta_d \sin 2\theta \cos(\phi - \phi_d) + 3 \sin^2\theta_d \sin^2\theta \cos 2(\phi - \phi_d)\}$$

$$d_x = \frac{1}{12}(15)^{1/2} P_2^2(\cos\theta') \cos 2\phi' = \tfrac{1}{2}(15)^{1/2}\{\sin^2\theta \cos 2(\phi - \phi_d) \cos 2\phi_d'$$

$$+ \tfrac{1}{2}(3\cos^2\theta - 1)\sin^2\theta_d \cos 2\phi_d' - \tfrac{1}{2}\sin^2\theta \cos 2(\phi - \phi_d)\sin^2\phi_d \cos 2\phi_d'$$

$$+ \sin^2\theta \sin 2(\phi - \phi_d)\cos\theta_d \sin 2\phi_d' - \sin 2\theta \sin(\phi - \phi_d)\sin\theta_d \sin 2\phi_d'$$

$$- \tfrac{1}{2}\sin 2\theta \cos(\phi - \phi_d)\sin 2\theta_d \cos 2\phi_d'\}.$$

By carrying the transformed p_z through a second rotation ϕ_d', θ_d, ϕ_d and expressing all angles θ and ϕ in terms of the original s, p, and d eigenfunctions we arrive at the expression given in the text for the most general eigenfunction.

The Smekal-Raman Spectra of $SiHCl_3$, $CHFCl_2$ and CF_2Cl_2

By CHARLES A. BRADLEY, JR.*
Department of Chemistry, Columbia University

(Received April 30, 1932)

The Smekal-Raman spectra of the compounds $SiHCl_3$, $CHFCl_2$ and CF_2Cl_2 have been investigated using a quartz mercury arc as the primary source. There are six frequency displacements in the case of silicochloroform all somewhat less than the corresponding displacements of chloroform. The so-called transverse hydrogen bond frequency is not observed. Eight frequencies of $CHFCl_2$ and nine of CF_2Cl_2 have been observed. The transverse hydrogen bond vibration is not observed in the former. An assignment of the observed frequencies to particular modes of vibrations is made.

INTRODUCTION

THE Smekal-Raman effect proves to be of great value in the study of molecular structure from a correlation between the observed frequencies and the mechanical modes of vibration of particular molecular models. Considerable success has been obtained in the explanation of the spectra of molecules of the type YX_4.[1] Thus it was thought that by observing the Smekal-Raman spectra of molecules in which some of the X atoms had been replaced by others more information could be gained concerning their structure and modes of vibration.

EXPERIMENTAL PROCEDURE

The apparatus used in these experiments was designed to serve for liquids boiling at $-40°$ to $-50°$C.[2] The observation tube was a Pyrex glass tube 2.5 cm in diameter with a plane window on one end, a straight portion of 12.5 cm length, and the lower portion tapering off to a point. The tapering portion was surrounded by a jacket filled with black enamel.[3] This took the place of the usual black curved light horn. A sidearm close to the window served for filling. The observation tube was mounted vertically in an unsilvered Dewar flask filled with anhydrous liquid ammonia. The outside of the Dewar, except for a narrow vertical strip, was covered with a piece of highly polished aluminum. Two Hanovia quartz mercury arcs operating on 220 volts were mounted vertically in front of the open strip in the aluminum. A piece of asbestos board was placed over the whole set-up, and the light scattered by the liquid in the observation tube was taken out through a small hole in the board, and reflected by a prism through a lens into the slit of a Hilger D78 glass spectrograph. The copper spectrum was used for comparison.

* Du Pont Fellow in Chemistry, 1930–1931.

[1] B. Trumpy, Zeits. f. Physik **66,** 790 (1930); H. C. Urey and C. A. Bradley, Jr., Phys. Rev. **38,** 1969 (1931).

[2] H. C. Urey and C. A. Bradley, Jr., Phys. Rev. **37,** 843 (1931).

[3] Black Duco of E. I. du Pont de Nemours and Company, Inc.

When one mercury arc was used and run hot, it gave out considerable continuous background. Two arcs were therefore mounted parallel and as close together as possible, and cooled with a current of air. This eliminated most of the continuous, and reduced the consumption of the ammonia. Ammonia was added as needed by pumping some in from a supply in another Dewar flask.

Some of the exposures were made on panchromatic plates, but the best spectra were obtained on Cramer Isopresto plates. The lengths of the exposures were ten and twenty hours.

The first compound studied was silicochloroform. It was prepared by passing dry hydrogen chloride over amorphous silicon at a temperature of 250° to 350°C. The product was condensed in a flask surrounded by solid CO_2. The product was fractionated into another flask, and sealed off. This fraction was distilled under vacuum into the observation tube.

The other compounds studied were dichloromonofluoromethane and dichlorodifluoromethane. These compounds were supplied to us by the Frigidaire Corporation through the kindness of Dr. R. M. Buffington and were reported by their laboratories as "better than 99 percent pure." They were redistilled twice in vacuo and finally distilled into the observation tube, and sealed off. The average measurements of several plates for each of these compounds are given in Tables I, II and III. The mercury arc lines from which Smekal-Raman lines were observed were λλ4047, 4078, 4348, 4358, 5462, 5771, 5792, 3985, 3907, 3651A. They are referred to in the tables as *a*, *b*, *e*, *f*, *g*, *i*, *m*, *n*, *o*, and *r* respectively.

TABLE I. *Silicochloroform*

$\tilde{\nu}$(cm^{-1})	Exciting line	$\Delta\tilde{\nu}$ (cm^{-1})	Note	$\tilde{\nu}$ (cm^{-1})	Exciting line	$\Delta\tilde{\nu}$ (cm^{-1})	Note
24885	*a*	+182	v.w.	22447	*a*, *f*	−2256, −491	s.b.
24454	*a*	−248	s.sh.	22350	*f*	−588	w.b.
24265	*b*	−248	w.	22256	*b*	−2257	w.
24215	*a*	−488	v.s.	22135	*f*	−803	w.b.
24116	*a*	−586	b.w.	20677	*f*	−2260	s.b.
24026	*b*	−488	s.sh.	18130	*g*	−178	m.
23906	*a*	−797	s.b.	18057	*g*	−250	w.
23717	*b*	−797	v.w.	17816	*g*	−491	m.s.
23428	*f*	+490	w.	17512	*h*	+185	v.w.
23171	*e*	+176	v.w.	17448	*i*	+185	v.w.
23114	*f*	+176	v.w.	17149	*h*	−178	w.sh.
22759	*f*	−179	w.	17087	*i*	−176	w.sh.
22685	*f*	−253	w.	16838	*h*	−489	w.sh.
22506	*e*	−490	v.w.	16775	*i*	−488	w.sh.

Notes: w. = weak; s. = strong; sh. = sharp; b. = broad; m. = medium; v. = very.

$CHCl_3$*		$SiHCl_3$		$CHCl_3$*		$SiHCl_3$	
$\Delta\tilde{\nu}$	*I*	$\Delta\nu$	*I*	$\Delta\tilde{\nu}$	*I*	$\Delta\tilde{\nu}$	*I*
261	4	179	5	762	3 *d*	587	4 *d*
367	5	250	6	1218	2 *d*	799	6 *d*
669	4	489	10	3019	3 *d*	2258	7 *d*

* Proc. Roy. Soc. **A127,** 360 (1930).

TABLE II. *Dichloromonofluoromethane*

$\tilde{\nu}$ (cm^{-1})	Exciting line	$\Delta\tilde{\nu}$ (cm^{-1})	Note	$\tilde{\nu}$ (cm^{-1})	Exciting line	$\Delta\tilde{\nu}$ (cm^{-1})	Note
24429	*a*	−273	m.d.	22662	*f*	−276	s.
24368	*r*	−3020	b.	22572	*n*	−3019	m.w.
24274	*o*	−3016	w.		*f*	−366	
24250	*a*	−453	s.sh.	22483	*f*	−455	s.sh.
24063	*b*	−451	w.	22213	*e*	−783	s.v.b. (band like)
	c	−270			*f*	−726	
23982	*a*	−721	v.b.s.	22152	*f*	−786	w.b.
23914	*a*	−789	v.w.	21687	*a*	−3016	m.
23792	*b*	−722	v.w.		*e*	−1309	
23397	*a*	−1306	m.	21631	*f*	−1307	w.
	f	+459		21493	*b*	−3021	v.w.
23215	*f*	+277	w.	19918	*f*	−3021	w.

$CHFCl_2$

$\Delta\tilde{\nu}$	*I*	$\Delta\tilde{\nu}$	*I*
274	7	786	4
366	4	(1065)*	1
454	7	1307	3
723	9	3019	5

* $\Delta\tilde{\nu} = 1065$ estimated from the microphotometer curve.

TABLE III. *Dichlorodifluoromethane*

	Exciting line	$\Delta\tilde{\nu}$	Note	$\tilde{\nu}$	Exciting line	$\Delta\tilde{\nu}$	Note
24443	*m*	−650	v.w.	23199	*f*	+261	v.w.
	a	−260		22677	*e*	−319	m.
24383	*a*	−320	v.w.		*f*	−261	
24272	*a*	−431	w.	22617	*f*	−321	w.
24249	*a*	−454	m.	22502	*f*	−436	w.
24060	*b*	−454	v.w.	22481	*f*	−457	m.
24040	*a*	−662	s.	22272	*f*	−666	s.
23850	*b*	−663	v.w.	22061	*f*	−877	v.w.
23626	*a*	−1076	v.w.	22019	*f*	−919	v.w.
23564	*a*	−1139	v.v.w.	21850	*f*	−1088	w.b.
23393	*f*	+455	v.w.	21782	*f*	−1156	v.w.

CF_2Cl_2

$\Delta\tilde{\nu}$	*I*	$\Delta\tilde{\nu}$	*I*
260	5	877	1
320	3	919	2
433	5	1082	3
455	7	1147	1
664	10		

THE MODES OF VIBRATION AND THE ASSIGNMENT OF FREQUENCIES

Brester[4] has determined the number of characteristic frequencies of these types of molecules and Dennison[5] has described the character of the vibrations of the chloroform and carbon tetrachloride types of molecules. Brester's

[4] C. J. Brester, Kristallsymmetrie und Reststrahlen, Dissertation, Utrecht, 1923.

[5] D. M. Dennison, Rev. Mod. Phys. **3**, 280 (1931).

work shows that the number of vibrational frequencies of CCl_4, $SiHCl_3$, CF_2Cl_2 and $CFHCl_2$ are 4, 6, 9, and 9 respectively.

In order to assign the frequencies one should have a physical idea as to the character of the motion. The simplest of the above types is carbon tetrachloride. Its four frequencies Brester calls A, B, C_1, and C_2. We may describe them in the following manner. Let the carbon atom be at the origin of the coordinate system. The axes are chosen so that they pass through the midpoints of the lines joining the corner chlorine atoms. Frequency A will consist of a perfectly symmetric motion of the chlorine atoms moving along the lines joining them to the carbon atom, which will remain stationary. This will be an inactive single vibration. Frequency B also is inactive and consists of a twisting motion of pairs of the chlorine atoms; i.e., the chlorine atoms move on the surface of a sphere. The pairs may be selected in three ways, but only two are independent. Thus B is a double frequency.

Frequencies C_1 and C_2 are of a similar character, but very different magnitude. The larger, which we will choose as C_1, will consist of a motion in which the chlorine atoms move nearly along the valence bonds, while for C_2 their motion will be more perpendicular to the bonds. In C_1 the chlorine atoms move in the positive while the carbon atom moves in the negative X direction; the two chlorine atoms with positive X coordinates move away from the X axis, while those with negative X coordinates move toward the X axis. There are three independent ways of choosing the axes in this manner, thus C_1, is a triple vibration. In C_2 the chlorine atoms with positive X coordinates move toward while those with negative X coordinates move away from the X axis, and this frequency is triple.

The most intense Smekal-Raman lines should be those corresponding to inactive frequencies. A will, of course, be larger than B, and more intense. B will be the smallest, C_1 the largest, and C_2 should lie between A and B.

In the Smekal-Raman spectrum of CCl_4 five frequency displacements have been observed. The appearance of the doublet $\Delta\tilde{\nu} = 760$ and 790 cm^{-1} probably is due to accidental degeneracy,[6] although it has been attributed to an asymmetry of the carbon atom.[7] Thus, the assignment for CCl_4 is $A = 460$ cm^{-1}, $B = 214$ cm^{-1}, $C_1 = 760$–790 cm^{-1}, and $C_2 = 311$ cm^{-1}.

In the case of CF_2Cl_2, all degeneracy has been removed, and nine frequency displacements are expected in the Smekal-Raman effect. We may describe the nine modes of vibration in the following manner. Let us take for the Z axis the symmetry axis, and let the origin be at the center of the mass. The two fluorine atoms may be considered as lying in the $X-Z$ plane, and the two chlorine atoms in the $Y-Z$ plane. There will be one frequency, A_1^1, which will be somewhat similar to the A vibration for CCl_4. However, it will be active in this case, and the electric moment will vibrate parallel to the Z axis. There will be two vibrations characterized by a twisting motion. We shall call these A_2 and A_1^2. A_2 will be an inactive frequency consisting of a twisting of the pairs of F atoms and Cl atoms about the symmetry axis. A_1^2

[6] E. Fermi, Zeits. f. Physik **71**, 250 (1931).
[7] A. Langseth, Zeits. f. Physik **72**, 350 (1931).

will consist of a sort of twisting of Cl–F pairs of atoms around some axis perpendicular to the Z axis. It will be an active vibration, and the electric moment will vibrate parallel to the Z axis.

The other six frequencies, we shall group as follows A_1^3, B_1^1, B_2^1 and A_1^4, B_1^2, B_2^2. The first group will be of a character similar to C_1 for CCl_4, and the second group similar to C_2. In A_1^3 the electric moment will vibrate $\parallel$ to the Z axis; in B_1^1 $\parallel$ to the X axis; in B_2^1 $\parallel$ to the Y axis. The motion of the corner atoms will be such that they move nearly along the bonds to the central atom. In A_1^4 the electric moment will be $\parallel$ to the Z axis, B_1^2 $\parallel$ to X, and B_2^2 $\parallel$ to Y and the motion is more perpendicular to the bonds.

It is impossible to assign every frequency displacement observed to the actual modes of vibration. However, it is possible to group them with considerable certainty. Since the F atoms are lighter than the Cl atoms, we would expect A_1^1, to be larger than the A for CCl_4, and to be rather intense. Thus $\Delta\tilde{\nu} = 664$ cm^{-1} becomes A_1^1; A_2 and A_1^2 should be the smallest frequency displacements, and become 260 cm^{-1} and 320 cm^{-1}. In assigning the groups A_1^3, B_1^1, B_1^2 and A_1^4, B_2^1, B_2^2 we expect the first to possess the largest frequencies, and all be rather closely grouped, while the second group should lie between 360 cm^{-1} and 664 cm^{-1}, and also all be rather close to one another. However, I find four frequency displacements in the region of the first group and two in the region of the second. In the first group I assign immediately $\Delta\tilde{\nu} = 1147$ cm^{-1} and 1082 cm^{-1}. The appearance of the two lines $\Delta\tilde{\nu} = 919$ cm^{-1} and 877 cm^{-1} may be due to combinations and accidental degeneracy, for we see that $260+664 = 924$ cm^{-1}, $455+433 = 888$ cm^{-1}, $1147-260 = 887$ cm^{-1}. Therefore, as in the case of C_1 for CCl_4, I must group the frequency displacements, 1147, 1082, 919, and 877 cm^{-1} in the group of vibrations A_1^3, B_1^1, B_1^2. For A_1^4, B_2^1, B_2^2, there are the frequencies $\Delta\tilde{\nu} = 455$ and 433 cm^{-1}. I should expect the third frequency to be close to these two. However, neither the original plate nor the microphotometer curve show any line in this region.

The case of $CHCl_3$ is somewhat simpler. Here one expects six frequency displacements, and they are all observed in the Smekal-Raman effect. Let us take the origin of the coordinate system at the center of mass of the molecule; the Z axis as the symmetry axis and the three chlorine atoms on a plane perpendicular to the symmetry axis. There will be three modes of vibration with the electric moment oscillating $\parallel$ to the Z axis, and three perpendicular to it. The first three will all be single, and the latter all double vibrations. We will call the $\parallel$ vibrations A, C_1^1, and C_2^1, and the perpendicular ones B, C_1^2, and C_2^2, corresponding to their similarity with CCl_4. The character of A will in this case be determined by the Cl atoms and consequently, while larger than A for CCl_4, will be of the same order of magnitude, and intense. Thus I ascribe $\Delta\tilde{\nu} = 669$ cm^{-1} to A. In the case of C_1^1 and C_2^1, the character seems to be determined mostly by the vibration of the hydrogen with respect to the rest of the molecule and is very large as a result. One thus expects C_1^1 to be 3019 cm^{-1} and $C_2^1 = 1218$ cm^{-1}. In order to justify this assignment I set up the equations of motion for the parallel vibrations assuming pure valency forces, and used the force constants calculated from CCl_4, (reference 1, p. 1972). The only change made being that one of the corner atoms now had 1/35 of the

previous mass. With these very simplifying assumptions, the numerical solution gave for the three parallel vibrations $\Delta\tilde{\nu} = 3015$, 1497, and 466 cm^{-1}; the agreement is quite as good as found in the case of CCl_4 assuming pure valency forces. Frequency B will again be a twisting motion, and the smallest observed frequency displacement; thus B is 261 cm^{-1}. C_1^2 and C_2^2 will be $\perp$ vibrations, as Dennision describes, as tilting of the plane containing the chlorine atoms relative to the line joining the carbon and hydrogen atoms. From analogy, I expect C_1^2 to be larger than C_2^2. Thus C_1^2 is 762 cm^{-1} and C_2^2 is 367 cm^{-1}.

In the case of $SiHCl_3$, again six frequency displacements are observed and they are all somewhat smaller than those for $CHCl_3$, as one would expect from the increased mass of the central atom. The intensities of the observed lines for $SiHCl_3$ are in the same order as those of $CHCl_3$. One may, therefore, immediately assign the frequencies as follows: A is 489 cm^{-1}, B is 179 cm^{-1}, C_1^1 is 2258 cm^{-1}, C_1^2 is 587 cm^{-1}, C_2^1 is 799 cm^{-1}, and C_2^2 is 250 cm^{-1}.

In the compound $CHFCl_2$, all degeneracy is removed and one expects nine frequency displacements in the Smekal-Raman effect. From the intensities of the observed lines, and comparison with the assignment of frequencies for $CHCl_3$, I make the following correlation: A, 723 cm^{-1}; B_1, and B_2, 274 cm^{-1}, and 366 cm^{-1}; C_1^1, 3019; C_1^2, 786 cm^{-1}; C_2^1, 1307 and C_2^2, 454 cm^{-1}. We still must find C_1^3 and C_2^3. C_1^2 shows on the microphotometer curve as being a very close doublet, and as one would expect C_1^3 to lie near C_1^2, 786 cm^{-1} may be both C_1^2 and C_1^3. However, a very faint line is observed also at $\Delta\tilde{\nu} = 1065$ cm^{-1}. This may be C_1^3; it may also be due to the combination $786+274=1060$ or $723+366=1089$. I expect C_2^3 to be close to C_2^2, but no line is observed in that region.

In Table IV I have collected and tabulated the observed frequencies and my assignment to the various types of vibration.

TABLE IV.

$CHFCl_2$	$SiHCl_3$	$CHCl_3$	CCl_4	CF_2Cl_2
$A-723$	$A-489$	A (single $-\parallel$ to Z) -669	$A-460$	$A_1^1-(\parallel$ to $Z)-664$
B_1-274 B_2-366	$B-179$	B (double $-\perp$ to Z) -261	$B-214$	A_2-(Inactive)-260 $A_1^2-(\parallel$ to $Z)\ 320$
C_1^1-3019 C_1^2-786 C_1^3-1065	C_1^1-2258 C_1^2-587	C_1^1 (single $-\parallel$ to Z) -3019 C_1^2 (double $-\perp$ to Z) -762	C_1-760 790	$A_1^3-(\parallel$ to $Z)\ 1147$ $B_1^1-(\parallel$ to $X)\ 1082$ $B_1^2-(\parallel$ to $Y)\ 919$ 877
C_2^1-1307 C_2^2-454 $C_2^3-?$	C_2^1-799 C_2^2-250	C_2^1 (single $-\parallel$ to Z) -1218 C_2^2 (double $-\perp$ to Z) -367	C_2-311	$A_1^4-(\parallel$ to $Z)$ $B_2^1-(\parallel$ to $X)\ 455$ $B_2^2-(\parallel$ to $Y)\ 433$

I should like to express my appreciation to Professor Harold C. Urey for his very helpful assistance and advice during the course of this work. I should also like to thank Dr. R. M. Buffington of the Frigidaire Corporation for the samples of $CHFCl_2$ and CF_2Cl_2. And I wish to express my appreciation to the E. I. du Pont de Nemours and Company, Incorporated for the awarding of a fellowship.

Note on a Relation between the Atomic Arrangement in Certain Compounds, Groups and Molecules and the Number of Valence Electrons

By W. H. ZACHARIASEN
Ryerson Physical Laboratory, University of Chicago

(Received April 20, 1932)

The atomic arrangement in compounds and groups $(A_mX_n)^{-p}$ for which $v=n\times 8+m\times 2$ is discussed, v being the total number of valence electrons per stoechiometric molecule or group. Available experimental data show that in such groups or compounds the atom A is usually displaced away from the center of the polyhedron formed by the surrounding atoms X. Simple rules for the amount of displacement are given. The interpretation of the observations in terms of the ionic theory and the theory of electron pair bonds is discussed.

IN THE following paper the crystal lattice of germano sulphide is described. GeS belongs to a large class of compounds, groups or molecules of the general formula $(A_mX_n)^{-p}$ which are characterized by the following features: None of the atoms A or X are transition elements. The total number of valence electrons per stoechiometric molecule or group, v, satisfies the condition $v=n\times 8+m\times 2$, or if atom X is a hydrogen atom, $v=n\times 2+m\times 2$.

On previous occasions I have had the opportunity to examine the atomic arrangement in several compounds or groups of this type.[1,2,3,4,5] In one important respect the results of these investigations were of exceptional interest. Usually in crystal lattices it is found that an atom is situated at the center of the polyhedron formed by the surrounding atoms. However, it was found in many cases, where the condition $v=n\times 8+m\times 2$ was satisfied, that the atom A was displaced away from the center of the polyhedron formed by the surrounding atoms X. Some examples may illustrate this statement: The groups $(SO_3)^{-2}$, $(ClO_3)^{-1}$, $(BrO_3)^{-1}$ have a pyramidal structure rather than the coplanar one found for $(NO_3)^{-1}$, $(CO_3)^{-2}$ and $(BO_3)^{-3}$.[4] The $(NO_2)^{-1}$ group has been found to be angular rather than collinear like CO_2[6]. And now in GeS we will see that Ge is not lying at the center of the sulphur octahedra, as does Mg in MgS.

However, there are definite exceptions. Tl in TlCl, TlBr, TlI[7] is not displaced away from the center of the cubes formed by the surrounding halogen atoms. The analogous thing is true for Pb in PbF_2, PbS, PbSe,

[1] W. H. Zachariasen, Norske Vid. Akad. Skr. Oslo **4**, 90 and 136 (1928).
[2] W. H. Zachariasen, Zeits. f. Krist. **71**, 501, 517 (1929).
[3] W. H. Zachariasen, Phys. Rev. **37**, 775 (1931).
[4] W. H. Zachariasen, Jour. Amer. Chem. Soc. **53**, 2123 (1931).
[5] W. H. Zachariasen and H. E. Buckley, Phys. Rev. **37**, 1295 (1931).
[6] G. E. Ziegler, Phys. Rev. **38**, 1040 (1931).
[7] P. P. Ewald and C. Hermann: Strukturbericht, 1913–1928, Leipzig, 1931.

PbTe, PbI_2,[7] for Bi in BiF_3 and BiI_3,[8] for Sn in SnTe,[7] and probably it is also true for Te in TeO_2[7] and for I in the alkaliiodates.[7,9] It is worth noticing, however, that the atomic number of atom A in all these cases is very high.

The empirical results we may formulate in a series of very simple rules:

In compounds or groups $(A_mX_n)^{-p}$ satisfying the condition: $v=8\times n+2\times m$ (or if the atom X is hydrogen, the condition: $v=2\times n+2\times m$) the atom A is displaced away from the center of the polyhedron formed by the surrounding atoms X.

The amount of displacement decreases: (1) With increasing principal quantum number of atom A; (2) With an increasing number of valence electrons on the neutral atom A; (3) With increasing principal quantum number of atom X; (4) and probably with a decreasing number of valence electrons on the neutral atom X.

The absence of any displacement in crystals like SnTe, PbTe, TlI may thus follow directly from rule 1 and 3.

By expressing the rules in terms of the number of valence electrons and principal quantum numbers we have deliberately avoided any interpretation on the basis of existing theories for the chemical binding.

If we choose to take the standpoint of ionic bindings in the compounds or groups which we have considered, we would have to explain our rules as being due to a polarization of the ions A. As a matter of fact the empirical rules we have given would be a direct consequence of the ionic interpretation. We cannot therefore draw the conclusion that the bonds are truly ionic in character. It illustrates, however, the value of the ionic theory as a working hypothesis. As a matter of fact I have been able to predict correctly the atomic arrangement in a number of groups on that basis.[1]

The rival to the ionic theory is, of course, the theory of the electron pair bond. It has been shown by Pauling[10] and by Slater[11] that the structure of many of the groups which we have dealt with here can be satisfactorily interpreted in terms of electron pair bonds. As a matter of fact this interpretation offers in many cases distinct advantages compared to the ionic interpretation. However, this is no proof of the existence of electron pair bonds. It seems to me that serious modifications of the ideas of Slater and Pauling are necessary in order to account for all our observations. In GeS we found that Ge formed six bonds with sulphur atoms, three corresponding to an interatomic distance 2.58A and the three others corresponding to 2.97A. In the isomorphous SnS the difference between the two distances undoubtedly is smaller than in GeS, and then finally in PbS (having the ideal NaCl structure) we have six equivalent bonds. A comparison between the interatomic distances in As_4O_6 and Sb_4O_6 also shows this gradual transition towards six equivalent bonds as we pass towards higher atomic numbers (compare rule 1). Three of the bonds in GeS, As_4O_6 and Sb_4O_6 may, of course, be in-

[8] H. Braekken, Zeits. f. Krist. **74**, 67 (1930).
[9] W. H. Zachariasen and F. A. Barta, Phys. Rev. **37**, 1626 (1931).
[10] L. Pauling, Jour. Amer. Chem. Soc. **53**, 1367 (1931).
[11] J. C. Slater, Phys. Rev. **37**, 481 and **38**, 325 (1931).

terpreted as electron pair bonds; but this interpretation is hardly satisfactory or justifiable in PbS for example.

It seems that the ideas of the electron pair bonds are fairly applicable in many cases for relatively low atomic numbers but of little use, in the present form at any rate, for high atomic numbers. In the lattices of As, Sb, Bi[7] each atom is surrounded by six other atoms, three at a distance d_1 and three at a distance d_2. The observed values of d_1 and d_2 are:

	d_1	d_2	α
As	2.51	3.15	97°
Sb	2.87	3.37	96°
Bi	3.10	3.47	94°

α is the angle between the three bonds corresponding to the distance d_1. Pauling in his paper states that the approach of the bond angle towards 90° in this series indicates the transition to electron pair bonds formed by pure p eigenfunctions. This statement seems to me to be somewhat misleading. If namely the bond angle is exactly 90°, there will be six equivalent bonds, instead of two sets of three bonds. Other eigenfunctions than those of s and p electrons would have to be involved in the formation of six equivalent bonds.

The Crystal Lattice of Germano Sulphide, GeS

By W. H. ZACHARIASEN
Ryerson Physical Laboratory, University of Chicago

(Received April 20, 1932)

The crystal lattice of germano sulphide, GeS, was examined by means of the Laue method, the powder method and the oscillating crystal method. The crystals are orthorhombic bipyramidal. The dimensions of the unit cell were found to be: $a=4.29\pm0.01$A, $b=10.42\pm0.03$A, $c=3.64\pm0.01$A. There are four molecules GeS in the unit cell and the calculated density is 4.24. The space group is Pbnm (V_h^{16}). The germanium atoms as well as the sulphur atoms are lying in the reflection planes: $(uv0)(\bar{u}, \frac{1}{2}-v, \frac{1}{2})(u+\frac{1}{2}, \bar{v}, \frac{1}{2})(\frac{1}{2}-u, v+\frac{1}{2}, 0)$. The values of the four parameters, u_1v_1 for Ge and u_2v_2 for S, were determined on the basis of intensity calculations, the final result being: $u_1=0.167$ (60°), $u_2=0.111$ (40°), $b_1=-0.125$ (−45°), $v_2=0.111$(40°). The crystal structure can be described as a deformed rocksalt lattice, the deformation being very great in the direction of the a axis. The germanium atoms are surrounded by distorted octahedra formed by sulphur atoms. The germanium atom is not lying at the center of the octahedron, but is displaced towards one of the octahedral faces. The distance from germanium to three of the sulphur atoms in this manner is distinctly smaller than to the three others. The two distances Ge-S are: 2.58A (average of 2.47, 2.64, 2.64) and 2.97A (average of 2.91, 3.00, 3.00). The closest approach between two sulphur atoms is 3.55A.

I. INTRODUCTION

FOR reasons which will be discussed in the following note, it appeared to be of special interest to examine the crystal lattices of compounds of divalent germanium.

The crystals of GeS used in this investigation were a gift from Professor W. C. Johnson of the department of Chemistry of this University. For particulars concerning the preparation of the crystals I may refer to a paper by Dr. Johnson soon to be published. The crystals form thin steel-grey plates of metallic luster. Laue photographs showed orthorhombic symmetry and gave axial ratios very similar to those of SnS. The isomorphism between GeS and SnS reported by Dennis[1] thus seems to be beyond doubt.

II. UNIT CELL AND SPACE GROUP

The Laue method, the oscillating crystal method and the powder method were employed. The dimensions of the orthorhombic unit cell were found to be:

$$a = 4.29 \pm 0.01\text{A}, \quad b = 10.42 \pm 0.03\text{A}, \quad c = 3.64 \pm 0.01\text{A}$$

corresponding to the axial ratios: 0.412:1:0.349. For SnS Groth[2] gives the ratios 0.3883:1:0.3566.

[1] L. M. Dennis and R. E. Hulse, J. Am. Chem. Soc. **52**, 3555 (1930).
[2] P. Groth, Chemische Krystallographie, Vol. 1, p. 150, Leipzig, 1906.

For the density of GeS, L. M. Dennis and R. E. Hulse[1] give the value 3.78, W. Pugh,[3] however, gives 4.012. These two values correspond to 3.57 and 3.78 molecules in the cell respectively. We have to assume therefore that there are four molecules GeS per unit cell. The calculated density is 4.24, so the experimental values are all low.

Reflexions from the following classes of planes were not observed in any of the photographs: $0kl$ if k is odd, and $h0l$ if $h+l$ is odd. The development of the crystal faces does not indicate any deviation from holohedral symmetry, so we will assume that the symmetry class is orthorhombic bipyramidal. All space groups except V_h^1, V_h^5, V_h^{13}, V_h^{16} are ruled out on the basis of present reflexions. A consideration of the general and special positions of these four space groups gives the result that only V_h^{16} can give an atomic arrangement that accounts for the observed intensities. In the new space group notation the symbol is Pbnm.[4]

As there are only four molecules in the unit cell, it follows that the four germanium atoms are equivalent; likewise the four sulphur atoms are structurally equivalent. The space group permits the following arrangements: (1) all atoms are lying in centers of symmetry; (2) germanium atoms are in centers of symmetry and sulphur atoms in reflexion planes, or vice versa; (3) all atoms are lying in the reflexion planes.

The possibility (1) is ruled out by the fact that the $h00$ and $0k0$ reflexions do not all have maximum of intensity. The alternative (2) must be rejected as it would result in a very weak 002 reflexion, whereas it actually appears with great intensity. Consequently both the germanium and the sulphur atoms are lying in the reflexion planes.

III. Determination of the Structure

The coordinates of the atoms are: 4 Ge in $(u_1v_10)(\bar{u}_1, \frac{1}{2}-v_1, \frac{1}{2})(u_1+\frac{1}{2}, \bar{v}_1, \frac{1}{2})$ $(\frac{1}{2}-u_1, v_1+\frac{1}{2}, 0)$, 4 S in analogous positions with parameters u_2 and v_2. The very strong 002 and 004 reflexions are accounted for by this arrangement; the structure amplitude for these reflexions will have the maximum value of 4 Ge+4 S.

Determination of parameters v_1 and v_2

The reflexions 040 and 080 occur with very great intensity whereas 020,060 and 0.10.0 are barely visible. v_1 and v_2 consequently must have values very close to $(2n+1)\times 45°$. The reflexion 021 occurs with medium intensity; $\sin 2v_1$ and $\sin 2v_2$ must have opposite signs, otherwise 021 would have shown maximum intensity. Hence we choose $v_1 \approx -45°$ and $v_2 \approx 45°$. The fact that 020,060 and 0.10.0 are present shows that v_1 and v_2 cannot both be numerically equal to 45°. More accurate values can be obtained from a comparison of the observed intensities for the reflexions 080,081,0.10.0 and 0.10.1. It is seen from table 4 that the parameter v_1 hardly can be different from $-45°$, whereas v_2 must be very close to 40°. The values $v_1 = -45°$; $v_2 = 40°$ are probably accurate to less than two degrees.

[3] W. Pugh, J. Am. Chem. Soc. **52,** 2372 (1930).

[4] Ch. Mauguin, Zeits. f. Krist. **76,** 542 (1931).

The value $v_2 = 50°$ gives the same intensities in the 0*kl* zone as does the value $v_2 = 40°$. However, when reflexions *hk*0 and *hkl* are also considered, the intensities are different for the two cases, so that we will have to consider also: $v_1 = -45°$; $v_2 = 50°$.

Determination of parameters u_1 and u_2

The very weak or missing reflexions 110,130 and 170 show definitely that $\cos u_1$ and $\cos u_2$ must both be positive or both negative. The strong 141 reflexion can be explained only if $\sin u_1$ and $\sin u_2$ both have the same sign. Consequently u_1 and u_2 are lying in the same quadrant. We can choose the range $0° - 90°$ for both u_1 and u_2.

TABLE I. *Spectra* 0*kl*.*

0*kl*	sin θ	Int. obs.	$\|F\|$	0*kl*	sin θ	Int. obs.	$\|F\|$
020	0.0676	vvw	10	080	0.2706	s	93
021	0.1190	m	55	062	0.2836	nil	15
040	0.1353	vvs	139	081	0.2872	w	19
041	0.1668	w	14	023	0.3018	w+	38
002	0.1966	vs	120	043	0.3236	vvw	9
060	0.2029	vw	18	082	0.3336	ms	83
022	0.2074	vvw	6	0.10.0	0.3382	vvw	20
061	0.2271	m	47	0.10.1	0.3513	wm	44
042	0.2380	s	106	004	0.3932	ms	80

* In this table and in subsequent tables the intensities are indicated in the order vvs, vs, s ms, mw, w, vw, vvw and nil. (v = very, s = strong, m = medium, w = weak).

TABLE II. *Spectra hk*0.

*hk*0	sin θ	Int. obs.	$\|F\|$	*hk*0	sin θ	Int. obs.	$\|F\|$
020	0.0676	vvw	10	170	0.2505	nil	1
110	0.0901	vw	13	310	0.2527	wm	41
120	0.1073	m	60	320	0.2593	wm	27
130	0.1312	nil	5	260	0.2624	vvw	3
040	0.1353	vvs	139	330	0.2702	m	36
140	0.1587	nil	9	080	0.2706	s	93
200	0.1673	wm	38	180	0.2825	vvw	12
210	0.1703	ms	86	340	0.2845	nil	9
220	0.1801	nil	1	270	0.2892	m	46
150	0.1882	m−	20	350	0.3019	w	42
230	0.1952	m	70	190	0.3149	w−	23
060	0.2029	vw	18	360	0.3219	w−	21
240	0.2146	w	34	400	0.3346	w	56
160	0.2212	m	49	370	0.3442	vw	30
250	0.2373	m	77	1.10.0	0.3476	w−	42

The relatively strong reflexions 210,230,250 and 270 show that $\sin 2u_1$ and $\sin 2u_2$ have the same sign, whereas the weak 200 reflexion indicates that $\cos 2u_1$ and $\cos 2u_2$ have opposite signs. It follows from this result that one of the parameters lies between 45° and 90°, the other between 0° and 45°.

Using the value $v_2 = 50°$ (and inserting the values of the scattering powers from Table V) we find for the structure amplitudes of 110 and 150:

$$|F|\ 110 = 77.5(\cos u_1 - 0.52 \cos u_2)$$

$$|F|\ 150 = 60(\cos u_1 - 0.58 \cos u_2).$$

The observed intensities of these two reflexions cannot be explained on the basis of the structure amplitudes given above. We must consequently use the value $v_2 = 40°$.

TABLE III. *Spectra hkl.*

hkl	sin θ	Int. obs.	$\|F\|$	*hkl*	sin θ	Int. obs.	$\|F\|$
111	0.1331	s	61	212	0.2597	m−	67
121	0.1453	nil	5	222	0.2662	nil	1
131	0.1638	s	47	171	0.2690	vw	29
141	0.1865	s	98	152	0.2718	w	17
211	0.1965	m	28	232	0.2767	m−	59
221	0.2050	m−	47	261	0.2819	vw	38
151	0.2110	s	54	242	0.2907	vw	29
112	0.2158	vw	11	162	0.2956	w	42
231	0.2185	w	19	181	0.2990	w	70
122	0.2235	m	46	252	0.3079	w	67
132	0.2359	nil	4	172	0.3181	nil	1
241	0.2360	nil	2	262	0.3291	vvw	2
161	0.2420	nil	10	191	0.3298	w	43
142	0.2523	nil	7	182	0.3439	nil	11
251	0.2568	w−	33	192	0.3710	w−	21

TABLE IV. *Determination of parameters v_1 and v_2.*

v_1 \ v_2	30°	35°	40°	45°	Observed	
	3	17	36	42	080	s
−35°	12	6	27	38	0.10.1	wm
	42	39	49	68	081	w
	74	85	81	61	0.10.0	vw
	39	59	78	84	080	s
	61	42	22	8	0.10.1	wm
−40°	18	14	25	44	081	w
	60	71	67	46	0.10.0	vw
	55	75	94	100	080	s
	82	64	44	30	0.10.1	wm
−45°	26	29	19	0	081	w
	13	24	20	0	0.10.0	vw
	39	59	78	84	080	s
	61	43	22	8	0.10.1	wm
−50°	69	73	62	44	081	w
	34	22	27	47	0.10.0	vw
	3	17	36	42	080	s
−55°	12	6	27	38	0.10.1	wm
	93	97	87	68	081	w
	48	36	41	61	0.10.0	vw

TABLE V. *F Curves.*[5]

sin θ	0	0.05	0.10	0.15	0.20	0.25	0.30	0.35	0.40
Ge	32	30	26.6	23.5	20.6	18.2	16.6	15.1	13.8
S	16	14.6	12.5	10.6	9.0	8.0	7.2	6.6	5.8

[5] The *F* curves for Ge and S were calculated by the method of *Thomas*, Proc. Cambridge Soc. **23**, 5, 542 (1927).

In order to get structure amplitudes for 130 and 170 that are approximately zero, we must require that $\cos u_1$ is somewhat less than $\cos u_2$. It follows that $u_1 > 45°$ and $u_2 < 45°$.

The best agreement between observed and calculated intensities was obtained with:

$$u_1 = 60° \qquad u_2 = 40°$$

the accuracy of the values being of the order of $\pm 5°$.

IV. Discussion of the Structure

In Figs. 1 and 2 are given projections of the structure on the *a* face and on the *c* face. The structure may be described as a highly deformed rocksalt

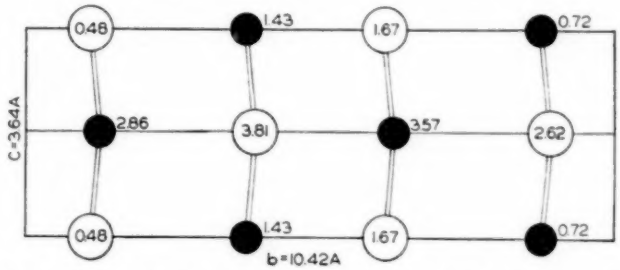

Fig. 1. This shows a projection of the structure on the *a* face. Germanium atoms are represented by solid circles, sulphur atoms by open circles. Numbers give heights of atoms above projection plane. The close approximation to the rocksalt lattice in the 100 zone is clearly shown in the drawing.

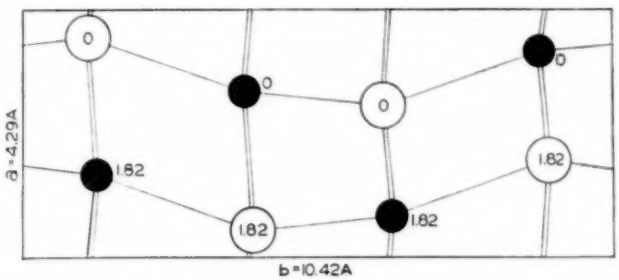

Fig. 2. Here is a projection on the *c*-face. The great deformation of the rocksalt arrangement in the direction of the *a*-axis will be noticed.

lattice. The observed axial ratio of 0.412:1:0.349 corresponds quite closely to $\frac{1}{2}(2)^{\frac{1}{2}}:2:\frac{1}{2}(2)^{\frac{1}{2}}$. It is readily seen from the figures that the deformation from the ideal rocksalt lattice is greatest in the direction of the *a* axis. The parameters of the ideal rocksalt lattice would be: $u_1 = 90°$ $u_2 = 90°$ $v_1 = -45°$ and $v_2 = 45°$, and the axial ratios would be: 0.3535:1:0.3535. We observed the values $u_1 = 60°$ $u_2 = 40°$ $v_1 = -45°$ $v_2 = 40°$ and $a:b:c = 0.412:1:0.349$. The axial ratios for SnS are 0.3883:1:0.3566 and indicate that the approximation to the ideal rocksalt lattice is closer than in the case of GeS.

A germanium atom is surrounded by six sulphur atoms at distances 2.47A (one S atom), 2.64A (two atoms), 2.91A (one atom) and 3.00A (two atoms). The six sulphur atoms around each germanium atom form a some-

what distorted octahedron. The germanium atom is not lying at the center of this octahedron but is displaced toward one of the octahedral faces. In that manner we get two principal distances between germanium and sulphur, and we may state that germanium is surrounded by three sulphur atoms at an average distance of 2.58A and by three other sulphur atoms at an average distance of 2.97A. The difference between these two average distances is far beyond any experimental error.

The distance of closest approach between two sulphur atoms is 3.55A, other distances being 3.64A and 4.29A.

I an indebted to Professor W. C. Johnson of the Chemistry Department of this University for the gift of excellent crystals of germano sulphide.

The Crystal Lattice of Potassium Pyrosulphite, $K_2S_2O_5$, and the Structure of the Pyrosulphite Group[1]

By W. H. ZACHARIASEN
Ryerson Physical Laboratory, University of Chicago

(Received April 8, 1932)

The crystal lattice of potassium pyrosulphite was examined in order to determine the structure of the pyrosulphite group. The Laue method and the oscillating crystal method were used. The dimensions of the monoclinic unit cell were found to be: $a=6.95$A, $b=6.19$A, $c=7.55$A, $\beta=102°41'$. The density determination gave 2.34 and corresponds to two molecules $K_2S_2O_5$ in the unit cell. The space group is $P2_1/m(C_{2h}^2)$. Two sets of four oxygen atoms are lying in general positions with coordinates $\pm(xyz)$ $\pm(x, \frac{1}{2}-y, z)$, while the remaining atoms are all lying in the reflection planes $\pm(u\frac{1}{4}v)$. The parameter values corresponding to the sixteen degrees of freedom were determined accurately and uniquely. No other assumptions than those underlying the theory for the diffraction of x-rays by crystals were made. The final parameters are:

	K I	K II	S I	S II	O I	O II	O III
x	0.22	0.65	0.70	0.01	0.07	0.63	0.67
y	0.25	0.25	0.25	0.25	0.06	0.06	0.25
z	0.95	0.67	0.22	0.32	0.24	0.31	0.03

In the lattice the potassium atoms are surrounded by nine or by seven oxygen atoms at average distances, respectively, of 3.01A and 2.78A. The pyrosulphite group can be described as a sulphite group and a sulphur dioxide molecule linked together by an electron pair bond between the two sulphur atoms. The sulphur to sulphur distance is 2.18A and the average sulphur to oxygen distance is 1.46A.* The atomic arrangement explains the observed cleavage and twinning.

1. INTRODUCTION

FOR several years the author has been interested in the determination of the shape and accurate dimensions of inorganic groups in crystals. The results of a large number of such investigations have been published in different journals during that time. However, there is yet a large field for studies along this line. Of the many different groups formed by sulphur and oxygen, for example, only the sulphate, the sulphite, and the dithionate groups have been examined.

It is a generally known fact that the determination of atomic arrangements involving 10 or more degrees of freedom is a problem of extreme difficulty. However, in many cases complicated crystal structures have been solved quite readily by utilizing empirical results deduced from already known atomic arrangements. To a large extent also chemical evidence has been used. However, when it is our object to get direct experimental data concerning the structure of unknown groups, it becomes clear that the purpose of the investigation fails, if the atomic arrangement is determined on the basis of assumptions of this kind.

* The bonds formed by sulphur atoms, whether three or four in number, are directed towards the corners of a regular tetrahedron to a close degree of approximation.

[1] Some of the results of this paper were given in a Letter to the Editor, Phys. Rev. **40**, 113 (1932).

Some time ago I started upon an examination of the structure of potassium pyrosulphite with the chief object of finding the shape and dimensions of the pyrosulphite group. In agreement with the statements given above no assumptions other than those underlying the theory for the crystal diffraction effects have been used in determining the parameter values corresponding to the 16 degrees of freedom involved. The labor necessary to solve the problem accurately and uniquely on such a basis naturally has been extreme. Nevertheless I have tried as far as possible to prepare the following account of the investigation in such a manner that each successive step of the solution may be retraced.

Crystals of potassium pyrosulphite are described in Groth's Chemische Krystallographie.[2]

The symmetry is monoclinic prismatic with the following elements: $a:b:c=1.4650:1:1.2222$, $\beta=131°43'$. Twins on 001 are very common. The crystals show a perfect cleavage parallel to $10\bar{1}$. The birefringence is strong and negative. The plane of the optical axes is 010 and the acute bisectrix makes an angle of 1°10′ with the c axis in the obtuse angle β. The angle between the optical axes is $2V=76\frac{1}{2}°$ for Na light. The refractive indices are not given, nor is the density.

I prepared crystals of $K_2S_2O_5$ by evaporating a concentrated solution of potassium carbonate which had been oversaturated with sulphur dioxide. Care was taken in order to prevent oxidation during the evaporation. The crystals were thick prisms parallel to the b axis. Twins seemed to be more common than single individuals. The following faces were identified: 102, $10\bar{1}$, $20\bar{1}$, 001, 110 and 210. An excellent crystal of approximate dimensions $0.7\times1.5\times0.7$ mm was selected, and all the observations were taken on this crystal. The density was determined by the suspension method and gave the value 2.34.

2. Experimental Methods

The Laue method and the oscillating crystal method were used. The photographs were indexed by means of the ordinary graphical methods,

Laue photographs were taken with the incident beam parallel to the three crystallographic axes and with the beam perpendicular to the a and c face. The lower wave-length limit in the incident beam was 0.27A and had been checked on a number of known crystals.

For the oscillation method Mo $K\alpha$ radiation was employed. The distance from crystal to photographic plate was 5.00 cm and was calibrated by means of calcite photographs. With the photographic plate at right angles to the incident beam reflections with glancing angles up to about 20° could be recorded. However, in several instances it was found desirable to measure reflections with greater glancing angles; the photographic plate was then set so as to make an angle of 30° with the direct beam. During each exposure the crystal was oscillated through 15°.

Thirty-five different photographs were taken and completely indexed,

[2] P. Groth, Chemische Krystallographie **2**, 305, Leipzig, 1908.

and the intensity of some 700 reflections from different atomic planes was recorded. In this manner all possible reflections with $\sin\theta/\lambda$ less than 0.5 were measured and in addition a large number of reflections with $\sin\theta/\lambda$ between 0.5 and 0.86. A suitable selection of about half of the observations are compiled in Tables IV, V, VI and VIII.

The F curve values used in the investigation were taken from James and Brindley's recent paper[3] and are given in Table I. In accordance with modern

TABLE I. *F curve values.*

$\sin\theta/\lambda$	0	0.10	0.20	0.30	0.40	0.50	0.60	0.70	0.80	0.90
K^{+1}	18	16.5	13.3	10.8	8.9	7.8	7.0	6.4	5.9	5.3
S^{+1}	14	12.1	10.1	8.8	7.8	6.9	6.0	5.2	4.5	3.9
O^{-1}	9	7.5	5.4	3.8	2.8	2.1	1.8	1.55	1.50	1.4

views the state of ionization was taken as K^{+1}, S^{+2}, O^{-1}. This assumption has no real physical meaning and is also of little consequence as far as the numerical values of the scattering powers are concerned, because of the small contribution from the valence electrons in the regions of $\sin\theta/\lambda$ where we have observations. The F curve values in Table I are not corrected for thermal motion; as we have only relative intensity measurements this correction is of little importance.

3. Unit Cell and Space Group

The choice of axes given by Groth is not very satisfactory. I have found it desirable to change the direction of the crystallographic a-axis so as to correspond to an angle β which is closer to 90°. This is accomplished by taking the a-axis in the direction with zone indices $[\bar{1}0\bar{1}]$. The new crystallographic elements then become: $a:b:c=1.1212:1:1.2222$, $\beta=102°\ 41'$. If $h'k'l'$ are the Miller indices referred to Groth's axes, hkl the Miller indices in the new set of axes, the transformation formulae will be: $h=-h'-l'$ $k=k'$ $l=l'$. In the following all indices are referred to the new axes.

All the observations agree with the following unit cell: $a=6.95$A $b=6.19$A $c=7.55$A $\beta=102°\ 41'$. The axial lengths are accurate to 0.02A. The axial ratios are: 1.123:1:1.220.

The observed density of 2.34 gives two (2.02) molecules in the unit cell. The calculated density is, conversely, 2.31.

The only class of absent reflections are the odd orders from 010. As the symmetry is monoclinic prismatic all space groups except the holohedral ones must be rejected. All the space groups except $P2/m(C_{2h}^1)$ and $P2_1/m$ (C_{2h}^2) are ruled out through observed reflections. The absence of odd orders from 010 shows that the b axis is a screw axis rather than a rotation axis. We conclude therefore that $P2_1/m$ is the correct space group.

4. Distribution of the Atoms among the Available Positions of the Space Group

In the space group $P2_1/m$ we may have twofold or fourfold positions. We get twofold positions by placing the atoms in centers of symmetry or in

[3] James and Brindley, Zeitschr. f. Krist. **78**, 470 (1931).

the reflection planes. The coordinates of the atoms are: centers of symmetry: $(000)(0\frac{1}{2}0)$, $(\frac{1}{2}00)(\frac{1}{2}\frac{1}{2}0)$, $(00\frac{1}{2})(0\frac{1}{2}\frac{1}{2})$, $(\frac{1}{2}0\frac{1}{2})(\frac{1}{2}\frac{1}{2}\frac{1}{2})$; Reflection planes: $\pm(u\frac{1}{4}v)$. The fourfold positions correspond to coordinates: $\pm(xyz)\pm(x, \frac{1}{2}-y, z)$.

Since there are ten oxygen atoms in the unit cell, it follows that at least two of them must lie in centers of symmetry or in reflection planes.

For reflections with $\sin\theta/\lambda$ greater than 0.4 we may with good approximation leave the oxygen contribution out of consideration because of the small scattering power. As the reflections 060,080 and 0.10.0 all are exceptionally strong, it follows that the contributions from potassium and sulphur atoms must be in phase. The potassium and sulphur atoms therefore must all have coordinates zero in direction of the b-axis, or they must all have coordinates $\frac{1}{4}$. The former possibility must be rejected as it cannot account for the great intensity of reflections from planes with odd index k (e.g., 510 and 470). Consequently the potassium and sulphur atoms all lie in the reflection planes; i.e. 2K I in $\pm(u_1\frac{1}{4}v_1)$, 2K II in $\pm(u_2\frac{1}{4}v_2)$, 2S I in $\pm(u_3\frac{1}{4}v_3)$ and 2S II in $\pm(u_4\frac{1}{4}v_4)$.

The contribution from potassium and sulphur to the structure amplitude of a reflection hkl is: a. k even,

$$(-1)^{k/2}2[K[\cos 2\pi(hu_1+lv_1)+\cos 2\pi(hu_2+lv_2)] + S[\cos 2\pi(hu_3+lv_3)+\cos 2\pi(hu_4+lv_4)]]$$

b. k odd,

$$(-1)^{(k+1)/2}2[K[\sin 2\pi(hu_1+lv_1)+\sin 2\pi(hu_2+lv_2)] + S[\sin 2\pi(hu_3+lv_3)+\sin 2\pi(hu_4+lv_4)]]$$

It is seen from these expressions that, except for the decrease in scattering power with increasing k, the contribution from potassium and sulphur is the same for reflections $h0l$, $h2l$, $h4l$ . . . with constant h and l, and also for reflections $h1l$, $h3l$, $h5l$ . . . If the oxygen atoms have no effect, or if they are lying all in the reflection planes, the intensities of reflection in the series $h0l$, $h2l$, $h4l$ . . . and $h1l$, $h3l$, $h5l$ . . . will decrease regularly with increasing k. This is not the case as the observations of Table III definitely show. In order to account for the great deviations from such a regular decrease it becomes necessary to put two sets of four oxygen atoms in general positions; i.e.,

$$4\text{ O I in }\pm(x_1y_1z_1)\pm(x_1\tfrac{1}{2}-y_1z_1)$$
$$4\text{ O II in }\pm(x_2y_2z_2)\pm(x_2\tfrac{1}{2}-y_2z_2).$$

At this stage of the investigation it is hardly possible to decide with any degree of certainty whether the two remaining oxygen atoms are situated in centers of symmetry or in reflection planes. This question we will therefore try to settle later (see page 929).

5. Determination of Parameters for Oxygen Atoms in General Positions

The observed intensities for the different $0k0$ reflections are given in Table II. The structure amplitudes are as follows (neglecting the contribution from the oxygen atoms in twofold positions).

TABLE II. *Reflections* 0*k*0.*

0*k*0:	020	040	060	080	0.10.0
$\sin\theta/\lambda$:	0.1616	0.3231	0.4847	0.6462	0.8078
Int. obs.:	vs	vs	ms	w	w−

TABLE III. *Prominent differences in intensity due to oxygen contribution.*

*h*0*l*	001 vw	002 vs	20$\bar{1}$ nil	201 vs	300 vs	103 nil	40$\bar{3}$ nil	10$\bar{5}$ w
*h*2*l*	021 wm	022 vw	22$\bar{1}$ vs	221 nil	320 w	123 w	423 m	125 s
*h*4*l*	041 vvw	042 w	24$\bar{1}$ w	241 w	340 m	143 vvw	443 vw	145 m
*h*1*l*	210 vs	013 ms	212 m−	11$\bar{4}$ w	410 w			
*h*3*l*	230 w	033 w−	232 nil	13$\bar{4}$ s	430 m			
*h*5*l*	250 m	053 w			450 vw			

* In this table and in subsequent tables the intensities are indicated in the order vvs, vs, s, ms, mw, w, vw, vvw, and nil. (v = very, s = strong, m = medium, w = weak).

$$(-1)^{k/2}(4K + 4S) + 4O(\cos 2\pi k y_1 + \cos 2\pi k y_2).$$

If the general decrease of intensity with increasing glancing angle is taken into consideration it becomes apparent that the fourth, sixth and tenth order are exceptionally strong reflections, whereas the second and eighth are relatively weak. These observations are explained if we choose:

$$2\pi y_1 = 20^\circ \qquad 2\pi y_2 = 20^\circ.$$

We will next try to fix the parameters x_1 and x_2 by making use of the observed intensities for reflections *hk*0 complied in Table IV. The structure amplitude for these reflections takes the form:

a. k even,

$$(-1)^{k/2}2[K[\cos 2\pi h u_1 + \cos 2\pi h u_2] + S(\cos 2\pi h u_3 + \cos 2\pi h u_4)] + 4O\cos k20^\circ[\cos 2\pi h x_1 + \cos 2\pi h x_2]$$

b. k odd,

$$(-1)^{(k+1)/2}2[K(\sin 2\pi h u_1 + \sin 2\pi h u_2) + S(\sin 2\pi h u_3 + \sin 2\pi h u_4)] - 4O\sin k20^\circ[\sin 2\pi h x_1 + \sin 2\pi h x_2].$$

From considerations of the relative intensities of reflections *h*00, *h*20, *h*40 . . . and of reflections *h*10, *h*30, *h*50 . . . the following conclusions as to the magnitude of $\cos 2\pi h x_1 + \cos 2\pi h x_2$ and of $\sin 2\pi h x_1 + \sin 2\pi h x_2$ can be drawn:

	$\cos 2\pi h x_1 + \cos 2\pi h x_2$	$\sin 2\pi h x_1 + \sin 2\pi h x_2$
$h = 1$	very small	small
2	medium small	very large
3	large	very small
4	large	medium large
5	small	large
6	medium small	small
7	large	small

Because of the space group symmetry, we may arbitrarily choose the parameter x_1 such that $0^\circ < 2\pi x_1 < 90^\circ$. The large value of $\sin 2\pi 2x_1 + \sin 2\pi 2x_2$ indicates parameters close to 45° and 225°. It is easily deduced from the above list that only the following two sets of parameter values are possible:

$$2\pi x_1 = 25^\circ,\ 2\pi x_2 = 225^\circ;\ \text{or}\ 2\pi x_1 = 45^\circ,\ 2\pi x_2 = 205^\circ.$$

TABLE IV. *Reflections hk*0.

sin θ/λ→				0.0737		0.1474		0.2211		0.2948		0.3685		0.4422		0.5159	
0				100 vvw	6	200 w	−23	300 vs	77	400 vw	−2	500 vvw	10	600 vw−	22	700 w−	−25
0.0808	010	nil	0	110 m	32	210 vs	−80	310 vvw	12	410 w	40	510 m	−50	610 w−	−24	710 nil	15
0.1616	020	vs	−75	120 vw	3	220 m	44	320 w	−39	420 w−	−28	520 vw	−7	620 w−	−36	720 nil	0
0.2423	030	nil	0	130 vw	−16	230 w	26	330 vw	−13	430 m	−49	530 w−	29	630 w−	30		
0.3231	040	vs	86	140 nil	3	240 w−	−24	340 m−	45	440 nil	15	540 vvw	8	640 vw−	27		
0.4039	050	nil	0	150 vw	19	250 m	−56	350 nil	6	450 vw	25	550 w	−48				
0.4847	060	ms	−73	160 nil	−4	260 vw	15	360 w−	−39	460 nil	−7	560 nil	−8				
0.5655	070	nil	0	170 vw	−11	270 w−	23	370 nil	−8	470 w	−31	570 vw	25				
0.6462	080	w	40	180 nil	2	280 w−	−20	380 w−	23	480 vvw	17	580 nil	5				
0.7270	090	nil	0	190 nil	10	290 vw	−27	390 vvw	8	490 vw	24	590 vw	−26				
0.8078	0.10.0	w−	−45	1.10.0 nil	−2	2.10.0 vvw	11	3.10.0 w−	−29	4.10.0 nil	−2						

TABLE V. *Reflections 0kl.*

sin θ/λ→				0.0679		0.1357		0.2036		0.2714		0.3393		0.4072		0.4750	
				001 vw	16	002 vs	−61	003 vs	−71	004 w	29	005 w	−17	006 nil	14	007 w	−37
0.0808	010	nil	0	011 m	−28	012 vw	2	013 m	49	014 w	26	015 w	−7	016 nil	5	017 vw−	11
0.1616	020	vs	−75	021 w	−23	022 vw	−12	023 s	−43	024 vvw	4	025 w−	3	026 nil	−19	027 w−	32
0.2423	030	nil	0	031 w	−23	032 nil	5	033 w−	−15	034 w	−32	035 nil	−3				
0.3231	040	vs	86	041 vvw	11	042 w	−19	043 w	41	044 nil	9	045 vw	−9				
0.4039	050	nil	0	051 w	−30	052 nil	−3	053 w	41	054 vw−	16	055 nil	−8				
0.4847	060	ms	−73	061 nil	−7	062 w−	20	063 w	−35	064 nil	−10	065 vvw	10				
0.5655	070	nil	0	071 nil	−3	072 nil	−3	073 vvw	−16	074 vw	−22	075 nil	0				
0.6462	080	w	40	081 nil	8	082 vw	1	083 vw	24	084 nil	−1						
0.7270	090	nil	0	091 nil	−5	092 nil	0	093 vvw	20	094 nil	17						
0.8078	0.10.0	w−	−45	0.10.1 nil	−5	0.10.2 vvw	18	0.10.3 vvw	−27								

These two sets are, however, equally justified as we can derive one from the other; it is therefore immaterial which of the two sets we choose. We therefore take:

$$2\pi x_1 = 25°, \quad 2\pi x_2 = 225°.$$

In order to determine the parameters z_1 and z_2 we proceed in a similar manner. From the observations compiled in Table V for reflections $0kl$ the following results are obtained

	$\cos 2\pi lz_1 + \cos 2\pi lz_2$	$\sin 2\pi lz_1 + \sin 2\pi lz_2$
$l=1$	small	very large
2	very large	very small
3	small	large
4	medium small	medium small
5	small	small
6	very small	very small
7	very small	

It is at once apparent from these conclusions that $2\pi z_1$ and $2\pi z_2$ both must be close to 90°. The most accurate parameter values were found on the basis of our observations for reflections $h0l$, $h2l$, $h4l$ . . . and $h1l$, $h3l$, $h5l$ . . . using the values for x_1 and x_2 which we determined previously. The final results of these calculations are:

$$2\pi z_1 = 85°, \quad 2\pi z_2 = 110°.$$

We are thus in the interesting situation that we have been able to fix the positions of some of the atoms without knowing anything about the arrangement of the rest of the atoms.

6. Determination of Parameter Values for Potassium and Sulphur Atoms

Knowing the oxygen lattice we can from an inspection of the observations on the basis of the expression for the structure amplitude, get definite information about the potassium plus sulphur contribution for each individual reflection.

The difference in scattering power between potassium and sulphur is small, in fact so small that it seems impossible to distinguish a potassium atom from a sulphur atom by means of intensity considerations alone. For a time we will therefore treat the potassium and sulphur atoms as if they were alike and give them a scattering power of $\frac{1}{2}(K+S)$. When we have fixed the positions of all the atoms in the unit cell, we will try to find a method by means of which a distinction can be made.

Let us at first determine the 4 parameters in the direction of the a axis, namely u_1 u_2 u_3 and u_4. For that purpose the observed intensities of reflections $hk0$ have to be used. Having determined the oxygen positions we are able to calculate the contribution of the oxygen atoms to the structure amplitude. We have, for example:

$$300 \quad 2K(S)[\cos 2\pi 3u_1 + \cos 2\pi 3u_2 + \cos 2\pi 3u_3 + \cos 2\pi 3u_4] + 3.88O \quad vs$$

$$320 \quad -2K(S)[\cos 2\pi 3u_1 + \cos 2\pi 3u_2 + \cos 2\pi 3u_3 + \cos 2\pi 3u_4] + 2.99O \quad w$$

$$340 \quad 2K(S)[\cos 2\pi 3u_1 + \cos 2\pi 3u_2 + \cos 2\pi 3u_3 + \cos 2\pi 3u_4] + 0.66O \quad m$$

In order to account for these observations we must have $\cos 2\pi 3u_1 + \cos 2\pi 3u_2 + \cos 2\pi 3u_3 + \cos 2\pi 3u_4$ very large and positive. Proceeding in this manner for all observations in Table IV we get the following conclusions:

	$\cos 2\pi hu_1+\cos 2\pi hu_2+\cos 2\pi hu_3+\cos 2\pi hu_4$	$\sin 2\pi hu_1+\sin 2\pi hu_2+\sin 2\pi hu_3+\sin 2\pi hu_4$
$h=1$	very small	small negative
2	medium large negative	very large positive
3	very large positive	very small
4	medium large positive	large negative
5	very small	large positive
6	medium small positive	medium large
7	medium large	very small

It is our task then to find values of the four parameters which satisfy the above results. This necessarily requires lengthy calculations, but can nevertheless be carried out uniquely. Definite starting points for the calculations are readily found. The very large contribution to the 210 reflection shows definitely that all the parameters lie within the ranges $0-0.25$ $0.50-0.75$. Since the contribution to the reflection 510 also is very large we must look for values in the ranges $0-0.10$ $0.20-0.25$ $0.60-0.70$. By continued calculations of this kind we can eventually find the accurate values. The best agreement was obtained with the following set: $2\pi u_1 = 80°$, $2\pi u_2 = 235°$, $2\pi u_3 = 250°$, $2\pi u_4 = 5°$. No other essentially different set can account for the observations.

The determination of the parameters v_1 v_2 v_3 and v_4 is carried out in the same manner. Besides the observations collected in Table V we are, however,

TABLE VI. *Reflections h0l.*

*h*00	*I*	*F*	*h*01	*I*	*F*	*h*02	*I*	*F*	*h*03	*I*	*F*	*h*04	*I*	*F*	*h*05	*I*	*F*	*h*06	*I*	*F*
600	vw−	22																		
500	vvw	10	501	vvw	−9	502	w	12												
400	vw	−2	401	nil	0	402	w	30	403	w	−14	404	w	−25						
300	vs	77	301	s	−55	302	ms	−66	303	m	38	304	vvw	0	305	w	−34			
200	w	−23	201	vs	−68	202	wm	−39	203	m−	35	204	nil	6	205	w	−37			
100	vvw	6	101	m	30	102	m	−28	103	nil	1	104	w	18	105	m	39	106	vw−	14
			001	vw	16	002	vs	−61	003	vs	−71	004	w	29	005	tw	−17	006	ni	14
$\bar{1}$00	vvw	6	$\bar{1}$01	w	−13	$\bar{1}$02	s	−49	$\bar{1}$03	wm	−27	$\bar{1}$04	w−	−4	$\bar{1}$05	wm	−43	$\bar{1}$06	vw−	−33
$\bar{2}$00	w	−23	$\bar{2}$01	nil	−4	$\bar{2}$02	w	−24	$\bar{2}$03	m	−42	$\bar{2}$04	w	−21	$\bar{2}$05	vw	11	$\bar{1}$06	w	14
$\bar{3}$00	vs	77	$\bar{3}$01	w	10	$\bar{3}$02	ms	−36	$\bar{3}$03	wm	41	$\bar{3}$04	w−	14	$\bar{3}$05	nil	14	$\bar{3}$06	m	60
$\bar{4}$00	vw	−2	$\bar{4}$01	wm	37	$\bar{4}$02	vw	5	$\bar{4}$03	nil	−1	$\bar{4}$04	w	33	$\bar{4}$05	vvw	−3	$\bar{4}$06	vw	−18
$\bar{5}$00	vvw	10	$\bar{5}$01	vw	7	$\bar{5}$02	vw	16	$\bar{5}$03	w	8	$\bar{5}$04	w	−31	$\bar{5}$05	vw	−23			
$\bar{6}$00	vw−	22	$\bar{6}$01	vvw	2	$\bar{6}$02	w	−26	$\bar{6}$03	vvw	1									

now also able to utilize the observed intensities of reflections *hkl*. From detailed calculations it can be shown that there is only one set of values which can satisfactorily account for the observations, namely the following:

$$2\pi v_1 = 340°,\ 2\pi v_2 = 240°,\ 2\pi v_3 = 80°,\ 2\pi v_4 = 115°.$$

7. Determination of Parameters for Oxygen Atoms in Twofold Positions

The effect on the intensity of the oxygen atoms in twofold positions we have so far left out of consideration. This effect is small because there are only two of these atoms and because their scattering power is small. However it is certainly large enough to be detected at small values of $\sin\theta/\lambda$. The parameters which we already have determined must be very accurate as there is a satisfactory agreement between observed and calculated intensities even for reflections corresponding to very large $\sin\theta/\lambda$.

If therefore discrepancies exist at small values of $\sin\theta/\lambda$, they cannot be accounted for by changes in the parameter values, and must consequently be attributed to the effect of the two oxygen atoms. In Table VII are seen a number of such discrepancies.

TABLE VII. *Calculated amplitudes without contributions from oxygen atoms in twofold positions.*

*h*0*l*	*I*	*F*	*h*1*l*	*I*	*F*	*h*2*l*	*I*	*F*	*h*3*l*	*I*	*F*
001	vw	0	011	m	−26	021	m	−13	031	wm	−24
100	vvw	14	110	m	19	120	vw	−4	130	w	−8
101	w	−3	11$\bar{1}$	nil	−10	12$\bar{1}$	w−	9	13$\bar{1}$	nil	7
101	m	27	111	vs	−67	121	nil	0	131	s	40
002	vs	−74	012	vw	6	022	vw	−3	032	nil	−8
102	s	−39	112	vs	−84	122	s	41	132	vs	78
200	w	−17	210	vs	−68	220	m	39	230	wm	19
20$\bar{1}$	nil	1	21$\bar{1}$	w	32	21$\bar{1}$	vs	64	23$\bar{1}$	nil	−6
102	m	30	112	vvw	−20	122	s	−58	132	vvw	1
201	vs	−61	211	w	−19	221	nil	−3	231	vw	8
202	w	−22	212	w−	20	222	w	−20	232	w	16
103	wm	−17	113	nil	−5	123	nil	−15	133	nil	8

For example, the calculated structure amplitude for the 100 reflection is too large, while it is too low for 110 and 120. The fact that discrepancies occur for reflections with odd k shows that the two oxygen atoms must lie in the reflection planes, i.e., $\pm(u_5\tfrac{1}{4}v_5)\cdot\cos 2\pi u_5$ and $\sin 2\pi u_5$ must be negative in order to explain the discrepancies mentioned; consequently $2\pi u_5$ must lie between 180° and 270°. The calculated structure amplitudes for the reflections 001, 011, 021 are all too low; $2\pi v_5$ must therefore lie between 0° and 90°. Detailed calculations of this kind give as result the accurate values:

$$2\pi u_5 = 240°,\quad 2\pi v_5 = 10°.$$

8. The Final Parameter Values

We have thus been able to determine all the 16 parameters in the structure on the basis of observed intensities alone. From careful considerations an accuracy of ± 0.01 can be claimed for all values except u_5 and v_5. For the latter parameters the accuracy is of the order ± 0.03. I wish to emphasize that the determination is unique; no other set of parameter values essentially different from the one given can account for the observed intensities. The agreement between observation and calculation no doubt can be slightly improved at large values of $\sin\theta/\lambda$ by minute changes in the parameter values within the limits given. No weight can be given to minor discrepanices due to the fact that the scattering power may be different in different directions from lack of spherical symmetry.

As previously stated we cannot distinguish between a potassium and a sulphur atom by means of intensity considerations alone. A large number of atomic arrangements containing potassium and oxygen atoms are known with great accuracy. The closest distance ever observed between potassium and oxygen atoms is of the order 2.7A. In the potassium pyrosulphite structure the atoms with coordinates u_1v_1 and u_2v_2 all have distances from adjacent oxygen atoms greater than 2.69A, whereas the atoms with coordinates u_3v_3

and u_4v_4 have distances from oxygen atoms as low as 1.45 and 1.44A. It is therefore reasonable to conclude that the former atoms are potassium, the latter sulphur.

The structure amplitudes calculated on the basis of the determined parameter values and with the proper F curve values are given in the Table IV, V, VI and VIII.

TABLE VIII. *Reflections hkl.* I is observed intensity; F is the calculated structure amplitude.

$\sin\theta/\lambda$	$h0l$	I	F	$h1l$	I	F	$h2l$	I	F	$h3l$	I	F	$h4l$	I	F
0.0679	001	vw	16	011	m	−28	021	m	−23	031	wm	−23	041	vvw	11
0.0737	100	vvw	6	110	m	32	120	vw	3	130	w	−16	140	vvw	3
0.0885	10$\bar{1}$	w	−13	11$\bar{1}$	nil	−1	12$\bar{1}$	w−	17	13$\bar{1}$	nil	0	14$\bar{1}$	w	−9
0.1106	101	m	30	111	vs	−55	121	nil	4	131	s	32	141	vw	7
0.1357	002	vs	−61	012	vw	2	022	vw	−12	032	nil	5	042	w	−19
0.1395	10$\bar{2}$	s	−49	11$\bar{2}$	vs	−76	12$\bar{2}$	s	49	13$\bar{2}$	vs	73	14$\bar{2}$	ms	−35
0.1474	200	w	−23	210	vs	−80	220	m	44	230	wm	26	240	w	−24
0.1481	20$\bar{1}$	nil	−4	21$\bar{1}$	w	20	22$\bar{1}$	vs	67	23$\bar{1}$	nil	1	24$\bar{1}$	w	−25
0.1680	102	m	28	112	vvw	−9	122	s	−56	132	vvw	−7	142	m−	31
0.1752	201	vs	−68	211	w	−27	221	nil	3	231	vw	14	241	w	−25
0.1770	20$\bar{2}$	w	−24	21$\bar{2}$	w−	9	22$\bar{2}$	w	−19	23$\bar{2}$	w	23	24$\bar{2}$	nil	1
0.2007	10$\bar{3}$	wm	−27	11$\bar{3}$	nil	0	12$\bar{3}$	nil	−7	13$\bar{3}$	nil	5	14$\bar{3}$	nil	−1
0.2036	003	vs	−71	013	ms	49	023	s−	−43	033	w−	−15	043	m	41
0.2165	30$\bar{1}$	w	10	31$\bar{1}$	m−	40	32$\bar{1}$	vw−	−6	33$\bar{1}$	w	−24	34$\bar{1}$	vw−	5
0.2211	300	vs	77	310	vvw	12	320	wm	−39	330	vw	−13	340	m	45
0.2212	202	wm	−39	212	m−	35	222	w	31	232	nil	−5	242	vw	−25
0.2235	20$\bar{3}$	m	−42	21$\bar{3}$	w−	−15	22$\bar{3}$	vw	−5	23$\bar{3}$	vw−	−12	24$\bar{3}$	vvw	−11
0.2312	103	nil	1	113	w	16	123	w	−24	133	vvw	7	143	vvw	10
0.2326	302	ms	−36	312	s	47	322	m	28	332	m	−38	342	w	−28
0.2451	301	s	−55	311	vw	−9	321	m	35	331	vw−	−11	341	m	−37
0.2651	10$\bar{4}$	w−	−4	11$\bar{4}$	w	25	12$\bar{4}$	vvw	0	13$\bar{4}$	s	−44	14$\bar{4}$	vvw	0
0.2655	30$\bar{3}$	wm	41	31$\bar{3}$	w−	13	32$\bar{3}$	wm	−38	33$\bar{3}$	vw−	−5	34$\bar{3}$	w	29
0.2714	004	w	29	014	w	26	024	nil	4	034	w	−32	044	nil	9
0.2763	203	m−	35	213	s	−51	223	vw	−4	233	m	42	243	w	17
0.2790	20$\bar{4}$	w	−21	21$\bar{4}$	wm	40	22$\bar{4}$	m	58	23$\bar{4}$	wm	−52	24$\bar{4}$	w	−31
0.2837	302	ms	−66	312	vw−	7	322	w−	26	332	nil	6	342	wm	−39
0.2876	40$\bar{1}$	wm	37	41$\bar{1}$	m	37	42$\bar{1}$	nil	−4	43$\bar{1}$	m	−49	44$\bar{1}$	vw	15
0.2948	400	vw	−2	410	wm	40	420	w−	−28	430	m	−49	440	nil	15
0.2962	40$\bar{2}$	vw	5	41$\bar{2}$	m−	−32	42$\bar{2}$	w−	23	43$\bar{2}$	m	53	44$\bar{2}$	nil	−8
0.2964	104	w	18	114	nil	−16	124	w	22	134	w−	26	144	nil	−4
0.3101	30$\bar{4}$	w−	14	31$\bar{4}$	nil	−2	32$\bar{4}$	w	−29	33$\bar{4}$	nil	−1	34$\bar{4}$	w−	17
0.3167	401	nil	0	411	nil	−3	421	vvw	−15	431	w−	18	441	nil	6
0.3193	40$\bar{3}$	nil	−1	41$\bar{3}$	vw	−7	42$\bar{3}$	m	−41	43$\bar{3}$	w	20	44$\bar{3}$	vw	19
0.3310	10$\bar{5}$	wm	−43	115	w−	−17	12$\bar{5}$	s	73	13$\bar{5}$	w−	16	14$\bar{5}$	m	−50

TABLE IX. *Final parameter values.*

Atoms	In angular measure			In fractions of cell dimensions		
	$2\pi x$	$2\pi y$	$2\pi z$	x	y	z
K I	80°	90°	340°	0.22	0.25	0.95
K II	235°	90°	240°	0.65	0.25	0.67
S I	250°	90°	80°	0.70	0.25	0.22
S II	5°	90°	115°	0.01	0.25	0.32
O I	25°	20°	85°	0.07	0.06	0.24
O II	225°	20°	110°	0.63	0.06	0.31
O III	240°	90°	10°	0.67	0.25	0.03

In Table IX are listed the final parameter values, expressed in angular measure and in fractions of the cell dimensions.

9. Discussion of the Atomic Arrangement

A projection of the atomic arrangement on the 010 face is reproduced in Fig. 1.

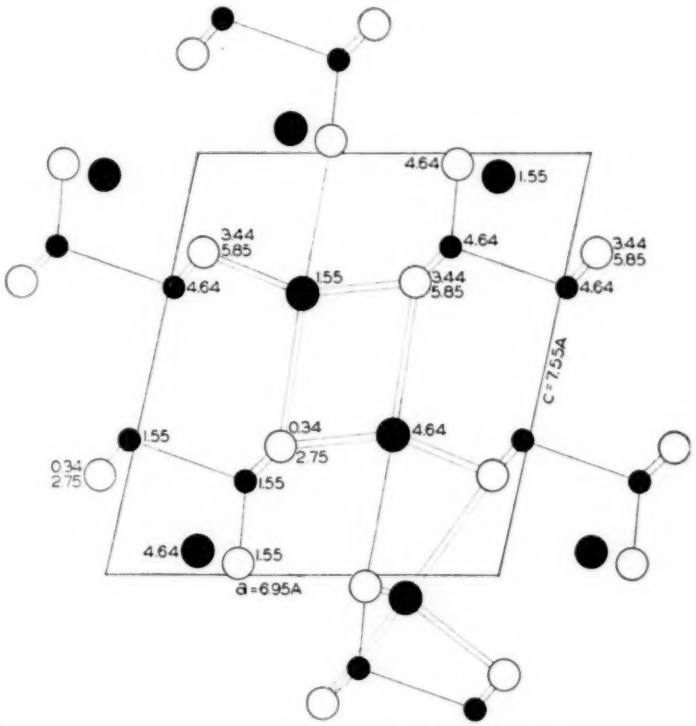

Fig. 1. The atomic arrangement projected on the *b* face. Large open circles represent oxygen atoms, large filled circles represent potassium atoms and small filled circles represent sulphur atoms. The attached numbers give the heights of the atoms above the projection plane expressed in *A*. Only some of the potassium to oxygen bonds are drawn.

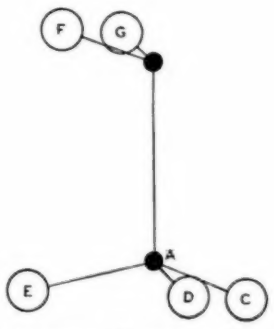

Fig. 2. The pyrosulphite group. Atoms denoted *A* and *B* are sulphur atoms, atoms denoted *CDEFG* are the oxygen atoms.

A potassium atom of the first kind (K I) is surrounded by nine oxygen atoms at approximately the same distance. There are two O I atoms at a distance of 2.88A, two O I atoms at 2.91A, two O II atoms at 3.02A, two O III

atoms at 3.21A and one O III atom at 3.01A. The average distance K I–O is 3.01A.

A potassium atom of the second kind (K II) is surrounded by seven oxygen atoms at an average distance of 2.78A. There are two O I atoms at 2.69A, two O II atoms at 2.74A, two O II atoms at 2.95A and one O III atom at 2.71A.

The fact that the average distance K I–O is greater than the average distance K II–O is in agreement with the empirical result that the interatomic distance increases with increasing coordination number. The distances K–O calculated for cordination numbers 9 and 7 from ionic radii published by the author are 2.93A and 2.85A,[4] against the values 3.01A and 2.78A observed.

The structure found for the pyrosulphite group is of exceptional interest. A drawing of the group is reproduced in Fig. 2. We may most conveniently describe the radical as consisting of a sulphite group and a sulphur dioxide molecule with a bond between the two sulphur atoms. The structural formula consequently has to be written as

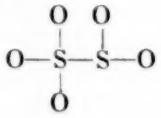

whereas the formula given by the chemists:

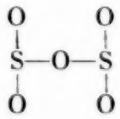

is incorrect.

The distances within the S_2O_5 group are: (the lettering referring to Fig. 2):

S I–S II	(*A–B*)	2.18A	O I–O I	(*F–G*)	2.41A
S I–O II	(*A–C, A–D*)	1.49A	O II–O II	(*C–D*)	241A
S I–O III	(*A–E*)	1.44A	O II–O III	(*C–E, D–E*)	2.49A
S II–O I	(*B–F, B–G*)	1.45A			

The angles between the four bonds of S I are: ($\sphericalangle BAC$ and $\sphericalangle BAD$) 105°, ($\sphericalangle CAD$) 108°, ($\sphericalangle CAE$ and $\sphericalangle DAE$) 116½°, ($\sphericalangle BAE$) 104°.

The angles between the three bonds of S II are: ($\sphericalangle FBG$) 112°, ($\sphericalangle ABF$ and $\sphericalangle ABG$) 102°.

The closest distance between oxygen atoms belonging to different pyrosulphite groups is greater than 3.4A, in harmony with predictions made by the author.[4] A further indication of the stability of the crystal lattice is the large distance between potassium atoms and between a potassium atom and a sulphur atom.

The reason for the observed cleavage parallel to the 001 face (the $10\bar{1}$ face according to Groth's axes) is obvious from Fig. 1. There are only four potassium to oxygen bonds per $42A^2$ of surface crossing the 001 face. The reported twinning after the $10\bar{1}$ face is due to the fact that the perpendicular to the twinning plane is a pseudo-twofold axis.

[4] W. H. Zachariasen, Zeitschr. f. Krist. **80**, 137 (1931).

The atomic arrangement is too complicated to allow a calculation of the optical properties. The acute bisectrix lies very nearly perpendicular to the connection line between sulphur atoms in the (S_2O_5) groups.

10. The Relations Between the Structure of the Pyrosulphite Group and that of Other Sulphur Oxygen Groups

The structures of the sulphate group,[5] the sulphite group[6] and the dithionate group[7] have been determined previously. The angles between the bonds are in all cases close to the tetrahedral angle ($109\frac{1}{2}°$). According to ideas presented by Pauling[8] and Slater[9] the angle between bonds which can be ascribed to p electrons tends to be 90°. If, however, the p and s eigenfunctions have lost their individuality due to the perturbations, the angles between the bonds will tend to be $109\frac{1}{2}°$.

All the groups $(S_mO_n)^{-2}$ can be interpreted by means of single electron pair bonds. Closed shells of four electron pairs are then formed around every atom in the group. The structure of the pyrosulphite group represented in two dimensions will be.:

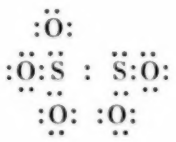

If we remove an oxygen atom in the dithionate group without altering the arrangement of the remaining atoms, we get the structure of the pyrosulphite group. In the pyrosulphite group the four atoms $ACDE$ of Fig. 2. give us an $(SO_3)^{-2}$ group of practically the same shape and dimensions as was found in the crystal lattice of Na_2SO_3. Analogously we would expect the three atoms BFG of Fig. 2 to represent the structure of the group $(SO_2)^{-2}$. The atoms AB give us an $(S_2)^{-2}$ group practically the same as found in FeS_2. Also the groups $(S_2O_2)^{-2}$, $(S_2O_3)^{-2}$ and $(S_2O_4)^{-2}$ can be represented by Fig. 2 if we remove some oxygen atoms. We do not know, however, which of the oxygen atoms we must remove. For example we can get two models for the structure of the $(S_2O_3)^{-2}$ group, either the atoms $ABCDE$ or the atoms $ABCDF$.

However, predictions of this kind need experimental verification. Investigations on the structure of other groups formed by sulphur and oxygen have been started in this laboratory.

[5] E.g., W. H. Zachariasen and G. E. Ziegler, Zeitschr. f. Krist. **81**, 92 (1931).
[6] W. H. Zachariasen and H. E. Buckley, Phys. Rev. **37**, 1295 (1931).
[7] M. L. Huggins, and Glenn O. Frank, Amer. Min. **16**, 580 (1931).
[8] L. Pauling, J. Amer. Chem. Soc. **53**, 1367 (1931).
[9] J. C. Slater, Phys. Rev. [2], **37**, 481 (1931).

Some Factors Involved in the Disappearance of Hydrogen in the Presence of Potassium or Lithium Ion Sources

By C. H. KUNSMAN AND R. A. NELSON
Fertilizer and Fixed Nitrogen Investigations Bureau of Chemistry and Soils, U. S. Department of Agriculture, Washington, D. C.

(Received April 26, 1932)

The rate of clean up of hydrogen was observed on potassium and spodumene glass surfaces, sources of K and Li ions respectively. Although there has been considerable difference of opinion as to the nature of this disappearance of hydrogen, i.e., whether it is a surface or gas phase reaction, our results show that the entire effect can be accounted for by a reaction on or within the hot glass, very likely the formation of water vapor.

CONSIDERABLE interest has recently been shown in the relative activity of positive ions and electrons in activation and chemical reaction. The experiments to be reported are concerned with the disappearance or clean up of gases in connection with hot surfaces used as positive ion sources and were conducted in the same manner as the recent experiments of Leipunsky and Schechter[1] and Mitchell.[2]

In the various experiments positive thermions of lithium, potassium or caesium were accelerated toward a collector with speeds up to 400 volts in a chamber containing hydrogen and immersed in liquid air. The disappearance of hydrogen was measured as a function of the positive ion current and speed of the positive ions. Leipunsky and Schechter used a platinum strip coated with an iron-aluminum-potassium oxide mixture and reported a clean up corresponding to 10 molecules of hydrogen per lithium ion at 125 volts to 1000 molecules of hydrogen per potassium ion at 270 volts, and observed some critical potentials.

Mitchell found an initial rate of decrease in the pressure of hydrogen due to the hot filament alone and an increased rate of decrease in pressure when lithium and caseium ions from spodumene and pollucite, respectively, left the surface and bombarded the hydrogen gas with from 15 to 320 volts speed. In this case the number of hydrogen molecules disappearing per positive ion varied from 0.01 to 0.5. The hydrogen clean up was independent of the voltage and no critical potentials were observed.

Although some of our preliminary experiments were carried out on supported iron-aluminum-potassium oxide surfaces, effective catalysts for ammonia synthesis, most of the work was done on glass coated filaments illustrated in Fig. 1. This source of positive ions has been previously described.[3] Either potassium glass or spodumene was drawn in the form of a tube and

[1] Leipunsky and Schechter, Zeits. f. Physik **59**, 857 (1930).
[2] Mitchell, J. Frank. Inst. **210**, 269 (1930).
[3] Cottrell, Kunsman and Nelson, Rev. Sci. Instr. **1**, 654 (1930).

sealed onto a platinum or tungsten core and mounted as the anode in a vacuum tube. The outer surface of the anode was coated by sputtering with a thin coating of platinum. This platinum coating was earthed or kept at

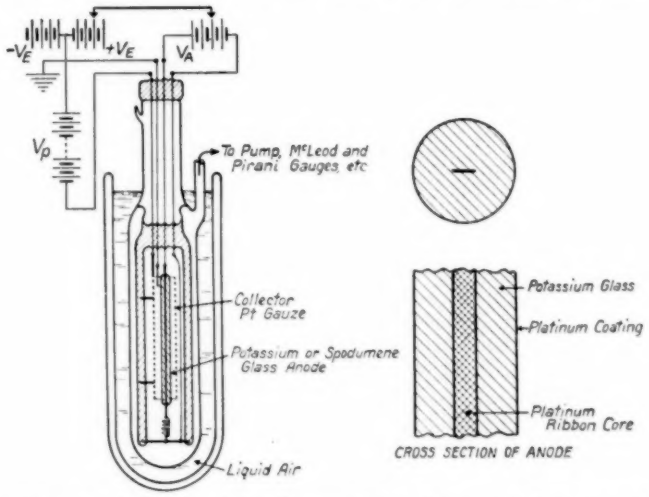

Fig. 1. Apparatus for the study of the disappearance of gases on glass coated filaments.

zero potential and a source of potential that could be varied applied to one end of the filament. With a current flowing through the core sufficient to heat the anode to a dull red temperature, an electrolytic potential will drive

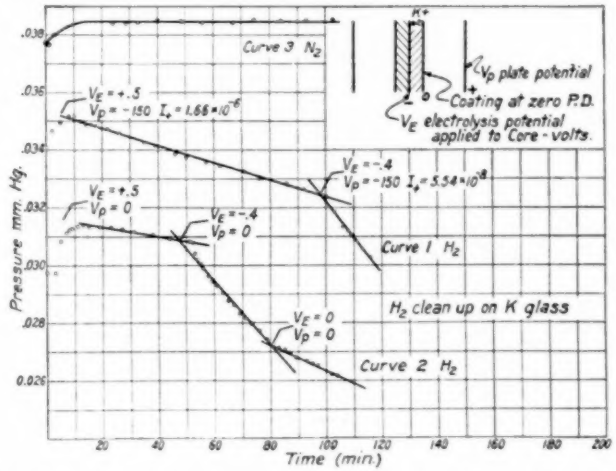

Fig. 2. H_2 clean up and arrangement of potentials with a potassium glass filament.

the potassium or lithium ions either to the core or to the platinum coated surface depending on the direction of the applied potential. The hot anode surface was about $2\frac{1}{2}$ cm². The positive ions were drawn from the surface through the hydrogen to the platinum gauze collector by placing a suitable potential on the latter. This source of ions has the advantage that at a given

temperature the positive ion current can be varied through wide limits. The volumes of the bulbs immersed in liquid air varied from about 200 cc to 250 cc. By means of the Pirani gauge 0.07 percent change in pressure could be detected between 0.01 mm and 0.1 mm, the pressure range studied. This was 30 to 100 times as sensitive as the McLeod gauge.

Fig. 2 gives the results for a potassium glass filament, a source of K^+ ions. In the upper right hand corner of the figure the arrangement of potentials to the elements of the tube is shown. As V_E is varied from positive to negative the K^+ ion current is decreased, so that the electrolytic decomposition of the glass and direction of mobility of the K^+ ions can be varied at will. The results of these curves show that for nitrogen (curve 3) there is no decrease in pressure or disappearance of gas whatsoever. Curve 1 for hydrogen shows an increase in the rate of decrease of the hydrogen pressure as the positive

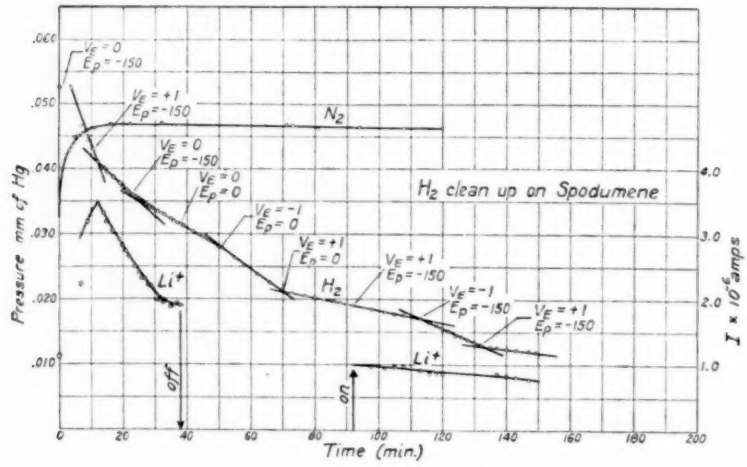

Fig. 3. H_2 clean up, lithium ion currents and potentials with a spodumene glass filament.

ion current is decreased or as K^+ is kept from going to the surface and entering the gas phase at 150 volts speed. In curve 2, $V_p = 0$, that is, no ions enter the gas phase and therefore no gas phase reaction takes place, the reaction of hydrogen clean up taking place on or within the hot surface. Curves 1 and 2 are practically identical and there is no indication in this or any similar test that the K^+ ions entering the hydrogen gas contributed a measurable amount to the decrease in the pressure of hydrogen. Our explanation of these results is that K^+ from K_2SiO_3 is electrolyzed through the glass, away from the surface and toward the core, leaving the SiO_3 ion temporarily free. Hydrogen soon replaces potassium giving H_2SiO_3, which decomposes to SiO_2 and H_2O. Thus what actually takes place is the formation of water vapor on the hot surface. Fig. 3 shows similar results for a spodumene filament, a Li^+ source. This curve is typical of a complete run starting with a new filament at room temperature. A period of approximately 25 minutes was required to reach a stable condition of temperature and surface in equilibrium with hydrogen. The factors concerned during this initial period are not too

well known. After this initial period the clean up of hydrogen is independent of the lithium ions entering the gas phase, and depends on the rate of electrolysis of lithium away from the surface toward the core. A similar reaction resulting in the formation of water vapor accounts for these results. Taylor[4] has advanced this explanation in connection with experiments on the clean up of hydrogen at glass surfaces under the influence of an electric discharge. Some study was made of the condensible products of the reaction. Of the hydrogen cleaned up about one half disappeared completely, the other half behaved like water vapor in that it was condensed at $-65°$ to $-75°$C at these pressures.[5] The part that disappeared completely could be accounted for by its adsorption as water vapor on the walls of the glass vessel. No effort was made to recover this by a heating of the glass bulb.

In none of our experiments was there an indication of a gas phase reaction between the alkali ions and hydrogen. By varying the electrolysis potential through the hot glass, rates were obtained comparable to those of Leipunsky and Schechter or Mitchell, calculated on the basis of hydrogen disappearing per alkali ion. The proportionality between positive ion currents and clean up observed by Mitchell was probably due to the fact that every alkali ion leaving the surface was replaced by hydrogen. Preliminary results on the iron-aluminum-potassium oxide catalysts indicate a decrease in hydrogen pressure, depending on the extent to which the catalyst oxide mixture was reduced, and on complete reduction there was no further clean up. It therefore appears that a calculation of the hydrogen disappearance on the basis of positive ions entering the gas phase is not tenable, but that a surface reaction, very likely the formation of water, was the controlling factor in these experiments.

[4] J. Taylor, Proc. Roy. Soc. **A123,** 252 (1929).
[5] N. R. Campbell, Proc. Phys. Soc. London **33,** 287 (1921)

Effects of Temperature and Nitrogen Pressure on the Afterglow of Mercury Resonance Radiation

By E. W. Samson
Palmer Physical Laboratory, Princeton University

(Received April 26, 1932)

Measurements have been made of the rate of decay of the λ2537 afterglow from an optically excited quartz cell containing 0.00236 mm of mercury vapor, and pressures of nitrogen ranging from 0.5 mm to 100 mm, at temperatures of 301°, 374°, and 486°K. The work was done with a rotating disk phosphoroscope so designed that two traces representing the decay of the afterglow were recorded on a photographic plate. Very pure nitrogen was necessary in order to obtain consistent results. The exponential decay constants ranged from 300 to 12,900 sec.$^{-1}$. A striking result was a very rapid increase of the decay coefficient with rise of temperature at high pressures. The rate of decay depends on the rates at which collisions with nitrogen molecules cause transitions of the mercury atom back and forth between the 2^3P_0 and 2^3P_1 states and possibly from either of these states to the normal state, on the rate of diffusion of metastable 2^3P_0 atoms to the walls of the vessel where they are reduced, and on the imprisonment of λ2537 radiation by successive absorptions and re-emissions of quanta before they escape from the cell. This latter factor depends on the frequency shape of the radiation emission and absorption coefficients and the geometry of the cell. It introduces such great mathematical difficulties into the theory that a rigorous solution for the decay constant in terms of conditions and atomic properties is not attempted here, but an approximate solution is given which, it is believed, considers all the important processes, is in excellent accord with the experimental results, and renders possible their interpretation in terms of *effective cross-sections*. From this theory and data the *effective temperature cross-sections* of excited mercury atoms for collisions with nitrogen molecules which give rise to energy transitions in the mercury atom were found to be, in the sense in which they are defined in this paper, independent of temperature in the range from 300°K to 500°K, and their mean values are:
for

$$^3P_0 \rightarrow {}^3P_1 \quad \sigma_0^2 = 6.7 \times 10^{-18} \text{ cm}^2$$
$$^3P_1 \rightarrow {}^3P_0 \quad \sigma_1^2 = 3.1 \times 10^{-17} \text{ cm}^2$$
$$^3P_1 \rightarrow {}^1S_0 \quad \Sigma_1^2 \leqq 2.2 \times 10^{-18} \text{ cm}^2$$
$$^3P_0 \rightarrow {}^1S_0 \quad \Sigma_0^2 \leqq 2.0 \times 10^{-22} \text{ cm}^2 \text{ roughly.}$$

The diffusion cross section for metastable atoms increases very slowly with temperature. The values found are 15.5×10^{-16}, 17.7×10^{-16}, and 18.4×10^{-16} cm^2 respectively at 301°, 374° and 486°K.

I. Introduction

EXPERIMENTS of R. W. Wood[1] on the fluorescence and absorption in a mercury resonance lamp excited by a mercury arc with and without other gases in the lamp showed distinctly that $^3P_0$ metastable mercury atoms were produced in large numbers when nitrogen was introduced at a few millimeters pressure. Stuart's[2] measurements of the quenching of fluorescence resonance radiation by foreign gases, including nitrogen, indicated that the number of $^3P_1$ atoms was reduced by collisions of the second kind with the

[1] Wood, Phil. Mag. **50,** 774 (1925); Phil. Mag. **4,** 446 (1927).
[2] Stuart, Zeits. f. Physik. **32,** 262 (1925).

foreign gas molecules. Asada, Ladenburg and Tietze,[3] and Asada[4] showed by a fluorescence and phosphoroscopic method that $^3P_0$ metastable atoms remain in the resonance lamp when nitrogen is present for almost one hundredth of a second. Zemansky,[5] in mercury vapor alone, by a phosphoroscopic method, measured the rate at which the re-emission of λ2537 died down after the exciting light was cut off, found that its decay rate was exponential, and too slow to be accounted for by imprisonment of the radiation by absorptions and re-emissions. He measured the decay constant as a function of mercury vapor pressure. He later[6] explained the curves by assuming that the long lifed $^3P_0$ metastable atoms are raised to the $^3P_1$ state on collision with other atoms, and that excited atoms diffuse to the walls, and are there reduced. Experiments on the lifetimes of rare gas atoms by Dorgelo and Washington,[7] Meissner and Graffunder,[8] Eckstein,[9] and Ebbinghaus,[10] also show that diffusion to the walls and collisions with other atoms serve to reduce metastable atoms.

Dorgelo[11] observed that rise of temperature decreased the lifetimes of metastable neon and mercury atoms, and explained the effect qualitatively as due to collisions. Cario and Franck[12] measured the quenching of mercury resonance radiation by nitrogen, by hydrogen, and by mixtures of the two at 750°C and at ordinary temperatures. It was found that nitrogen did not quench the radiation, that hydrogen did, and that adding nitrogen to hydrogen increased the quenching at the high temperature, while at low temperature both nitrogen and hydrogen quench and their effects are additive. These phenomena they explained very beautifully in a qualitative way on the basis of diffusion of metastable atoms to the walls, interchange between $^3P_0$ and $^3P_1$ states of mercury by collisions with nitrogen, and reduction of $^3P_0$ or $^3P_1$ atoms to the normal state by collisions with hydrogen, and rapid increase of the number of $^3P_0 \rightarrow {}^3P_1$ transitions on collision with nitrogen because many more collisions would have the required 0.218 electron-volts of relative kinetic energy at high temperatures.

An interesting early paper by Foote[13] which attempted to interpret Stuart's quenching curves, gave a clear exposition of the processes involved in such experiments, and included absorption and re-emission of the radiation, but omitted reduction of excited atoms at the walls, which is important.

The present research was undertaken with the object of determining how the collision processes for excited mercury atoms with nitrogen molecules are

[3] Asada, Ladenburg and Tietze, Phys. Zeits. **29,** 549 (1928).
[4] Asada, Phys. Zeits. **29,** 708 (1928).
[5] Zemansky, Phys. Rev. **29,** 513 (1927).
[6] Zemansky, Phys. Rev. **34,** 213 (1929).
[7] Dorgelo and Washington, Kon. Ak. v. Wet. Amst. **35,** 1009 (1926).
[8] Meissner and Graffunder, Ann. d. Physik **84,** 1009 (1927).
[9] Eckstein, Ann. d. Physik **87,** 1003 (1928).
[10] Ebbinghaus, Ann. d. Physik **7,** 267 (1930).
[11] Dorgelo, Physica **5,** 429 (1925).
[12] Cario and Franck, Zeits. f. Physik **37,** 619 (1926).
[13] Foote, Phys. Rev. **30,** 288 (1927).

affected by temperature. The method chosen was phosphoroscopic observation of the rate of decay of the λ2537 afterglow due to $^3P_1$ atoms produced by collisions, after the cutting off of optical excitation, over a range of temperatures and nitrogen pressures.

To account for the results and interpret them quantitatively it was found necessary to evolve a more comprehensive theory than any hitherto given, of the processes influencing the rate of decay. Since the theory is complicated it is perhaps best to describe the experiments, show that the results fit the derived formula over a large range of measurements, and evaluate the empirical constants, before proceeding to discuss the theory and the interpretation of the constants in terms of atomic properties.

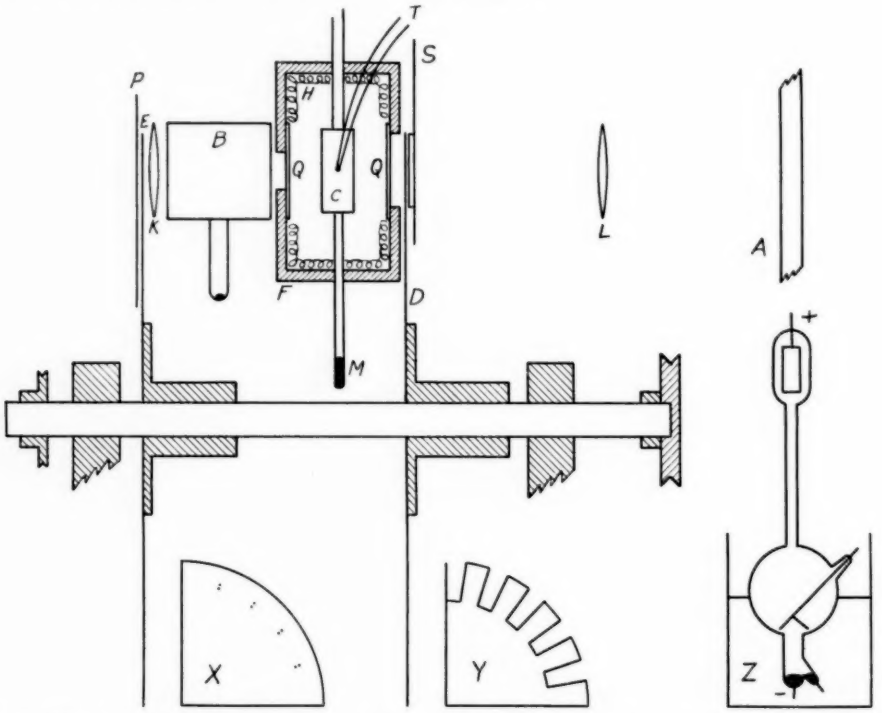

Fig. 1. The measuring apparatus. Insets: *X*—quadrant of disk *E*; *Y*—quadrant of disk *D*; *Z*—details of mercury arc *A*.

II. The Experimental Apparatus and Methods

The aim of the experiment was to measure the rate of decay of the λ2537 afterglow emitted from a quartz cell containing a small amount of mercury vapor, and several millimeters of nitrogen, after it had been excited optically for a while and the exciting light shut off. The apparatus of Fig. 1 was employed. It is essentially similar to that used by Zemansky,[5] and other workers at Columbia University.

The source of exciting light was the mercury arc at *A*, (shown in detail, at *Z*), the base of which was water cooled. The arc, once started, ran between the top and bottom electrodes at about 7 amperes, 40 volts. It was not mag-

netically deflected. The light was focussed by the lens L on the slit at S, which was about 2 mm wide and 3 cm long. It was then interrupted periodically by the rotating toothed wheel D, which is shown more clearly in the inset at Y. It then passed through the quartz window Q of the asbestos board furnace F, into the quartz cell C containing mercury vapor and nitrogen, where it periodically excited the mercury vapor.

Light passing through the cell or emitted by it passed out at the other window Q, through the quartz cell B which contained bromine vapor for the purpose of filtering out light due to the phosphorescence of the quartz cell C, then through the lens K which served to collimate it, and then through small holes in the rotating disk E, shown more clearly in the inset at X, onto the photographic plate at P, where it recorded a pair of traces such as shown in Fig. 2, due, during the period of the afterglow to λ2537 light only.

Fig. 2. Photographic traces representing the decay of λ2537.

The rotating disks were of 15 cm radius. The interrupting disk had twenty teeth 10 degrees wide, with spaces 8 degrees. The second disk had twenty 1 mm holes 18 degrees apart at 13.15 cm from the center, and twenty at 12.85 cm from the center on the same radii. The disks were set relatively to each other so that the part of the traces representing the afterglow light fell on the axial line of the cell. The cycle of excitation and afterglow was repeated twenty times per revolution of the disks. The decrease of density of the photographic trace with the angle thus represented the decrease of intensity of the afterglow with time, when the speed of the disks was known. The speed was measured with a tachometer.

Over each of the outer set of holes was cemented a piece of cellophane which transmitted 65.2 percent of λ2537 light, as determined by measurement with a photocell spectrometer apparatus. Thus the density of one trace at a given angle represented 65.2 percent of the intensity of the other trace at the same angle. A small correction was made to this for the smaller exposure time of the outer trace due to the slightly greater radius. The reciprocity law is accurate enough for such a correction. The densities of the two traces were measured and plotted as a function of angle (or time), as in Fig. 3. Since the decay of the afterglow is very nearly exponential the horizontal distance between the two traces should be constant and give the time of decay to 65.2 percent of the intensity, thus determining the decay constant β where

$$I = I_0 e^{-\beta t}$$

represents the decrease of intensity with time. This distance was not ac-

curately constant, but was greater at the beginning than at the end. This however, is attributed to geometrical imperfections in the arrangement of the apparatus and the value at the center should be correct. The average distance was actually used to determine β and is believed to be correct within about 3 percent.

The use of cellophane to give a diminished intensity trace for calibration of the plates eliminated the intermittency errors which would occur if some

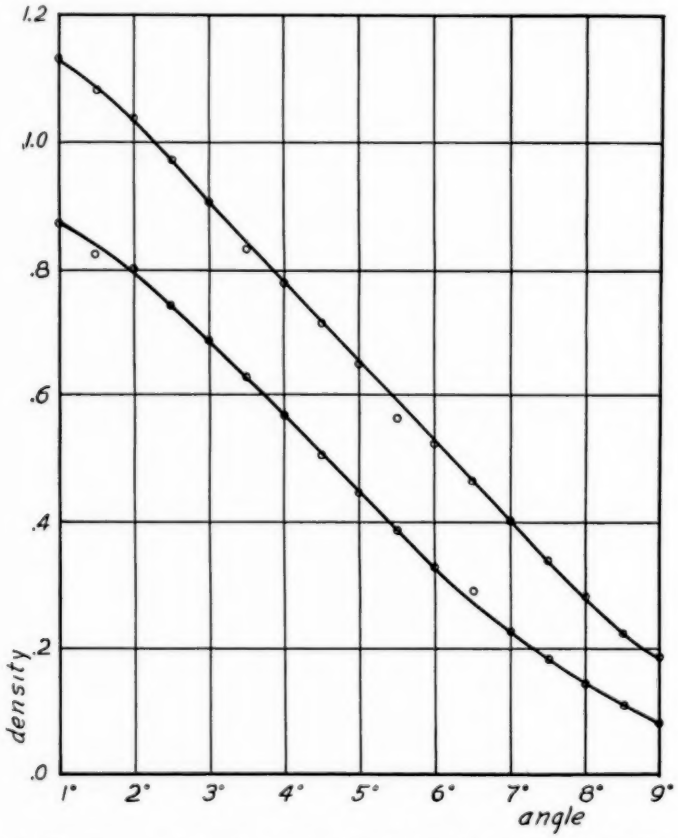

Fig. 3. The curves of density against angle for the photograph of Fig. 2. (Time is proportional to angle.)

of the holes were plugged according to Zemansky's procedure. The two traces are strictly comparable. It is perhaps worth while to mention that when cellophane is used for such purposes it must be pre-exposed to the light of the arc as its transmission increases several percent during the first few hours exposure, for $\lambda 2537$ light, then becomes constant, at least over reasonable periods of time. (A sample of German cellophane was found to fluoresce.)

The bromine filter in the path of the emergent light was found to be necessary to remove light due to phosphorescence of the quartz[14] of which the experimental cell was made. This phosphorescence was very intense and had

[14] Webb and Miss Messenger, Phys. Rev. **34**, 1463 (1929).

a decay period right in the region of measurement, having a constant of roughly 3000 to 4000 sec^{-1}. Its wave-length, however, is in the blue and near ultraviolet and it was almost completely distinguished by the bromine filter which was made of quartz chosen specially because it had very little fluorescence. Tests with a spectrograph showed the filter to be entirely adequate and also showed that no light other than $\lambda 2537$ was present in the afterglow after passing through the filter, so that it was legitimate to dispense with the spectrograph in making the measurements.

The furnace was heated by coils *H* of nichrome wire evenly distributed on its inside surface, leaving sufficient space for good circulation of air about the cell, and the temperature was measured by means of a thermocouple *T*, placed at the edge of the cell.

The pressure of mercury vapor inside the cell was determined by the drop of mercury in the appendix *M* which remained at room temperature, about 28 degrees, all the time.

Extreme purity of the gas was found to be an essential factor in obtaining consistent measurements. When impurities were present the rate of decay became very high and the intensity of the afterglow very low. This led to difficulties in the early stages of the work until their cause was ascertained and a good method of purification was adopted.

The nitrogen was prepared by the action of bromine on ammonia. Water vapor and excess ammonia were removed by allowing it to stand over phosphorus pentoxide for a considerable time. It was then admitted at a pressure of about 180 mm to a system in which it was kept in continual circulation through a mixture of copper and copper oxide at about 350°C, a trap containing glass beads at liquid air temperature, and a bulb containing phosphorus pentoxide. The gas was circulated by convection, one arm of the system being heated to about 200°C, and the process was continued for several days before the gas was used. The purification system was connected with the experimental system through a Toeppler pump equipped with a mercury seal which could be opened at will with an electromagnet. The direction of pumping was towards the purification side. When an experiment was to be performed the gas was allowed to flow very slowly through the ground surfaces of the unsealed Toeppler valve into the experimental system, and it passed through another trap with glass beads at liquid air temperature before reaching the cell *C*. The rate of flow was such that it took about twenty minutes to get 10 mm pressure in the cell. When all these precautions were taken it was found that consistent measurements could be obtained. The variations due to impurities were found to be much greater at high nitrogen pressures.

Before making measurements the quartz cell was thoroughly baked out so that there was no danger of gas coming off the walls of the cell. The cell was baked for an hour and a half at 450°C, and then for about the same time at 550°C, then for about 20 hours at 475°C, with the pumps on all the time. Then with the pumps shut off for $2\frac{1}{2}$ hours at the same temperature the pressure rose only to about 1 or 2×10^{-5} mm. Since the highest temperature used in the experiments was 215°C, and even before careful baking a test had

shown that raising the cell to 300°C for an hour and a half between two measurements of the rate of decay at room temperature made a difference of less than 10 percent in the measurements, it was considered that this was sufficient care to ensure that no impurities arose from the cell walls during the experiment.

III. Measurements and Experimental Formulas

Measurements of the rate of decay were made as described and the exponential constants β were calculated, over a range of nitrogen pressures

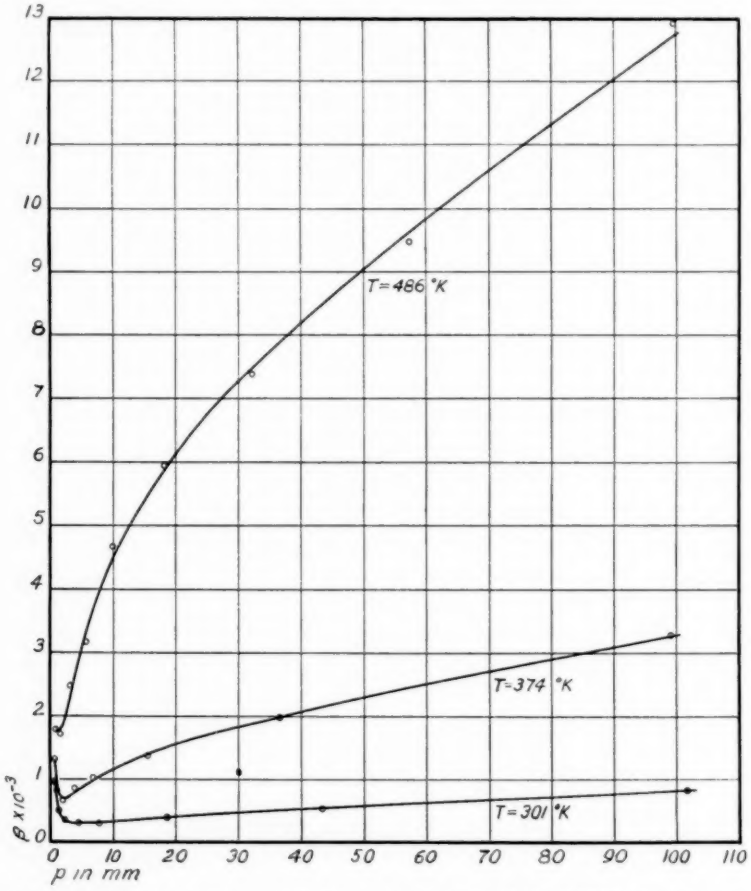

Fig. 4. Curves showing the exponential decay constant β, of the λ2537 afterglow against the pressure of the nitrogen at three temperatures.

roughly from 0.5 mm to 100 mm, with mercury vapor at 0.00236 mm at the three temperatures 301°K, 374°K, and 486°K. The decay constants ranged from 300 to 12,900, the speed of the disks from 190 to 3660 r.p.m. The times of exposure required ranged from 2 minutes to two or three hours. It was not considered worth while to attempt to make measurements at higher temperatures because the decay constants became too large for the available speed of the disks at high pressures, and a short curve is insufficient for the evaluation of the constants in the formula.

At each temperature the procedure employed was to introduce gas very slowly into the cell until the highest pressure was reached, to make a photograph suitable for measurement, then to reduce the gas pressure to the next convenient point and make another, and proceed in this way until the pressure was the lowest convenient for making good photographs. Thus a whole set of measurements was made with the same gas, the pressure being highest for the first measurements. This procedure was adopted because it was convenient experimentally, any impurities introduced during the experiments would tend to be partially pumped out between successive pictures, and minor variations in the purity of the gas would not occur from one experiment to the next so that the curve of decay constant against pressure would be somewhat smoother and easier to fit with the formula.

Altogether about 110 photographs were taken and a great many of them measured in overcoming experimental difficulties before any of the final measurements reported in this paper were made.

The theoretical formula reduced to the form used for fitting the curves of decay constant against nitrogen pressure is

$$\beta = \frac{X}{p} + \frac{Yp + Wp^2}{p + Z} \tag{1}$$

where p is the nitrogen pressure in mm, X, Y, Z, and W are constants to be determined from the curve at each temperature, and β is the decay constant. The results are tabulated in Table I and the curves are shown in Fig. 4. The curves are plotted from the formula and the experimental points put in.

TABLE I.

p (mm)	β obs.	β calc.	% Diff.		
0.61	957	905	+5.4	$T=301°K$	
1.18	516	520	−0.8	$X=526$	
2.25	359	355	+1.0	$Y=365$	
4.4	306	306	0.0	$Z=4.7$	
7.8	301	319	−5.5	$W=4.94$	
18.6	394	393	+0.2	$E_\beta=2.6\%$	
43.3	540	535	+0.9		
101.5	832	833	−0.1		
0.57	1307	1250	+4.6	$T=374°K$	
1.02	818	847	−3.4	$X=637$	$E_X=4\%$
1.95	663	710	−6.6	$Y=1685$	$E_Y=9\%$
3.78	846	795	+6.4	$Z=6.80$	$E_Z=15\%$
6.8	1023	997	+2.6	$W=18.0$	$E_W=12\%$
15.6	1367	1409	−3.0	$E_\beta=3.80\%$	
36.6	1977	1993	−0.8		
99.2	3274	3252	+0.7		
0.87	1787	1774	+0.7	$T=486°K$	
1.57	1711	1801	−5.0	$X=909$	$E_X=7\%$
3.07	2480	2380	+4.2	$Y=7150$	$E_Y=6\%$
5.65	3160	3333	−5.2	$Z=7.75$	$E_Z=10\%$
10.0	4657	4488	+3.8	$W=65.5$	$E_W=9\%$
18.2	5935	5897	+0.6	$E_\beta=2.9\%$	
32.2	7382	7488	−1.4		
57.3	9467	9618	−1.6		
99.7	12,900	12,700	+1.6		

Several points of interest are to be noted about the shape of the curves, regarded independently of the formula. First, the rise towards a vertical asymptote at zero pressure, very marked in the two lower curves and not quite reached in the upper curve, is due to the rapid increase of diffusion of excited atoms to the walls as the pressure decreases, and indicates quite clearly that they are there removed permanently from the excited states. Second, the minimum of each curve and then the rise with increasing pressure, shows that the diffusion decreases in importance and collision processes become the dominating influence by either removing the excited atoms to some permanent state or to a state where they can radiate their energy. Third, the fact that the curves are decidedly concave downward at medium pressures and appear to be approaching an asymptote with an upward slope is an important point. If there were only interchange between the 2^3P_0 and the 2^3P_1 states to consider besides radiation, the result at high pressure would be a constant ratio of the numbers of atoms in the two states due to the rapidity of the interchange, and consequently a constant decay coefficient, and the curves would be concave downward as they rose with pressure towards this constant value. The final upward asymptote must be attributed to some process of collision which hastens the decay rate with rise of pressure for all pressures, and hence must be of the nature of removal to the normal state on collision, or else some more abstruse effect. It will be seen in the theory that it may be due partly to collision broadening of the $\lambda 2537$ line. Finally the great increase of β with temperature at high pressures is very striking. It indicates a rapid increase with pressure of some collision process. Since the metastable 2^3P_0 atoms are the only ones which have a long natural lifetime they control the slowness of the decay in order of magnitude at least and so it seems *a priori* that the process which increases so very rapidly with temperature must be removal of metastable atoms by collision. This is borne out by the theory. The curves themselves thus give a preliminary indication of the nature of the processes which must be considered in the theory.

In finding the best formulas to fit the curves a method of successive approximation was used for that at room temperature, but for the other two the least squares method was used because it was little if any more difficult and gave some information about probable errors, and the manner in which they increased with subsequent calculations based on the constants of the formulas. The probable errors of β, X, Y, Z, and W are represented in Table I by E_β, E_X, E_Y, E_Z, and E_W as they were found in the calculations. They thus represent only the magnitudes of random errors and deviations from the formula. For room temperature, since E_β is smallest, it was assumed that the magnitudes of the probable errors of the constants are about the same as for the highest temperatures.

IV. Equations for Solution of the Problem

The Problem.

A cylindrical cell containing a small amount of mercury vapor, and a relatively very great amount of nitrogen, is excited by light from a mercury arc

for a time, and then the exciting light is stopped. We wish to express in terms of atomic properties the manner in which the intensity of the light thereafter radiated from the cell will decrease with time.

We shall throughout this paper use the terms n, 0, and 1 to denote the normal, 2^3P_0 (metastable) and 2^3P_1 states of the mercury atom, and these terms shall be used as subscripts to denote quantities pertaining to the corresponding states.

During excitation a concentration of metastable 0-atoms is built up by absorption of λ2537 and subsequent collisions of the 1-atoms with nitrogen molecules which reduce them to the 0-state. 2^3P_2 atoms may be produced during excitation by stepwise excitation, but are very rapidly removed as a result of the close resonance with a vibration level of nitrogen at 0.571 electron-volts, being reduced to $^3P_1$, so that no appreciable concentration is present at any time.[15] Their production during the decay will be very improbable because relatively few collisions have the required kinetic energy. We shall therefore neglect them.

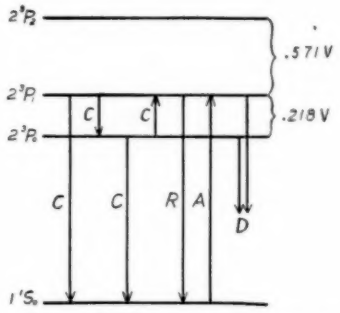

Fig. 5. Important transition processes for the mercury atom. *C*—produced by collisions; *R*—emission of λ2537; *A*—absorption of λ2537; *D*—diffusion to the walls; *V*—electron volts.

Fig. 5 indicates the types of transition which may occur by collisions with nitrogen, to radiation or absorption of λ2537, and to diffusion of excited atoms, during the afterglow period. There is interchange between the 0 and 1 states on collision, and there may be reduction of either 0- or 1-atoms to the normal state on collision. 1-atoms are reduced to the normal state by radiation of λ2537. Excited atoms lose their energy if they strike the walls of the cell and hence diffusion must be considered. This involves the geometry of the cell.

A quantum of light of λ2537 may be absorbed and re-emitted several times before it finally escapes from the cell. The frequency distribution of the absorption line of the vapor, and the frequency distribution of the radiation density determine the number of quanta of radiation absorbed by any given element of volume. Thus consideration must be given to the diffusion of the radiation in the cell. This also involves the geometry of the cell.

All the important processes have now been enumerated, and we must proceed to express them mathematically.

[15] Pool, Phys. Rev. **38**, 955 (1931).

The following notation will be used:

n_0, n_1, n = numbers of atoms per cc at a point in the states 0, 1, and n respectively.

N = number of nitrogen atoms per cc.

p = pressure of nitrogen in mm of mercury.

D = diffusion coefficient for 0-atoms or 1-atoms.

k_0, K_0, k_1, K_1 = numbers of effective collisions per second per mercury atom at 1 mm nitrogen pressure giving rise respectively to the transitions $0\rightarrow 1$, $0\rightarrow n$, $1\rightarrow 0$, and $1\rightarrow n$.

$\rho(\nu)d\nu$ = radiation density between the frequency ν and $\nu+d\nu$ within the $\lambda 2537$ line.

$b(\nu)\,\rho(\nu)\,d\nu dt$ = probability that an n-atom will absorb a quantum in the range between ν and $\nu+d\nu$ in the time dt. This defines the coefficient $b(\nu)$.

A, B, B_{1n} = the Einstein coefficients for emission, absorption, and stimulated emission, respectively, of quanta of $\lambda 2537$ radiation by mercury atoms.

g_0, g_1, g_n = statistical weights of 0-, 1-, n-states, respectively.

l = length of the cell. $l = 1.65$ cm.

c = radius of the cell. $c = 2.16$ cm.

We may immediately set up the equation for the rate of change of 0-atoms at a point. It is the number coming in by diffusion plus the number formed by collisions minus the number removed by collisions. Thus

$$\partial n_0/\partial t = pk_1 n_1 - p(k_0 + K_0)n_0 + D\nabla^2 n_0 \tag{2}$$

In finding $\partial n_1/\partial t$ radiation enters. Stimulated emission of radiation is negligible because of the Einstein relation $Bg_n = B_{1n}g_1$ and the fact that $n_1 \ll n$, whence $n_1 B_{1n}\rho(\nu) \ll nB\rho(\nu)$, or the number of stimulated emissions is much smaller than the number of absorptions, whence radiation in the afterglow capable of being absorbed must be almost entirely due to spontaneous emission. Further, we may put the diffusion coefficient the same for 1- as for 0-atoms because the states are so close that there is no reason to expect any difference of behaviour for a process such as diffusion, which involves *no internal effects* on the atoms.

Thus we may write finally

$$\partial n_1/\partial t = pk_0 n_0 + n\int_0^\infty b(\nu)\rho(\nu)d\nu - n_1(A + pk_1 + pK_1) + D\nabla^2 n_1. \tag{3}$$

We must solve Eqs. (2) and (3) in accordance with the boundary conditions

$$n_1 = n_0 = 0 \text{ at walls.} \tag{4}$$

So far our procedure has been rigorous, but the radiation integral in the above equation makes the problem exceedingly complicated. $b(\nu)$ depends on the five components of the line, Doppler and pressure broadening. $\rho(\nu)$ de-

pends on $b(\nu)$ and also on the position of the point and the distribution of 1-atoms in the cell. It becomes necessary to make an approximation in dealing with the radiation terms, which gives finally a reasonably satisfactory solution.

V. The Solution

First, we shall assume that $\rho(\nu)$ is chiefly due to the radiating atoms in its immediate neighbourhood, so that it is proportional to n_1 at the same point. Then the absorption term may be represented by Ln_1, where L is an unknown coefficient which does not depend on the position of the point. Now if we put $A-L=P$ we have P representing a *resultant radiation coefficient* for the cell and each element of volume in it, and we may rewrite Eq. (3) thus,

$$\partial n_1/\partial t = pk_0n_0 - n_1(pk_1 + pK_1 + P) + D\nabla^2 n_1. \tag{5}$$

We must now solve Eqs. (2) and (5) with the boundary conditions (4). Now it is easily proved by substitution that if $\psi(x,y,z,t)$ is a solution of

$$\partial\psi/\partial t = D\nabla^2\psi \tag{6}$$

and $f_0(t)$ and $f_1(t)$ are solutions of

$$df_0/dt = pk_1f_1 - p(k_0 + K_0)\, f_0 \tag{7}$$

$$df_1/dt = pk_0f_0 - f_1(pk_1 + pK_1 + P) \tag{8}$$

then

$$n_1 = f_1(t)\psi(x,y,z,t) \tag{9}$$

$$n_0 = f_0(t)\psi(x,y,z,t) \tag{10}$$

are solutions of the complete Eqs. (2) and (5). Only the function ψ is affected by the geometrical boundary conditions (4).

Hence we may solve Eqs. (7) and (8) first. Eliminating df_0/dt and f_0 by differentiation and solving the resulting equation gives

$$f_1 = F\exp\left[-\tfrac{1}{2}\{U + (U^2 - 4V)^{1/2}\}t\right] + G\exp\left[-\tfrac{1}{2}\{U - (U^2 - 4V)^{1/2}\}t\right] \tag{11}$$

where

$$U = (pk_1 + pK_1 + pk_0 + pK_0 + P) \tag{12}$$

and

$$V = [(pk_0 + pK_0)(pk_1 + pK_1 + P) - p^2k_0k_1]. \tag{12a}$$

From the experiments of R. W. Wood[1] on absorption by 1- and 0-atoms during the steady state with illumination by λ2537 in the presence of nitrogen it is apparent that $n_1 \ll n_0$. But in that case Eq. (2) holds with $\partial n_0/\partial t = 0$, and diffusion tends to remove metastable atoms to the walls, so that

$$k_0 + K_0 \ll k_1 \tag{13}$$

Using this relation to simplify Eq. (11) we may show first that $V \ll U^2$ whence f_1 reduces first to $Ge^{-Vt/U}$ and then using Eq. (13) again, finally

$$f_1 = Ge^{-\alpha t} \tag{14}$$

where

$$\alpha = \frac{p(k_0 + K_0)P + p^2(K_0K_1 + K_0k_1 + k_0K_1)}{p(k_1 + K_1) + P}. \tag{15}$$

Similarly

$$f_0 = G'e^{-at}. \tag{16}$$

Now the solution of Eq. (6) in accordance with the boundary conditions, in cylindrical coordinates, assuming any symmetrical distribution as initial condition, gives for solution a series of terms of which only the first is of importance because the rest decay very rapidly, whence

$$\psi = G''J_0(\mu_1 r/c)\cos(\pi x/l)e^{-\gamma t} \tag{17}$$

where

$$\gamma = \left(\frac{\pi^2}{l^2} + \frac{5{\cdot}81}{c^2}\right)D. \tag{18}$$

Finally by Eqs. (14), (16), (17), (9), and (10) we see that

$$n_1 = C_1n_0 = C_2(r, x)e^{-(\alpha+\gamma)t}. \tag{19}$$

Since the radiated intensity is proportional to n_1 our experimental decay coefficient is the above exponential coefficient $\alpha+\gamma$, whence

$$\beta = \alpha + \gamma. \tag{20}$$

It is convenient at this point to introduce a small correction to the *resultant radiation coefficient* P, which is a function of the line shape. Now the line shape is affected chiefly by Doppler effect which is a function only of temperature, but it is also affected by Lorentz collision broadening, which is a function of pressure. It is desirable to reserve the term P for the result of Doppler effect and express the increase of the resultant radiation coefficient which is due to pressure broadening of the line by an added term ap, which would naturally be chosen as a first order approximation. An examination of Zemansky's[16] data on the pressure broadening effect for λ2537 with nitrogen in the same pressure range provides a rough confirmation of the view that the term ap is adequate for the purposes of this paper, that is, that it is accurate within the limits of error of the experiment. Hence we shall replace P by $P+ap$.

Then expanding our value for β, using Eqs. (15) and (18)

$$\beta = \left(\frac{\pi^2}{l^2} + \frac{5{\cdot}81}{c^2}\right)\Delta + \frac{p(k_0 + K_0)P + p^2[K_0k_1 + (k_0 + K_0)(K_1 + a)]}{p(k_1 + K_1 + a) + P}. \tag{21}$$

Since $D \sim 1/N \sim 1/p$ (See Eq. (31)) we may rewrite Eq. (21) in a form suitable for application to experimental results thus:

$$\beta = \frac{X}{p} + \frac{Yp + Wp^2}{p + Z} \tag{22}$$

[16] Zemansky, Phys. Rev. **36**, 219 (1930).

where X, Y, Z, and W are constants at a given temperature. Their values are clear by comparison with Eq. (21). The experimental results were found to agree with this formula (Section III) over a wide range of measurements.

VI. Requirements for Interpretation of Data

The first step in the interpretation is to note that by comparison of Eqs. (21) and (22)

$$k_0 + K_0 = Y/Z \tag{23}$$

$$k_1 + K_1 + a = P/Z \tag{24}$$

$$\frac{K_1 + a}{k_1 + K_1 + a} + \frac{k_1}{k_1 + K_1 + a} \cdot \frac{K_0}{k_0 + K_0} = \frac{WZ}{Y} \tag{25}$$

$$D = \frac{X}{p(\pi^2/l^2 + 5.81/c^2)} . \tag{26}$$

Now Y, Z and W are known from the experimental data and are given in Table I. The value of P must be determined at each temperature by a calculation of the effect of diffusion of radiation. This calculation is a problem in itself, and the method used may have some interest apart from its application in this paper. Since it would appear in the nature of a digression here, it is carried out in Appendix B, at the end of the paper.

In order to evaluate the 'effective temperature cross sections for the various processes,' we also require the following formulas expressing k_0, K_0, k_1, and K_1 in terms of the corresponding 'cross sections' σ_0^2, Σ_0^2, σ_1^2, and Σ_1^2, for the processes involving energy transitions, and for D in terms of σ_d^2 the diffusion cross section. μ = reduced mass for mercury and nitrogen, T = temperature, k = Boltzmann's constant.

$$k_0 = \frac{2N\sigma_0^2}{p}\left(\frac{2\pi kT}{\mu}\right)^{1/2}\left(1 + \frac{\epsilon}{kT}\right)e^{-\epsilon/kT} \tag{27}$$

$$k_1 = \frac{2N\sigma_1^2}{p}\left(\frac{2\pi kT}{\mu}\right)^{1/2} \tag{28}$$

$$K_0 = \frac{2N\Sigma_0^2}{p}\left(\frac{2\pi kT}{\mu}\right)^{1/2} \tag{29}$$

$$K_1 = \frac{2N\Sigma_1^2}{p}\left(\frac{2\pi kT}{\mu}\right)^{1/2} \tag{30}$$

$$D = \frac{1}{3\pi\sigma_d^2 N}\left(\frac{8kT}{\pi\mu}\right)^{1/2} . \tag{31}$$[17]

The factor $(1+\epsilon/kT)e^{-\epsilon/kT}$ in Eq. (27) represents the fraction of all collisions within a distance σ_0, which possesses relative kinetic energy $\geqq \epsilon$, or sufficient to produce the upward transition $0 \rightarrow 1$ in the mercury atom.

Since a discussion at this point of the definitions and nature of 'effective velocity and temperature cross sections for various processes' and derivation

[17] Tolman, *Statistical Mechanics*, p. 228, Eq. (525) and p. 63, Eq. (95).

of formulas would again be a digression, it has been placed in Appendix A at the end of the paper.

VII. Results Independent of P

Since the calculation of P involves a further approximation, we shall first discuss those results which are independent of it.

The diffusion cross sections are calculated from the experimental values of X in Table I, by means of Eqs. (26) and (31), giving the results[17a] in Table II, under σ_d^2. They show a slow increase with temperature. Since the expected deviations would be about 6 percent this rise is probably a real one, but is slower than the square root of the absolute temperature. The sum σ of the gas-kinetic radii of the nitrogen molecule and the mercury atom results in a value $\sigma^2 = 11.2 \times 10^{-16}$ whence it appears that the cross section for metastable mercury atoms is somewhat larger than for normal atoms, as would be expected for excited atoms. This fact indicates that the assumption that all metastable atoms lose their energy at the walls is justified by the experiment. A few percent might be reflected unchanged without greatly affecting the results, but most of them are certainly reduced at the walls.

Table II.

$T°K$	σ_d^2 cm²	WZ/Y	$e^{\epsilon/kT}/(1+\epsilon/kT)$	k_0	σ_0^2 cm²
301	15.5×10^{-16}	0.0636	477	77.65	7.21×10^{-18}
374	17.7×10^{-16}	.0724	111.6	247.8	5.99×10^{-18}
486	18.4×10^{-16}	.0710	29.41	922.5	6.71×10^{-18}
	Mean Values	0.0690			6.66×10^{-18}

In order to find k_0 and σ_0^2 we must first note that by comparison of Eq. (25) with the values of WZ/Y in Table II

$$K_0 \ll k_0 \qquad K_1 + a \ll k_1 \tag{32}$$

at all three temperautres, and the maximum possible value of the ratios of K_0 to k_0 and $K_1 + a$ to k_1 is of the order of 7 percent which is within the range of possible errors of k_0 and k_1. Actually it appears later that K_0 is exceedingly small compared to k_0. We may then evaluate k_0 from Eq. (23) neglecting K_0. The values are listed in Table II.

The rapid increase of k_0 with temperature is very striking. It corresponds to a rapid rise with temperature of the number of $0 \rightarrow 1$ transitions produced by collisions, and accounts for the rapid divergence of the different (β, p) curves at high pressures as due to a rapid increase in the rate of removal of metastable atoms, in agreement with the interpretation placed on that divergence when the curves were examined.

The effective cross sections σ_0^2 may now be found from Eq. (27). The values in Table II show that within our probable random errors, which are

[17a] Webb and Miss Messenger, since this paper was written, have published in a letter (Phys. Rev. **40**, 466, 1932) the value $\sigma_d = 3.7 \times 10^{-8}$ cm, at room temperature, which compares well with our value $3.9 = 10^{-8}$. Their experimental method and that of the author are very similar. Both are based on that of Zemansky, referred to before.

about 15 percent, σ_0^2 does not vary with temperature in the range from 300° to 500°K. It should be emphasized here that there is no *a priori* reason to expect σ_0^2 to be constant. It is shown in the appendix that an *effective temperature cross section* of this nature, from the way it is defined, must be expected to be a function of temperature. Hence our result is not merely confirmation of an *a priori* expectation, and may not hold for temperatures very different from those of the measurement.

The rapid increase of k_0 with temperature is due principally to the factor $(1+\epsilon/kT)e^{-\epsilon/kt}$ in Eq. (27) which represents the fraction of all collisions within the distance σ_0 that have sufficient relative kinetic energy ($\geqq\epsilon$) to produce the upward transition 0→1 in the mercury atom. This illustrates quantitatively the explanation advanced by Cario and Franck[12] for the fact that nitrogen does not quench resonance radiation at 750°C, as mentioned in our introduction.

The fact that σ_0^2 is constant implies that the corresponding *velocity cross section*, Q_0^2, must be nearly constant over the important range of velocities just above the critical relative velocity V_c corresponding to the relative kinetic energy ϵ. Since the important range of velocities is that just above the critical velocity ($\epsilon\gg kT$), the value of Q_0^2 must rise abruptly, within a few hundredths of an electron volt, from zero at the critical velocity, to its nearly constant value above it, or σ_0^2 would not appear to be independent of temperature. Thus Q_0^2 must be nearly equal to σ_0^2 in this range.

It is well to point out here that although we have referred to the nitrogen molecule as though it were a definite molecule in a definite state, the *normal state*, this is not strictly true. Actually there is a distribution of molecules among the rotational states of the lowest electronic and vibration state, due to the temperature, and principally determined by the Boltzmann factor. Since they must all be very close to the lowest state at the temperatures of our experiments, however, and it is quite impossible to differentiate between them, we have simply neglected the effect throughout.

VIII. Results Depending Partially on P

Before we can evaluate k_1 and σ_1^2 we must know the values of P at the three temperatures. These values are calculated in Appendix B, to which the reader is referred, by a method involving an approximation which is consequently involved in the following calculations. The values of k_1 are obtained from Eq. (24) neglecting (K_1+a) on account of Eq. (32), using values of Z from Table I. σ_1^2 is then found by Eq. (28). The values of P, k_1 and σ_1^2 are listed in Table III.

Table III.

T°K	P	k_1	σ_1^2 cm^2
301	0.761×10^6	1.62×10^5	3.15×10^{-17}
374	0.882×10^6	1.30×10^5	2.82×10^{-17}
486	1.058×10^6	1.36×10^5	3.37×10^{-17}
Mean $\sigma_1^2=3.11\times10^{-17}$			

Now σ_1^2 may also have random errors of the order of 15 percent whence it is also apparently independent of temperature within the limits of error of the experiment in the range from 300° to 500°K. If we take this as correct it again implies that the velocity cross section, Q_1^2, is nearly constant and equal to σ_1^2 over the important range of velocities.

We have now found that both σ_0^2 and σ_1^2 are independent of temperature, and it is reasonable to assume that Σ_0^2 and Σ_1^2 will be essentially independent of temperature also, in order to make inferences from Eqs. (25), (29) and (30). We may then substitute in Eq. (25) from Eqs. (29) and (30), again neglecting small quantities according to Eq. (32), and get

$$\frac{a}{k_1}+\frac{\Sigma_1^2}{\sigma_1^2}+\frac{\Sigma_0^2}{\sigma_0^2}\,\frac{e^{\epsilon/kT}}{(1+\epsilon/kT)}\,. \tag{33}$$

Now k_1 varies as $T^{1/2}$, the variation of a with temperature is unknown but probably slow so that a/k_1 varies slowly; Σ_1^2/σ_1^2 is constant, but the third term varies very rapidly due to the factor $e^{\epsilon/kT}/(1+\epsilon/kT)$. (See Table II.) Whence if Σ_0^2 has any appreciable magnitude, WZ/Y should also vary rapidly with the temperatue. Table II shows that WZ/Y is unaffected by this factor, whence we conclude that Σ_0^2 is zero within the experimental accuracy. If we attribute the 0.01 increase of WZ/Y to this term we find $\Sigma_0^2=2\times10^{-22}$ as a possible order of magnitude. Hence we may say roughly

$$\Sigma_0^2 \leqq 2\times10^{-22}\ \text{cm}^2$$

and this means that few if any metastable 2^3P_0 atoms are reduced to normal $^1S_0$, or otherwise permanently removed by collisions with nitrogen. This result agrees with many others which indicate that processes which take place on collision have much smaller probability for larger required change of kinetic energy.

We can now reduce Eq. (33) to

$$\frac{a}{k_1}+\frac{\Sigma_1^2}{\sigma_1^2}=\frac{WZ}{Y}\,. \tag{34}$$

It can be shown that a/k_1 may account for an appreciable proportion (35 percent) of the magnitude of WZ/Y by a rough argument based on the data in Table IV Appendix B, and Zemansky's pressure broadening data, but its magnitude is uncertain so that from the above equation and Table II we may only assign an upper limit for Σ_1^2

$$\Sigma_1^2 \leqq 2.15\times10^{-18}\ \text{cm}^2.$$

It does seem probable however, that Σ_1^2 has a magnitude of this order, because the value of WZ/Y is about three times the estimated collision broadening term in Eq. (34). In this case the question arises as to why Σ_1^2 should be 10,000 times greater than Σ_0^2. Several suggestions may be offered, but without undue emphasis because the subject is uncertain. There might be close resonance with the nitrogen molecules or with an impurity, so that the

energy of $^3P_1$ could go mostly into excitation energy and require but a small change in kinetic energy, while the resonance with $^3P_0$ is relatively poor. Or the difference might be due to an inherent difference between optically allowed and forbidden transitions. Or it might be that a collision is capable of stimulating radiation of the allowed line λ2537. This last seems to be the most plausible way of accounting for the large ratio, particularly in view of the experiment of Cario and Franck[12] referred to before, for if Σ_1^2 has a value which does not signify production of radiation, there should be quenching at all temperatures.

IX. Summary and Remarks

The values of the effective cross sections may now be gathered together. Those involving energy changes of the mercury atom on collision with nitrogen have all been found to be, within the limits of random error, independent of temperature in the range from 300° to 500°K. It was inferred that the corresponding velocity cross sections are nearly constant over the important range of velocities. The values of the temperature cross sections are:

$$\sigma_0^2 = 6.66 \times 10^{-18}\ \text{cm}^2, \qquad \Sigma_1^2 \leqq 2.15 \times 10^{-18}\ \text{cm}^2,$$

$$\sigma_1^2 = 3.11 \times 10^{-17}\ \text{cm}^2, \qquad \Sigma_0^2 \leqq 2.00 \times 10^{-22}\ \text{cm}^2 \text{ roughly}.$$

The first of these is the most reliable because it does not depend on the assumption used in evaluating P, the *resultant radiation coefficient.*

The diffusion cross section, σ_d^2, was found to increase slightly with temperature. The values are 15.5×10^{-16}, 17.7×10^{-16}, and $18.4\times10^{-16}\text{cm}^2$, at the temperatures 301°, 374°, and 486°K, respectively. These values are also independent of P. They are in good agreement with the assumption that metastable mercury atoms are reduced at the walls.

The theory presented in this paper and the appendix concerning the value of P appears to be quite well justified by the nature and the coherence of the results. The same kind of argument may be followed in the problem of quenching of resonance radiation, and similar approximations may be employed.

M. L. Pool[15] in a recent paper has described measurements of the rate of decay of metastable atoms of mercury in the presence of nitrogen, by a method which uses the absorption of λ4047 ($2^3P_0 - 2^3S_1$). He emphasizes the result that the decay is not strictly exponential but is faster at the beginning, and attributes the effect to the presence of excited metastable nitrogen atoms in the level of vibration quantum number 1 produced by previous collisions with mercury atoms in the $^3P_1$ state. His theory, however, neglects the important influence of the reduction of $^3P_1$ atoms to the normal $^1S_0$ or metastable $^3P_0$ states and imprisonment of λ2537 radiation, so that his numerical calculations of cross sections cannot be compared with those of the present paper. His measurements cover less than half the range of nitrogen pressures used in this paper, and the more rapid rise of his final exponential decay constant with pressure was the effect observed in the present investigation when traces of impurity were present. The effect of more rapid initial decay may

indeed be in part due to the excited nitrogen molecules, but it should be borne in mind that some of this effect is naturally to be expected anyway in the transition from the state of affairs during excitation to the different state of affairs which holds during the decay after sufficient time has elapsed. This transition period is represented in the theory by terms of higher decay rate which have been neglected as dropping out rapidly. To justify Pool's interpretation would require a detailed examination of these terms which would be very difficult. The present experiments made no effort to detect this deviation from the exponential character, the value taken as the actual decay rate was the mean value at periods rather later than those used by Pool.

Zemansky's[18] value of the quenching cross section, 1.92×10^{-17}cm^2 for mercury resonance radiation in nitrogen, should agree with our value of $\sigma_1^2+\Sigma_1^2=(3.1+0.2)10^{-17}=3.3\times10^{-17}$, if, as he assumes, the pressure in his experiments was so low that the number of $0\rightarrow1$ transitions was negligible. The difference in these two values is apparently due to the difference in his treatment of the diffusion of radiation. Two assumptions appear implicitly in his paper. The first is that a quantum of radiation, in being absorbed and re-emitted a number of times, retains the same frequency. That this is not true may be seen by considering the Doppler effect on a quantum absorbed and then reradiated at right angles, when the absorbed and emitted frequencies are totally independent. The second assumption is that the calculations may be carried out for an element of the line and integrations with respect to frequency performed afterwards. It is impossible to estimate the error due to this procedure. However, the assumptions were made to deal with the same difficulties as those of our treatment of radiation. It does not seem possible to treat our problem by Zemansky's method, but it is possible to recalculate his quenching cross-section by methods analogous to ours. Zemansky has kindly recalculated his result for nitrogen in this way and gets the value 2.7×10^{-17}cm^2, in close agreement with our value of 3.3×10^{-17}. Since the conditions of his experiment were considerably different, such an agreement seems to provide an excellent check on the accuracy of our treatment of problem of diffusion of radiation.

The author wishes to express his sincere appreciation to Professor K. T. Compton for suggesting the subject of this investigation, to Dr. M. W. Zemansky for advice during its early stages, to Professor L. A. Turner for a great deal of helpful advice and criticism during the later parts of the work and in the preparation of this paper, and to the Department of Physics at Princeton for continued support throughout a rather prolonged research.

Appendix A

Collision statistics

The conception of a collision between molecules is indefinite because molecules do not have definite boundaries, but we may call a (V, q) collision one in which the relative velocity is V and the distance from the center of one molecule to the line of the relative velocity V through the center of the

[18] Zemansky, Phys. Rev. **36**, 919 (1930).

other is q. For a (V, q) collision there is a probability $\phi(V, q)$ that a given process, say a transition of energy state, may take place, for a given pair of molecules. We know very little of the nature of the function $\phi(V, q)$. For statistical purposes however, we may define an *effective velocity cross section, Q^2, for the given process* by calculating the number of collisions within a distance Q at the velocity V, denote it $Z(V, Q^2)dV$ and equate it to the actual number of effective collisions at this velocity, which may be found experimentally, thereby determining Q^2. (The cross-section area is really πQ^2, but it is convenient to drop the π and refer simply to Q^2 as the cross section. This convention has been adopted with reference to all the cross sections in this paper.) Q^2 is clearly a function of velocity and of the process considered.

Since actual experiments usually do not differentiate between velocities but are carried on at a known temperature, it is convenient to make a similar definition of an *effective temperature cross-section for the given process*. If $Z(T, \sigma^2)$ represents the total number of collisions of all velocities within the distance σ at temperature T then

$$Z(T, \sigma^2) = \int_0^\infty Z(V, Q^2)dV. \tag{1}$$

We find it convenient in this paper to modify the definition slightly for the case where an amount of relative kinetic energy ϵ is required to produce the transition and equate the total number of effective collisions to the total number of collisions within a radius σ *which have sufficient relative kinetic energy* to produce the transition. Thus

$$Z(T, \epsilon, \sigma^2) = \int_{V_c}^\infty Z(V, Q^2)dV \tag{2}$$

where V_c is the critical velocity corresponding to the energy ϵ.

The σ^2 is in each case a function of temperature on account of Q^2 being a function of velocity. It is also clear from this derivation that σ^2 has no relation to the gas-kinetic radii of the atomic bodies concerned, and may be quite different for different processes. If σ^2 is known accurately as a function of temperature then Q^2 may be determined as a function of velocity through the above equations, but further information it is impossible to obtain from the results of statistical measurements alone.

To ascertain how these effective temperature cross sections depend on temperature is one of the objects of the present work. The right hand members of the above equations have occurred in our theory in the form knp, the total number of effective collisions per cc per second. The left member is easily calculated on the basis of the Maxwellian distribution[19] of velocities, and the resulting equations are Eqs. (27) to (30) of Section VI.

Appendix B

Diffusion of radiation and evaluation of P

In Section V of this paper the effect of diffusion of radiation was treated by the introduction of a resultant radiation coefficient, P, which was as-

[19] Tolman, *Statistical Mechanics*, p. 69, Eqs. (121) and (122a).

sumed to be the same for every element of volume and for the cell as a whole. We wish to evaluate this coefficient. In order to do so we note that it concerns *only emission and absorption of radiation*. If our cell had no other processes occurring than these the radiation emitted would decay according to the law $I = I_0 e^{-Pt}$ and P would be the exponential decay coefficient for the cell. We shall then determine P theoretically by calculating what the decay coefficient would be if only emission and absorption of λ2537 radiation occurred.

Now this problem was solved by E. A. Milne[20] for a simplified case, namely that of atomic absorption and emission coefficients which were constant over the breadth $\Delta\nu$ of the line, and an infinite plane slab of gas. His result is that the decay is dominated by the first term of a series of exponentials, and the decay coefficient of this term is (expressed in our notation),

$$P = \frac{A}{1 + (\kappa l/\lambda)^2} \tag{1}$$

where κ is the absorption coefficient, l the thickness of the slab, and λ is the root which lies between 0 and $\pi/2$ of the equation

$$\lambda \tan \lambda = \kappa l, \tag{2}$$

He interprets

$$\kappa l = C \tag{3}$$

as the *opacity* of the slab, presumably because for a collimated beam of the frequency shape assumed shining through the slab, the total transmitted intensity $I(l)$ is to the total incident intensity $I(0)$ in the ratio

$$I(l)/I(0) = e^{-\kappa l} = e^{-C}. \tag{4}$$

In an experimental case, he suggested that the opacity of the slab should be determined by measurement, and used to calculate P. This clearly is intended as a way of finding a suitable type of mean value for P, in consideration of the fact that the absorption and emission coefficients actually depend on the frequency.

In Milne's theory P is a function only of $I(l)/I(0)$, or of the fraction of incident light transmitted by the slab when the absorption and emission coefficients are independent of frequency over the breadth of the line. This fact suggests the assumption that P is a function only of the transmission (or absorbing power) of the slab even when the absorption and emission coefficients do depend on the frequency, and that the function itself is unchanged. Since we can determine the ratio $I(l)/I(0)$ we can evaluate P on the basis of this assumption, so that it is a convenient one to make for our present problem, and we shall proceed to use it. Its accuracy is perhaps open to some question, but it is hoped that it affords a good approximation. The discussion moreover, contains many ideas which are essential to any more rigorous theory. The assumption agrees with Milne's suggestion, but requires

[20] Milne, Jour. Lon. Math. Soc. I, Part I, p. 40 (1926).

the added rather obvious statement that the light whose transmission we determine has intensity corresponding in frequency distribution to the natural radiation coefficients of the gas in the cell. We may then calculate $I(l)/I(0)$ from the known value of A, and through it obtain the value of P.

The use of a value of P derived for an infinite plane slab in the case of our cell which is cylindrical is roughly justified later, by consideration of the dimensions of the cell, in relation to the probability of a quantum escaping at the edge.

We shall calculate P for a line affected by Doppler broadening only. The effect of pressure broadening was considered before and expressed by another term, ap, so it need not be discussed here.

A consideration of the Doppler principle applied to a system of atoms moving with velocities according to the Maxwell-Boltzmann velocity distribution formula, and the definition of the half breadth of a line as the breadth $\Delta\nu$ at half the maximum height of the line, leads[21] to the formula

$$\phi(\nu)d\nu = \phi(\nu_0)e^{-4\log 2(\nu_0-\nu)^2/\Delta\nu^2}d\nu \tag{5}$$

for the probability that a quantum emitted or absorbed with proper frequency ν_0 will appear to the observer to be of frequency ν, where $\phi(\nu_0)$ is the maximum, occurring at ν_0, and

$$\Delta\nu = \left[\frac{8kI\nu_0^2}{mc^2}\log 2\right]^{1/2} \tag{6}$$

is the half breadth.

If we put

$$\omega^2 = \frac{4(\nu_0 - \nu)^2}{\Delta\nu^2}\log 2 \tag{7}$$

then the absorption coefficient

$$\kappa(\nu) = \kappa(\nu_0)e^{-\omega^2}. \tag{8}$$

Also if $I(0, \nu)$ is the intensity incident on the slab at ν, and $I(1, \nu)$ is the intensity transmitted at ν, then

$$I(0, \nu) = I(0, \nu_0)e^{-\omega^2} \tag{9}$$

in accordance with our assumption that the incident light must have the same frequency distribution as the radiation coefficients.

Then the transmitted intensity at ν is

$$I(l,\nu) = I(0, \nu)e^{-\kappa(\nu)l} = I(0, \nu_0)\exp\left[-\omega^2 - \kappa(\nu_0)le^{-\omega^2}\right]. \tag{10}$$

The total incident intensity is

$$I(0) = \int_0^\infty I(0, \nu_0)e^{-\omega^2}d\nu. \tag{11}$$

[21] Müller-Pouillet's, *Lehrbuch der Physik*, 11 Ed. V. 2, Part 2, V. 1. Article by Minkowski discusses factors affecting shape of spectrum lines.

A similar integration of Eq. (10) gives the total transmitted intensity $I(l)$. Then, changing $d\kappa$ into terms of $d\omega$ and changing the integrations to correspond (0 becomes effectively $-\infty$), and integrating the denominator gives the required ratio

$$\frac{I(l)}{I(0)} = \frac{1}{\pi^{1/2}} \int_{-\infty}^{\infty} \exp\left[-\omega^2 - \kappa(\nu_0) l e^{-\omega^2}\right] d\omega. \tag{12}$$

The integral may be computed graphically when $\kappa(\nu_0)$ is known.

Now when a collimated beam $I(\nu)$ goes a distance dx the energy absorbed per cm^2 in $d\nu$ is $\kappa(\nu) I(\nu) d\nu dx$, but it is also $nh\nu\rho(\nu) b(\nu) d\nu dx$, and since $c\rho(\nu) = I(\nu)$ we find that

$$\kappa(\nu) = nh\nu b(\nu)/c. \tag{13}$$

From Eq. (5) it is apparent that $B\phi(\nu) = b(\nu)$, and since a quantum must appear to be absorbed at some frequency $\int_0^\infty \phi(\nu) d\nu = 1$ whence

$$\int_0^\infty b(\nu) d\nu = B. \tag{14}$$

Further, the Einstein relation[22] of radiation coefficients is

$$B = g_1 c^3 A / 8\pi g_n h\nu^3. \tag{15}$$

The value of A is known quite accurately whence, through Eqs. (13), (14), (15), (8) and (7), and assuming (as Zemansky[16] did) that the five components of the line are approximately equal, we get $\kappa(\nu_0)$ as one fifth of the value it would have if there were only a single component, namely,

$$\kappa(\nu_0) = \frac{(2 \log 2)^{1/2}}{40\pi} \frac{g_1 \lambda^2 A}{g_n} \cdot \frac{n}{\Delta\nu}. \tag{16}$$

Using the[23] value 8.75×10^6 for A

$$\kappa(\nu_0) = 1.64 \times 10^{-4} n/\Delta\nu. \tag{17}$$

The Doppler half breadth, by Eq. (6), is

$$\Delta\nu = 5.97 \times 10^7 T^{1/2} \tag{18}$$

and since the mercury vapor pressure in the experiments was that of the liquid at 28°C, namely 0.00236 mm

$$n = 2.295 \times 10^{16}/T. \tag{19}$$

Whence finally

$$\kappa(\nu_0) l = 1.04 \times 10^5 T^{-3/2}. \tag{20}$$

[22] Ruark and Urey, *Atoms, Molecules, and Quanta*, p. 60.

[23] Ladenburg and Wolfsohn, Zeits. f. Physik **65**, 207 (1930).

Thus P may be calculated at each temperature through Eqs. (20), (12), (4), (3), (2), and (1). The course of the calculation is indicated in the following table.

TABLE IV.

$T°K$	$\kappa(\nu_0)l$	$I(l)/I(0)$	C	λ	P
301	19.9	0.0158	4.15	1.273	0.761×10^6
374	14.4	0.0233	3.76	1.251	0.882×10^6
486	9.7	0.0375	3.29	1.216	1.058×10^6

A rough justification of the assumption that our cell is a fairly good approximation to an infinite plane slab may be obtained from the figures of Table IV. Our method depends on the fact that the rim is relatively farther than the face of the cell so that a quantum of radiation has less chance of escaping there. Hence, we should consider the situation at the highest temperature, where the transmission is greatest, to strengthen the argument. The value of $\kappa(\nu_0)\ l$ at 1.65 cms is 9.7 whence at 2.16 cm, the radius of the cell, it would be 12.7. Now consider points on the axis of the cell. A rough interpolation gives $I(l)/I(0)=0.028$ for $\kappa(\nu_0)l=12.7$ and this is the chance of a quantum going far enough unabsorbed to escape at the rim. The solid angle is roughly $2\pi\times2.16\times1.65/2.16^2=4\pi\times0.38$. Thus the total probability of a quantum emitted at the axis of the cell escaping at the rim is $0.028\times0.38=0.0106$.

Now the probability of a quantum being emitted by a 1-atom in time dt is $A\,dt$, and the probability of a quantum escaping from an infinite plane slab is $P\,dt$, whence the probability of an already emitted quantum escaping from the slab is $P/A=1.058\times10^6/8.85\times10^6=0.12$. Thus the added probability of escape due to the cylindrical shape of the cell, for quanta emitted close to the axis, where observations are made, is only one tenth of the total. This affords justification for the belief that the assumption is a good one, involving at least no greater error than the use of Milne's theory.

Hyperfine Structure and the Polarization of Mercury Resonance Radiation

By ALLAN C. G. MITCHELL
Department of Physics, New York University, University Heights

(Received April 28, 1932)

The general theory of the calculation of the polarization of resonance radiation is discussed for the case when hyperfine structure has to be considered. The polarization of mercury resonance radiation is computed for various orientations of electric vector and magnetic field, use being made of the hyperfine structure data of Schüler and his collaborators. The polarization of the stepwise radiation of mercury is also calculated and the results compared with the experiments of Richter. Fair agreement between theory and experiment is found. von Keussler's method of calculating the polarization is discussed and it is shown that his method leads to incorrect results.

SINCE the recent analysis of the hyperfine structure of mercury by Schüler and Keyston[1] and Schüler and Jones[2] several writers have made use of these data to calculate the polarization to be expected for the resonance radiation of mercury and for lines excited in stepwise radiation. Thus Larrick and Heydenberg[3] and von Keussler[4] have calculated the polarization to be expected for the resonance line λ2537 of mercury, have compared their results with the experiments of von Keussler[5] and Olson[6], and have found good agreement between theory and experiment. Further von Keussler made the calculation for the separate hyperfine structure components of λ2537, which he found to be in substantial agreement with the experiments of Ellett and McNair[7], and also for the polarization of the stepwise lines in mercury as observed by Richter[8].

Larrick and Heydenberg have carried through the calculation for the case in which the resonance tube is in a zero magnetic field, or in which it is in a magnetic field parallel to the electric vector of the exciting light. The case in which the magnetic field is perpendicular to the electric vector of the exciting light was not considered. von Keussler, on the other hand, did not correctly take into account the relative populations of the upper Zeeman levels of the several hyperfine structure components and was led thereby to erroneous conclusions.

It is the purpose of this paper to review the general method for obtaining theoretically the polarization of any resonance line showing hyperfine structure and to apply it to the problem of mercury resonance radiation and stepwise radiation in mercury.

[1] Schüler and Keyston, Zeits. f. Physik **72,** 423 (1931).
[2] Schüler and Jones, Zeits f. Physik **74,** 631 (1932).
[3] Larrick and Heydenberg, Phys. Rev. **39,** 289 (1932).
[4] v. Keussler, Zeits. f. Physik **73,** 565 (1932).
[5] v. Keussler, Ann. d. Physik **82,** 793 (1927).
[6] Olson, Phys. Rev. **32,** 443 (1928).
[7] Ellett and McNair, Phys. Rev. **31,** 180 (1928).
[8] Richter, Ann. d. Physik **7,** 293 (1930).

General Method

A general method for calculating the polarization of resonance radiation has been given by Van Vleck[9] and applied by the writer[10] to the case of cadmium resonance radiation in which hyperfine structure is involved. To carry out the calculation one usually assumes that the resonance tube is in a magnetic field strong enough to separate the Zeeman levels for each hyperfine structure component but still not strong enough to cause Paschen-Back effect of hyperfine structure. The Zeeman transition diagrams for each hyperfine structure component must then be drawn and the relative transition probabilities for each Zeeman component computed from the usual sum rules. These relative transition probabilities must now be readjusted in such a way that the chance of leaving any magnetic sublevel of any hyperfine structure component will be the same for all such levels. This assumption, equivalent to the statement that the mean life of any upper magnetic sublevel is the same for each such level of any hyperfine structure component, has been justified theoretically. Such a procedure serves to place the absorption coefficients and relative emission intensities of the various Zeeman components of the resonance radiation on a correct scale so that there is no further need for consideration of relative intensities of lines coming from various magnetic states.

Hyperfine structure is ascribed to the spin moment $\boldsymbol{i}$ of the nucleus of a given atom. This nuclear moment vector $\boldsymbol{i}$ then combines with the spin and orbital angular momentum vector of the electrons $\boldsymbol{j}$ to form the total angular momentum of the atom $\boldsymbol{f}$ ($\boldsymbol{f}=\boldsymbol{i}+\boldsymbol{j}$). Thus, for a given electronic state j there may be several hyperfine structure states with different values of f. Each of these states splits into $2f+1$ states in a magnetic field. It is found further that the value of the nuclear moment i is dependent on the isotopic constitution of any given element. Thus, isotopes of even atomic weight usually show no nuclear moment and those of odd atomic weight show some multiple of $\frac{1}{2}$.

If a resonance tube containing a vapor of an element consisting of various isotopes is radiated by a light source containing this element, the intensity distribution of the resonance radiation will depend on the intensity distribution of the light from the source, the relative number of atoms of different isotopic constitution in the resonance lamp, and on the absorption coefficient for the light of a given frequency.

In order to include both resonance radiation, in which an atom goes from a lower level to an upper level under absorption of frequency ν and returns to the same level under emission of light of the same frequency, and other types of radiation, in which it returns to other lower levels with emission of a different frequency, one may consider the following diagram.[11] The atom, originally in one of the hyperfine states (f', j_0), absorbs radiation of intensity I_ν

[9] Van Vleck, Proc. Nat. Acad. Sci. **11**, 612 (1925).

[10] Mitchell, Phys. Rev. **38**, 473 (1931). See however a correction by Ellett and Larrick, ibid. **39**, 294 (1932).

[11] The writer is indebted to Professor G. Breit for this method of presentation.

$[I(f''', j_1; f', j_0)]$, reaches the upper state (f''', j_1), and returns with emission of light to the state (f'', j_2). The number of atoms of isotope A, having a nuclear spin i_A, in the lower state f_A is

$$N = \frac{(2f_A + 1)N_A}{(2j_0 + 1)(2i_A + 1)}.$$

Since to every level f_A there are $2f_A+1$ magnetic levels, the number of atoms of isotope A in any such level is

$$N_{m'} = \frac{N_A}{(2j_0 + 1)(2i_A + 1)}.$$

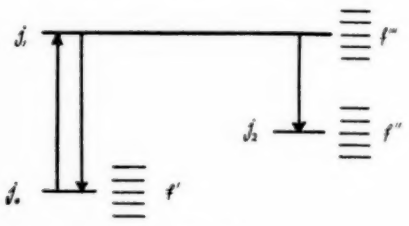

Fig. 1.

Let the transition probability between a magnetic sublevel $m'(f_A', j_0)$ of a hyperfine level f_A' of j_0 to a magnetic sublevel $m'''(f_A''', j_1)$ of a hyperfine level f_A''' of j_1 be for a π component

$$\gamma(m', f_A', j_0; m''', f_A''', j_1),$$

and for a σ component

$$\Gamma(m', f_A', j_0; m''', f_A'''j_1).$$

If the resonance tube be situated in a magnetic field making an angle θ with the electric vector of the exciting light, then the chance of reaching a given upper magnetic level $(m'''f_A'''j_1)$ by the absorption of π and σ components, respectively, is proportional to

$$N_{m'}I(f_A''', j_1; f_A', j_0)\gamma(m'f_A'j_0; m'''f_A'''j_1)\cos^2\theta$$

$$\tfrac{1}{2}N_{m'}I(f_A''', j_1; f_A', j_0)\Gamma(m'f_A'j_0; m'''f_A'''j_1)\sin^2\theta.$$

If the radiation is observed at right angles to the direction of the exciting beam and to the plane of the magnetic field, and if ξ and η are the intensities of radiation polarized along and perpendicular to the direction of the field, respectively, then for the contribution to the intensity from the upper level $(m'''f_A'''j_1)$ we have (omitting the common factor $2j_0+1$)

$$\xi_A = kI(f_A'j_0; f_A'''j_1)\frac{N_A}{2i_A + 1}\gamma(m'''f_A'''j_1; m''f_A''j_2)\{\gamma(m'f_A'j_0'; m'''f_A'''j_1)\cos^2\theta + \tfrac{1}{2}\Gamma(m'f_A'j_0; m'''f_A'''j_1)\sin^2\theta\}$$

and

$$\eta_A = \tfrac{1}{2}k\frac{N_A}{2i_{A+1}}I(f_A'j_0;\, f_A'''j_1)\Gamma(m'''f_A'''j_1;\, m''f_A''j_2)$$
$$\left\{\gamma(m'f_A'j_0;\, m'''f_A'''j_1)\cos^2\theta + \tfrac{1}{2}\Gamma(m'f_A'j_0;\, m'''f_A'''j_1)\sin^2\theta\right\}.$$

For the total intensity in each direction one must sum over all magnetic levels, hyperfine levels and isotopes.

$$\xi = k\sum_{ABC\cdots}\sum_{f'f''f'''} I(f_A'j_0;\, f_A'''j_1)\frac{N_A}{2i_A+1}\sum_{m''',m'',m'}\left\{\gamma(m'''f_A'''j_1;\, m''f_A''j_2)\right.$$
$$\left.\cdot\left[\gamma(m'f_A'j_0;\, m'''f_A'''j_1)\cos^2\theta + \tfrac{1}{2}\Gamma(m'f_A'j_0;\, m'''f_A'''j_1)\sin^2\theta\right]\right\} \qquad (1)$$

$$\eta = \tfrac{1}{2}k\sum_{A,B,C\cdots}\sum_{f',f'',f'''} I(f_A'j_0;\, f_A'''j_1)\frac{N_A}{2i_A+1}\sum_{m''',m'',m'}\left\{\Gamma(m'''f_A'''j_1;\, m''f_A''j_2)\right.$$
$$\left.\cdot\left[\gamma(m'f_A'j_0;\, m'''f_A'''j_1)\cos^2\theta + \tfrac{1}{2}\Gamma(m'f_A'j_0;\, m'''f_A'''j_1)\sin^2\theta\right]\right\}. \qquad (2)$$

The polarization is then given by

$$P = \frac{\xi - \eta}{\xi + \eta}.$$

The Polarization of Mercury Resonance Radiation (λ2537)

In order to explain the hyperfine structure of mercury, Schüler and Keyston assumed that the even atomic weight isotopes ($N_x = 69.88$ percent of an ordinary mixture) show no nuclear moment, the isotope of atomic weight 199 ($N_{199} = 16.45$ percent) shows a moment $i = \frac{1}{2}$, and that of atomic weight 201 ($N_{201} = 13.67$ percent) shows a moment $i = 3/2$. Fig. 2 shows the Zeeman transition diagrams for the various hyperfine structure states. Below each line are given the adjusted transition probabilities and at the right of each upper level is given the population per unit light intensity per atom in each lower level. To conserve space only half of the transitions for the odd atomic weight isotopes are given.

The resonance line of mercury shows five hyperfine structure components. As may be seen from Fig. 3 the lines from the even isotopes do not all come at the same wave-length and furthermore lines from some isotopes may coincide with lines from others. The numbers next each line give the relative intensity of each component as observed by Schüler and Keyston and the wave-length separations in milliangstroms are given below.

In the practical problem of observing the polarization of resonance radiation the exciting light source is usually run at fairly high current density. This means that the vapor pressure in the arc is high enough so that some of the radiation is absorbed by cold atoms near the walls. This tends to make the intensity of all the hyperfine structure components about equal. If the current in the arc is kept very low, the intensity distribution tends more toward the theoretical intensities. These two conditions are usually designated by *broad line* and *narrow line* source respectively.

The calculation has therefore been carried out for these two cases. For the broad line condition formulae (1), (2), and (3) are used and $I(f_A'j_0; f_A'''j_1)$ is made the same for every term of the sum. For the narrow line source, the intensities of the components as given in Fig. 3, together with the number of atoms of a given kind capable of absorbing these frequencies, are used.

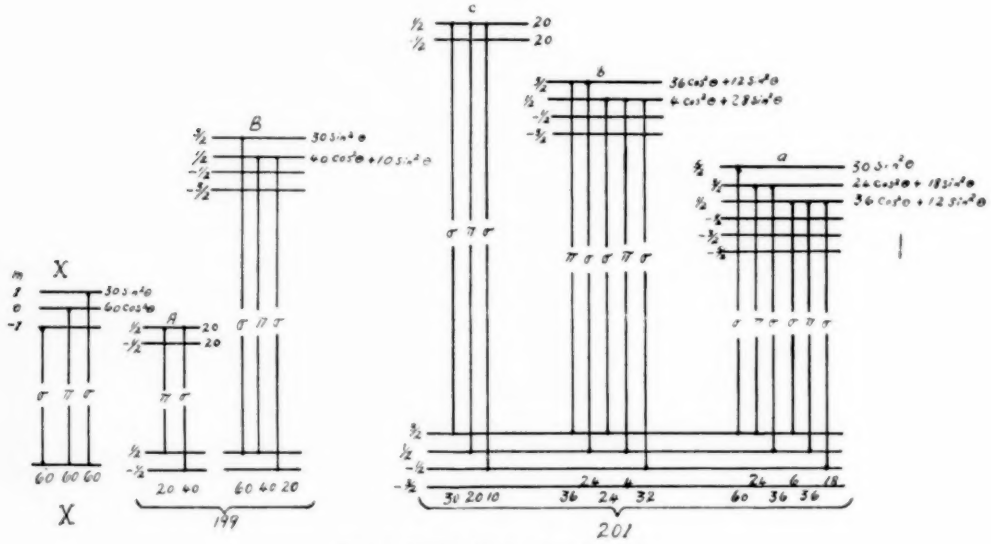

Fig. 2. Hyperfine levels of λ2537.

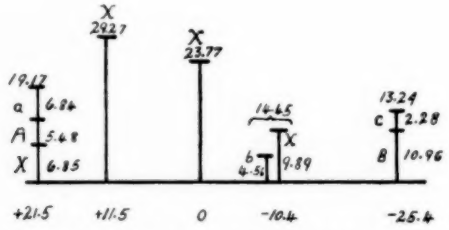

Fig. 3. Hyperfine structure of λ2537.

The results of the calculation are given in Table I for the cases in which the electric vector of the exciting light is parallel ($\theta=0$) or perpendicular

TABLE I. *Polarization of mercury resonance radiation*

Excitation	Polarization (percent)	
	$\theta=0$	$\theta=\pi/2$
Broad line	84.7	73.5
Narrow line	88.7	81.2

($\theta=\pi/2$) to the field. If the experiment is performed in the absence of a magnetic field, spectroscopic stability insures that the correct value will be given by placing $\theta=0$.

The results are in substantial agreement with experiment. von Keussler[5] using a broad line source, found 79.5 percent polarization, while Olson[6] varied the current in his source and found 79 percent with a current of 3.5 amperes, 84 percent at 1 ampere, and 86 percent at 0.4 amperes. Both experiments were performed in a zero magnetic field.

The results of Table I are, of course, in agreement with those of Larrick and Heydenberg who used the same method, but not in agreement with the calculations of von Keussler[4] who obtained 83.4 percent polarization for $\theta=0$. This descrepancy, although not large, is due to a fundamentally incorrect method of calculation as will be shown later.

Polarization of the Separate Hyperfine Structure Components of λ2537

Ellett and McNair[7] measured, by means of a Wollaston prism and a Lummer plate, the polarization of the five hyperfine structure components of the resonance line λ2537 separately. They showed that the three inner components (11.5, 0, −10.4 m.A.) were practically completely polarized, whereas the two outer components showed incomplete polarization. Recently Ellett[12] measured the polarization of resonance radiation containing only the two outer components and found the degree of polarization to be not more than 60 percent.

Table II gives the results of the calculation by the methods outlined above for a case in which the source shows broad lines and when the experiment is carried out in a zero magnetic field.

Table II.

Component	Polarization in percent	
	This method	von Keussler's method
21.5	55.9	54.3
11.5	100	100
0.0	100	100
−10.4	84.8	76.4
−25.4	51.4	51.4

The two components 11.5 and 0.0 show 100 percent polarization as would be expected since they arise from isotopes that show no nuclear spin. As an example of the use of formulae (1) to (3) the calculation of the polarization of the 21.5 m.A. component will be carried out in detail. Fig. 3 shows that this component is made up of the three components I_x, I_A, and I_a of Fig. 2. The polarization will then be given by

$$P=\frac{(450I_xN_x+63I_aN_{201})(3\cos^2\theta-1)}{450I_xN_x(\cos^2\theta+1)+200I_AN_{199}+9I_aN_{201}(7\cos^2\theta+31)}.$$

Substituting $I_x=I_A=I_a$, $N_x=0.0685$, $N_{199}=0.1645$, and $N_{201}=0.1367$, and $\theta=0$, one obtains the result given in the table.

[12] Ellett, Phys. Rev. **37**, 216 (1931).

The results of the calculation are in good agreement with experiment. Owing to the difficulties of the experiment the deviation of the -10.4 m.A. component from 100 percent would not be expected to be observed.

Polarization of Stepwise Radiation

Richter radiated a mixture of mercury vapor and nitrogen with polarized light containing all the lines of the mercury spectrum and observed the radiation given off from the resonance tube in a direction at right angles to the exciting light beam for polarization. He confined his measurements to the visible triplet (λ4047, λ4358, λ5461) from the 7^3S_1 state, and the ultraviolet

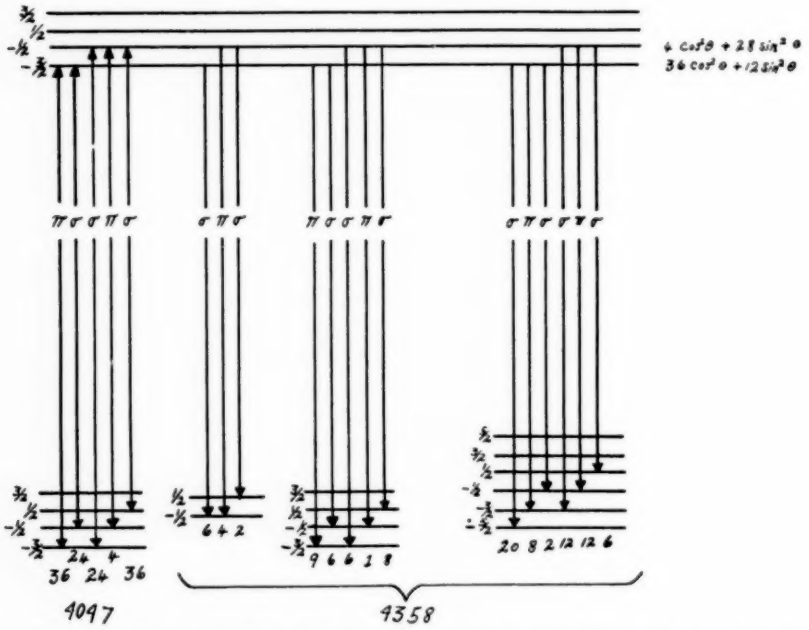

Fig. 4. Excitation of stepwise lines λ4047, λ4358 from isotope 201, upper level $f=3/2$.

triplet (λ2967, λ3131, λ3663) from the 7^3D_1 state, and found these lines to show various degrees of polarization. In order to reach these higher states, normal mercury atoms must absorb λ2537, reach the 6^3P_1 state, be transferred to the 6^3P_0 state by collision with nitrogen, and absorb either λ4047 ($6^3P_0 - 7^3S_1$) or λ2967 ($6^3P_0 - 7^3D_1$) from the arc.

The calculation of the polarization of these lines will be carried out for a broad line source. One must first find the relative number of atoms in any sublevel $(m', f_A' j_0)$ of the 6^3P_0 state at any time. During the excitation to the 6^3P_1 state the relative number of atoms of a given isotopic kind reaching the upper state will be directly proportional to the relative abundance of isotopes in the ground state. Assuming that the mean radiation life for each hyperfine structure component is the same and that the chance of being brought to the 6^3P_0 state by collision with nitrogen is the same for all isotopes, it follows that the relative number of isotopes in the 6^3P_0 state after the process will

be the same as that in the ground state. It must be assumed further that collision with nitrogen leads to an equal distribution of atoms among the magnetic sublevels of a given hyperfine state. Since 6^3P_0 has the same structure as the ground state the distribution of atoms among the magnetic sublevels can be taken to be the same as in the ground state.

On account of the many levels involved, the complete level scheme for these transitions can not be given here. As an example, however, the diagram for the excitation of the $f=3/2$ state of the 7^3S_1 state for the isotope 201 is given in Fig. 4. The state is reached by the absorption of one of the hyperfine structure components of 4047 and from it are radiated the three visible lines. The transition[13] probabilities are given at the foot of the diagram and the relative population of each upper level on the right. The transitions for the line λ5461 are not shown.

Richter measured the polarization of the stepwise lines in the two cases $\theta=0$ and $\theta=\pi/2$. A comparison between his experimental results (the mean of all observations for a given orientation of field and electric vector) and calculated values of the polarization is given in Table III. In column 5 of

TABLE III. *Polarization of stepwise radiation*

$7^3S_1-6^3P_{0,1,2}$

Line	Condition	Polarization in percent Observed	Calculated	v. Keussler
λ4047	$\theta=0$	72 ± 6	84.7	83.4
	$\theta=\pi/2$	56 ± 14	73.5	
λ4358	$\theta=0$	49 ± 6	44.6	71.5
	$\theta=\pi/2$	22 ± 4	18.2	
λ5461	$\theta=0$	13 ± 1	3.44	8.7
	$\theta=\pi/2$	8.5 ± 1	3.66	

$7^3D_1-6^3P_{0,1,2}$

Line	Condition	Polarization in percent Observed	Calculated	v. Keussler
λ2967	$\theta=0$	67 ± 7	84.7	83.4
	$\theta=\pi/2$	37 ± 7	73.5	
λ3131	$\theta=0$	29 ± 7	44.6	71.5
	$\theta=\pi/2$	25 ± 1	18.2	
λ3663	$\theta=0$	42 ± 4	3.44	8.7

[13] The adjusted transition probabilities are not given for the hyperfine structure components of λ4358 and λ5461. The adjustment of the figures given (relative transition probabilities) to make the transition probability from any upper magnetic sublevel the same for all such levels is best accomplished during the calculation by using

$$\frac{\gamma(m'''f_A'''j_1;\ m''f_A''j_2)}{\gamma(m'''f_A'''j_1;\ m''f_A''j_2)+\Gamma(m'''f_A'''j_1;\ m''f_A''j_2)} \quad \text{and} \quad \frac{\Gamma(\ )}{\gamma(\ )+\Gamma(\ )}$$

for each Zeeman component in question instead of γ or Γ as given in Eq. (1).

the table are given von Keussler's calculated values. The following observations were obviously not included: (1) When the electric vector of the exciting light was parallel to the observation direction and the magnetic field was zero; and (2) when the magnetic field was in the direction of observation. Only the degree of polarization is given in the table without respect to the direction of the plane of polarization of the fluorescence. One might add that in all cases the calculated and observed direction of polarization are in agreement.

One may see from the table that there is fair agreement between theory and experiment for the visible lines with exception of λ5461. For the two lines λ4047 and λ4358 the decrease in polarization to be expected when the field is perpendicular to the electric vector is observed. For the line λ5461 there seems to be considerable disagreement between theory and experiment. This is probably due to the fact that such a small degree of polarization as that shown by this line is difficult to measure.

For the ultraviolet lines the agreement is not quite so good. The reason may be twofold. In the first place the hyperfine structure of these lines has not been measured, and the calculation was made on the assumption that they follow the same scheme as the visible lines. In the second place the observations are more difficult to make since the lines are weaker. The line λ3663 is seen to be in bad disagreement with theory. This may have its origin in the fact that this line is probably a composite of the three lines λ3663, λ3650, and λ3654.[14]

There still remains one point of divergence between the calculated and observed values. It will be noted that the mean of the observed values of the polarization for λ4047 lies below that calculated while for λ4358 and λ5461 the reverse is true. One would expect that the observed polarization would always lie below the calculated value due to the effect of collisions and imprisoned resonance radiation. Richter has shown, however, that the polarization of λ4047 and λ4358 is practically independent of the nitrogen pressure. The fact that the observed values of the polarization for λ4358 and λ5461 lie above the calculated might be explained if the λ4047 line in the arc were not quite a broad line. In this case one would expect the hyperfine structure components due to the even isotopes to be stronger than those due to the isotopes 199 and 201. This would result in a relative increase in the number of even isotopes in the 7^3S_1 state, and since the polarization of the components due to the even isotopes is higher than that due to the odd there would be a consequent increase in the polarization of all three lines. The effect would be a differential one, however, and would tend to increase the polarization of λ4358 and λ5461 relatively more than that of λ4047. This is due to the fact that the former lines have more hyperfine structure components coming from the upper levels of the odd isotopes than does λ4047, and these components are, in general, weakly polarized.

[14] See Mitchell, Phys. Rev. **36**, 1589 (1930).

Remark on von Keussler's Method

von Keussler calculated the polarization for the mercury lines for the case in which there is no magnetic field, using a method different from the one employed here. He considered first each hyperfine structure component separately and wrote down the relative intensities of each π and σ component of the Zeeman pattern. He then appears to have assumed that those states which are reached by the absorption of σ components alone are not excited and that those which are excited by absorption of π components are all *equally populated*. The degree of polarization for the resonance radiation from this one component would then be

$$P = (J_x - J_y)/(J_x + J_y) \tag{4}$$

where $J_x = \Sigma J_\pi$; $J_y = \Sigma J_\sigma$ (the sum of the intensities of π and σ components, respectively, emanating from upper Zeeman levels). Instead of using the polarization P as written he made use of the notion of spatial polarization defined by

$$P' = (J_x - J_y)/(J_x + 2J_y)$$

where J_x and J_y have the same significance as in (4), and the denominator is the total intensity radiated in all directions of space. Finally he assumed that the spatial polarization of a group of hyperfine structure components would be given by

$$P' = \frac{\sum_k J_k P_k'}{\sum_k J_k},$$

where J_k is the intensity of the kth component and is proportional to $(2f_k+1)/(2i_k+1)N_k$. The observed polarization is given by

$$P = \frac{3}{1 + 2/P'}.$$

The error in the method is, of course, the assumption that all of the upper magnetic levels which are reached by the absorption of π components are equally excited. This may be seen not to be true in general by inspection of Fig. 2. Table III, for the polarization of the five hyperfine structure components of $\lambda 2537$ illustrates this point. The table shows that there is agreement between von Keussler's method and the one used here for all except the two components 21.5 and -10.4 m.A. It is just these two components for which the assumption of equal population of upper magnetic levels does not hold.

The Relative Intensities of Multiplet Transitions in Complex Spectra

By C. W. UFFORD
Palmer Physical Laboratory, Princeton University

(Received April 23, 1932)

From the wave functions of the multiplets of Slater's theory of complex spectra, the relative transition probabilities of multiplet transitions have been calculated for Russell-Saunders coupling for the electron configurations $p^3s-p^2s^2$, p^3s-p^1, p^2s-p^3, $p^4s-p^3s^2$, $p^1s^2-p^5s$, p^2s-ps^2, p^4s-p^5 and the quintet transitions of d^3p-d^3s. The calculated quintet transition probabilities of d^3p-d^3s are compared with the values measured in Ti I.

I. INTRODUCTION

THE relative transition probabilities of multiplet transitions have been calculated for Russell-Saunders coupling for configurations containing only s and p electrons with more than two electrons, and for the quintet terms in the electron configuration d^3p-d^3s. The relative transition probabilities for the electron configurations $p^5p'-p^5s$ are the same as those of the simple configurations $pp'-ps$, the p^5 group, lacking one electron of being a closed shell, behaving in a manner similar to that of a single p electron. Similarly the relative transition probabilities in d^9p-d^9s are the same as those in $dp-ds$. The relative transition probabilities for these two pairs of two electron configurations found by the method of the present paper agree with those found by the method of Kronig[1] which gives the relative transition probabilities of multiplet transitions in two electron spectra.

The transition probabilities in Russell-Saunders coupling for some cases in which the jumping electron does not belong to a group of more than two equivalent electrons have been calculated by Johnson[2] by coupling the angular momentum vectors in a prescribed order.

The method used in the present paper is to find the transition probability for a single electron jump by using the wave functions of the multiplets of Slater's[3] theory of complex spectra which can be found by the methods given by Gray and Wills,[4] Wigner,[5] Bartlett,[6] or Johnson.[7] From this transition probability, the transition probability for the entire multiplet transition may be got by use of the summation rules of Ornstein and Burger given in Born and Jordan.[8]

These methods determine the wave function completely for a multiplet

[1] R. de L. Kronig, Zeits. f. Physik **33**, 261 (1925).
[2] M. H. Johnson, Jr., Phys. Rev. **40**, 133 (1932).
[3] J. C. Slater, Phys. Rev. **34**, 1293 (1929).
[4] N. M. Gray and L. A. Wills, Phys. Rev. **38**, 248 (1931).
[5] E. Wigner, Gruppentheorie, 1931, p. 206.
[6] J. H. Bartlett, Jr., Phys. Rev. **38**, 1623 (1931).
[7] M. H. Johnson, Jr., Phys. Rev. **39**, 197 (1932).
[8] M. Born and P. Jordan, Elementare Quantenmechanik, J. Springer, 1930, p. 160.

in case only one of its kind belongs to the configuration. If several multiplets of the same kind are given by a configuration, one must assume that each of them is coordinated with a parent term in the limit configuration in a definite way in order to get completely determined wave functions. Of course this assumption may break down, for it corresponds to neglect of the matrix components of the Hamiltonian connecting the two multiplets; but it frequently corresponds to a good approximation to actual conditions in the atom. It is this assumption that corresponds to the grouping of multiplets into triads, pentads, etc. in actual analyses of spectra. This assumption is used in but one place in this paper, i.e., to determine the wave functions for the two ^5D multiplets in the d^3p configuration.

II. Method of Calculating Transition Probabilities

In order to find the wave functions for the configuration d^3p or d^3s by Wigner's[5] method it is first necessary to know the functions for d^3 to which is then added a p or an s electron to give d^3p or d^3s. To find d^3, first two equivalent d electrons must be combined to give d^2; and then to d^2 a third equivalent d electron must be added. In this way the wave functions $d^3p\ ^5G$ and $d^3s\ ^5F$ are found to be:

$$d^3p^5G_{32} = \frac{1}{96^{1/2}}\left\{3^{1/2}\left|\alpha^{-1}\alpha^1\alpha^2\alpha_p{}^1\right| + \left|\alpha^0\alpha^1\alpha^2\alpha_p{}^0\right|\right\}$$
$$d^3s^5F_{32} = \frac{1}{24^{1/2}}\left|\alpha^0\alpha^1\alpha^2\alpha_s\right|, \tag{1}$$

where the subscript 3 of $^5G_{32}$ is the z component, m_L, of the total orbital angular momentum, L; and the subscript 2 is the z component, m_S, of the total spin angular momentum, S. α^{m_l} represents the central field wave function of a d electron with $m_s = \frac{1}{2}$, β^{m_l} a d electron with $m_s = -\frac{1}{2}$; and the superscript, m_l, gives the z component of the orbital angular momentum, l, of the electron. The s and p electrons are distinguished by a subscript from the three d electrons. Each term in the linear combination going to make up the wave functions is a determinant of the central field wave functions of single electrons since any complete wave function must be antisymmetric. The first letter in each determinant corresponds to the first electron, the second letter to the second electron, etc. Thus $\left|\alpha^{-1}\alpha^1\alpha^2\alpha_p{}^1\right| = -\left|\alpha^1\alpha^{-1}\alpha^2\alpha_p{}^1\right|$.

Now the transition probability[9] between these states depends on the quantity P given by

$$P = \int d^3p^5G_{32}r\overline{d^3s\ ^5F_{32}}d\tau', \tag{2}$$

where r is the sum of the radius vectors of the four electrons, and $d\tau'$ indicates integration over the three coordinates of each of the four electrons and summation over the spins. Because of the orthogonality of the central field wave functions, this integral vanishes[10] unless three of the electrons in

[9] See for example E. U. Condon and P. M. Morse, Quantum Mechanics, McGraw-Hill, 1929, p. 100.

[10] E. U. Condon, Phys.Rev. **36**, 1131 (1930).

$d^3p\ {}^5G_{32}$ agree in all their quantum numbers with those of $d^3s\ {}^5F_{32}$, and unless for the fourth electron $\Delta m_s = 0, \Delta m_l = 0, \pm 1$ and $\Delta l = \pm 1$. This gives:

$$P = \frac{1}{96^{1/2}} \frac{1}{24^{1/2}} \int \left| \alpha^0\alpha^1\alpha^2\alpha_p{}^0 \right| r \left| \overline{\alpha^0\alpha^1\alpha^2\alpha_s} \right| d\tau'. \tag{3}$$

Now each term in the first determinant times the second determinant yields 24 integrals. However, each of the 24 terms in the first determinant yields the same 24 integrals so that the integral becomes:

$$P = \tfrac{1}{2} \int \alpha^0\alpha^1\alpha^2\alpha_p{}^0 r \left| \overline{\alpha^0\alpha^1\alpha^2\alpha_s} \right| d\tau'. \tag{4}$$

The component coordinate of r for which the integral does not vanish is determined by the change in m_l. Since $\Delta m_l = 0$ in this case, all integrals except the one involving the z component of r for the unequal electrons vanish. Also the first three electrons in the term from the determinant must equal those in the term from $d^3p\ {}^5G_{32}$ giving:

$$P = \tfrac{1}{2} \int \alpha_p{}^0 z \bar{\alpha}_s d\tau, \tag{5}$$

as the integration over the coordinates of the first three electrons gives 1 on account of the normalization of the central field wave functions.

To find the total transition probability of the multiplet transition, the sum must be taken over all allowed transitions between the different values of m_L for each multiplet. This sum is given by the rules of Ornstein and Burger[8] with j replaced by L for Russell-Saunders coupling.

In addition to the factors given by Ornstein and Burger, there must be a factor $2S+1$ to express the result of summing over the different values of m_S. Thus for $d^3p\ {}^5G_{32} - d^3s\ {}^5F_{32}$,

$$J^{L,L-1} = (2S+1) \frac{L(2L-1)(2L+1)}{L^2 - m_L{}^2} J^{L,L-1}(m_L, m_L), \tag{6}$$

or on substituting $L = 4$, $m_L = 3$ and $S = 2$,

$$J^{4,3} = 45 \left[\int \alpha_p{}^0 z \bar{\alpha}_s d\tau \right]^2, \tag{7}$$

where $J^{L,L-1}$ represents the total transition probability for a multiplet transition in which L changes from L to $L-1$, and $J^{L,L-1}(m_L, m_L)$ represents the transition probability where the total orbital angular momentum L changes from L to $L-1$ with m_L remaining unchanged. $J^{L,L-1}(m_L, m_L)$ is proportional to the square of the quantity P in Eq. (5).

III. Theoretical Relative Transition Probabilities

Following the general method of section 2, the relative transition probabilities for all configurations involving s and p electrons (except those for which the Kronig rules suffice for a complete determination of the relative

transition probability) have been calculated. The results are given in Tables I to IV. The intersystem transitions forbidden by the selection rule for the spin quantum number, $\Delta S=0$, are marked x, and those forbidden by the selection rule for total orbital angular momentum, $\Delta L=0, \pm 1$, are marked y. There are as yet no experimental measurements of intensities with which these theoretical formulas can be compared.

TABLE I. *Relative multiplet transition probabilities in Russell-Saunders coupling for the transitions p^2s-ps^2 and p^4s-p^5.*

	p^2s or p^4s			
ps^2 or p^5		^2S	^2P	^2D
	^2P	1	9	5

TABLE II. *Relative multiplet transition probabilities in Russell-Saunders coupling for the transition $p^4s^2-p^5s$.*

	p^4s^2			
		^3P	^1D	^1S
p^5s	^3P	9	x	x
	^1P	x	5	1

TABLE III. *Relative multiplet transition probabilities in Russell-Saunders coupling for the transitions p^2s-p^3 and $p^4s-p^3s^2$.*

	p^2s or p^4s				
		^4P	^2D	^2P	^2S
p^3	^4S	12	x, y	x	x
or	^2D	x	15	15	y
p^3s^2	^2P	x	5	9	4

TABLE IV. *Relative multiplet transition probabilities in Russell-Saunders coupling for the transitions $p^3s-p^2s^2$ and p^3s-p^4.*

	p^3s					
		^3S	^3P	^3D	^1P	^1D
p^2s^2	^3P	12	9	15	x	x
or	^1S	x	x	x	4	y
p^4	^1D	x	x	x	5	15

IV. COMPARISON WITH OBSERVED INTENSITIES

In view of the scarcity of experimental measurements of relative intensities of multiplet transitions in complex spectra at present, it was not considered worth while to work out the transition probabilities for the more complicated configurations. However, the measurements of Harrison and Engwicht[11] of the strong quintets arising from d^3p to d^3s in Ti I are suitable for a test of the theory, so that this case will now be considered in detail.

In these configurations, the quintet triads of d^3p and monads of d^3s, which result from adding a p and an s electron respectively to the several multiplets of the d^3 configuration of Ti II, are well separated. It is therefore significant to regard the two ^5D's of d^3p as having definite parentage in the d^3 configuration. This assumption leads to vanishing transition probabilities between multiplets in d^3p and d^3s which have different parents in d^3.

That such multiplet transitions are actually very weak relative to the others is shown even by the rough intensity data in Russell's[12] analysis of Ti I. They are not entirely absent, however, indicating some departure from the condition of exact parentage assignment for the multiplets in d^3p and d^3s. The intensities of these weak multiplet transitions were not measured by Harrison and Engwicht so for them only a very rough indication of their intensities can be given by converting the visual estimates into approximate

[11] G. R. Harrison and H. Engwicht, J.O.S.A. and R.S.I. **18,** 287 (1929).
[12] H. N. Russell, Astrophys. J. **66,** 283 (1927).

relative intensities by using Russell's[13] empirical rule that intensity varies as the square root of numbers assigned on the visual scale.

The experimental data used here are those of Harrison and Engwicht[11] to which small corrections have been applied according to the ideas of Harrison and Johnson[14] to allow for the slight alterations produced by the partial break-down of Russell-Saunders coupling, which permits weak transitions between multiplets of differing multiplicity.

In this work the most difficult point, in attempting to infer relative transition probabilities from the observed intensities, is that which refers to the relative numbers of atoms in the initial states under the actual conditions of excitation in the source. This was an arc, and the conditions are certainly not those corresponding to thermal equilibrium at any definite temperature. Nevertheless in the absence of any better way to treat the data, Harrison and his co-workers have adopted the procedure of correcting approximately for the distribution of atoms in various initial states by supposing it to correspond to thermal equilibrium at a temperature T, that is, that the number in an initial state of energy E_i and of statistical weight, g_i is proportional to

$$g_i e^{-E_i/kT}.$$

The question is then whether the observed intensities correspond to theoretical transition probabilities with a reasonable supposition as to T.

The situation is presented in Fig. 1. In Fig. 1a, the relative transition probabilities are plotted as ordinates against various assumed values of T. The points are the values obtained from the experimental data. The points are joined by vertical lines with the theoretical values with which they should agree. It will be seen that the order of increasing transition probabilities obtained theoretically agrees with experiment for all values of T in the range considered. The experimental values have been multiplied by a factor to make their sum equal to the sum of the theoretical values.

In Fig. 1b, the relative transition probabilities of different multiplet transitions associated with each triad are compared with their theoretical ratios. Here the experimental values are multiplied by a factor to make the middle component of each triad agree with the theoretical values. The agreement is quite good for $T = 10{,}000°\text{K}$.

In Fig. 1c, the ratio of the total transition probability for the two triads, as inferred from the measured intensities for several assumed values of T, is compared with the theoretical value which is $7/3$. This ratio is more sensitive to the assumed temperature of the arc than the relative transition probabilities within each triad because the two triads are separated by about 5700 wave numbers, whereas adjacent multiplets within a triad are separated by at most 2000 wave numbers. Fig. 1c shows that at 10,000°K the triad with the lower initial state is almost twice as strong as it should be. This probably indicates a departure from the assumed equilibrium distribution in the arc. Also the two limit terms d^3b^4F' and d^3a^4P' in Ti II lie exceptionally

[13] H. N. Russell, Proc. Nat. Acad. Sci. **11**, 322 (1925).

[14] G. R. Harrison and M. H. Johnson, Jr., Phys. Rev. **38**, 757 (1931).

close to other limit terms of the same species coming from d^2s, so that the possibility of perturbation is by no means to be excluded.

For each multiplet involved in these transitions, the wave number separation of the term with the highest J value from the term in Ti I with lowest energy, $d^2s^2a^3F_2'$, is given in Fig. 1d.

It is a pleasure to thank Professor E. Wigner for his constant assistance throughout these calculations, and Professor H. N. Russell and Professor E. U. Condon for their many helpful suggestions.

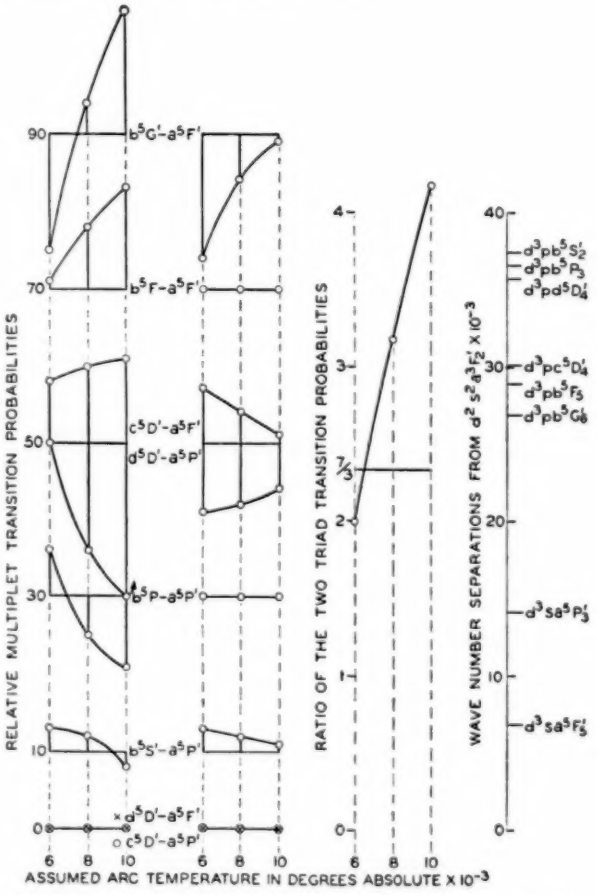

Fig. 1a Fig. 1b Fig. 1c Fig. 1d

Fig. 1. Relative multiplet transition probabilities and term values. The horizontal lines in Figs. 1a, 1b and 1c represent the theoretical values. The circles are the experimental points, each point being joined by a vertical line to the theoretical value with which it should agree. In Fig. 1a, the experimental values for each temperature have been multiplied by a factor to make their sum agree with the sum of the theoretical values. In Fig. 1b, the experimental values for each triad transition have been multiplied by a factor to make the central multiplet transition probability agree with the theoretical value. The points in Fig. 1c are the ratio of the sum of the three upper points in Fig. 1a, belonging to the triad transitions with a^5F' as the lower multiplet, to the sum of the three lower points belonging to the triad transitions with a^5P' as the lower multiplet. Figure 1d gives the wave number separation of the term with the highest J value from the term $d^2s^2a^3F_2'$ in Ti I with the lowest energy, for each quintet involved in the transitions of Figs. 1a, 1b and 1c.

Photoelectric Currents in Gases between Parallel Plates as a Function of the Potential Difference

By NORRIS E. BRADBURY
Physical Laboratory, University of California

(Received May 3, 1932)

If one of two parallel plate electrodes in a gas emits photoelectrons, the current received at the collecting electrode is a function of the potential difference, the gas pressure, the initial velocity of the photoelectrons, and the mobility of the carrier. In the experiments reported here, a quartz mercury arc and a plane zinc electrode were used as the source of photoelectrons. Current:potential-difference curves were obtained for different gas pressures in hydrogen and nitrogen, and the ratio of the current, i, to the saturation current, I_0, obtained in each case. A theoretical equation of J. J. Thomson gives the relation

$$i=\frac{I_0(6\pi)^{\frac{1}{2}}kX}{C+(6\pi)^{\frac{1}{2}}kX}$$

where X is the field strength; k, the mobility of the carrier; and C, its random velocity. The validity of this equation is established by the experimental data which permit the values of the electron mobility k to be determined as a function of X/p. Values so obtained agree well with those obtained by Loeb and by Townsend and Bailey. An equation recently given by Langmuir (Phys. Rev. **38,** 1656 (1931)) is shown to be applicable only at low pressures where it yields a satisfactory value of the mean free path of the electron.

INTRODUCTION

IF ONE of two parallel plate electrodes in a gas emits photoelectrons, the current which will be received at the positive collecting electrode varies with the potential across the plates and the pressure of the gas. This phenomenon has been investigated by several observers.[1,2,3,4] It was treated theoretically by J. J. Thomson[5] in 1906 who proposed the equation

$$i=\frac{I_0(6\pi)^{1/2}kX}{c+(6\pi)^{1/2}kX}$$

in which k is the mobility of the carrier; X the field strength at which the current i is measured; c, the random velocity of the electrons; and I_0 the saturation current. Prior to 1926, however, no satisfactory comparison between theory and experiment had been made. In 1926 in this laboratory, Woolsey, in an unpublished thesis, attempted to verify this equation taking into account the electron mobility. He measured the current which passed between

[1] Stoletow, Journal de Physique **9,** 468 (1890).
[2] Schweidler, Comptes Rendus **127,** 224 (1898).
[3] Lenard, Ann. d. Physik **2,** 359 (1900).
[4] Varley, Phil. Trans. **A202,** 439 (1904).
[5] J. J. Thomson, Cond. Elec. through Gases (Cambridge University Press, Cambridge, 1928) p. 466.

two parallel plates at various potential differences and for different gas pressures, when one of the plates, of speculum metal, was illuminated with ultraviolet light. He was unable to determine accurately the saturation current; the exact interpretation to be placed upon the meaning of c was not clear; and the experiments were not conclusive.

In a recent article, Langmuir[6] proposed an equation of the form

$$i = 4I_0\lambda\phi/3a$$

in which ϕ is a function of the potential across the plates and the initial energy with which the photoelectron is liberated; λ is the mean free path of the electron in the gas; and a is the distance between the plates. Since this equation predicted a ratio of i/I_0 of a somewhat different order than that found by Woolsey, it seemed of interest to carry out the experiments with greater accuracy to determine the applicability of the above equations. Consequent to the refocussing of attention on this problem by Langmuir the meaning to be attached to c in Thomson's equation was clarified by Professor L. B. Loeb who put the equation into a suitable form for verification. The experiments in consequence were carried out under improved conditions and have led to the results reported here.

Apparatus and Procedure

The essential features of the apparatus are shown in Fig. 1. A quartz mercury arc was used as a source of ultraviolet radiation. The light from the arc was focused on the plate by means of quartz lenses and passed through a plane quartz window sealed to the chamber by a Pyrex-quartz graded seal. The plates and supports were entirely of zinc save for the tungsten-Pyrex leads. The upper plate was surrounded by a grounded guard ring and equipotential vanes were inserted midway between the plates to maintain a uniform field. The upper collecting plate, to which was connected the electrometer system, thus received only electrons which had traveled in a uniform field. The area of the collecting plate was 20.9 cm and the plates were 3.00 cm apart. They were kept parallel during the glass blowing by an accurate spacing block.

Potentials were applied to the lower plate by means of a bank of storage cells. The equipotential vanes were connected to the midpoint of a 100,000 ohm resistance inserted between the lower plate and ground. Field strengths as high as 300 volts/cm could be employed.

Hydrogen and nitrogen were chosen as the gases to be studied as they do not attach electrons when adequately purified. The purification was carried out in the manner previously described for the mobility experiments in pure gases. The chamber could be evacuated to better than 10^{-6} mm for determining the saturation current and before filling with purified gas.

The procedure in the experiments was carried out as follows. After the polished and cleaned zinc plates had been allowed to come into equilibrium with the gas to be studied, the chamber was pumped out and the saturation

[6] Langmuir, Phys. Rev. **38**, 1656 (1931).

current determined. The chamber was then filled to the desired pressure with pure gas, and the current:potential-difference curve taken for the range of potentials between zero and as high as conditions permitted. The chamber was then re-evacuated and the saturation current again determined. The agreement of this value with the one taken at the beginning of the experiment was considered sufficient evidence that the photoelectric effect had not varied during the course of the measurement.

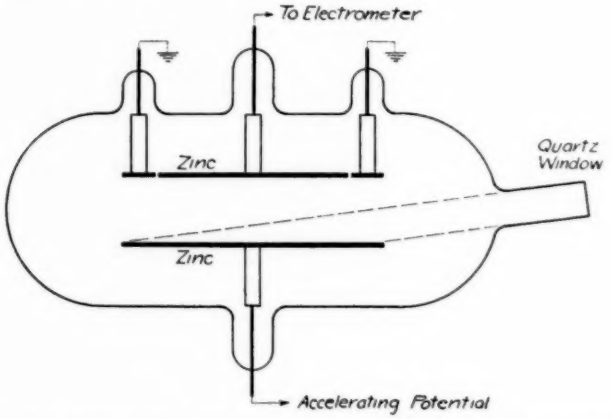

Fig. 1. Diagram of chamber showing plane parallel zinc electrodes.

Experimental Results

A series of curves for hydrogen at different pressures is shown in Figs. 2 and 3. Curve *A* was taken with the highest attainable vacuum. The lack of saturation at the lower values of *V* is due to the finite size of the collecting

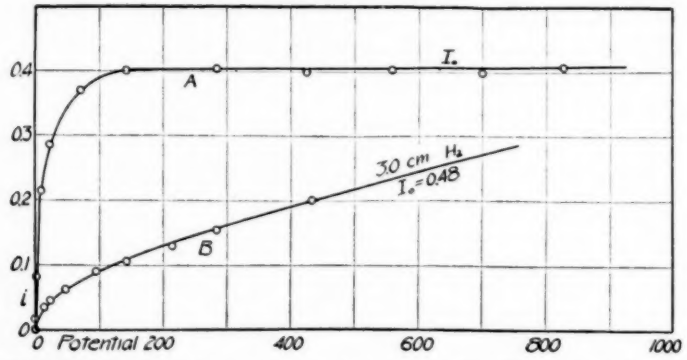

Fig. 2. Saturation current in vacuum and at 3.0 cm H_2. The current is in arbitrary units and the potentials in volts.

electrode and the random direction of emission of the photoelectrons from the cathode. Curve *B* is that obtained for hydrogen at 3 cm and *C* for hydrogen at 9.5 cm. Curves *D*, *E*, are for 33 and 67 cm hydrogen respectively. Fig. 4 shows curves for hydrogen at 1 mm pressure and at 2 mm pressure. Curves were also taken in nitrogen at 33 cm and 67 cm pressure. Their appearance is not greatly different from those reproduced here.

THEORETICAL

The theoretical equation developed by J. J. Thomson is of the utmost simplicity. As the electrons are ejected from the cathode by the incident light, they collide with the gas molecules above the plate. A certain number diffuse

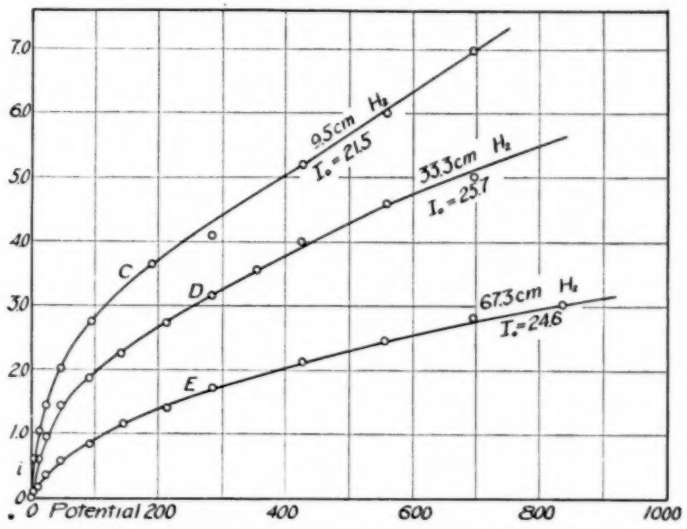

Fig. 3. Current:potential-difference curves for various pressures of hydrogen.

back to the plate in consequence and contribute nothing to the current through the gas. The resultant current is, then, that due to the total charge given off by the cathode, minus the amount returned to it by diffusion. The number of electrons which strike unit area of the plate in unit time is given by

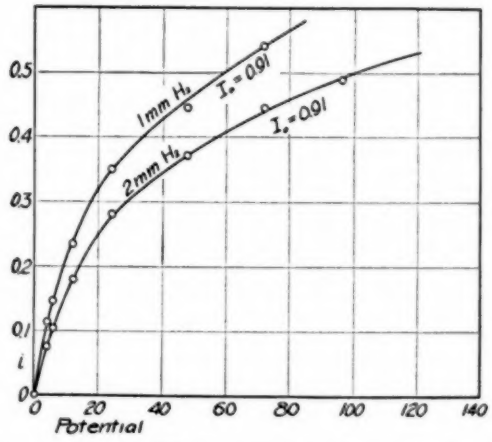

Fig. 4. Current:potential-difference curves at low pressures of hydrogen.

the expression $nc/(6\pi)^{1/2}$ where c is the root mean square velocity of translation of the electrons and n their density. Similarly the current will be given by

$$i = nekX \tag{1}$$

where k is the mobility and X the field strength. If the total number of electrons given off by the cathode be n_0, then we can write

$$n_0 e = cne/(6\pi)^{1/2} + nekX = I_0 \qquad (2)$$

Eliminating n from (1) and (2) we may write

$$i = \frac{I_0(6\pi)^{1/2}kX}{c + (6\pi)^{1/2}kX}$$

where i and I_0 represent the current at a field strength X and the saturation current respectively. We are now faced with the proper evaluation of c. Heretofore this has been considered to be either the velocity of thermal agitation of electrons in equilibrium with the gas, or the energy as deduced from field strength and mobility considerations. It is obvious, however, that the greater part of the diffusion process is going to occur in the immediate vicinity of the plate *before* the electrons have reached thermal and field equilibrium. While they are then in the vicinity of the plate, they possess, owing to the small inelasticity of their impacts with gas molecules, most of the initial energy with which they were ejected. It is this energy that determines the number of collisions made and, hence, the extent of the diffusion back to the electrode. Accordingly, it seems reasonable to assign to *c the most probable velocity with which the electrons leave the plate.* This initial energy can be easily calculated from the wave-length of the incident light and the work function of the metal. The latter constant is a source of uncertainty inasmuch as it varies quite appreciably with the condition of the surface. In these experiments it was not possible to measure the work function. Accordingly the value was taken to be 3.57 volts, as given in a table by Hughes and DuBridge.[7] The conditions of the experiments were such that the 2536A line of mercury was the only exciting radiation of importance. This, with the work function given, leads to a value of 1.29 volts for the maximum energy of emission. Since it has been shown[8] that the *most probable velocity* is approximately 0.6 that corresponding to maximum energy, the value of c has been chosen as

$$c = 0.6 \times 1.29 \times 5.94 \times 10^7 \text{ cm/sec.}$$
$$= 4.58 \times 10^7 \text{ cm/sec.}$$

With this value of c, the equation of Thomson may be put into the form

$$\frac{I_0}{i} - 1 = \frac{c}{(6\pi)^{1/2}k_0 Xp/760} = \frac{4.58 \times 10^7}{(6\pi)^{1/2}k_0 Xp/760}$$

from which it is possible to calculate the values of k_0 from the data given in Fig. 2 and 3. The values of k_0 so obtained are plotted against X/p and the results shown in Fig. 5. Similar calculations carried out for nitrogen are shown in Fig. 6. The trend of the curves is exactly that obtained by Loeb[9] and the

[7] Hughes and DuBridge, Photoelectricity (McGraw Hill, N. Y., 1932) p. 76.
[8] Lukirsky and Prilezaev, Zeits. f. Physik **49,** 236 (1928).
[9] L. B. Loeb, Kinetic Theory of Gases (McGraw-Hill, N. Y., 1927). p. 504.

absolute values differ less than might be expected from the uncertain value employed for the work function of the zinc electrode. An increase of 0.3 volt in the work function would bring them into almost exact agreement. In the case of hydrogen the measurements at low pressures enabled k_0 to be found for values of X/p as great as 20. At this point the value of k_0 was found to be 845 cm/sec per volt/cm. Townsend and Bailey[10] have studied k_0 for values of X/p as high as 0.85 where they found a value of k_0 of approximately 1600.

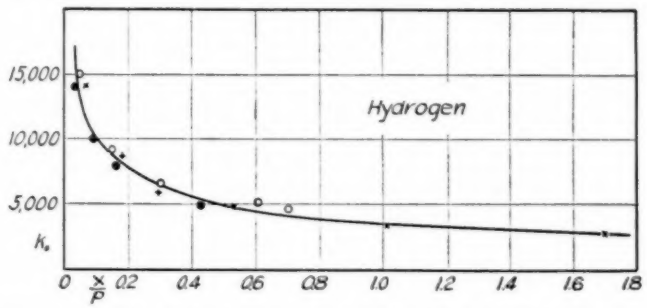

Fig. 5. Electron mobility in hydrogen as a function of X/p. The circles are values computed from data taken in hydrogen at 33.3 cm pressure; the crosses at 9.5 cm pressure; and the remaining points at 67.3 cm pressure.

As far as is known, the present measurements are the only ones that have been attempted at such high values of X/p. While, owing to the approximate nature of the calculations involving an average energy of emission and a doubtful value of the work function, too much confidence cannot be placed

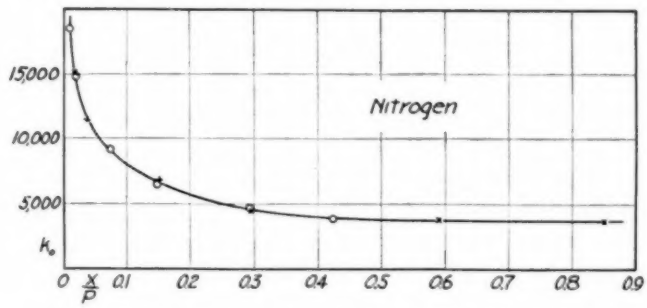

Fig. 6. Electron mobility in nitrogen as a function of X/p. The circles are values computed from data taken at 68 cm, and the crosses data taken at 33 cm.

on this procedure as a method of accurately determining electron mobilities, the method is useful in giving orientating data in this field. In any case, it is clear that the Thomson equation adequately accounts for the facts within the limitations of the calculations.

One may now turn to a test of the equation recently proposed by Langmuir. The derivation of this relation is based on a well-known diffusion equation of electrons in an electric field proposed by G. Hertz.[11] Substantially the

[10] Townsend and Bailey, Proc. Roy. Soc. **A87,** 357 (1912).

[11] G. Hertz, Zeits. f. Physik **32,** 298 (1925).

derivation is carried out on the same principles as the Thomson equation, i.e., to consider the number of electrons lost from the initial saturation current by diffusion back to the emitting electrode. The form of the equation which applies to parallel plate electrodes is given by

$$i = \frac{4}{3}\frac{I_0\lambda}{a}\frac{V}{V_0}\frac{1}{\log\left[(V+V_0)/V_0\right]}$$

where V is the potential across the plates and V_0 the energy with which the electron is ejected from the cathode, and the other symbols have been defined above. The function ϕ has been replaced by its definition in terms of V and V_0 in this equation.

In deducing this relation, however, a natural assumption is made which is barely applicable at a pressure of 1 mm in hydrogen and certainly not applicable at greater pressures. It is assumed that an electron starting out with an energy V_0 and going through a potential field to a point of potential V will have its kinetic energy expressable by

$$\tfrac{1}{2}mv^2 = (V_0 + V)e.$$

This is correct provided the electron does not lose energy in its impact with gas molecules. Compton and Benade[12] have shown that even in He, an electron loses a fraction f of its energy in collision with a gas molecule where f is approximately equal to $2m/M$; and more recently Harries[13] has shown that even greater losses can occur in CO and N_2. Therefore, if the Compton[14] theory of electron behavior in gases is correct, the electron continually loses energy to the gas molecules as it gains it from the field between mean free paths, and eventually reaches a steady state where it possesses its terminal energy. To gain an idea of the error introduced by neglecting this loss of energy in the case of hydrogen, it is easy to calculate the energy of an electron after it has gone a distance of 1 cm in H_2 gas in a field of unit gradient. The results are shown in Table I. The assumption that the electron gains the

TABLE I.

p (mm)	X	Distance	Energy (volts)
1	1	1	0.94
2	1	1	0.804
30	1	1	0.075

entire energy of the field through which it has passed would lead to a value of the energy of one volt in each case. It is thus seen that such an assumption is barely sufficient at pressures of 1 mm and fails very badly at higher pressures. Accordingly we would not expect the Langmuir theory to be applicable in the region to which we have successfully applied the Thomson equation.

[12] Compton and Benade, Phys. Rev. **9**, 187 (1918).
[13] Harries, Zeits. f. Physik **42**, 26 (1927).
[14] Compton, Phys. Rev. **22**, 333 (1923).

We should, however, expect it to apply with fair accuracy to the data taken at 1 and 2 mm pressure. Computation of the experimental results given above in Figs. 2, 3, and 4 on this basis lead to the results given in Table II. The

TABLE II. *Computed values of mean free path.*

Pressure	I_0	i	V	Mean free path
1	0.91	0.145	6	1.76×10^{-5}
1	0.91	0.23	12	1.80
1	0.91	0.50	60	1.17
2	0.91	0.10	6	2.44
2	0.91	0.16	12	2.50
2	0.91	0.39	60	1.77
30	0.96	0.14	60	9.4
95	2.15	0.22	60	20.8
330	7.15	0.42	60	41.0

kinetic theory mean free path for H_2 to which the values given above should correspond (the value of λ determined from Langmuir's equation having been reduced to 760 mm and multiplied by $4(2)^{1/2}$), is variously given, but 1.8×10^{-5} cm is an average value. It is seen that at low pressures and voltages, the Langmuir equation gives excellent agreement—probably better than the data warrant. At higher pressures, where the assumptions of his derivation do not apply, we find the expected deviation. It might be noted that in Langmuir's equation there is a fortuitous escape from the dangers of the assumption that $\frac{1}{2}mv^2=(V+V_0)e$. This happens because of the fact that in the final equation, V appears in the equation independently of this assumption, V_0 is a true representation of the electron energy where most of the diffusion to the electrode is taking place; and as a result, only the function log $[(V_0+V)/V_0]$ neglects the loss of energy to gas molecules. In consequence, the deviation in λ above computed at higher pressures is much less than might be expected from Table I. An attempt was made to carry through an analogous derivation employing the Compton equations for the rate of energy gain as the electron moves through the gas. The resulting equation, however, was a complicated function of X/p and λ and was totally unsuited to experimental comparison. It is not reproduced here in view of the fact that the Thomson equation satisfactorily accounts for the observed phenomena.

In conclusion, it is desired to extend sincere thanks to Professor L. B. Loeb for his continual interest and inspiring suggestions during the course of these and previous experiments.

Investigations in the Field of the Ultra-short Electromagnetic Waves III. Electronic Oscillations in Vacuum Tubes and the Causes of the Generation of the Dwarf Waves

By G. Potapenko*

Norman Bridge Laboratory of Physics, California Institute of Technology

(Received April 12, 1932)

The purpose of this paper is the elucidation of the causes of the generation of the dwarf waves i.e., of waves with frequencies exceeding many times the frequency of the oscillations of the electrons about the grid of the tube. The existing theories of the generation of ultra-short waves cannot give a satisfactory explanation of the origin of dwarf waves of different orders. This is due to the simplifying assumptions made by the theories in the conditions of the problem. The phenomena of generation of ultra-short waves are closely connected with the motion of electrons. Therefore, in order to obtain the explanation in question an investigation was made of the motion of the electrons in tubes generating ultra-short waves. The motion of the electrons was investigated graphically by means of special diagrams which simultaneously represented the trajectories of the electrons and the alternating potentials at the electrodes of the tube. In this manner it was shown that the reason a vacuum tube can generate dwarf waves is because the tube can transmit energy into the oscillating circuit coupled with it and transmit it periodically with a period equal to the natural period of the circuit not only when this period T is equal to the period of the electronic oscillations τ (normal waves), but also when $T=\tau/2$, $T=\tau/3$, $T=\tau/4$, $\cdots$ (dwarf waves). This property of the tube depends on the fact that in all the cases described a periodic division of the electrons into two groups is possible. According to the theory of E. Gill and J. Morrell this division determines the transmission of energy into the oscillating circuit. The above property of the tube means also that the dynamic resistance of the tube is negative under these conditions. The diagrams of the trajectories and the velocities of the electrons, constructed on the basis of the computations of G. Kreutzer, confirmed the above deductions.

§1. Introduction

IN THE two preceding papers[1] we described some of the results of the investigations of the generation of ultra-short waves by vacuum tubes on the grid of which is impressed a high positive potential with respect to the filament and the plate. In this case, as we know, the electrons issuing from the filament can oscillate about the grid of the tube as a position of equilibrium. The period of oscillation and the corresponding wave-length λ can be determined from Barkausen's approximate formula:

$$\lambda^2 E_g = d_a^2 \times 10^6 \tag{1}$$

where d_a is the diameter of the plate of the tube (in cm) and E_g is the positive grid potential (in volts).

* Carnegie Fellow.

[1] G. Potapenko, Phys. Rev. **39**, 625, 638 (1932). These articles will be referred to as I and II respectively.

We have shown that in reality, together with the waves of a length approximately corresponding to the Barkhausen's formula (normal waves), the vacuum tubes can also generate waves whose length is approximately 2, 3, 4, $\cdots$, times shorter than that given by this formula (dwarf waves). Furthermore, investigations have shown that all of these waves belong to the same type of GM-oscillations, i.e., they are oscillations of the oscillating circuits connected with the tube. Hence, it follows, that these circuits are excited in such a manner that during one period of electronic oscillations or, in other words, during the time τ the electrons take to pass from the filament to the plate and back, the circuits execute two complete oscillations (dwarf waves of the 1st order), three complete oscillations (dwarf waves of the 2nd order), etc.

We have not yet explained why dwarf waves can be generated by vacuum tubes. In other words, we did not explain why it is that in oscillating circuits connected with the tube oscillations can be maintained having integral relations between the period of the circuit and the period of electronic oscillations. This is one of the fundamental questions. In the present paper we shall attempt to answer it.

§2. On the Theories of Generation of Ultra-short Waves

Several papers can be mentioned where attempts were made theoretically to solve the problem as to what should be the relations between the period of the oscillating circuit T and the time τ of the passage of the electrons in order that the vacuum tube be capable of generating oscillations.

E. Gill and J. Morrell[2] were the first to attempt to give an energetic theory of the generation of ultra-short waves. They showed that the tube can give energy to the circuit and, consequently, maintain its oscillations at different relations between the period T and the time of passage τ. Among others they made the following two fundamental assumptions: (1) the electrons which had already passed the grid and are moving back toward the filament are completely detained by the grid and (2) all the electrons have the same speed when they are moving across the grid. It is easily seen that the first assumption confines the problem to the case of oscillations generated by tubes with very closely wound grids when electrons can actually have such trajections, as it was shown by H. Hollmann.[3] The second assumption is generally incorrect,[4] if only because it contains an assumption of the absence of an alternating field between the grid and the filament. Because of these two assumptions the results obtained by E. Gill and J. Morrell can be considered only as an indication of a theoretical possibility of oscillations at $T \neq \tau$. Unfortunately, it is not possible to make any numerical comparisons of these results with the results of our experiments. O. Pfetscher[5] made the same assumption of the equality of speeds of electrons passing across the grid. His theory showed two relations between the period of oscillations T and the

[2] E. W. Gill and J. H. Morrell, Phil. Mag. **44,** 161–178 (1922).
[3] H. E. Hollmann, Ann. d. Physik **86,** 129–188 (1928).
[4] See also E. W. Gill, Phil. Mag. **12,** 843–853 (1931).
[5] O. Pfetscher, Phys. Zeits. **29,** 449–478 (1928).

time τ_{ga} the electrons take to pass from the grid to the plate. One of them corresponds to the condition $T=2.94\tau_{ga}$, the other, with a lower energy of oscillations, corresponds to the condition $T=\tau_{ga}$. The first condition corresponds rather closely to normal waves, since $\tau\sim 3\tau_{ga}$ for the usual type of tubes. The second condition must in this case correspond to dwarf waves of the 2nd order, as it can be seen that the ratio of the wave-lengths of these two oscillations is equal to 2.94. O. Pfetscher's theory gives thus an indication of the possibility of dwarf waves of the 2nd order. The theory differs, however, from the results of experiments in so far as dwarf waves of the 1st, and 3rd orders are concerned. To these waves must correspond the conditions $T\sim 1.5\tau_{ga}$ and $T\sim 0.73\tau_{ga}$, when the generation of waves is impossible according to this theory.

J. Sahánck[6] gave also a theory of the generation of ultra-short waves, based on calculations of energy. According to his theory, oscillations can be maintained only when there exists one of the following three relationships between the period of oscillations T and the time of passage of electrons τ. In our usual notation[7] these relationships are:

$$\begin{aligned} 1.35\tau &\geqq T \geqq 0.50\tau \\ 0.34\tau &\geqq T \geqq 0.25\tau \\ 0.20\tau &\geqq T \geqq 0.165\tau. \end{aligned} \tag{2}$$

The middle points of these regions correspond to the conditions: $T=0.925\tau$, $T=0.295\tau$ and $T=0.183\tau$. The first of these relationships is near to that which must exist in the case of normal waves. The second relationship is near to the one existing in the case of dwarf waves of the 2nd order. Passing now to the wave-lengths and dividing the first equality by the second we get $\lambda_2=\lambda_0/3.14$, which is really close to the expression for dwarf waves of the second order, which we had mentioned previously (II, Eq. 3). The third relation is close to the one which must exist for the case of dwarf waves of the 4th order. Passing now to wave-lengths[8] and dividing the third expression by the first we get $\lambda_4=\lambda_0/5.05$, which is also close to the relationship which we found for the case of dwarf waves of the 4th order. Thus, J. Sahánck's theory permits us to expect dwarf waves of the first two even orders. It differs from the results of experiments, as far as the dwarf waves of odd orders are concerned. The results of our previous paper show that these waves are no less intensive than the others, while from the relationships (2) it is seen that the conditions $T=0.5\tau$ (dwarf waves of the 1st order), $T=0.25\tau$ (dwarf waves of the 3rd order) and $T=0.165\tau$ (dwarf waves of the 5th order) correspond to the boundaries of the possible regions of oscillations. Therefore, according to A. Sahánck's theory under these conditions there should be no waves of any

[6] J. Sahánck, Phys. Zeits. **26,** 368–376 (1925); **29,** 640–654 (1928); Zeits. f. Hochfreqn. **38,** 78–80 (1931).

[7] Sahánck uses the time of passage of electrons in one direction. We take the time of passage of electrons from the filament to the plate and back to the filament, which corresponds to the complete period of oscillation of electrons about the grid.

[8] In passing to wave-lengths we denote, as we usually did, $cT=\lambda_0$ for the case of normal waves and $cT=\lambda_2$ and $cT=\lambda_4$ for the case of dwarf waves of the 2nd and 4th orders.

appreciable intensity. However, these waves are not entirely "prohibited," as it is the case in the theory of O. Pfetscher. The theory of J. Sahánck differs still in another respect from the results of experiments. It concerns the dimensions of the tube. His theory shows that oscillations are possible only when

$$2.0 < r_a/r_g < 5.0 \tag{3}$$

where r_a and r_g are the radii of the plate and the grid respectively. However, oscillations are observed even at such values of r_a/r_g which lie outside these limits. For example, N. Kapzov[9] observed oscillations with a tube for which $r_a/r_g = 1.75$ and A. Scheibe[10] obtained oscillations with a tube for which $r_a/r_g = 5.81$. The disagreement between the theory of A. Sahánck and the experimental results[11] is apparently due to the fact that his formulas were derived for the case of a tube with two electrodes (diode), and their extension to the case of a tube with three electrodes is not entirely faultless. Moreover, the theory assumes plane electrodes in the tube and a uniform field between the electrodes, while the experimental results were obtained with tubes with cylindrical electrodes and therefore the field between them was not uniform.

Thus, so far, we have no theory which would enable us to compute the values of the relations between T and τ, for which oscillations can exist in tubes under actual experimental conditions. The lack of success of the attempts made so far can be attributed to the simplifications introduced into the conditions of the problem. The results of the above investigations are important, however, in that respect that they permit us to foresee the possibility of the generation of waves corresponding to the condition $T \ll \tau$, i.e., oscillations having frequencies considerably exceeding the frequencies of the electronic oscillations.[12]*

[9] N. Kapzor, Zeits. f. Physik **35,** 131 (1925).

[10] A. Scheibe, Ann. d. Physik **73,** 79 (1924).

[11] L. Tonks, Physik Rev. **30,** 501–511 (1927) in determining theoretically the conditions under which the so-called "negative reistance" appears in tubes, also indicates $r_a > 2.1$ as the condition under which oscillations can appear. He attributes the results of N. Kapzov to the presence of traces of mercury vapor in his tube. In evaluating the results of A. Scheibe it must be borne in mind that the grid of his tube had a square cross-section and the relation given above is equivalent.

[12] K. Schuster, Ann. d. Physik **7,** 54–64 (1930), has recently investigated the problem of the generation of ultra-short waves from the point of view of wave mechanics. His fundamental ideas are as follows. High potential gradients exist at the surface of the electrodes. Therefore, the de Broglie waves, corresponding to the oscillating electrons, must be totally reflected from the surfaces of plate and of the filament and must form standing waves between these surfaces. The equation of Schrödinger gives for this case discrete energy levels. Their differences determine the frequencies of the electromagnetic waves which, in principle, can be observed. Hence it follows that to any frequency of electronic oscillations must correspond a whole series of frequencies of electromagnetic waves. The theory shows that these frequencies are analogous to band spectra; the boundary of the "head line" of this series corresponds exactly to the period of electronic oscillations and the remaining bands have frequencies higher than this initial one. The initial conditions assumed by this theory correspond, strictly speaking, to the case of BK-oscillations and therefore we shall not examine them in detail. They show us, however, a new path toward the explanation of the origin of oscillations with frequencies higher than the frequency of the electronic oscillations.

§3. The Motion of Electrons in Vacuum Tubes

The phenomena of generation of ultra-short waves are most intimately connected with the motion of electrons in the tube. Therefore, a study of this motion is a most natural procedure in trying to find an answer to the question as to why dwarf waves appear in vacuum tubes. The simplest and the clearest way will be a graphic representation of the electronic trajectories by means of specially constructed diagrams. We shall discuss them now.

We have already mentioned that all the ultra-short waves which we had obtained belonged to the type of GM-oscillations. We shall examine them.

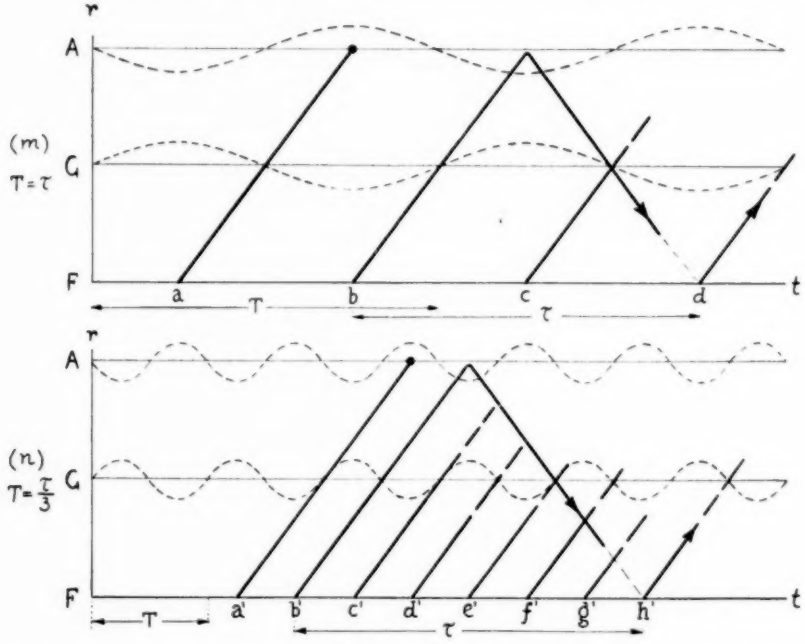

Fig. 1. Diagram of the motion of electrons in the tube; (m) the period of the generated oscillations T as equal to the time τ the electrons take to pass from the filament to the plate and back to the filament, (n) the period of the generated oscillations T is equal to one third of the time τ.

The characteristic feature of GM-oscillations is their dependence on the oscillating circuit connected with the tube (II, §4). Therefore the diagrams of electronic motion which we have to construct must give a simultaneous representation both of the electronic trajectories and of the alternating potentials of the electrodes of the tube which characterize the oscillations of the circuit.

Let us plot the time along the x-axis and the distances of the electrons

* *Note added to proof.* A Rostagni, Atti della R. Ac. di Torino 16, 217–223 (1931), has recently given a new theory of the generation of oscillations in which he took into account the natural period of the space charges in the interval grid-plate of the tube. The former he determined in a manner analogous to the determination of the natural period of an ionized gas. This theory led him to the relationship between the periods of the normal and of the dwarf waves which he had obtained.

from the filament—along the *y*-axis. Let *FG* be the distance (in arbitrary units) from the filament to the grid and *FA* be the distance (in the same units) from the grid to the plate (Fig. 1*m*). Let the alternating potentials at the grid and the plate with respect to the filament be represented by two sinusoidal curves of an arbitrary period. Since a constant difference of phase of 180° must exist between the oscillations of potentials at the grid and at the plate, these two sinusoidal curves will be mirror images of each other. It must be also remembered that the constant grid potential is the larger quantity and therefore the grid will always remain positively charged. At the same time, the constant plate potential is always equal to zero and therefore during oscillations the plate will alternately have positive and negative potentials (with respect to the filament). The oscillations of the potential at the filament can be disregarded because in our generator the oscillating circuits were connected only to the plate and the grid. Furthermore, special chokes were connected in the heating circuit (see I, Fig. 1) which precluded appreciable alternating potentials at the filament.

Let us take two electrons *a* and *b* and plot their trajectories. Let us assume, moreover, that the constant grid potential E_g is so selected that the time τ the electrons take to pass from the filament to the plate and back to the filament, is equal to T, the natural period of the oscillating circuit, or in other words to the period of the alternating potentials at the grid and at the plate. The electron *a* will issue from the filament at the moment the grid potential will have its maximum value. On its path toward the grid its acceleration will also have its maximum possible value; the electron will be able to pass across the grid with a high velocity. On its path toward the plate the electron will be acted upon by a retarding field, which will be weaker than the accelerating field that had acted upon the electron on its path from the filament to the grid. This will be caused by two circumstances: the grid potential will no longer be so high as before and the plate will have a positive potential. Therefore, the electron will strike the plate and impart to it its remaining energy. The electron *b* will issue from the filament at the moment when the grid potential is at its minimum. On its path toward the grid the electron *b* will have an acceleration smaller than the one the electron *a* had on the same path. Therefore, it will pass across the grid with a lower velocity. The retarding field on its path from the grid to the plate will act on the electron more strongly than the accelerating field on the first part of its path, because now the grid potential will be higher than before and the plate-potential will be negative. Therefore, the electron *b* will not reach the plate and after coming to rest it will start moving toward the grid, will again be able to pass across the grid and so forth.

The same difference as between electrons *a* and *b* will exist between electrons *c* and *d*. Therefore, because of the presence of alternating potentials at the electrodes of the tube the electrons will be sorted out into two groups. One part of them will not be able to produce oscillations and coming to the plate will give rise to a current in the plate circuit of the generator. The other part will be able to oscillate and in passing from the plate to the grid will

reduce the current flowing through the tube. Thus, there will be a certain order in the motion of the electrons and the current flowing through the tube will oscillate. Besides these two groups there will be other electrons which after issuing from the filament will come to the grid and will be captured by it. The majority of electrons will belong to this group, as it could be seen from a comparison of the currents flowing through the grid circuit and the plate circuit of the tube. These electrons, however, do not disturb the process of oscillations and we shall not consider them.

The electrons which lose their energy in coming from the filament to the plate and which return to the grid impart their energy to the oscillating circuit.[13] For this reason, the periodic oscillation of the current flowing through the tube indicates that small amounts of energy are periodically imparted to the oscillating circuit, the period being equal to the natural period of the circuit. The oscillations of the circuit will be maintained in this manner, if the energy received will be sufficient to cover the losses in the circuit.

Let us assume now a three-fold decrease in the natural period of the circuit and therefore, in the period of oscillations of the potentials of the grid and the plate, with which the circuit is connected. At the same time let the constant grid potential and therefore the time τ of the passage of electrons remain unchanged. In this case instead of the condition $T=\tau$ we shall have $T=\tau/3$. This case is represented on Fig. 1*n*. Again, let us take two electrons a' and b'. It is easily seen that the electron a' will be under conditions analogous to those of electron a. It will come to the plate and will strike it. The second electron, b', will be analogous to the electron b. It will not reach the plate, will come to rest in the vicinity of it and will start moving toward the grid. In other words it will be capable of oscillating about the grid. For similar reasons electrons c', e', g', $\cdots$, will be captured by the plate and electrons $d', f', h', \cdots$, will start moving toward the grid and will be able to oscillate about it. Thus a perfectly definite order in the electronic motions will be established in this case, i.e., when $T=\tau/3$. As before, part of the electrons will settle on the plate, producing plate current, and another part will come back from the plate to the grid, thus decreasing the current flowing through the tube. It is easily seen that this current through the tube will oscillate periodically, performing three oscillations during each period τ. Hence, it again follows that periodically, three times during every period τ, energy will be imparted to the oscillating circuit connected to the tube. Due to this energy oscillations of the period $\tau/3$ will be maintained in the circuit. Of course the resistance of the oscillating circuit should not be too great, so that the energy supplied could cover its losses.

From the above, it follows that if oscillations are possible, i.e., if they can be maintained by the tube when $T=\tau$, then they are possible when $T=\tau/3$.

[13] See, for example, E. W. Gill and J. H. Morrell, Phil. Mag. **44**, 171 (1922). A certain amount of energy will be taken from the oscillating circuit and transformed into heat on the plate by electrons, the velocity of which will increase under the influence of the alternating potentials. However, this amount of energy will be less (under definite conditions) than that imparted to the circuit by electrons losing their velocity.

Using a similar argument it can be shown that oscillations are possible when $T=\tau/2$, $T=\tau/4$, $T=\tau/5$ etc. This is essentially an answer to the question as to why dwarf waves can appear. It is easily seen that this answer can be formulated as follows: *The reason a vacuum tube can generate dwarf waves is because the tube can transmit energy into the oscillating circuit connected with it and transmit it periodically with a period equal to the natural period of the circuit not only when this period T is equal to the period of the electronic oscillations τ (normal waves) but also when $T=\tau/2$, $T=\tau/3$, $T=\tau/4$, $\cdots$,* (dwarf waves). It is quite evident that the energy supplied periodically can maintain oscillations of a corresponding period.

We considered the process of sorting out of electrons in two groups, assuming that the constant potential at the plate with respect to the filament is equal to zero. Even if there had been a sufficiently large negative potential at the plate and the electrons were quite unable to reach the plate, the presence of alternating potentials at the electrodes would cause a division of the electrons into two groups. These two groups would differ in the amplitude of electronic oscillations and in the time τ of passage of electrons. This case, as well as the one considered above, was first indicated by E. Gill and J. Morrell.[2] It was recently examined by H. Möller[14] under the name of "sorting out by phases" ("Phasen Aussortierung"). It approaches very closely the scheme of oscillations, which was proposed by F. Harms.[15]

The division of electrons into two groups permits us to explain why oscillations can be observed at all in circuits connected with the tube. The mere presence of electronic oscillations cannot explain this fact. If the oscillations of electrons about the grid were disorderly, no oscillations or waves could, evidently, be observed outside the tube. If oscillations are observed, it means that the electronic oscillations about the grid are in some way regulated. From the above, we see that this regulation has a perfectly definite sense. When speaking of electronic oscillations it must be borne in mind that only an observer watching the separate groups of electrons would be able to observe the presence of such groups which actually oscillate periodically about the grid and are periodically replenished by an influx of new electrons (b, d, $\cdots$, etc., see Fig. 1m). At the same time, an observer watching what takes place at some given point between the electrodes of the tube, would have at any given moment electrons moving at different velocities from the filament to the plate and from the plate to the filament. Such an observer could easily call this motion disorganized (especially in the case of dwarf waves) and the only periodic process which he would observe would be the oscillation of the density of current flowing through the tube.

§4.

The oscillation of the density of the current flowing through the tube and the process of transmission of energy into the oscillating circuit could formally be ascribed to the presence of the so-called "negative resistance" between the

[14] H. Möller, Elektr. Nachr. Techn. **7**, 293–306 (1930).

[15] F. Harms, Verh. d. Deutsch. phys. mediz. Ges. **51**, 136–144 (1926).

electrodes of the tube. This idea was first expressed by V. Pagliarulo.[16] It is also consistently carried out in the works of K. Kohl.[17]

The concept of negative resistance is generally used in the radio engineering. It is applied in the cases of the presence of the so-called "falling characteristic" (for example, in the case of arc, dynatron, negatron, etc.). The concept of a negative resistance receives a different interpretation when applied to the description of the phenomena of the generation of ultra-short waves. In the first place, the presence in an oscillating circuit of a negative resistance, as it is usually understood, permits to obtain in this circuit oscillations corresponding to its natural frequency and within wide limits independently of what this frequency may be. On the other hand, in the case of ultra-short waves the vacuum tube can maintain oscillations only when there exists a very definite relation between the period of these oscillations and the time of passage of electrons. This distinction is very essential. Evidently, it is caused by the fact that in the region of ultra-short waves the periods of the generated oscillations are of the order of magnitude of the time of electronic passage. On the other hand, in schemes similar to the one with which we were obtaining ultra-short waves, the vacuum tube has no falling characteristic. Therefore, the term negative resistance must in our case be used only in the sense of a dynamic negative resistance. A. Sahánck,[6] as far as we know, was the first one to indicate the possibility of the existence of such a resistance, in other words, the possibility of a transition of the usual static characteristic into a falling dynamic characteristic. L. Tonks[18] and O. Pfetscher[5] gave a detailed theoretical investigation of the conditions under which the resistance of the tube may become negative.

Applying the concept of negative resistance to our results we can say that *a vacuum tube has the character of a dynamic negative resistance if the period of the oscillating circuit connected with it and the time the electrons take to pass from the filament to the plate and back to the filament, satisfy approximately the conditions* $T=\tau$, $T=\tau/2$, $T=\tau/3$, $\cdots$, When we explain the phenomena of generation of ultra-short waves from the point of view of electronic processes we give a physically correct explanation as to why under precisely these conditions the resistance of the tube becomes negative.

§5.

The above considered scheme of electronic motions is, of course, merely an illustration of the fundamental idea which explains the causes of the experimentally observed fact of the generation of ultra-short waves with different relations between T and τ. For example, this scheme does not make it clear whether the electrons, issuing at the time the grid potential is at its maximum (electrons b, d, b', d', etc.,) will have the maximum velocity, or whether it will be the electrons which issue from the filament a little before that moment. The same can be said, of course, of the electrons having the

[16] V. Pagliarulo, Phys. Rev. **23,** 300 (1924).
[17] K. Kohl, Ann. d. Physik **85,** 1–62 (1928); Erg. d. ex. Naturwiss. **9,** 324 (1930).
[18] L. Tonks, Phys. Rev. **30,** 501–511 (1927).

lowest velocity. Our scheme gives no indications as to how great will be the number of electrons which can oscillate about the grid as compared with the number of electrons which fall on the plate. Finally, it is not clear whether only those oscillations are possible for which $T<\tau$ or also those for which $T>\tau$. The answer to these questions must be given by the theory.

To obtain a more exact picture of the motion of the electrons we must construct more accurate diagrams capable of presenting in some definite units both the trajectories and the speeds of electrons for different working conditions of the tube. These diagrams can be constructed if we determine the trajectories and the speeds of the electrons from their equations of motion. We can make use of the results of computations made at our suggestion by G. Kreutzer in 1929.

All the vacuum tubes with which we succeeded in obtaining ultra-short waves had cylindrical electrodes, symmetrically arranged (I, §5). The equations of motion of the electrons will take into account this fact. Let r_f, r_g and r_a be the radii of the filament, grid and plate respectively. The constant potentials of the filament and the plate will be assumed equal to zero. Let E_g be the constant positive potential of the grid with respect to the filament. In the presence of oscillations alternating potentials must appear on the grid and the plate. Let E_0 be their amplitude. Since a constant phase difference of 180° must exist between these two potentials, the actual potentials of the grid and the plate will be

$$[E_g] = E_g + E_0 \sin \omega t \quad [E_a] = - E_0 \sin \omega t \tag{4}$$

where ω is the angular frequency of oscillations. According to what we said before, we neglect here the alternating potentials at the filament.

The field between the electrodes of the tube will be logarithmic and the equations of motion of the electrons can be written as follows:[19]

$$\frac{d^2r}{dt^2} = K_1 \frac{1 + \alpha \sin \omega t}{r} \quad \text{(for the interval filament-grid)}$$

$$\frac{d^2r}{dt^2} = - K_2 \frac{1 + \beta \sin \omega t}{r} \quad \text{(for the interval grid-plate)} \tag{5}$$

where

$$K_1 = \frac{eE_g/m}{ln(r_g/r_f)} \quad K_2 = \frac{eE_g/m}{ln(r_a/r_g)} \quad \alpha = \frac{E_0}{E_g} \quad \beta = \frac{2E_0}{E_g}$$

and r is the distance of the electron from the filament. In deriving these equations neither the space charge nor the initial velocity of electrons issuing from the filament were taken into account.

It is easily seen that the above equations have two groups of parameters. Some of them —r_f, r_g, r_a—are given by the dimensions of the tube; others —ω, E_g, E_0—can be selected quite arbitrarily. Also, the frequency ω corresponds to the natural period T of the oscillating circuit coupled with the tube;

[19] N. Kapzov, Zeits. f. Physik **49**, 395–427 (1928).

E_g determines the period τ of electronic oscillations and the number of electrons falling on the plate depends on E_0. E_0 can be selected in agreement with the experimental data. As to the selection of ω and E_g, we shall distinguish several cases, depending on the resulting relations between T and τ: $T=\tau$ (normal waves) and $T=\tau/2$, $T=\tau/3$, $T=\tau/4$, $\cdots$, (dwarf waves).

The equations of motion of the type written above cannot be integrated in known functions. When expanded they give very slowly converging series.[20] Therefore, numerical or graphical integration is the only method of solving them.

(a). Normal waves, $T=\tau$. For this case, the numerical integration of the equations was performed by N. Kapzov.[19] His results show that those electrons do not reach the plate which issue from the filament at moments corresponding to the phases of oscillation of the grid potential within the limits from $-80°$ to $+60°$. Here the phase $0°$ corresponds to the beginning of the positive half period of oscillation. The electrons which correspond to the phase $-80°$ have a minimum velocity in passing across the grid; the electrons which correspond to the phase $+80°$ have in this case a maximum velocity and fall on the plate.[21] Computations have also shown that electrons corresponding to the phases $-70°$ and $+70°$ do not fall upon the filament on their motion toward it and can, therefore, perform several oscillations about the grid.

F. Sears[22] has recently performed a graphic integration of equations (5) by means of an integraph. His results are in agreement with those of N. Kapzov.

(b). Dwarf waves; $T=\tau/2$, $T=\tau/3$, $T=\tau/4$, $T=\tau/5$. These cases are of particular interest to us. At our suggestion G. Kreutzer performed the integration of Eq. (5) for all of these cases,[23] using the method of Runge-Kutta.[24] This work is very fatiguing and demands a great deal of attention. It was assumed that: $r_f=0.006$ cm, $r_g=0.31$ cm, $r_a=0.8$ cm, $E_g=100$ v, $E_0=10$ v. N. Kapzov and later F. Sears used the same conditions. Therefore, all of these results are easily comparable. The time of passage of electrons under these conditions was calculated from the formula of A. Scheibe[10] which takes into account the cylindrical shape of the electrodes and is more accurate than formula (1). This time of passage was found to be equal to 0.507×10^{-8} sec. T, the period of oscillations was, therefore, taken as being equal to $\frac{1}{2}$, $\frac{1}{3}$, $\cdots$, of this magnitude. Computations were made in such a manner that for each of the cases indicated above the trajectories and the velocities of the electrons issuing from the filament were successively determined for different moments of time. For dwarf waves of odd orders computations were made for moments corresponding to the phases $0°$, $90°$, $180°$, $270°$

[20] S. Zilitinkewitsch, Arch. f. Electrotech. **15**, 470–484 (1926).

[21] Compare Fig. 1*m*, electrons *a* and *b*. No computations were made by N. Kapzov for electrons corresponding to the phases $-90°$ and $+90°$.

[22] F. Sears, Journ. Franklin. Inst. **209**, 459–472 (1930).

[23] See preliminary report: G. Potapenko, Zeits. f. Physik **10**, 542–548 (1929).

[24] See C. Runge und H. König, "Numerisches Rechnen," pp. 286, 311 (1921)

and for dwarf waves of even orders computations were made only for 0° and 180°. The latter was done to shorten the computations as it was found that these two electrons represented the two groups in which we were interested.

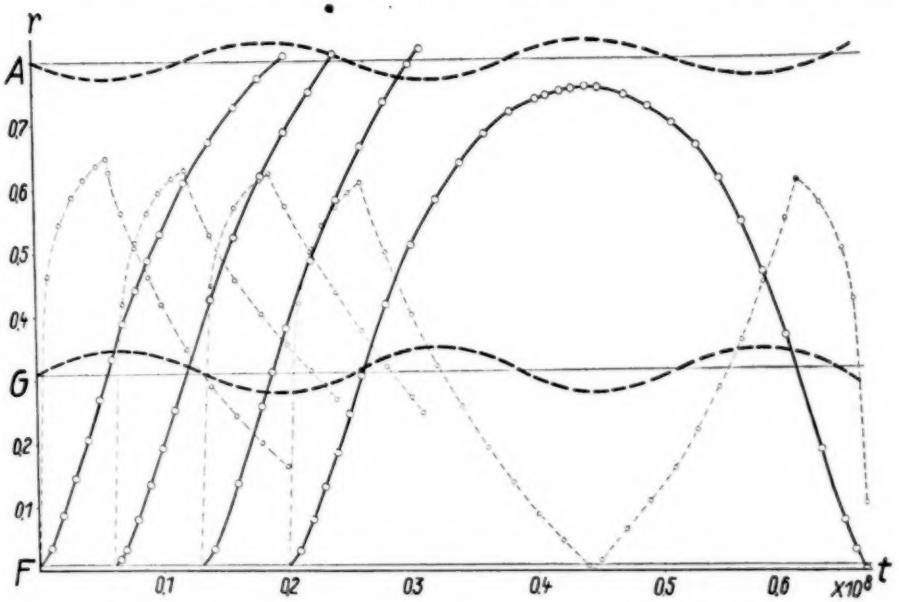

Fig. 2. Trajectories and velocities of the electrons for the case $T=\tau/2$.

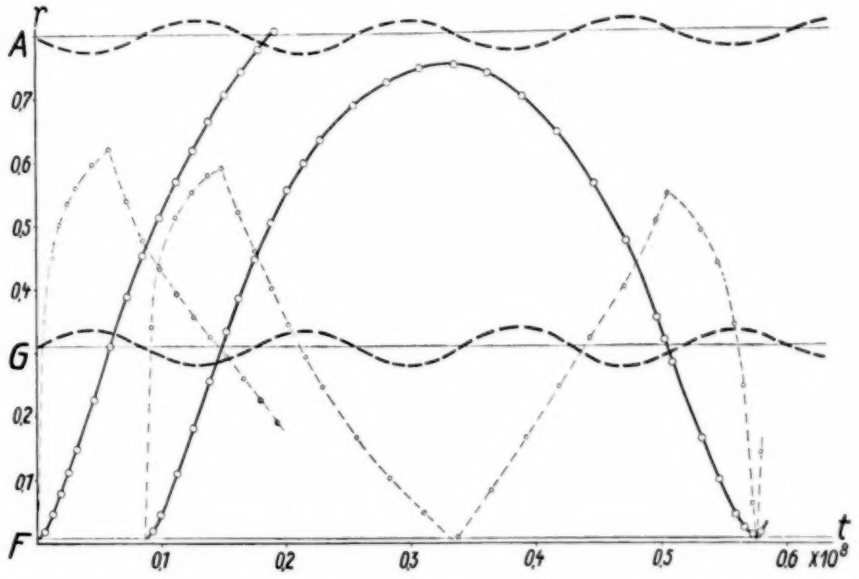

Fig. 3. Trajectories and velocities of the electrons for the case $T=\tau/3$.

The results of computations are given in Figs. 2–5. The continuous lines represent the paths of the electrons and the dotted lines—their velocities.

Figs. 2–5 show that in all cases without exception there actually exists a

division of electrons into two groups; some of them reach the plate and fall on it, others lose their velocity before reaching the plate and start moving back toward the plate. This fully confirms the scheme of electronic motions,

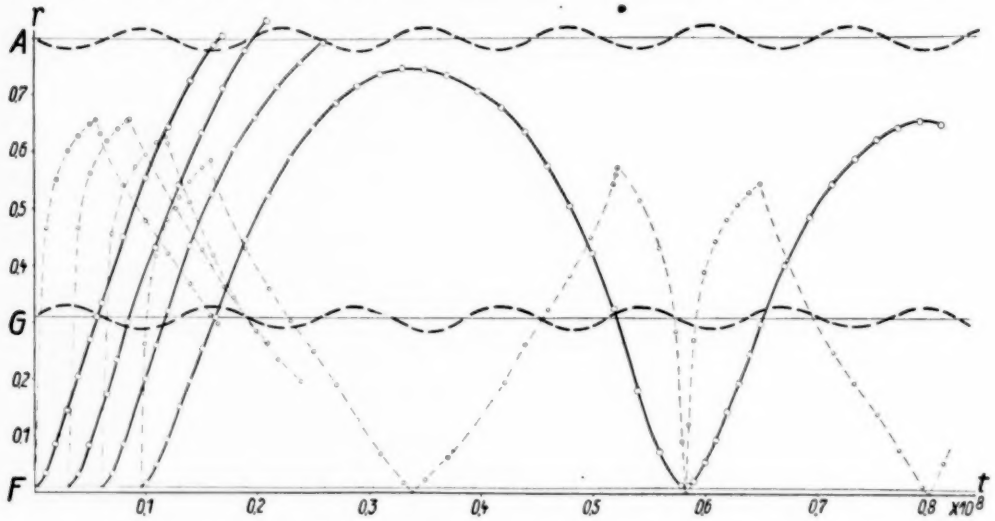

Fig. 4. Trajectories and velocities of the electrons for the case $T=\tau/4$.

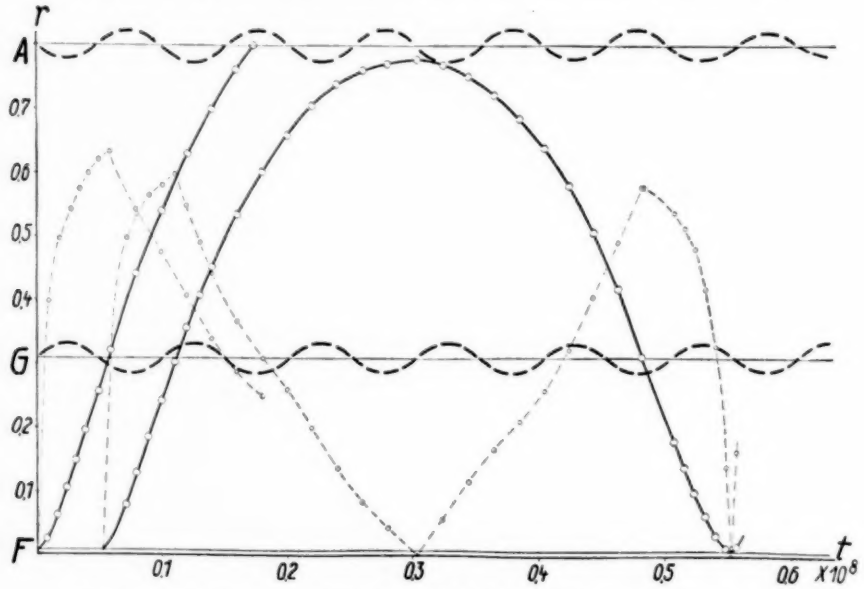

Fig. 5. Trajectories and velocities of the electrons for the case $T=\tau/5$.

given above, and thus fully confirms our basic idea as to the causes of the origin of dwarf waves.

The diagrams show also that the group of electrons moving from the plate toward the filament corresponds in different cases to different phases ω. At $T=\tau/2$ and $T=\tau/4$ only those electrons will move back toward the fila-

ment which issue from it at $\omega = 270°$ or, which is the same thing, at $\omega = -90°$. When $T = \tau/3$ and $T = \tau/5$ the electrons issuing from the filament at $\omega = 180°$ will also be able to move back toward the filament. The alternating potential at the grid is of decisive importance in the division of electrons into two groups. This is particularly clearly seen when $T = \tau/2$. In this case the electrons issuing at $\omega = 0°$ and $\omega = 270°$ approach the plate when it has approximately the same positive potential. Nevertheless, only the first electron will strike the plate, the second does not reach the plate and starts moving back. The trajectories and also the velocity curves show, moreover, that the electrons after passing the grid for the second time can fail to reach the filament and will thus be able to oscillate several times about the grid. It is of interest, that under the conditions which we selected, the period of the electronic oscillations, as determined from the trajectories of the electrons, will be a little shorter than the one previously computed from A. Scheibe's formula. Their ratio is 1.02–1.05. This difference must be ascribed to the influence of the alternating potentials which is not taken into account by the formula of A. Scheibe. It must be mentioned that in the case $T = \tau$ the difference between these two periods is considerably greater. According to the results of N. Kapzov[19] their ratio is 1:15 under the same amplitudes of oscillations. Hence it follows that the influence of the alternating potentials decreases as the difference between T and τ increases. This is easily understood, for the more often the field alternates during, the time of passage of the electrons, the more there will be of a summation and mutual cancellation of the influence of the separate phases of oscillations.

In conclusion the author wishes to express his gratitude to the Carnegie Corporation of New York for the grant of a Fellowship and to Professor R. A. Millikan for the facilities of the Norman Bridge Laboratory.

Magnetic Properties of Magnetite Crystals at Low Temperature

By CHING HSIEN LI
University of Illinois

(Received April 11, 1932)

Thin circular disks cut parallel to the 100, 110 and 111 planes of magnetite crystals were prepared. The components of the intensity of magnetization normal and parallel to the magnetic field at temperatures down to that of liquid air were investigated by the method of torsion. It was found that the magnetic properties of the crystal abruptly changed at about $-160°$C. This temperature corresponds exactly to the temperature at which the specific heat of magnetite increases suddenly to a maximum as was found by Millar two years ago. X-ray photographs taken at room temperature and at liquid air temperature show no difference indicating that there is no change in the distribution of the points of diffraction. The intensity of the two patterns requires further measurements. Weiss' theory of the molecular field cannot be applied as $-160°$C is not a Curie point.

INTRODUCTION

IN HIS investigation on the heat capacities of ferrous oxides at low temperatures Russell W. Millar[1] found that the specific heat of magnetite (Fe_3O_4) rises suddenly to a maximum at 114.15°K. He assumed that this maximum is due to a change in the magnetic properties.

P. Weiss and P. N. Beck[2] have measured the specific heat of iron, nickel, and magnetite at various temperatures, and found an increase of specific heat of these substances near their critical points. Weiss explained this change as due to the change of magnetic energy. He showed that the magnetic energy per cubic centimeter of a ferromagnetic substance is:

$$E = -\tfrac{1}{2}H_m I = -\tfrac{1}{2}NI^2$$

where I is the magnetic moment per unit volume, H_m the molecular field and N is a constant depending on the substance. The negative sign indicates that it is necessary to supply heat to demagnetize the substance. Therefore

$$\frac{dE}{dT} = -\frac{N}{2}\frac{d(I^2)}{dT}$$

where T is the temperature. The increase of specific heat is

$$C_m = \frac{1}{\rho J}\frac{dE}{dT} = -\frac{1}{2}\frac{N}{\rho J}\frac{d(I^2)}{dT}$$

where ρ is the density of the substance and J is the mechanical equivalent of heat. With this formula Weiss found a very good agreement between the theory and the experiment.

[1] Russell W. Millar, Jour. Amer. Chem. Soc. **51**, 215 (1929).
[2] Weiss and Beck, Journ. de Physique [4] **7**, 249 (1908).

Therefore it is of interest to investigate the magnetic properties of magnetite at low temperatures to see whether there are any changes at the point where the specific heat increases and to see whether these changes can be explained by Weiss' theory. It is the purpose of the present work to investigate this point. The magnetic properties of magnetite crystals at ordinary temperatures have already been investigated by V. Quittner,[3] so the present investigation is limited to low temperatures and especially to temperatures from $-150°$C to -170C.

Method of Investigation

Magnetite crystals from West Lessetsk, Ural, with an octahedral habit, were obtained from Ward's Natural Science Establishment at Rochester, New York. They were found to have a great homogeneity. Three circular disks parallel to the planes 100, 110 and 111 were carefully prepared by grinding a crystal (one for each disk) on the grinding machine to suitable dimensions for the investigation. The dimensions of the disks are as shown in Table I.

Table I.

Plane of disk	Diameter in cm	Thickness in cm	Volume in cc
100	0.95	0.096	0.0674
110	1.08	0.079	0.0723
111	0.83	0.083	0.0449

The volumes of the disks were calculated from their weight and density the latter having been determined from a large crystal.

The investigation was divided into two parts: (1) The determination of the component of intensity of magnetization normal to the magnetic field at temperatures between $-150°$C and $-170°$C; (2) The determination of the parallel component between the same temperatures.

The methods used in determining these components are essentially the same as those used by P. Weiss[4] in his experiments on pyrrhotite crystals. The crystal disk is suspended between the pole pieces of an electromagnet and the couple exerted on the crystal by the magnetic field is determined by balancing it against the couple of the suspending wire.

In measuring the normal component, the crystal disk is suspended with its plane horizontal in a horizontal magnetic field. Suppose the intensity of magnetization I makes an angle ϕ with field H, then the couple exerted by the field on the crystal of volume V is

$$N = VHI \sin \phi.$$

Now $I \sin \phi$ is the component of intensity of magnetization perpendicular to the field H. Therefore

$$I_{\perp} = \frac{N}{VH} = \frac{k\theta}{VH}$$

[3] V. Quittner, Arch. des Sci. [4] **26,** 358, 455, 585 (1908); also Ann. d. Physik [4] **30,** 289 (1909).

[4] P. Weiss, Jour. de Physique [4] **4,** 469 (1905).

where k is the torsion constant of the suspension and θ is the angle of deflection of the crystal. Thus the normal component, $I_\perp$, for different directions in the crystal in a constant field can be measured by rotating the crystal in the magnetic field.

The parallel component of magnetization is determined by suspending the disk in a vertical position in a horizontal magnetic field with its plane making a small angle α with the direction of the field. Then, under the action of the field, the disk is rotated about a vertical axis through a small angle ρ. Let R (Fig. 1) be the disk and H the direction of the field. Then the torque exerted on the disk by the field is

$$\begin{aligned} N &= I \cos\phi HV \sin(\alpha - \rho) \\ &= I_\parallel HV \sin(\alpha - \rho) \\ I_\parallel &= N/[HV \sin(\alpha - \rho)] = K\rho/[HV \sin(\alpha - \rho)]. \end{aligned}$$

By orientating the disk in the field the parallel component in different directions in the crystal can be obtained.

The apparatus employed was essentially a rotating electromagnet with a system of suspension similar to that used by Weiss.

The thermocouple, used to measure the temperature at which the crystal is maintained, is made with No. 40 copper and constantan wires. One of its junctions is maintained in melting ice and the other is placed close to the disk. The thermocouple was calibrated both before and after the experiment against the fixed freezing points of the following substances and liquid air temperature, determined by means of an oxygen vapor pressure thermometer:

Mercury	−39°C	Toluene	−95.1°C
Chlorobenzene	−45.2°C	Carbon disulfide	−111.6°C
Ethyl acetate	−83.6°C	Liquid air	−190.7°C

The cooling system consists of a Dewar flask and a copper tube. The copper tube has an inner diameter of about 3 cm and a total length of about 18 cm. The tube is capable of adjustment to different heights thus exposing part of its surface to the air outside of the Dewar flask. The temperature inside the tube depends on the area which is exposed to the air and on the depth to which the tube is immersed in the liquid air. By experimenting and adjusting the height of the copper tube any desired temperature can be maintained constant inside providing liquid air is added to the flask from time to time.

Procedure

After the magnetic field and the thermocouple have been calibrated and the torsion constant of the suspension determined, the magnetite crystal is set in position. The suspension is adjusted until the crystal is in the middle of the field and the zero position in the absence of the magnetic field is noted.

In measuring the component of magnetization normal to the field the crystal disk is put in the horizontal position. A field is applied to the disk and the magnet is rotated around its axis several times before any measure-

ment is taken in order that the crystal may be uniformly magnetized. After the crystal is magnetized the magnet is set in a definite position and the deflection of the disk noted. The magnet is then turned through 10 degrees and the deflection again noted. This process is continued until the magnet has been rotated 360 degrees. The direction of rotation of the magnet is then

Fig. 1.

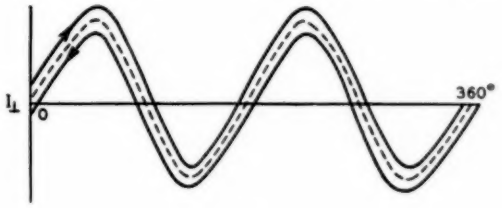

Fig. 2.

reversed and readings taken every 10 degrees until it reaches its initial position.

The normal component of magnetization is calculated from the equation $I_\perp = K\theta/VH$. Plotting the results with the angles of rotation of the magnetic field as abscissas and $I_\perp$ as ordinates, two curves are obtained as shown in Fig. 2. One of the curves is obtained when the field is rotated from 0° to

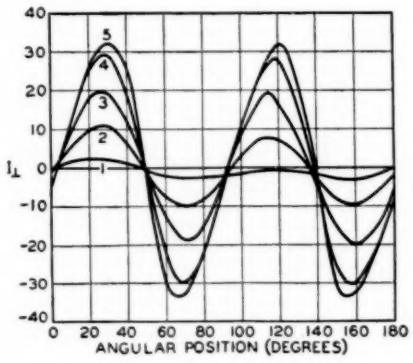

Fig. 3. Normal component of intensity of magnetization in plane (100). At temperature −155°C. 1, $H=282.75$ gauss; 2, $H=435.00$ gauus; 3, $H=489.37$ gauss; 4, $H=598.12$ gauss; 5, $H=696.00$.

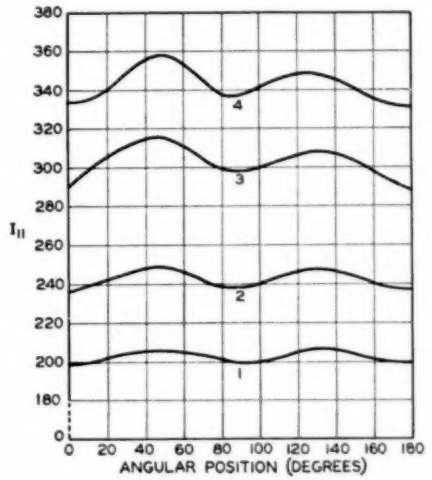

Fig. 4. Parallel component of intensity of magnetization in plane (100). At temperature −155°C. 1, $H=282.75$ gauss; 2, $H=369.75$ gauss; 3, $H=435.00$ gauss; 4, $H=489.37$ gauss.

360° and the other is obtained when it rotated back from 360° to 0°. The area between the two curves increases with increase in the hysteresis loss due to rotation.

By taking the average of the ordinates of these two curves as the ordinate of the third, we obtain a curve of I corrected for hysteresis. That this is true

has been proved experimentally by V. Quittner.[5] All the curves of the normal components of magnetization which are shown in the next section are plotted this way.

In determining the parallel component of magnetization the crystal is set in the vertical position and the zero position noted in the absence of the magnetic field. The field is applied and before taking any reading the crystal is rotated several times about a horizontal axis. The direction of the magnetic field is then adjusted by rotating the magnet until there is no deflection of the crystal. In this position the direction of the field is in the same plane as the direction of the intensity of magnetization. The magnet is then turned to the right or left through an angle of 5 degrees and the deflection of the crystal noted.

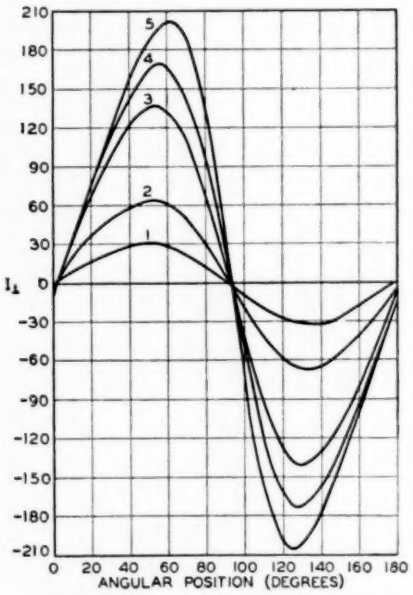

Fig. 5. Normal component of intensity of magnetization in plane (100). At temperature −166°C. 1, $H=184.87$ gauss; 2, $H=282.75$ gauss; 3, $H=435.00$ gauss; 4, $H=489.37$ gauss; 5, $H=598.12$ gauss.

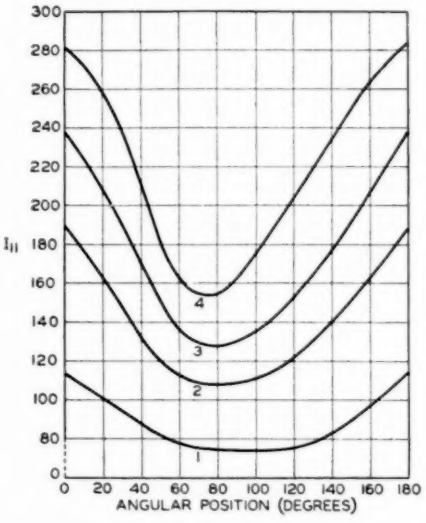

Fig. 6. The parallel component of magnetization in plane (100). At temperature −166°C. 1, $H=184.87$ gauss; 2, $H=282.75$ gauss; 3, $H=369.75$ gauss; 4, $H=489.37$ gauss.

The field is removed, the crystal rotated 10 degrees about the normal passing through its center, and the measurements repeated in this position. By this process the disk is rotated in steps of 10 degrees until 360° is reached. $I_\parallel$ is then calculated from the equation

$$I_\parallel = K\rho/[VH \sin(\alpha - \rho)].$$

The Experimental Results

Figs. 3 and 4 show respectively the variation of the normal and parallel components of magnetization in the disk parallel to the 100 plane at tem-

[5] V. Quittner, Arch. des Sci., [4] **26**, 456 (1908).

perature −155°C. Both of these components have two maxima and two minima in 180 degrees. The two maxima and also the minima differ a little from each other. The parallel component has maximum and minimum values when the field is in the directions of the tetragonal and diagonal axes respectively, while the normal component has its maximum and minimum values when the field has directions between these axes. The amplitude of these curves increases as the field strength increases. It would probably reach a maximum and then decrease to zero when the field is increased to a point where the crystal is saturated.

Figs. 5 and 6 also show these two components of magnetization in the 100 plane, but at a temperature −166°C. It can be seen that both of these components have now a period of 180° and the amplitude of the curves become far greater than before.

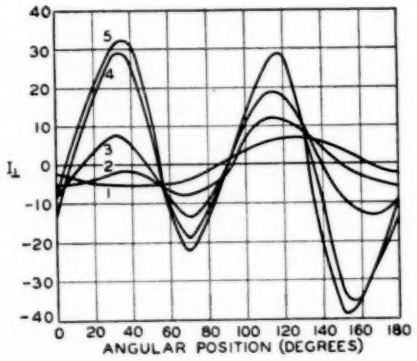

Fig. 7. Normal component of intensity of magnetization in plane (110). At temperature −155°C. 1, $H=184.87$ gauss; 2, $H=282.75$ gauss; 3, $H=369.75$ gauss; 4, $H=489.37$ gauss; 5, $H=598.12$ gauss.

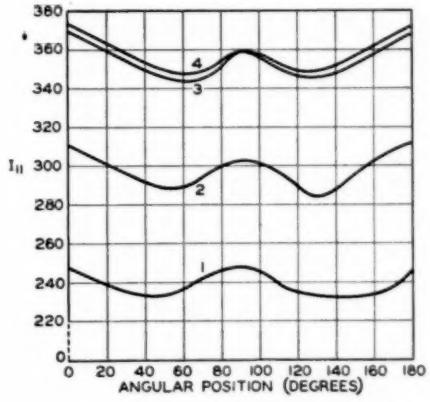

Fig. 8. The parallel component of intensity of magnetization in plane (110). At temperature −155°C. 1, $H=282.75$ gauss; 2, $H=369.75$ gauss; 3, $H=489.37$ gauss; 4, $H=598.12$ gauss.

Figs. 7 and 8 show these two components in the disk cut parallel to the 110 plane and at temperature −155°C. At the field of 184.9 gauss the curve for the normal component has only one maximum and minimum in 180 degrees and the amplitude is rather small. As the field increases the number of maxima and minima increases to two instead of one. And the two maxima and also the minima are different from each other. Both the curves of the two components show apparently a period of 180 degrees. For the parallel component the maxima and the minima are in the directions of the tetragonal, digonal and trigonal axes, while the normal component has its maximum and minimum between these three axes.

Figs. 9 and 10 show these two components in the same 110 plane, but at the temperature −166°C. The curves show again a great change as in the 100 plane and the form of the curves of the two components are somewhat similar to those obtained in 100 plane at the same temperature, −166°C.

Figs. 11 and 12 show the two components in the 111 plane at temperature

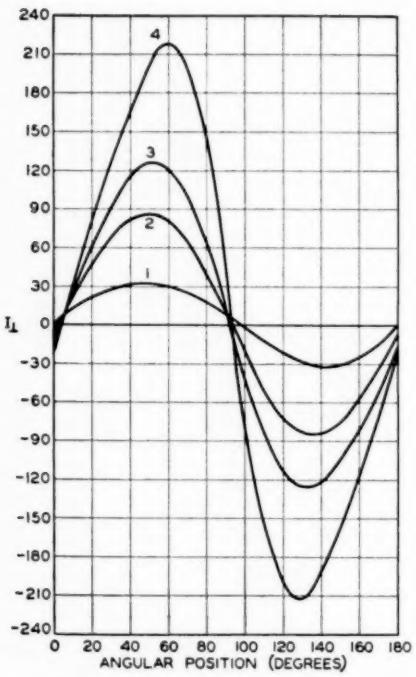

Fig. 9. Normal component of intensity of magnetization in plane (100). At temperature −166°C. 1, $H=184.87$ gauss; 2, $H=282.75$ gauss; 3, $H=369.75$ gauss; 4, $H=489.37$ gauss.

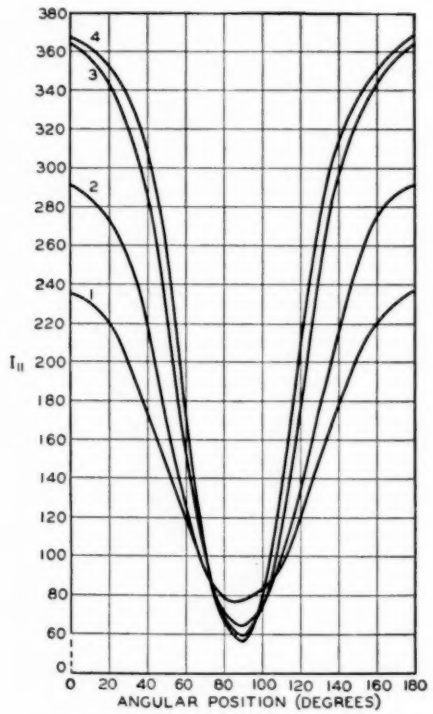

Fig. 10. Parallel component of magnetization in plane (110). At temperature −166°C. 1, $H=282.75$ gauss; 2, $H=369.75$ gauss; 3, $H=489.37$ gauss; 4, $H=598.12$ gauss.

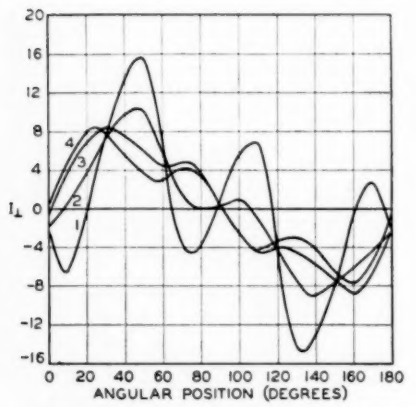

Fig. 11. Normal component of intensity of magnetization in plane (111). At temperature (111). At temperature −155°C. 1, $H=435.00$ gauss; 2, $H=543.75$ gauss; 3, $H=435.00$ gauss; 4, 783.00 gauss.

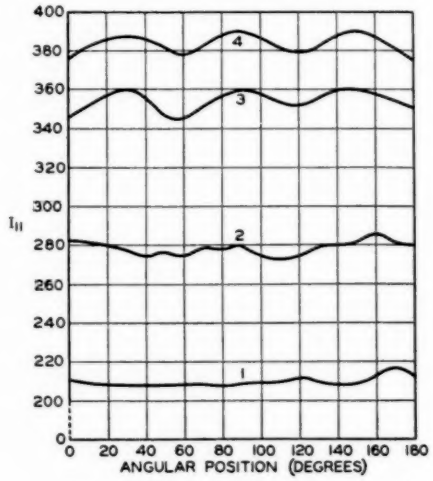

Fig. 12. The parallel component of intensity of magnetization in plane (111) At temperature −155°C. 1, $H=184.87$ gauss; 2, $H=282.75$ gauss; 3, $H=435.00$ gauss; 4, $H=598.12$ gauss.

-155°C. The forms of the curves of these two components vary as the field varies. For the normal component it has three maxima and minima in 180 degrees with amplitudes all different. As the field changes, the maximum and minimum points shift and show a phenomenon which is very complicated. For the parallel components there are three maxima and minima in 180° when the field is large but the curves become irregular when the field is small.

Figs. 13 and 14 show the two components in the same plane, 111, but at temperature -166°C. The curves again are greatly changed and they have forms somewhat similar to that obtained in 100 and 110 planes. Instead of three maxima and three minima in 180 degrees as at temperature -155°C there is now only one maximum and one minimum.

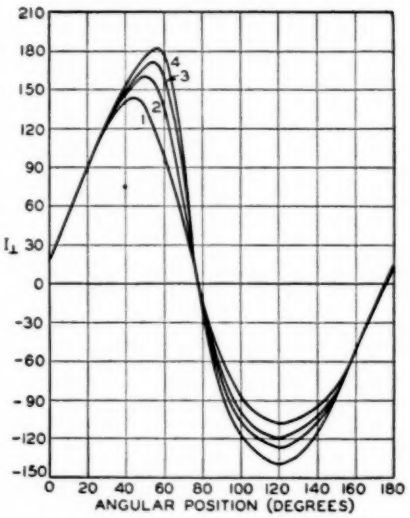

Fig. 13. Normal component of intensity of magnetization in plane (111). At temperature -166°C. 1, $H=435$ gauss; 2, $H=543.75$ gauss; 3, $H=619.87$ gauss; 4, $H=783.00$.

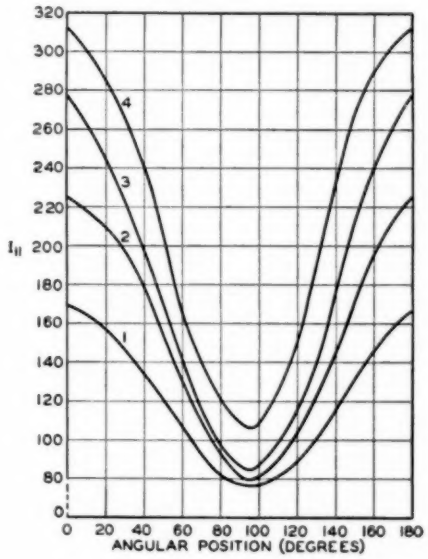

Fig. 14. Parallel component of intensity of magnetization in plane (111). At temperature -166°C. 1, $H=184.87$ gauss; 2, $H=282.75$ gauss; 3, $H=435.00$ gauss; 4, $H=696.00$ gauss.

From the above data we can see plainly that there is a great change in magnetic properties when the magnetite crystal is cooled through the range of temperature from -155°C to -166°C.

In order to show definitely at what temperature this change takes place the normal component in a definite direction in the disk is determined by applying a given field and, at the same time, varying the temperature. Fig. 15 shows the variation of the normal component in a certain direction in the 111 plane when the applied field is 696 gauss. The temperatures are plotted as abscissas and the deflections, which are proportional to $I_\perp$, are plotted as ordinates. The curve shows clearly that the change takes place at about -160°C. In the other directions in the disk the variation is not so large but

one can always find such a variation at about $-160°C$. Thus we see that a change takes place at that temperature which is just the temperature at

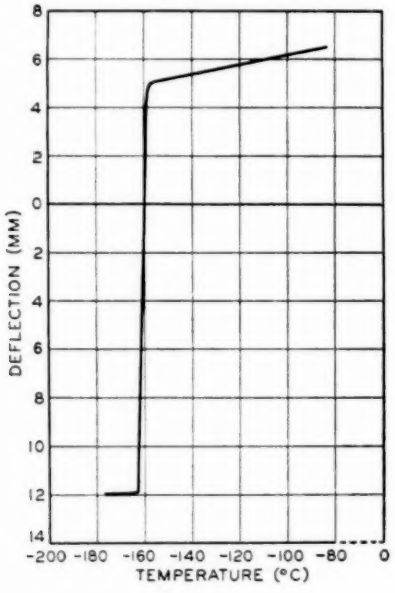

Fig. 15.

which the specific heat of magnetite increases to a maximum as has been mentioned in the introduction.

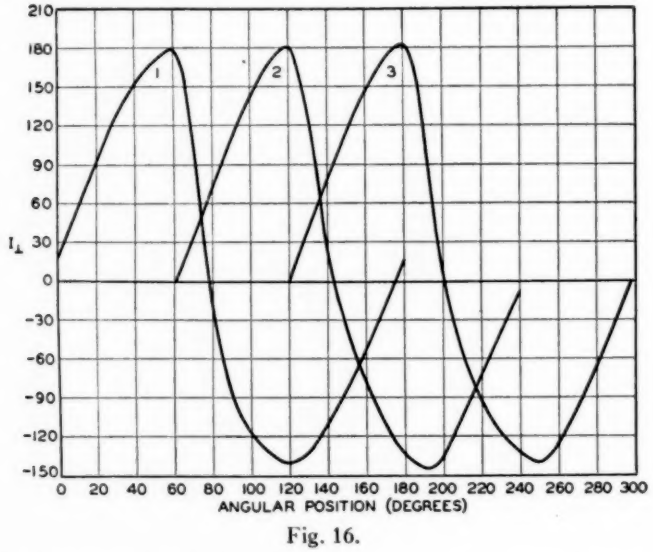

Fig. 16.

Furthermore the position of the maximum and the minimum of the curves of the two components obtained at temperatures lower than $-160°C$ depends upon the direction in which the magnetic field is applied during the

process of cooling. Fig. 16 shows this effect for $I_\perp$. Curve 1 is obtained after the disk 111 is cooled through the temperature $-160°C$ with the direction of the field applied along the direction marked zero. Curve 2 is obtained when the field is applied in a direction 60 degrees from the previous position during the process of cooling and curve 3 is obtained similarly when the field is applied in a position 120 degrees from the first position.

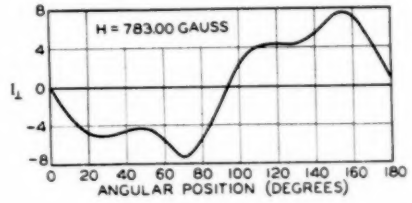

Fig. 17. Normal component of magnetization in 111 plane at temperature $-166°C$. When the crystal is cooled in the absence of the field.

This phenomenon of the shifting of the position of maxima and minima of the normal component was found in all three disks. A similar shifting was also found for the parallel component. It seems as if we can locate the position of maxima and minima of the curves of these two components in any position that we please, depending on the position of the crystal in the field when it is cooling.

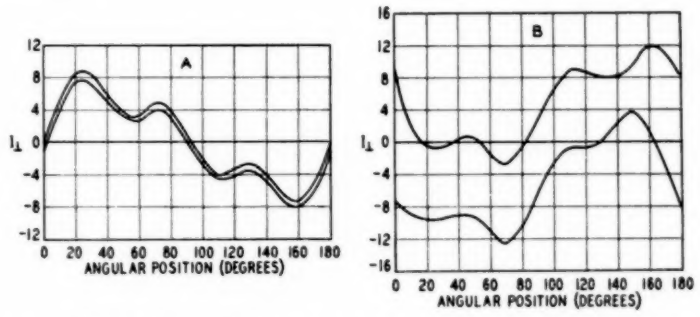

Fig. 18. *A*, Rotating hysteresis-loop in 111 plane at temperature $-155°C$. *B*, Rotating hysteresis-loop in 111 plane at temperature $-166°C$ after the crystal is cooled in the absence of the field.

On the other hand, if the crystal was cooled through the range of temperature from $-155°C$ to $-166°C$ in the absence of the magnetic field, then the change will be different. Fig. 17 shows the normal component of magnetization in 111 plane taken at temperature $-166°C$ after it has been cooled to that temperature in the absence of an external field. This curve still has three maxima and three minima in 180 degrees, but they are shifted 90° as we see if we compare it with curve 4, Fig. 11. The hysteresis of rotation in this case is about ten times as large as compared with that which was obtained at $-155°C$ (Fig. 18).

Discussion of Results

From previous investigations made on magnetic crystals at room temperatures, V. Quittner has shown that magnetite, so far as its magnetic properties are concerned, possesses the symmetry of the orthorhombic system. According to that symmetry, the normal component of the intensity of magnetization in the 111 plane should have, between 0° and 180°, three different waves with the possibility that one or even two of these waves may disappear completely. This is what has been found in the present investigation at the temperature −155°C. The curves obtained at −155°C in all the disks have similar forms to those found by Quittner at room temperature. Thus we can conclude that the magnetic symmetry of the magnetite has not been changed when cooled down to the temperature −155°C. But the forms of the curves are completely changed when the crystal is cooled in the magnetic field below −160°C. Therefore, the magnetic symmetry of magnetite must be changed from the magnetic point of view at least.

Weiss' theory of the Curie point cannot be applied to the phenomenon discovered because −160° is not a curie point. We might of course consider a double change, a sudden loss of magnetism and an increase of magnetism is the neighborhood of −160°C. We would have to introduce a second constant of another internal magnetic field N_3 which would be equal to 33800 approximately. But this attempt is unsatisfactory and the theory of the phenomenon requires further experiments.

X-ray photographs both at room temperature and at liquid temperature were taken. The distribution of the points in both pictures is the same, but the question of the intensities remains open.

Acknowledgment

The writer wishes to express his sincere appreciation to Professor J. Kunz for his suggestion of the problem and to him and to Professor E. H. Williams for their constant encouragement and suggestions during the investigation. Thanks are also due to Professor F. W. Loomis for his permission to use the laboratory, to Mr. N. P. Goss for his help in taking the x-ray photographs, and to the Rockefeller Foundation which provided him with a fellowship.

LETTERS TO THE EDITOR

Prompt publication of brief reports of important discoveries in physics may be secured by addressing them to this department. Closing dates for this department are, for the first issue of the month, the twenty-eighth of the preceding month; for the second issue, the thirteenth of the month. The Board of Editors does not hold itself responsible for the opinions expressed by the correspondents.

The Relation of Branching of Lightning Discharges to Changes in the Electrical Field of Thunderstorms

C. T. R. Wilson,[1] Schonland,[2] Schonland and Craib,[3] and others have published reports based on investigations in England and in South Africa which indicate that thunderstorms are bipolar with the upper pole positive in a majority of cases. The mechanism of the thunderstorm as described by Simpson,[4] and based on his breaking-drop theory, requires that the anterior active portion of the cloud, where convection currents of ascending air are formed, shall be positively charged. Above and to the rear of this active area there are less concentrated negative charges. This theory has been elaborated by Humphreys[5] and recent field investigations by Banerji[6] at Bombay are in general agreement with it.

Based on experiments with influence machines in the laboratory in which the branching of the discharge always goes from the positive pole toward the negative, Simpson[7] has used as the criterion for determining the polarity of any portion of a cloud from which lightning flashes proceed the direction of observed branching. A study of 328 lightning photographs collected by him from various sources gave a ratio of more than 3 from positive clouds to 1 from negative. In view of the fact that the active part of the cloud should be small compared with the remainder, this is a surprisingly large ratio. It is also contradictory to the recent papers by Lewis and Foust,[9] Peek[10] and others which show that almost all of the direct lightning strokes to transmission lines are from negative clouds and that the negative discharges are much more severe than the positive.

The writer has been making observations on the electrical field of thunderstorms for more than seven years, and summaries of the results obtained have been previously reported.[8] During the last two years our efforts have been concentrated on an attempt to obtain as many lightning photographs as possible for which the corresponding field changes were observed. The field changes were obtained by the use of an insulated metal deck connected through a sensitive galvanometer to ground. A beam of light through a right-angle prism to the galvanometer mirror and back to a revolving drum made the electrical record semi-automatic. Special care was taken to keep accurate and specific notes by the photographer as well as by the observer in charge of the electrical apparatus, the two observers being in constant telephone communication as well, so as to identify definitely each picture with the corresponding galvanometer record. A battery of four micro-barographs, three in a north-and-south line 8.5 miles long, and the fourth four miles to the west, gave an accurate record of the path of the storm.

[1] Wilson, Phil. Trans. Roy. Soc. **A221,** 73–115 (1920).

[2] Schonland, Proc. Roy. Soc. **A118,** 233–251 (1928).

[3] Schonland and Craib, Proc. Roy. Soc. **A114,** 229–243 (1927).

[4] Simpson, Proc. Roy. Soc. **A114,** 376–401 (1927).

[5] Humphreys, Monthly Weather Rev. **42,** 348–380 (1914).

[6] Banerji, Jour. Roy. Meteor. Soc. **56,** 305–355 (1930).

[7] Simpson, Proc. Roy. Soc. **A111,** 56 (1926).

[8] Jensen, Monthly Weather Rev. **58,** 115–116 (1930).

[9] Lewis and Foust, Gen. Elec. Rev. 452–458 (1931).

[10] Peek, Jour. A.I.E.E., **48,** 306 (1931).

In twelve night storms during which pictures have been taken, all within the Schonland reversal distance, a total of 366 flashes have been photographed and the field change deflections have been observed for 185. Of these, 77 show downward branching in discharges which reached the ground and the accompanying galvanometer deflections indicated positive field changes, requiring the lower pole of the cloud to be negative. Thirteen discharges which reached the ground showed negative field changes and came from a positive portion of the cloud. Several of these are striking examples of positive branching with their many fine streamers. Eight discharges reaching the ground have distinct upward branching, four being accompanied by positive field changes and four by negative. Eighteen show no branching although they clearly reached the ground. In some cases the fine streamers were obscured by clouds and rain. Forty-eight show branching across the sky but do not reach the earth, 29 having a positive field change and 19 a negative one. The remaining 21 are indeterminate. It will be seen from the above summary that either there *can* be branching downward from a negative cloud, or the observations are self-contradictory.

Schonland and Allibone[11] have shown that by the use of an impulse generator delivering over 3,000,000 volts they have been able to obtain branching *from* a negative point *to* a positive grounded plane. F. W. Peek, Jr., has sent me two photographs made in the General Electric laboratories which show branching *from* a negative point, one to a plane and the other to a point raised from a plane. He has also supplied photographs showing branching from a positive point to a negative plane, the streamers in this case being more numerous and attenuated. It is characteristic of my own photographs from a negative cloud that they consist of a very bright principal channel with but few light streamers, while those from a positive cloud are less concentrated and have many more streamers. This agrees well with the experience of the electrical engineers already cited that negative hits on their lines predominate over the positive and carry much larger charges.

From the above facts it is evident that Simpson's criterion for determining the polarity of a thundercloud by the direction of branching can no longer be accepted, and that his theory relative to the mechanism of thunderstorms will probably require revision at some points. The studies are being continued.

J. C. JENSEN

Nebraska Wesleyan University,
Lincoln, Nebraska,
May 12, 1932.

[11] Schonland and Allibone, Nature, **128,** 794 (1931).

An Attempt to Determine the Nuclear Moment of Beryllium

The evaluation of the nuclear moment of beryllium has become a matter of interest to physicists in general since the identification of the neutron by Chadwick,[1] as well as to spectroscopists. For if one assumes that there is conservation of angular momentum, then the neutron must have a spin equal to that of the beryllium nucleus. The collision of an α-particle with a Be^9 atom giving rise to a C^{12} atom plus a neutron leads to this result provided the above assumption is made.

The resonance line of beryllium, 2348.6A, has been photographed in the sixth order of a 21-foot grating (90,000 lines). The grating is mounted stigmatically and the dispersion for that order and region is 0.692A/mm. The line was excited by means of a helium-filled Schüler lamp. Eastman Hyperpress plates were used for the exposures which lasted 30 hours. The line appears quite as sharp as one would expect a sixth order line to appear. Nor does a microphotometer trace taken with a Koch-Goos recording microphotometer show any evidence of there being a hyperfine structure associated with this transition.

The resonance line of beryllium is a transition from a $2\,{}^1S$ to a $2\,{}^1P$ level and it is in the latter level that the hfs splittings occur, a level which might not be expected to have too large a hfs pattern. If one could obtain some Be III lines in a region where high dispersion and resolution are available, splittings comparable to those for Li II might be observed provided that Be^9 has a nuclear moment differing from zero.

With this same source an attempt was made

[1] J. Chadwick, Nature **129,** 312 (1932).

to find a band system due to Be_2 in order to determine the nuclear spin by means of the alternation of intensities. According to Furry and Bartlett[2] there should be such a band system in the infrared. Exposures of eight hours duration were taken with Xeno-cyanine plates in the first order of the grating but these failed to reveal such a band system which doubtless lies still farther out in the infrared.

ALLAN E. PARKER

Sloane Physics Laboratory,
New Haven, Connecticut,
May 14, 1932.

[2] W. H. Furry and J. H. Bartlett, Jr., Phys. Rev. **39,** 210 (1932).

The Transformation Product of Potassium

Potassium is known to emit beta-particles. Furthermore, there is evidence in support of the view that only one of the two isotopes of potassium is responsible for this radioactivity, namely, the isotope of mass 41.[1,2] The emission of a beta-particle should change this isotope into an isotope of calcium of mass 41, which is intermediate between the masses 40 and 44 of the two known isotopes of calcium. The amount of calcium 41 which would thus accumulate in potassium minerals since the consolidation of the earth's crust has been estimated to be from 0.01 to 0.1 percent.[3]

If calcium 41 is generated in this manner by radioactive potassium, it should be quite possible to detect its presence in potassium minerals of practically any age by the magneto-optic method[4] because of the great sensitivity of the apparatus. This method of attack has another advantage in that the potassium in transforming into calcium would change its valence from one to two. The "minimum" of light intensity characteristic of the calcium isotope would therefore appear on the scale at a point widely separated from the scale reading of its parent potassium isotope in all compounds in which they are studied, in consequence of the relationship between scale readings (or differential time lags) and combining equivalents of the cations.

We have examined for calcium 41 four samples of sylvite, in each of which we find a minimum of light intensity intermediate on the scale between the minima of calcium 40 and 44 and appropriate to calcium 41. The results are given below, the percentages being very rough estimates:

Sylvite	Approximate percentage of calcium 41	Approximate percentage of ordinary calcium
Sample		
No. 1, from Stassfurt, Prussia (purchased from Ward)	0.2	0.04
No. 2, from U.S. Potash Company, New Mexico (purchased from Mackay)	0.1	0.2
No. 3, from U.S. Potash Company, New Mexico (supplied by the company)	0.1	0.005
No. 4, Source unknown	0.02	0.005

It will be noted that the concentration of what appears to be Ca^{41} is surprisingly high in comparison with that which is calculated.[3]

In preparing the solutions for analysis, an amount of sylvite crystals weighing from 0.1 gm to 1 gm was used. As a check on the work, the calcium was examined in the chloride, sulphate, hydroxide and phosphate forms and in each case a minimum which may be attributed to Ca^{41} was found between the two minima of ordinary calcium. The scale readings, in the order of calcium 40, 41 and 44, for these compounds are:

[1] See Radiations from Radioactive Substances by Rutherford, Chadwick and Ellis, MacMillan Company, pages 541–544, and the references therein cited.

[2] Frost and Frost, Nature **125,** 48 (1930). Holmes and Lawson, same reference.

[3] Hevesy, Nature **120,** 838 (1927); Hevesy, Seith and Pahl, Zeits. f. phys. Chem., Bodenstein-Festband, pp. 309–318 (1931).

[4] Allison, Ind. Eng. Chem. (Analyt. Ed.) **4,** 9 (1932). Detailed description of apparatus *in press,* Preprints of American Inst. Mining and Metall. Eng.

$CaCl_2$	18.66	18.54	18.44
$CaSO_4$	12.05	11.80	11.54
$Ca(OH)_2$	12.57	12.49	12.37
$Ca_3(PO_4)_2$	23.52	23.38	23.20

Several commercial (C.P.) preparations of potassium compounds were also examined for this transformation product, with the following results:

Compound	Approximate percentage of calcium 41	Approximate percentage of ordinary calcium
KCl (Merck's)	3×10^{-6}	2×10^{-3}
K_2SO_4 (Merck's)	2×10^{-6}	4×10^{-4}
KOH (Merck's)	1×10^{-6}	1×10^{-3}
K_3PO_4 (Baker's)	3×10^{-3}	4×10^{-3}

Miss Edna R. Bishop kindly recrystallized some of the commercial (C.P.) KCl listed above, whereby we found the amount of the compound which may be ascribed to Ca^{41} to have been reduced by about ten fold.

The minimum attributable to Ca^{41} was looked for in fourteen commercial preparations (C.P.) of calcium, in six of which it occurred in traces, while its presence could not be detected in the other eight. It is therefore concluded that the minimum is not caused by a third isotope of ordinary calcium.

Since the functional dependence of scale reading upon atomic mass is not definitely known, we are unable to assign a mass of 41 rather than 42 or 43 to the calcium in question, but the evidence is positive that its mass lies between 40 and 44. We have searched, without success, for a third isotope of potassium which might be responsible for the radioactivity of this element and which might be the parent of a calcium atom of mass other than 41.

A search failed to reveal a minimum corresponding to a calcium isotope of mass 39 associated with sylvite, thus indicating that the isotope K^{39} does not take part in the radioactivity of potassium.

Since the minimum of light intensity in the several compounds investigated occurs at a point which corresponds to a calcium isotope of mass greater than 40 and less than 44 and since we know of no other compound to which this minimum can be assigned, the results above reported seem to present strong experimental evidence in support of the view that the transformation product of potassium is calcium, whose atomic mass is probably 41.

FRED ALLISON
ROY GOSLIN

Department of Physics,
Alabama Polytechnic Institute,
Auburn, Alabama,
May 14, 1932.

Note on Accommodation Coefficients

Michels[1] has shown that his determination of the ratio of the accommodation coefficients of helium and argon on a tungsten surface is not satisfactorily interpreted by the writer's theoretical considerations.[2]

These considerations were based upon the observation that under certain experimental conditions the probability that the solid suffers a change of quantum numbers during the reflection of a gas atom from its surface is much less than unity, i.e.

$$S \ll 1 \qquad (1)$$

Here S is the sum of all transition probabilities as calculated by a first order perturbation method. Under these conditions a good approximation to the energy transfer may be obtained by the first approximation in a perturbation scheme, permitting the accommodation coefficient to be readily calculated. For helium and argon gas with a tungsten surface at room temperature, $S \geq 0.15$, 0.54 respectively, according as $d \leq 0.25\times10^{-8}$cm, where d occurs in the repulsive potential $\exp(-r/d)$. Hence we should not expect the calculation to be applicable to argon at such a high temperature. Unfortunately the writer was originally too optimistic in stating the condition $S<1$ in place of (1).

The theoretical expression for the accommodation coefficient, (3) of reference 2, should be multiplied by 1/2. This error arose in the definition of t_0', which should be $\Delta E = k(t_0' - t_0)$.

In the calculation of the transition probability,[3] it was assumed that

$$a \ll d$$

[1] W. C. Michels, Phys. Rev. **40**, 472 (1932).
[2] C. Zener, Phys. Rev. **40**, 335 (1932).
[3] C. Zener, Phys. Rev. **37**, 556 (1931).

where a is the average displacement of a surface atom from its position of equilibrium. This assumption may be avoided, and the same results obtained, provided

$$a \ll \lambda$$

where λ is the wave-length of the gas atom. Both conditions are satisfied with helium and tungsten.

CLARENCE ZENER
National Research Fellow,
Palmer Physical Laboratory,
Princeton, N. J.
May 19, 1932.

The Ultimate Lines of Element 87

In a communication to the Physical Review the writer presented an estimate of the wave-lengths of those lines which may be expected to appear when a sample containing traces of the element of atomic number 87 is examined spectroscopically.[1] The numerical value of each line is dependent on the quantum defects of two levels, and as an error of ± 0.005 in the estimation of the latter produces an uncertainty of about $\mp 180\nu$ in the term value, the wave-lengths can be off by as much as 200A should the errors in the estimation of the levels be of opposite sign. It is therefore desirable to form an independent estimate of the wave-lengths of the first two doublets in the principal series spectrum of ekacaesium by a method which involves one, instead of two extrapolations, and for which data are available to test its reliability in constructing the known spectrum of radium.

TABLE I. *Spectrum of singly ionized radium.*

N_a	λ_a	N_b	λ_b	λ_a/λ_b
$1^2S-2^2P_2$: $\lambda_a/\lambda_b=0.006139N_a+1.7799$				
38	4077.714	30	2025.5	2.01319
56	4554.037	48	2144.39	2.12370
88	3814.44	80	1649.8	2.31206
	(3828)			(2.3201)
$1^2S-2^2P_1$: $\lambda_a/\lambda_b=0.007439N_a+1.7618$				
Sr	4215.515	Zn	2061.9	2.04448
Ba	4934.09	Cd	2265.03	2.17838
Ra	4682.20	Hg	1942.3	2.41065
	(4693)			(2.4164)

A method of extrapolation which fulfills these requirements assumes a linear relationship between the atomic number (N) and the ratio (λ_a/λ_b) of the wave-lengths of corresponding lines belonging to the spectrum of elements of sub-groups a and b with total quantum numbers $n+1$ and n respectively. Thus, in the second periodic group of elements the ratio of the wave-lengths of the *raies ultimes* emitted by strontium and zinc, barium and cadmium, and radium and mercury are proportional to the atomic numbers of either sub-group of elements. Table I shows that the wave-lengths of the radium lines can be closely approximated by this method, the estimates being 3828A and 4693A, whereas the observed lines of the doublet reside at 3814.44A and 4682.20A. Again, the difference between the wave-numbers of the two lines is 4818ν which compares favorably with the measured doublet separation of 4857.2ν.

TABLE II. *Red lines of neutral ekacaesium.*

N_a	λ_a	N_b	λ_b	λ_a/λ_b
$1^2S-2^2P_2$: $\lambda_a/\lambda_b=0.010860N_a+2.0001$				
37	7800.30	29	3247.548	2.40190
55	8521.15	47	3280.67	2.59738
87	(7150)	79	2427.96	(2.9449)
$1^2S-2^2P_1$: $\lambda_a/\lambda_b=0.012014N_a+1.9830$				
Rb	7947.63	Cu	3273.964	2.42753
Cs	8943.6	Ag	3382.89	2.64378
87	(8104)	Au	2675.95	(3.0282)

TABLE III. *Violet lines of neutral ekacaesium.*

N_a	λ_a	N_b	λ_b	λ_a/λ_b
$1^2S-3^2P_2$: $\lambda_a/\lambda_b=0.007464N_a+1.7994$				
37	4201.81	29	2024.33*	2.07557
55	4555.3	47	2061.19*	2.20992
87	(4225)	79	1725.5†	(2.4488)
$1^2S-3^2P_1$: $\lambda_a/\lambda_b=0.007668N_a+1.7973$				
Rb	4215.58	Cu	2025.67*	2.08097
Cs	4593.2	Ag	2069.85*	2.21899
87	(4328)	Au	1756.0†	(2.4644)

[1] H. Yagoda, Phys. Rev. **38**, 2298 (1931).

* A. Fowler, "Report on Series in Line Spectra," p. 111 (1922) London.
† W. M. Hicks, Phil. Mag. (6) **38**, 26 (1919).

A similar set of operations on the members of group I may be expected to yield equally reliable results in the estimation of the corresponding lines of element 87. These calculations are presented in Tables II and III;

quantities in parentheses indicating extrapolated values. Unless otherwise noted the wave-lengths are those given in the International Critical Tables.[2] A comparison of the new estimates with the values secured from the quantum defect relationship (Table IV) shows that only in the case of the $1^2S-2^2P_2$

TABLE IV. *Ultimate lines of element 87.*

Method	Red doublet $1^2S-2^2P_2$	Red doublet $1^2S-2^2P_1$	Violet doublet $1^2S-3^2P_2$	Violet doublet $1^2S-3^2P_1$
Quantum defects	7460	8130	4260	4310
Sub-group ratios	7150	8104	4225	4328

line of the red doublet do the two methods yield markedly different results. The doublet separations of 1646ν in the red, and 558ν in the violet region are in good agreement with independent estimates for these intervals, the mean of which are $1690 \pm 100\nu$ and $550 \pm 50\nu$.[3]

Judging from the nature of the agreement between the calculated and observed spectral lines in the case of the radium spectrum, it may be concluded that in the spectrophotographic examination of mineral concentrates lines in the region of 4225 ± 15A and 4328 ± 15A will be observed should the sample contain ekacaesium. The investigation also indicates that the first doublet of the principal series will appear in a region that is better adopted for its visual observation than has been supposed by previous workers.[4]

HERMAN YAGODA

New York University,
Washington Square East,
May 19, 1932.

[2] Inter. Critical Tables **5,** 323 (1929).

[3] Detailed calculations will be published in the July or a later issue of the Journal of the American Chemical Society.

[4] K. T. Bainbridge, Phys. Rev. **34,** 752 (1929); J. Papish and E. Wainer, J. Am. Chem. Soc. **53,** 3818 (1931); W. F. Meggers, Science Supplement **74,** No. 1926, 10 (1931)

Absorption of Oxygen in the Region of Short Wave-lengths

The dispersion of oxygen between the visible and 1900A can be described quantitatively[1] by two resonance wave-lengths $\lambda_1 = 1469$A and $\lambda_2 = 544$A with the corresponding number of oscillators $f_1 = 0.20$ and $f_2 = 5.93$.

In order to study the physical significance of this result we have investigated the absorption of oxygen down to 300A by means both of a small fluorite and a large grating spectrograph. The latter, designed by Compton and Boyce,[2] was used for qualitative measurements only. Flowing oxygen was introduced into the spectrograph at pressures between 0.25 and 0.002 mm. Besides the oxygen, only some helium, at about 0.001 mm pressure, coming from the light source, was in the spectrograph. The light source was an uncondensed capillary discharge at 0.1 mm pressure in helium containing perhaps one percent of impurities. This gave emission lines distributed over the whole of the spectral range investigated. The conspicuous impurities were oxygen, hydrogen and nitrogen.

The results confirm some of the earlier experiments of Lyman, Leifson and Hopfield. There are two strong absorption regions in oxygen, one between 1750 and 1300, with a maximum in the neighborhood of 1400A, and another below 1100A and still quite strong at 300A, separated by a gap which is transparent for a 4 meter path of pure O_2 at 0.25 mm pressure. As nitrogen proved to be also transparent in this region, it seems hopeful to use wave-lengths between 1300 and 1100A for photochemical reactions, the light source and the reaction chamber being separated by CaF_2 or LiF windows and a few millimeters of air. Such a light source is under construction.

The two resonance wave-lengths calculated from the dispersion measurements correspond obviously to the two observed absorption regions. Their positions are in fair agreement with the estimated centers of gravity of the absorption bands.

For quantitative measurements we used a fluorite spectrograph, like one constructed by Cario and Schmidt-Ott,[3] the hydrogen spectrum of a capillary tube as light source and

[1] R. Ladenburg and G. Wolfsohn, Phys. Rev. **40,** 123 (1932).

[2] K. T. Compton and J. C. Boyce, Phys. Rev. **40,** 1038 (1932).

[3] G. Cario and H. D. Schmidt-Ott, Zeits. f. Physik **69,** 719 (1931).

the photographic photometric method to determine the absorption coefficient in the continuous absorption of the Schumann-Runge bands. The dissociation of the O_2 molecule by the influence of light in this region of the spectrum is so strong that by illuminating a closed cell of 10 cm length for 1450A to about one-half of its intensity, i.e., as much as metallic absorption. The absorption in the band lines is incomparably smaller. This is just what we should expect from the above mentioned dispersion measurements as well as from the application of the Franck-Condon principle to the potential energy

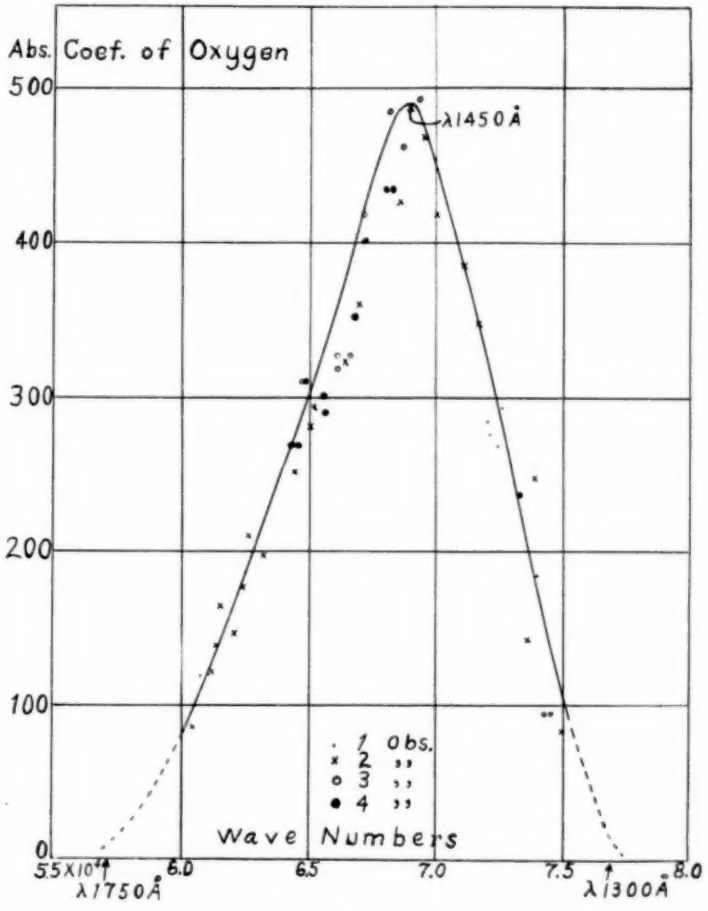

Fig. 1.

some minutes the greater part of the oxygen disappears, the O atoms probably being absorbed by the walls of the cell.

The results of our measurements are shown in the graph, the abscissae being wave numbers ($1/\lambda$), the ordinates, absorption coefficients α defined by the equation

$$I = I_0 \epsilon^{-\alpha l}$$

and reduced to 76 cm pressure and 0°C, l being in cm. Therefore a length of 0.0014 cm of O_2 at NPT reduces light of wave-length curves of O_2 calculated by Morse[4] and Stueckelberg.[5]

Finally we can compute from the graph of the absorption coefficient the f value, assuming the classical relation between absorption and dispersion[6]

[4] P. M. Morse, Phys. Rev. **34,** 57 (1929).

[5] E. C. G. Stueckelberg, Phys. Rev. **34,** 65 (1929).

[6] R. Ladenburg, Verh. d. D. Phys. Ges. **16,** 769 (1914); Zeits. f. Physik **4,** 451 (1921).

$$\int \alpha d\nu = \pi N f e^2/mc = f \times 7.12 \cdot 10^{17}$$

where N means the number of molecules at NPT. Thus we get for the absorption of oxygen in the Schumann region the value

$$f = 0.193 \text{ and } \lambda_{max} = 1450\text{A}$$

in very good agreement with the conclusions drawn from the dispersion curve.

Regarding the second resonance wavelength in the region of 544A, our qualitative measurements by means of the grating spectrograph show that the absorption coefficient is here of the same order of magnitude as in the Schumann region. On the other hand the corresponding f value as deduced from the dispersion measurements turned out to be about 30 times as large as f_1. This can be accounted for if we assume that the absorption region extends from 1100A to 160A, an assumption compatible with our experiments which showed a quite considerable absorption at 303A with a column of 4 meters of oxygen at 0.002 mm pressure.

So we may say that our absorption measurements of the O_2—molecule confirm the conclusions drawn from the dispersion curve and the classical relation between absorption and dispersion, heretofore verified only for monatomic gases.

R. Ladenburg
C. C. Van Voorhis
J. C. Boyce
Palmer Physical Laboratory,
Princeton University,
May 25, 1932.

Measurements of the Height of a Large Drop of Mercury

A recent paper in this journal by the present writer[1] gave for the surface tension of mercury in vacuum values ranging from 438.4 ±0.3 dynes per cm at 12.5° to 423.9 ±0.6 dynes per cm at 67°—determined by the flat-drop method. The accuracy of results obtained by this method have been questioned by R. S. Burdon in a letter to Nature.[2] His contention is that there is a possibility that the readings were taken on "the lowest curve of the drop which will reflect rays coming from the top of the ground-glass window," instead of on the real summit of the drop. Needless to say a point so important as the exact definition of the top of the drop was not overlooked in the original experiment. Between March 31 and July 26, 1930, fifty-four sets of readings, each set consisting of at least nine trials, were discarded chiefly because the definition of the top of the drop was not considered sufficiently exact. Two layers of heavy asbestos paper wrapped around the large tube containing the dish of mercury restricted the entrance of light to a circular opening less than 1 cm in diameter. As the top of the opening was approximately 1 mm above the top of the drop the source of error mentioned by Burdon was practically eliminated.

However, in spite of the care taken in the original experiment, to ascertain the true top of the drop, efforts have since been made, in accordance with Burdon's suggestion,[2] to check the readings previously taken. A summary of the work follows.

The apparatus was reset and the lighting conditions duplicated. The horizontal microscope was focused on the center of the drop's meniscus, the line which gives the sharpest focus. A set of readings was taken. Then the light was blocked out from the top of the window until the verge of invisibility was reached. The averages given below speak for themselves.

Full window.....	0.8182 ±0.0001 cm
1 cm window	0.8183 ±0.0001 cm
Blocked window....	0.8183 ±0.0001 cm

A facsimile of the dish was set up in the open laboratory. The room was darkened and the lamp encased in a box the only opening of which was covered with unglazed paper. The top of the drop was first located by means of oblique lines[3] ruled on a card which was placed directly behind the dish. The cross hairs, focused on the intersection of the slanting lines and their reflection, remained unchanged upon the removal of the card. Nor did the use of a spherometer point, as suggested by Burdon, produce any change in the setting.

As a further test that the conditions under which readings were taken on the top of the drop were not precisely the same as those de-

[1] M. Kernaghan, Phys. Rev. **37,** 990–997, (1931).

[2] R. S. Burdon, Nature **128,** 456, (1931).

[3] S. G. Cook, Phys. Rev. **34,** 513–520, (1929).

scribed by Burdon for the encased drop, efforts were made to reproduce his experiment.[2] A drop 6 cm in diameter was encased in a closed box. The drop was illuminated through a ground-glass window 6 cm in diameter and arranged symmetrically with

TABLE I.

Diamter of window in cm	Height from top of drop to top of window in cm	Reading of microscope set on apparent top of drop in cm
6	2.5	0.5531 ± 0.0001
	0.2	0.5640 ± 0.0001
	0.1*	0.5725 ± 0.0001
4	1.5	0.5579 ± 0.0001
	0.2	0.5643 ± 0.0002
	0.1*	0.5745 ± 0.0001
2.8	0.9	0.5617 ± 0.0001
	0.2	0.5645 ± 0.0001
	0.1*	0.5746 ± 0.0001
1	0.15 (approx)	0.5733 ± 0.0001
	0.1*	0.5746 ± 0.0001

* or less.

reference to it. The distance between the center of the drop and the window was 9 cm. Light was admitted through apertures 6 cm, 4 cm, 2.8 cm and 1 cm respectively and in each case it was blocked out by steps. Table I gives the results.

Burdon gets a difference of 0.121 mm in the reading for the apparent top of the drop for heights of 1 mm and 8 mm respectively. In the above table the difference is 0.129 mm for heights 1 mm and 9 mm respectively. The distance between the lamp and the center of the drop was in one case 4 cm and in the other case 9 cm.

Since the opening used in the original experiment was 1 cm in diameter and the top of this opening was about 1 mm or even less above the top of the drop it is felt that Burdon's criticism does not apply. It is likewise felt that the readings were taken on the true summit of the drop and consequently the value for the surface tension of mercury in vacuum computed from those readings is deemed the correct value.

The writer wishes to thank Doctor F. E. Poindexter for his keen interest and cooperation in this work.

MARIE KERNAGHAN, R.S.C.J.
Maryville College,
St. Louis, Missouri,
May 25, 1932.

An Experiment in Support of the Hypothesis of a Time Lag in the Faraday Effect

There has been an accumulation of experimental evidence in our studies with the magneto-optic method of analysis which seems to favor the view that the nature of the phenomena underlying this method is associated with a time lag in the Faraday effect.[1,2] The present experiment, which was suggested by Professor J. W. Beams, appears to be difficult of explanation upon any other hypothesis. A mixture of compounds possessing both positive and negative Verdet constants (a water solution of salts of cerium) was prepared which when placed between crossed Nicols in a steady magnetic field of at least 2000 gauss showed zero Faraday effect for monochromatic light. The cell containing this solution was then placed in one of the coils in the magneto-optic apparatus, the other coil being empty, and subjected to the field produced by the high potential current surges ordinarily employed. Upon application of this field, there was observed a brightening of the light transmitted by the second Nicol. As it was not possible to secure a solution free of a certain amount of color and as the absorption of light was therefore considerable, all observations were made after the manner of Faraday by slightly uncrossing the Nicols until there was a threshold of visibility of the light in the absence of the magnetic field, so that a rotation of the plane of polarization would be perceptible. The observations were made when the analyzing Nicol was in this slightly uncrossed position both in the clockwise and the counterclockwise directions. In neither setting of the analyzer could any brightening be detected when the steady field was applied, while there was definitely produced, with both settings of the analyzer, an increase in the light intensity upon application of the transient field. The monochromatic light used was the Mg 4481A spark line. The neutral solution

[1] Allison and Murphy, J. Am. Chem. Soc. **52,** 3796 (1930).

[2] Allison, Christensen and Waldo, Abstract, Washington Meeting of the American Physical Society.

was obtained after a considerable amount of rather tedious experimentation by the trial and error method.

Since the solution contains positive and negative compounds (and traces of numerous impurities), the brightening of the transmitted light under the influence of the transient magnetic field can be accounted for upon the hypothesis that the compounds present in the solution have different Faraday time lags and thus set up rotation of the plane of polarization at different times after the application of the field. The maximum instantaneous field due to the high tension transient currents, as computed from our experimental data, is less than the strength of the steady magnetic field which gave no rotation.

FRED ALLISON
JOHN L. CONDON
Department of Physics,
Alabama Polytechnic Institute,
May 28, 1932.

Dependence of the Ionization Produced by the Cosmic Penetrating Radiation upon Pressure and Temperature

Compton, Bennett and Stearns[1] have recently offered an explanation of the ionization-pressure relation at high pressures in terms of a selective recombination at these pressures. On this basis they have been able to approximate closely the experimental ionization-pressure curves and to explain to some extent the difference in the ionization produced by the penetrating radiation in different gases.

An interesting feature of this explanation is that it indicates a dependence of the ionization produced in a given quantity of gas upon the temperature of the gas. According to the theory the variation with temperature is negligible at pressures in the neighborhood of 1 atmosphere but increases with pressure and becomes considerable in the neighborhood of 100 atmospheres.

In testing the theory, Compton[1] and his associates found that "Two series of readings on air at 100 atmospheres pressure, taken between 0° and 30°C and between 0° and 37°C, showed greater ionization at the higher temperature by 7.8 percent and 8.3 percent respectively. Only one set of temperature readings was made at a lower pressure. This was for nitrogen at 20 atmospheres. The observed effect was 0.0000 ± 0.0003, whereas the predicted value of $\beta(=\delta i/\delta T)$ for nitrogen at this pressure is 0.0004."

The ionization in the above work was produced by gamma-rays. Stearns informs me that he has recently investigated the temperature variation of the ionization produced by the cosmic penetrating radiation in oxygen at a pressure of 70(?) atmospheres, and has found an effect corresponding to that previously observed with the gamma-ray ionization at 100 atmospheres.

Wolff[2] has very recently investigated the temperature variation of the gamma-ray ionization in CO_2 and N_2 at 21.5 atmospheres. He observed an increase of 10 percent in the ionization in CO_2 and 5.3 percent in that in N_2, upon increasing the temperature from 1° to 38°C.

The writer has investigated the temperature effect in the ionization produced by the penetrating radiation in the 13.8 liter spherical chamber described elsewhere[3] in detail, with the 5.5–6 ft. water shield. With constant amount of air and a mean pressure of 162.1 atmospheres, the ionization was observed to increase 7.0 percent of the smaller value when the temperature was increased from 7.5° to 40.5°C. Under similar conditions but with a mean pressure of 23.3 atmospheres, the ionization increased 8.7 percent of the smaller value when the temperature was increased from 14.45° to 47.25°C. These values are without corrections for variations in barometric pressure or for variations in the density of the shields. The barometric pressure was practically the same during the high and low temperature observations at the higher pressure, but at the lower pressure the barometric pressure during the high temperature observations was low, perhaps enough to have augmented the variation in ionization by an amount of the order of 1 percent. However, intermediate temperature observations at the higher pressure indicate that the variation of the ionization with temperature is greater at

[1] A. H. Compton, R. D. Bennett and J. C. Stearns, Phys. Rev. **39**, 873 (1932).

[2] Kurt Wolff, Zeits. f. Physik **75**, 570 (1932).

[3] J. W. Broxon, Phys. Rev. **37**, 1320 (1931).

higher temperatures. In fact, when the temperature rate of variation of the ionization at the high and low pressures is considered as a function of the temperature, the indication is that the temperature effect may be nearly independent of the pressure.

Apparent slight dependence of the ionization upon time rate of change of temperature or upon the previous condition of the gas has also been observed. Soon after filling the chamber to a high pressure very large ionization values (sometimes about twice the equilibrium values) were observed, even though the gas appeared to have assumed a nearly constant temperature and the ionization current had been flowing for several minutes. Soon after reducing the pressure the ionization was also somewhat greater than the final steady value, but no differences as large as those following compression were observed.

JAMES W. BROXON

University of Colorado,
May 30, 1932.

PROCEEDINGS OF THE AMERICAN PHYSICAL SOCIETY

MINUTES OF THE WASHINGTON MEETING APRIL 28–30, 1932

The 177th regular meeting of the American Physical Society was held in Washington, D. C. at the Bureau of Standards on Thursday and Friday, April 28 and 29, and at the National Academy of Sciences on Saturday, April 30, 1932. The first session began at ten o'clock on Thursday morning. There were three parallel sessions for the reading of the ten minute contributed papers on Thursday morning, three on Thursday afternoon, two on Friday morning, two on Friday afternoon and two on Saturday afternoon. The presiding officers were W. F. G. Swann, President of the Society, Paul D. Foote, Vice-President, K. K. Darrow, W. J. Humphreys, H. E. Ives, C. E. Mendenhall, F. K. Richtmyer and E. B. Stephenson.

On Saturday morning from ten to eleven-fifteen o'clock there was a symposium on "Electric and Magnetic Units." This program was arranged by Professor A. E. Kennelly of Harvard University on behalf of the International Electrotechnical Union and the International Union of Pure and Applied Physics. The program consisted of five contributed papers, abstracts of which, numbers 95, 96, 97, 98 and 121, appear in the following pages. After considerable discussion the meeting passed a resolution that the President of the American Physical Society appoint a committee to consider the question of what action the Physical Society should take in regard to the adoption of electrical and magnetic units and report, if possible, to the Council and the Society at the New Haven meeting.

The session on units was followed at eleven-fifteen o'clock by a second symposium on "Structure of Solids." This consisted of two invited papers. The first was on "The Mosaic Structure in Metal Crystals" by Professor A. Goetz from the California Institute of Technology. The second paper was "On Newly Discovered Effects in Ferromagnetic Crystals" by Dr. Francis Bitter from the Westinghouse Electric and Manufacturing Company, Pittsburgh.

On Friday evening the Society held a dinner at the Hotel Washington with 186 present. The President presided and the after dinner speakers were K. T. Compton, Paul D. Foote, D. C. Miller and Professor Franz Simon visiting from the University of Breslau, Germany.

Meeting of the Council: At its meeting held on Thursday, April 28, 1932, the deaths of three fellows, Louis A. Bauer, B. A. Behrend and C. Leo Mees, and one member, F. M. Hartmann, were reported. One person was transferred from membership to fellowship and eighty-two were elected to mem-

bership. *Transferred from Membership to Fellowship:* S. Herbert Anderson. *Elected to Membership:* Carl D. Anderson, Oscar E. Anderson, Prescott N. Arnold, Benito E. Artau, Richard M. Badger, S. S. Barker, Baronig Baron, Norris E. Bradbury, Weldon G. Brown, Florence C. Burmann, William E. Bush, Milton A. Chaffee, Stuart H. Chamberlain, George Collins, Frederick P. Cowan, Howard J. Curtis, Ardith P. Davis, Wallace deLaguna, Joseph H. Dexter, John S. Donal Jr., Hugh L. Donley, George A. Downsbrough, Frank G. Dunnington, P. Whitfield Durkee, John P. Elting, Gladys D. Finney, Alfred B. Focke, Milton E. Gardner, Fred Goeddeke, Hyman H. Goldsmith, J. C. Gray, L. R. Hafstad, C. L. Haines, Harry H. Hall, Thomas M. Hammond, Maurice F. Hasler, Robert J. Hopkins, Archer Hoyt, Howard C. Hoyt, Andrew Hustrulid, Chih K. Jen, C. R. Jeppesen, P. Kapitza, Edward H. Kurth, Joseph K. Leibing, Leo H. Linford, M. Stanley Livingston, William M. Lobenstine, Dorothea Lyford, J. Adair Lyon, Millard F. Manning, Emmett V. Martin, C. H. Matz, John W. Mauchly, J. H. McLeod, Austin McTigue, Kenneth R. More, Harold E. Mott, George F. Moynahan, Philip Nolan, Floyd Ostenson, Charles G. Patten, A. L. Patterson, James C. Scott, David H. Sloan, Dwight O. Smith, Noyes D. Smith, Jr., J. Edward Spike, Jr., Robert G. Stokely, Charles A. Swartz, John G. Tappert, D. Oscar Trauger, Edwin A. Uehling, Robert N. Varney, Ernst Weber, Howard W. Weinhart, Frederick E. White, Harry J. White, C. T. Wood, George H. Worrall, Ta-You Wu, and John Wulff.

At this meeting the Council approved with a few modifications the Constitution presented by the executive committee of the newly formed New England Section. The members of this executive committee are: Professor E. C. Kemble (Harvard) chairman, Professor P. M. Morse (M.I.T.) secretary, Professor G. F. Hull (Dartmouth), Professor Louise S. McDowell (Wellesley) and Professor S. R. Williams (Amherst).

The Council also approved the Constitution of the American Institute of Physics as presented by its secretary, G. B. Pegram.

The regular scientific program of the Society consisted of 122 papers. Numbers 1, 11, 31, 38, 51, 54, 76, 106, 108, 117 and 119 were read by title. The abstracts of these papers are given in the following pages. An *Author Index* will be found at the end.

W. L. SEVERINGHAUS, SECRETARY

1. The mechanism of atomization accompanying solid injection. R. A. CASTLEMAN, JR., *Bureau of Standards.*—A brief historical and descriptive account of solid injection is followed by a detailed review of the available theoretical and experimental data that seem to throw light on the mechanism of this form of atomization. It is concluded that this evidence indicates that: (1) the atomization accompanying solid injection occurs at the surface of the liquid after it issues as a solid stream from the orifice; and (2) such atomization has a mechanism physically identical with the atomization which takes place in an air stream, both being due merely to the formation, at the gas-liquid interface, of fine ligaments under the influence of the relative motion of gas and liquid and to their collapse under the influence of surface tension to form the drops in the spray. This simple theory, previously proposed by the author, is the most satisfactory and fits the observations the best of any yet advanced. It is recommended that the use of the term "atomization" be restricted to a certain range in which its use is sound etymologi-

cally and physically. This analysis is to appear in detail as a Technical Report of the National Advisory Committee for Aeronautics.

2. The mechanics of effervescence. OTTO STUHLMAN, JR., *University of North Carolina.*—Bubbles of gas when released in a liquid at depths great compared to their diameters on reaching the surface burst and eject droplets of the fluid into the air. Each bubble whose diameter is less than a critical value, as determined by the characteristics of the liquid, on bursting simultaneously ejects many droplets. Their distribution in height is logarithmic with the greater difference in height between the higher ones. For water at 21°C maximum droplet ejection was 14 cm for a critical bubble diameter of 0.12 cm; benzene is less stable but gives 9.0 cm height for 0.15 cm at 22°C. Bubbles less than 0.10 cm diameter eject droplets to heights proportional to three halves power of the radius. Bubbles having diameters greater than the above critical values burst irregularly. Irregularity is attributed to instability of the bubble. Variation in distribution amongst any given group of droplets at a given height is nearly Maxwellian. Lower boundary is sharp with a more straggling distribution for larger values of height. The theory of ejection herewith developed pictures the bursting bubble accompanied by a gas vortex ring which assists in raising the liquid jet of contour $hx=$constant, and volume $hx^2=c$. Instability in raising a volcano-like jet produces drop formation, which vortex ring redistributes so that log h decreases proportionally as the number of drops increases linearly.

3. Diagonal symmetry in Chladni plates. R. C. COLWELL, *West Virginia University.*—Ritz has shown that all the figures of a Chladni plate may be developed from the equation $w=\Sigma\Sigma u_m(x)v_n(y)$. For high vibrations two terms of the series will give a very close approximation to the sand nodes. The equation then takes the form $w=Au_mv_n+Bu_nv_m$, in which u_m and v_n represent the solutions of a bar fixed at the center. These terms contain both hyperbolic and trigonometric functions. The only diagonal type investigated by Ritz was the simple form where $m=n+1$. This gives one diagonal and a group of wavy lines parallel to it. With an electric valve oscillator which forces the plate into very high vibrations, it is possible to form many complicated figures with symmetry about the diagonal. Several of these will be shown.

4. Ultrasonic absorption in gases. J. C. HUBBARD, *The Johns Hopkins University.*—Electrodes of the piezoelectric plate of an acoustic resonator interferometer (J. C. Hubbard, Phys. Rev. **38,** 1011, (1931)) are connected to the variable capacity of a tuned circuit including thermo-galvanometer. The circuit is excited at the crevasse frequency of the resonator plate, the circuit being tuned to resonance. Simple relationships are expected and found between thermo-galvanometer current and path-length r in the interferometer fluid. If σ be the ratio of current to resonance maximum current with the interferometer disconnected, σ_0 at loops (constant), σ_m at nodes, then for small values of r, $[\sigma_m/(1-\sigma_m)-\sigma_0/(1-\sigma_0)](r\alpha+\beta)=$const., where α is the attenuation factor of particle velocity in the fluid, and $\beta=-\log\gamma$, where γ is the coefficient of reflection. Correction must be made when α is large (CO_2). A simple method of evaluating α and γ is derived from peak widths of the σ, r curve. For room air the above relation exactly describes results, but α is several times larger than would be expected for dry, CO_2—free air, being 0.25 at 500 kc and 24°C. Experiments are in progress with pure gases.

5. The electric network equivalent of a piezoelectric resonator. K. S. VAN DYKE, *Wesleyan University.*—The decrement of a quartz resonator is measured by observing in a cathode-ray oscillograph the decay of its free vibrations. The measured logarithmic decrement is a linear function of the external load resistance when electrodes are plated on the quartz, which function yields the resistance and inductance elements of the network. For a quartz rod $40\times5\times5$ mm vibrating lengthwise in its fundamental compressional mode (67.5 k.c.) the inductance is thus measured to be 395 henries. Comparison of this value with the formulas previously derived (Phys. Rev. **25,** 895, (1925)) for the elements of the network yields a value of the piezoelectric constant for quartz in agreement with the statically determined value preferred by the International Critical Tables. After eliminating the uncertainties of mounting, the decrement is found to be a linear function of the pressure of the surrounding atmosphere and to be proportional to the radiation resistance of the particular gas used. The residual decrement in vacuum for resonance frequencies between 50 and 100 k.c. varies between 10^{-5} and 5×10^{-5} for

different resonators tried. It is 1.6×10^{-5} for the resonator studied above, which indicates a resistance element of 950 ohms. This corresponds to an internal friction constant (Kimball's ξ, Phys. Rev. **30**, 956 (1927)) of 0.018×10^{-15}.

6. Hydrodynamic characteristics of twelve symmetrical hydrofoils. R. C. DARNELL, *U. S. Experimental Model Basin, Washington, D. C.*—The center of pressure and coefficients of lift, drag, and absolute moment have been determined for 12 hydrofoils of symmetrical section and 0.25 sq. ft. area at a Reynolds number of approximately 175,000. The hydrofoils were towed (leading edge vertical) in the tank of the Model Basin beneath a special flat bottomed float that carried the dynamometer by which the lift, drag, and torque were measured. The angle of attack was varied from 0° to 45° and the interval between the top of the hydrofoil and the bottom of the float from 0 to 2 in. The aspect ratios studied were 0.5, 1.0, 1.5, and 2.0. In general up to the burbling point the lift coefficient can be represented with fair accuracy by the equation

$$C_L = \frac{\alpha}{0.182 + \frac{1}{\pi R}}$$

where α is the angle of attack in circular measure and R the aspect ratio. For $R=1$ the flow breaks down at $\alpha=32°$ and for $R=2$ at about 20°. The center of pressure remains at approximately the quarter chord point up to about 15°; in the interval of 15°−25° it moves rapidly towards the trailing edge and between 25° and 45° is located about 40 percent of the chord from the leading edge.

7. The radon content of soil gas. HOLBROOK G. BOTSET. *Gulf Research Laboratory.—Introduced by Paul D. Foote*—An electroscope and apparatus for sampling and measuring the radon content of soil gas are described. A study of the radon content of soil gases under varying conditions and over extensive areas gave the following results: There is apparently no correlation between radon content and depth from which the gas sample is taken; radon content during rainy weather appears to be higher than in dry weather; certain soil formations appear to have more or less characteristic radon contents. There is great local variation in the radon content of soil gas. Measurement of the radon content over a known salt dome showed a definite increase in radon content along the edge of the dome. This was an eroded structure and soil along its edge was enriched in heavy mineral. A determination of the heavy mineral content of the soil showed a definite correlation with the radon content of the soil gas, whence it is found that this is an indirect qualitative measure of the heavy mineral content of the soil.

8. Flow of liquids through porous materials under the action of gravity. R. D. WYCKOFF, H. G. BOTSET, M. MUSKAT. *Gulf Research Laboratory.*—Recent published results of studies on the flow of liquids through porous materials under the action of gravity have resulted in rather wide disagreement in both the formulation and interpretation. This paper presents the experimental results obtained by the authors, together with an analysis and final empirical formulation of the flow equations. Typical of the results is the equation for the gravity flow in a radial system given by:

$$Q = \frac{\pi K\gamma g(Z_1^2 - Z_2^2)}{\ln \frac{r_1}{r_2}}$$

where K = permeability of the medium, γ = density of fluid, g = acceleration of gravity, r_1 = reservoir radius, r_2 = well radius, Z_1 and Z_2 = hydrostatic head of fluid observed at the bottom of the sand at r_1 and r_2 respectively. The paper extends the analysis to include the case of composite flow in which gravity and pressure drive exist simultaneously. Experimental data on this case are presented. Finally the analysis is extended to cover general gravity flow systems whose geometry is other than radial.

9. Capillary action at low pressures. F. W. CONSTANT, *Duke University.*—Consideration of the pressure just beneath the meniscus of a liquid in a capillary tube shows that the rise of a liquid due to capillary action is limited at low pressures or for very fine capillaries by the air

pressure above the liquid, although the simple theory of surface tension does not predict this. Thus as the air pressure is gradually reduced a capillary column of water, say 30 cm high, is at first unaffected, then falls steadily, showing no rise in a vacuum. This was confirmed experimentally, the effect being somewhat complicated by the slower diffusion of the vapor through the fine capillary. Capillary action in tall trees is hence limited to about 32 feet. No effect occurs for liquids which are depressed in capillary tubes, such as mercury in glass.

10. Viscosity and particle shape in colloid solutions. LARS ONSAGER, *Brown University.*—Einstein has shown that spherical particles in solution will increase the viscosity by a factor $\Delta\eta/\eta=1+2.5\phi$, where ϕ is the fraction of the total volume occupied by the solute. For an extension to ellipsoidal particles, the necessary hydrodynamic calculations have been made by Jeffery (Proc. Roy. Soc. **A102,** 161 (1922)). Presently, the Brownian motion is taken into account. For ellipsoids of rotation, with semi-major axes $a \gg b=c$, the factor 2.5 in Einstein's formula is replaced by $4a^2/15b^2 \log (a/b)$. The time of relaxation for rotation is $\tau=\rho/6kT$, where $\rho=\eta\times 8\pi a^3/3 \log (a/b)$, e.g., for $\eta=0.01$ and $a=100b=5\times 10^{-5}$ cm. The calculated viscosities are much greater than those measured by Staudinger for solutions of paraffins in tetralin, etc., which indicates that such molecules do not retain a straight linear shape in solution. In addition, it seems necessary to assume slip at the surface of a hydrocarbon molecule.

11. The relationship of gravitation and electromagnetism. WILLIAM A. TRIPP, *Medford, Mass.*—The law of gravitation is deduced on a purely electromagnetic basis. The formula for the attractive force between bodies is derived and shown to be equivalent to the usual gravitational formula in the case of bodies at rest, but relative motion affects the value of the force if the bodies are not at rest. The analysis is based on the present day concept of atomic structure which postulates relatively stationary protons and rapidly moving electrons, coupled with an application of electromagnetic phenomena interpreted in terms of electronic reactions. Gravitation thus appears, not as a vague individual phenomenon, but as the statistical residue of electromagnetic attractions and repulsions on all the individual particles of matter in a body, the attractive forces predominating.

12. Aberration of the second order in the Michelson-Morley experiment. N. GALLISHOHAT, *Helen Schaeffer Huff Memorial Research Fellow, Bryn Mawr College.*—The theory of the second-order aberration in application to the Michelson-Morley experiment has been further developed. *Summary.* The phase-effect must be compensated by Lorentz-FitzGerald contraction. The displacement of fringes observed by D. C. Miller is due to aberration of the interfering rays. The horizontal displacement Δl_H of fringes in *D. C. Miller experiment,* recomputed in terms of the horizontal component of v, $\Delta l_H=l/2(v^2/c^2)\sin^2(v,z)\sin 2\psi$, ($z$-vertical, ψ-azimuth), shows a shift of the azimuth-curve by 45°, the velocity v (data of D. C. Miller) is 460 km/sec. in the direction found by D. C. Miller. *Michelson's repetition:* the line of sight l and fringes—stationary; thus, no aberration could be observed. *Joos' repetition:* stationary l, but rotating fringes; $\Delta l=l/2(v^2/c^2)\sin 2(v,z)\cos\alpha$ (α-angular displacement of fringes) represents a full-period effect, actually observed by Joos but eliminated by averaging the readings for both halves of the interferometer's revolution. *Piccard repetition:* classical form of interferometer, horizontal fringes; thus, full-period vertical effect: $\Delta l_V=l/2(v^2/c^2)\sin^2(v,z)\cos\psi$, again excluded by averaging. *Kennedy's repetition:* photometric method with broad fringes (nearly parallel beams), sensitivity 2×10^{-3} (fringe). In order to detect aberration (about 7×10^{-3} mm), this would require fringes about 4 mm—too narrow for the method used. *Conclusion.* The zero-result of the various repetitions of the Michelson-Morley experiment is *not inconsistent* with the result of D. C. Miller, considered as second-order aberration.

13. Graphical presentation of compressibility data. W. EDWARDS DEMING AND LOLA E. SHUPE. *Bureau of Chemistry and Soils, Washington, D. C.*—By plotting Δ against density in isobars and isotherms, the compressibility data for a gas can be exhibited on a small size graph that renders easy a quick estimation of the remaining p, v, T coordinate when two of them are given. $\Delta\equiv v(pv/RT-1)$. With a little more effort, this coordinate can be calculated accurately by reading the ordinate Δ from the graph at the point corresponding to the two given p, v, T coordinates, and solving for the remaining (unknown) one in $\Delta=v(pv/RT-1)$. This graph thus

affords two kinds of interpolation; one is rapid estimation of the unknown p, v, T coordinate, and the other is an easy calculation of its value that gives results as accurately as the original data are known. This method of presentation also shows trends of the deviation from $pv=RT$. Graphs for nitrogen, carbon monoxide, and hydrogen are shown.

14. Transport phenomena in Einstein-Bose and Fermi-Dirac Gases, E. A. UEHLING AND G. E. UHLENBECK, *University of Michigan.*—The theory of gases in non-stationary states, given by Lorentz and Enskog, is generalized for the quantum statistics to give the hydrodynamical equations and the distribution function in first and second approximation, and formal expressions for the viscosity and heat conductivity coefficients. These results are valid for all statistics and for all degrees of degeneration. Two essential points contribute to this generality: (a) Exact expressions independent of statistics and degeneration can be given for the coordinate and time derivatives of the coefficient A of the equilibrium distribution function in terms of the pressure and temperature gradients and time derivatives, though a closed expression for this coefficient as a function of v and T is known only in limiting cases. (b) The function W of the general equation of state for ideal gases in all statistics

$$pv = \frac{RT}{M} W(v^{2/3}T)$$

is adiabatically invariant. Numerical values of the viscosity and heat conductivity coefficients, which should come out of the formal theory on the introduction of special assumptions about the molecular forces, have not yet been obtained. It is our hope that these results, when found, may furnish an experimental test of the existence of Bose statistics in real gases, as is required by theory.

15. The equation of state of a non-ideal Einstein-Bose or Fermi-Dirac gas. G. E. UHLENBECK AND L. GROPPER, *University of Michigan.*—With regard to the question whether from isotherm measurements one can obtain an experimental test for the existence of Bose statistics in real gases, as is required by theory, we could prove the following general theorem. The "Zustandsumme" of a non-ideal Bose or Fermi gas is given by the classical integral provided one replaces the Boltzmann $exp(-V_{ij}/kT)$ factor by:

$$e^{-V_{ij}/kT}\left\{1 \pm \exp\left(-\frac{4\pi^2 mkT}{h^2} r_{ij}^2\right)\right\} \tag{1}$$

for each pair of molecules (i, j). For the second virial coefficient B, this has, i.e., in a Bose gas, as a consequence that:

$$B = B_{non\text{-}id.\ class} + B_{ideal,\ Bose} + B' \tag{2}$$

where:

$$B' = 2\pi N \int_0^\infty dr r^2 (1 - e^{-V/kT}) e^{-4\pi^2 mkT^2/h^2}. \tag{3}$$

Only at very low temperatures the last two terms in (2) become appreciable. They are then of the same order of magnitude, but have opposite signs. Due to this fact, due to the lack of precise knowledge of the molecular forces, and due to the absence of accurate measurements of B at very low temperatures, one can as yet not decide from isotherm measurements alone whether or not real gases obey the Bose statistics.

16. The theory of the atom of energy. E. K. PLYLER, *University of North Carolina.*—In the quantum theory of Planck it is postulated that energy is absorbed and radiated in definite amounts equal to $h\nu$. In the present theory it is postulated that there is a minimum of energy which may be emitted or absorbed and that all other amounts of energy are a multiple or this minimum. Whenever an electron absorbs energy its linear velocity will increase if no spin is produced. By the conservation of energy principle an equal amount of energy will be emitted when the electron is brought to its original velocity. In the case of the production of x-rays by the bombardment of a target with a stream of electrons, the collisions which decrease the velocity to zero at one time will produce the maximum or threshold frequency. Other types of

collisions will cause the emission of smaller quanta of energy and these will make up the continuous spectrum which, is really a closely grouped discontinuous spectrum being made of various multiples of the atom of energy. More applications from optics and other branches of physics will be given and the more complete theory will be stated.

17. The Dirac electron in simple fields. MILTON S. PLESSET, *Yale University.*—The Dirac electron is considered first in one-dimensional fields in which the potential function $V(x)$ is a polynomial of any degree in x. By writing the equations of Dirac in a "canonical" form it is possible to attain an analytical symmetry which facilitates a detailed investigation of the behavior of the solutions at the singular points of the equations. It is found that there is no quantization in any of these cases taking the usual boundary condition of quadratic integrability. The particular case of the simple harmonic oscillator, $V=ax^2$, is discussed in detail. For the oscillator in space, $V=ar^2$, it is also found that there is no quantization. This treatment may be extended to show that Dirac's equations for any central field in which the potential function $V(r)$ is a polynomial in r give solutions with a continuous energy spectrum.

18. Calculation of first order atomic energies for configurations involving almost closed shells. GEORGE H. SHORTLEY, *Princeton University.*—A method is developed for calculating the electrostatic energy matrix for a configuration consisting of a closed shell minus ϵ electrons plus η other electrons with the same simplicity as for the corresponding configuration consisting of just $\epsilon+\eta$ electrons. One classifies the states according to the quantum numbers of the "missing" and of the added electrons and calculates Slater's integral $(J-\delta K)$ for each pair of electrons in the usual way except that one attaches a negative sign to an integral connecting a "missing" with an added electron. One obtains in general quite different formulas for the electrostatic energies for the two configurations mentioned above. This means, in the Russell-Saunders case, that one obtains in general quite different multiplet separations and ordering of the multiplets. In the particular case $\eta=0$, however, one obtains the same formulas in the two cases, as has been shown by Heisenberg. It is then shown quite generally that the matrices of magnetic interaction are identical in LS coupling for the two configurations mentioned above except for a reversal of sign of the spin-orbit coupling parameter corresponding to the almost closed shell.

19. A rigorous treatment of assemblies containing crystals, in quantum and classical statistical mechanics. T. E. STERNE, *National Research Fellow, Harvard University and the Massachusetts Institute of Technology.*—The "Fowler-Darwin" method of finding the number C of linearly independent wave functions capable of representing an assembly with both crystalline and gaseous phases, of X similar systems and of total energy E, is to express C in the form of a double complex integral, and evaluate this by the method of steepest descents. Although the method of steepest descents when applied to this integral leads to the correct physical results, such use is not rigorous because the denominator of the integrand contains the expression $1-x\kappa(z)$ where x is a selector variable and $\kappa(z)$ is the crystalline partition function per system. A rigorous procedure is to find the number C_p of wave functions capable of representing the assembly of total energy E when there are P systems in the crystal, by the use of the method of steepest descents, in this case rigorous. To find C one then sums the resulting expression over all P less than X. The usual results of statistical mechanics follow directly. The method may be used for assemblies containing mixed crystals.

20. A graphical projection method of determining the coordinates of point-groups. DAN MCLACHLAN, *The Pennsylvania State College.* (*Introduced by Wheeler P. Davey.*)—The study of the 32 point-groups has so far required either that the student follow analytical methods blindly without visualizing the symmetry operations point by point, or that he follow, in imagination, the effect of rotating three-dimensional configurations of points about various axes. This paper describes a graphical scheme which enables a student to visualize the various symmetry operations by means of appropriate projections. For point-groups of cubic symmetry the whole cube is projected on its (111) plane, so that the cubic axes appear in projection as three equal lines spaced 120° apart. A template is made to the same scale, showing the projec-

tions of the three axes and showing, to the same projection, the coordinates of some point P. Mechanical manipulations of the template are described for showing the effects of various symmetry operations on the coordinates of P. Similar procedures are described for rhombohedral point-groups both with rhombohedral and with hexagonal axes. The use of triangular coordinate paper is described in making projections of hexagonal point-groups.

21. The principles of a new portable electrometer. Ross Gunn, *Naval Research Laboratory, Washington, D. C.*—A new type of sensitive electrometer, sufficiently rugged for use on aircraft or shipboard and employing a standard portable microammeter for an indicator, is described. The instrument is a true electrometer and its leakage depends only on the amber insulation and the ionization of the surrounding air. The voltage sensitivity of a typical instrument is 10,000 microamperes (divisions) per volt. Sensitivities one hundred times this seem attainable after certain refinements in design are completed. The effective capacities of the instruments already built approximate 25 cm.

22. The x-ray scattering curves for NH_4 and I in NH_4I at various temperatures. G. A. Morton, *Massachusetts Institute of Technology.* (*Introduced by B. E. Warren.*)—The f-curves for NH_4 and I have been determined for the two polymorphic forms of ammonium iodide for various temperatures. Measurements were made with an x-ray powder spectrometer using the $K\alpha$ radiation of molybdenum. Intensity measurements were made on the high temperature form between $+175°$C and $-50°$C at intervals of 75°, and on the low temperature form at $-20°$C and $-70°$C. The form of the resulting f-curves is discussed and curves of the effective distribution of scattering matter in the crystal are given.

23. The shape of an x-ray line. Archer Hoyt, *Cornell University.* (*Introduced by F. K. Richtmyer.*)—An x-ray emission line as measured by the double crystal spectrometer ("anti-parallel" position) can be represented very accurately by means of a simple empirical formula of the type

$$y = \frac{a}{1 + (x/b)^2} \tag{1}$$

where the ordinate y represents the intensity $I(\lambda)$ as a function of $x \equiv (\lambda_0 - \lambda)$, b *the half-width at half-maximum*, a the maximum ordinate of the spectral line, and λ_0 the wave-length of that ordinate. Some uses for the formula are (1) location of background under the $K\alpha$ doublet, (2) the calculation of the separation of close components from measured points used in the empirical formula. Formula (1) appears to be a function of a very fundamental type since it is also a good representation of rocking curves obtained in the "parallel" position of the spectrometer. A search for theoretical justification of this type of formula has brought to light the curious result that although the application of the Dirac quantum theory of the radiation field yields a formula of the same type, the maximum ordinate predicted is independent of the spontaneous transition probability; whereas, certain experimental work indicates that the maximum ordinate is a good measure of the line intensity. This is very disturbing since the assumption is usually made that the line intensity *is* proportional to this Einstein coefficient of spontaneous transition.

24. Refraction of x-rays by calcite crystals. J. A. Bearden and C. H. Shaw, *Johns Hopkins University.*—Previous measurements of the refraction of the molybdenum K series by calcite have given values of $\delta = 1 - \mu$ which are about 7 percent higher than the calculated values. The present measurements have been made using a 90 degree prism in which the refracting surface was polished optically flat and approximately parallel to the (100) plane. The prism edge was carefully prepared according to the method described in Phys. Rev. **39**, 1 (1932). However, the refracted lines were not as narrow as they should have been, which indicates that it is very difficult to obtain a "perfect" prism edge with calcite. Two experimental methods were used; in the first the x-rays struck the refracting surface externally and in the second internally. The theoretical values were calculated from the quantum theory of dispersion using the crystal wave-lengths. The results are shown in the following table:

Line	λ	Method	δ(exp.)10^6	δ(theory)10^6
Mo K_β	0.6314A	First	1.465	1.467
Mo K_α	0.7093	First	1.852	1.853
Mo K_β	0.6314	Second	1.448	1.467
Mo K_α	0.7093	Second	1.827	1.853
Cu K_β	1.389	First	7.07	7.14
Cu K_α	1.538	First	8.67	8.76

The experimental and theoretical values are thus in agreement within the experimental error.

25. The reflecting and resolving power of calcite for x-rays from 0.21 to 2.3A. SAMUEL K. ALLISON, *University of Chicago.*—Using a precision double crystal spectrometer, the rocking curves from three pairs of calcites in the (1, −1) position were observed for 7 wave-lengths from 0.21A (W $K\alpha$) to 2.3A (Cr $K\alpha$). Three quantities were observed at each wave-length, (1) the percent reflection ($\%R$), defined as the ratio of the maximum ionization current obtainable from crystal B to the ionization current produced by the x-rays incident on B from A, (2) the reflection coefficient (R), defined as the ratio of the area of the rocking curve from B to the intensity incident on B from A, (3) the half width at half maximum of the rocking curve from B. One of the pairs was obviously more perfect than the others. It is shown that none of the three quantities defined above is simply related to the analogous observations on a single crystal with monochromatic, parallel, incident x-rays, but that numerical predictions of the values of the above quantities may be obtained from somewhat laborious calculations based on Darwin's theory of diffraction by a perfect crystal as modified by Prins to take account of absorption. At present a complete calculation has only been carried out for the reflection of Cr $K\alpha$. Results: $\%R$ predicted, 55.7; observed, 55.4: R pred., 4.25×10^{-5}; obs., 4.7×10^{-5}: half width pred., 6.5 seconds; obs., 7.1 sec. On the basis of this agreement it can be stated that it is possible to find specimens of calcite for which there is no evidence for a mosaic structure from intensity of reflection measurements.

26. Wave-lengths of the tungsten K-series spectrum with the double-crystal x-ray spectrometer. JOHN H. WILLIAMS, *National Research Fellow, University of Chicago.*—Using a Société Genevoise double-crystal x-ray spectrometer and the method devised by Compton (R. S. I. **2,** 365, (1931)), the K-series wave-lengths of tungsten were determined from the diffraction angles in the first order from calcite. The results, corrected for slit heights (Compton, Letter to the Editor, Phys. Rev., in press) and reduced to 18°C, are:

Line	Angle	Wave-length in X.U.
W $K\alpha_2$	2° 01′ 06.3″	213.37
W $K\alpha_1$	1° 58′ 22.3″	208.56
W $K\beta_2$	1° 44′ 51.4″	184.75
W $K\beta_1$	1° 44′ 24.8″	183.97
W $K\gamma$	1° 41′ 37.7″	179.06

The wave-lengths were calculated assuming the grating constant $d=3.02904$A at 18°C. The probable errors of the angle measurements are about $\pm0.2''$ except for $K\gamma$ and the random errors in the scale rulings of these instruments are approximately $\pm0.4''$. The separation of α_1, α_2 agrees exactly with the energy difference $L_{II}-L_{III}$. The β_1, β_3 lines were easily resolved in the first order and give a separation of 0.78 X.U. agreeing closely with the energy difference $M_{II}-M_{III}$.

27. Forbidden x-ray lines in the *L* series. S. KAUFMAN AND F. K. RICHTMYER, *Cornell University.*—On some of the long-exposure plates taken to bring out satellites, faint lines have been observed in the region of the $L\beta_2$ line of several heavier elements from $77Ir$ to $90Th$. These lines have been identified as diagram lines, forbidden by the usual x-ray selection rules and belonging to the two series $L_{22}-N_{21}$, $L_{22}-O_{21}$, $L_{22}-P_{21,22}$ and $L_{22}-N_{22}$, $L_{22}-O_{22}$. The first member of each series $L_{22}-M_{21}$ and $L_{22}-M_{22}$ has been found by Idei for several elements in the same atomic number range. Ross has recently reported "forbidden" lines in the K series. Search for other "forbidden" lines is being continued.

28. The production of the molybdenum $L\alpha$ satellites by fluorescent absorption of silver $L\alpha$ radiation. F. R. HIRSH, JR. AND F. K. RICHTMYER, *Cornell University.*—The molybdenum $L\alpha$ satellites have been obtained by fluorescent absorption of silver $L\alpha$ radiation, by means of a special x-ray tube designed for use with a Siegbahn vacuum-spectrograph. An exposure of 40 hours, with the x-ray tube running at 20 k.v. and 30 m.a. brought out satellites of easily observable intensity. A plate taken by cathode ray excitation, with the same intensity of molybdenum $L\alpha_1$, shows satellites of about the same intensity as in fluorescence. This is in disagreement with the results of Coster and Druyvesteyn who found the intensity of the satellites to be much less for fluorescent excitation, as compared with cathode ray excitation. Work is in progress to show whether the satellites on the fluorescent plate are due to true fluorescence or merely to the high speed photoelectrons ejected by high energy white radiation quanta, which are able to doubly ionize atoms in the molybdenum fluorescent anticathode.

29. Satellites near the $K\beta_1$ line. O. REX FORD AND C. B. POST, *West Virginia University* —For the elements Sc(21), Ca(20) and K(19) the *B*-satellites are found to be more numerous than previous literature reports them. A satellite of shorter wave-length than $K\beta^{III}$ has been found in the elements K(19) to Sc(21). This satellite is given the name $K\beta^{IV}$. Another satellite, very close and on the short wave length side of $K\beta_1$ is found in the elements K(19) and Ca(20). The semi-Moseley diagram of these two new satellites has the same behavior as in the case of the other satellite lines. Experimental evidence is offered to show that all the *B*-satellites present a much greater regularity when referred to $K\alpha_2$ as the parent line instead of $K\beta_1$ as has been customary. If the *B*-satellites are related to the $K\alpha_2$ line rather than $K\beta_1$ a new classification of the *K*-satellites is demanded, in which there are no satellites on the long-wave-length side of the parent lines. The semi-Moseley diagrams are very valuable in the investigation of new elements.

30. Comparison of effects produced by 200 k.v. x-rays. 700 k.v. x-rays and gamma-rays. G. FAILLA, *Memorial Hospital, New York. (Summary of results obtained by different investigators at Memorial Hospital.)*—The influence of wave-length *per se* on the effects produced by ionizing radiations is being investigated intensively at the Memorial Hospital from different angles. The results reported at this time are based on the following effects: *Biological:* (1) reduction in linear growth of roots and shoots of wheat seedlings, (2) killing of fruit fly eggs, (3) reduction in linear growth of the tails of young mice, (4) epilation of a section of the tail, (5) severance of the end of the tail beyond the irradiated section, (6) epilation of the ears of rabbits, (7) erythema (reddening) of the human skin. *Chemical:* (8) precipitation of mercurous chloride from Eder's solution, (9) decomposition of potassium iodide in acid solution, (10) darkening of photographic film, with and without intensifying screens. *Physical:* (11) ionization in different ionization chambers. The results show that wave-length plays an important part in the degree of effect produced. From a practical standpoint the most important result is that human skin and other living tissues (all made up of low atomic number elements) do not react in the same way to the three qualities of radiation.

31. The reduction by x-rays of aqueous chromic acid solutions and the influence of added organic substances. HUGO FRICKE AND MARTHA WASHBURN. *The Walter B. James Laboratory for Biophysics, Cold Spring Harbor, L. I.*—A study has been made of the reduction of solutions of chromic acid in concentrations varying from N/500 to N/36000 chromate by irradiation with different dosages of x-rays. It is concluded that the effect is due to a primary activation of the water by the rays. Various organic substances increase the action of the rays, some having a marked effect in as low a concentration as 10^{-7} molar. The effect of the organic substance decreases in low concentration, according to a relationship which may be accounted for by assuming that organic molecules take part in the reaction when they encounter activated molecules which exist for a limited time only. The dependence of the effect on chemical composition forms an interesting subject which has been studied to some extent. For example, the effectiveness of the normal monobasic acids of the paraffin series increases rapidly with the length of the chain, valeric acid being over 100 times more active than acetic acid.

32. Further x-ray evidence as to the size of a gene; and as to the energy of mutation by ultraviolet rays. OSWALD BLACKWOOD, *The University of Pittsburgh.*—The author's previous minimum value, (130A), of the radius of the gene nucleus of the fruit fly is changed to 200A when x-ray bulb absorption is taken into account. In causing mutation by x-rays only one ion pair is produced if the radius is 130A and thirty if Muller's maximum value, (600A), is correct. The threshold frequency limit for ultraviolet capable of causing mutation probably lies below the window glass limit, 3150A. It certainly is above the shortest mercury arc line, 2480A. The corresponding energy excitation values of the gene are four and five electron volts. The spectral transmission of fruit fly larva "skins" has been determined by the author. With Altenberg's data the energy to cause mutation is determined. The value depends upon the assumption as to the threshold limit and is between 50 and 1800 times that for x-rays. The number of quants absorbed in the gene is between 300 and 10000. This low efficiency suggests that multiple excitations are necessary which progressively raise the energy to a value adequate for mutation.

33. Methods for computing lattice energy constants, R. H. CANFIELD, *Naval Research Laboratory, Anacostia, D. C.*—The classical methods of calculating lattice energies depend on the existence of special functions which limit the symmetry of the lattices to which they may be applied. The present paper describes two methods applicable to lattices of any symmetry. The first method, applied to the Coulomb potentials, involves the calculation of the potential of an ion at the center of an ever-enlarging sphere of crystal-lattice. At each step a special correction layer is added, such that the net charge of the whole sphere is zero and the volume integral of the potential energy is zero. This progression approaches a limit which may be determined to four digits by plotting. The second method is applied to potentials having exponents of $1/r$ higher than three. In this method the energy is computed exactly for a large sphere of surrounding atoms, and the remainder of the crystal to infinity replaced by a volume integral over a uniform distribution of matter. The lower limit of this integral is the boundary of a sphere containing matter equal to the actual content of the crystal sphere which furnishes the main term. This method gives results to six digits. Numerical results are given.

34. Molecular rotation in the solid state and the polymorphic relations of the univalent nitrates. F. C. KRACEK, TOM F. W. BARTH AND C. J. KSANDA. *Geophysical Laboratory, Carnegie Institution of Washington.*—The group of univalent nitrates affords a particularly important array of closely related structural types. The K, NH_4, Rb, Cs, Tl and Ag nitrates all exhibit polymorphism; crystallographic observations indicate that certain structural types may be common to two or more members of the series. Li and Na nitrates are not polymorphic, but $NaNO_3$ exhibits a gradual transition ending at 275°C which has been interpreted in terms of a gradual initiation of rotation of the nitrate group (J. Am. Chem. Soc. **53,** 3339 (1931)). In NH_4NO_3 the nitrate group rotation is initiated at a polymorphic inversion (Nature **128,** 410 (1931)). In some of the other members of the series the rotation of the nitrate group is likewise initiated at a polymorphic inversion. Thus, in KNO_3, the room temperature orthorhombic modification KNO_3(II) inverts to a holohedral trigonal form, KNO_3(I) at 127.7°C. The intensities of x-ray diffraction from KNO_3(I) ($a_0=4.50$A, $\alpha=73°\ 30'$, space group D_{3d}^5, $d=2.03$ calcd. with 1 KNO_3 per unit of structure, obsd. $d=2.03$) are explainable only on the assumption of the nitrate group being in motion about the trigonal axis. On cooling KNO_3(I) to below 125°C the salt inverts metastably to a pressure modification KNO_3(III) by a single crystal transformation. KNO_3(III) is ditrigonal pyramidal, space group C_{3v}^5, $a_0=4.37$A, $\alpha=76°\ 55'$, one KNO_3 per unit of structure, $d=2.13$ calcd., $d>2.10$ obsd. The NO_3 groups in this modification occupy fixed positions. Other examples will be considered.

35. The unit of structure of the minerals of the sodalite family. TOM F. W. BARTH. *Geophysical Laboratory, Carnegie Institution of Washington. (Introduced by F. C. Kracek).*—Minerals of this family are made up of the following three silicates (formulae for the full unit cells are given):

I. $Na_8Al_6Si_6O_{24}Cl_2$; II. $Na_8Al_6Si_6O_{24}SO_4$; III. $Ca_{4-5}Al_6Si_6O_{24}(SO_4)_{1-2}$.

I = sodalite, II = noselite, III is present in hauyne. An atomic arrangement for noselite in which two Na-atoms have no fixed positions in the lattice ("vagabonding ions") has been proposed by

Jaeger. But this hypothesis is not in agreement with the known facts. The structure of sodalite as proposed by Pauling is correct, but does not explain the isomorphous relationship to silicates II and III. The following table shows, however, that the sodalite structure also can be described as belonging to space group T_d^1 (by applying the principle of variat atom equipoints) whereby the relationship to noselite and hauyne becomes evident.

	Space gr.	Na_8	Al_6 Si_6	O_{24}	Cl_2, S	O_4
Sodalite (Pauling)	T_d^4	8*a*	6*g* 6*f*	general	2*a*	
Sodalite (Barth)	T_d^1	4*a*+4*a*	12*f*	12*g*+12*g*	1*a*+1*b*	
Noselite { II	T_d^1	4*a*+4*a*	12*f*	12*g*+12*g*	1*a*	4*a*
Hauyne { III	T_d^1	4*a*[+¼(4*a*)]	12*f*	12*g*+12*g*	1*a*(+1*b*)	4*a*(+4*a*)

The varying composition of ultramarines (which also belong to the sodalite family) is explained as a consequence of the variate atoms encountered in the position 12*f*.

36. New orientations forming in a crystal of Ag-Cu during precipitation. C. S. BARRETT AND H. F. KAISER, *Naval Research Laboratory, Washington, D. C.*—The orientation of individual grains of a solid solution of Cu in Ag (4 weight percent Cu) has been studied by x-rays before and after annealing, with surprising results. X-rays reflected from a single grain in the quenched homogeneous alloy give strong and well defined spots, but these spots completely disappear after annealing treatments varying from 7 to 38 hours at 300°C. Before the original spots have vanished new reflections appear, weak and elongated. These occur at diffraction angles indicating reflection from the solid solution instead of the precipitate. These reflections are not destroyed by further annealing. Photograms of these reflections on a Davey-Wilson camera, when analyzed by stereographic projection, disclose a series of new orientations of fragments of the original crystal. The new orientations are related to the orientation of the original crystal by rotations covering the angular range 36° to 54° about each of the axes [100], [010] and [001] of the original matrix. There is a preference for rotations of approximately 42° and 48° about these axes corresponding to the fragmentation of a single crystal into crystallites with six different orientations. No type of twinning previously observed in metals accounts for such an effect; it can be explained by twinning only by going to high index planes as twinning planes, such as those of the form {830}, {940} or one intermediate between these. Photomicrographs were taken of the different stages of the process, and although the grains ceased to have the appearance of a homogeneous solid solution, characteristic twinning structures did not appear, nor did the usual Widmanstätten structure.

37. X-ray study of the plastic working of Mg-alloys. L. G. MORELL AND J. D. HANAWALT, *The Dow Chemical Company, Midland, Michigan.*—An x-ray study has been made of the structure of Mg-alloys fabricated at various temperatures. Different processes of working such as rolling, forging, or extruding result in characteristic fiber structures as seen by the x-ray photograms. These patterns are identified by comparing with computed patterns for the hexagonal system with axial ratio $c/a=1.62$. In this way it is found that a forged Mg-alloy possesses a [001] fiber axis lying in the direction of forging, while extruded Mg-alloys show a [210] fiber axis lying in the direction of extrusion. These results are understood in terms of the planes and direction of gliding in the micro crystals in polycrystalline Mg. The x-ray diagrams serve also to show the grain size and distortion of the micro crystals as a function of the temperature and the degree of working.

38. Molecular structure of ice and water. E. L. KINSEY AND O. L. SPONSLOR, *University of California at Los Angeles.*—A new lattice for ice, so far as the hydrogen positions are concerned is proposed, based on the oxygen positions given by Barnes. The units H^+ and $H_3{}^-O_2$ appear, the latter built with three hydrogens forming an equilateral triangle in a plane midway between the oxygens. Large polarization effects arise and reasons are given to show why a lattice in which they are produced is preferred to a coordination structure in which they are not. The lattice provides dihydrol as the polymer in ice and water, and qualitatively explains many of the substance's abnormalities. The model is used to calculate the oxygen-hydrogen angle θ

in the $H_3^+O_2$ unit, for the unit within the lattice, and within dihydrol, regarded as isolated. Approximate calculations indicate $\theta=30°$ to within a few degrees for the unit in the lattice. The effect of the lattice on θ is small (several degrees) whereas, it acts to increase the polarization at an oxygen nearly three fold. Use is made of this to account for the stability of dihydrol in the crystal lattice.

39. Lorentz double refraction in cubic crystals. F. SEITZ, *Princeton University.*—In 1878 Lorentz pointed out that the classical crystal optics is a first approximation which neglects variations in the electric intensity of the light wave over the lattice. He returned to the problem in 1921 and gave an incomplete theory and performed experiments showing that rocksalt is not optically isotropic. In this paper the basis for an extension of the classical theory is given by writing

$$P_i = \alpha_{ij}E_j + \beta_{ijk}\frac{\partial E_j}{\partial x^k} + \gamma_{ijkl}\frac{\partial^2 E_j}{\partial x^k \partial x^l}$$

for the electric moment in unit volume P_i due to the electric intensity, E_j. The tensor α corresponds to classical theory. Voigt (1905) shows essentially how β is responsible for optical activity of crystals. The tensor γ gives rise to double refraction in addition to that due to α, so that double refraction may occur even where crystal symmetry makes α isotropic. For the cubic system γ has three independent non-vanishing components. Double refraction is predicted for wave-fronts in all planes except the (100) and the (111) planes so that a cubic crystal has seven optical axes with regard to the Lorentz double refraction due to γ. More experimental data are needed before the predictions can be checked.

40. Quantum analogue of Lorentz broadening of spectral lines. HENRY MARGENAU, *Yale University.*—Recently the effect of interatomic perturbations upon the position and breadth of absorption lines has been calculated. The broadening thus computed agreed with the observed half width as to order of magnitude, but left room for the simultaneous existence of other causes. Hence the question as to the significance of "collision broadening" arises. Clearly, the classical mechanism of this phenomenon, as suggested by Lorentz, has become illusory. A Fourier analysis of the incident radiation, leading to Lorentz' formula, is also to be rejected. There is, however, a possible quantum analogue of this phenomenon. Suppose that the intensity of the incident light which is being absorbed by a given atom varies in its intensity so strongly that it may be regarded as intermittent. If this intermittence is due to the screening by other atoms its period may be smaller than the average life time of the excited state. In that case it is easy to show, by the usual perturbation methods, that the half width of the absorbed line, $\Delta\nu$, depends on the period of intermittence, t. The result, $\Delta\nu=.45/t$, is practically identical in form with Lorentz' formula, $\Delta\nu=0.32/\tau$, τ being the mean time between two collisions.

41. Theory of inelastic collisions. E. C. G. STUECKELBERG, *Princeton University.*—A theory of inelastic collisions very similar to the one by London (recently published in the Zeitschr. f. Physik) has been developed. If only two stationary states of the two colliding systems are considered and if the nondiagonal interaction energy matrix elements depend on distance only, the problem reduces to two simultaneous differential equations. For a rather special case of this nondiagonal interaction energy the problem can be solved for all velocities. It is interesting to observe the deviation from the Born-Dirac Collision theory. In the case of exact resonance (i.e., if the kinetic energy before and after collision is the same) a general solution can be given within the region of validity of the Wentzel-Brillouin-Kramers approximation. The interesting feature is that with increasing interaction-energy we find an increase in transition probability. But after this probability reaches one it begins to oscillate between 0 and 1 in a way which depends on the exact nature of the interaction energy.

42. Double Stern-Gerlach experiment and related collision phenomena. N. ROSEN AND C. ZENER (*National Research Fellow*), *Mass. Inst. of Tech. and Princeton University.*—The experiment of Phipps and Stern on the behavior of atoms in a rotating magnetic field led to results at variance with the theoretical predictions of Güttinger. A possible explanation is that the latter's calculations involved an abrupt change in the rate of rotation of the field that certainly

was not present in the experiment. To mend this, the rate of rotation is represented by a continuous smooth function having a maximum at $t=0$ and going to zero at $t=\pm\infty$. An exact solution of the problem for a function of this type is obtained and it is found that the expression for the fraction of electrons that have reversed their spins with respect to the field at the end of the rotation is considerably different from Güttinger's and in complete agreement with the experiment of Phipps and Stern. The same analysis may be generalised to all classes of collision phenomena in which only two quantum states need be considered, and in which the difference in eigenwert of these two states, ΔE, is small in comparison to the relative translational energy. If $f(t)$ is the matrix element, with respect to the two states, of the perturbation, and $A=2\pi/h \int_{-\infty}^{\infty} f(t)dt$, then the transition probability is given by

$$\left(\frac{\sin A}{A}\right)^2 \cdot \left| \int_{-\infty}^{\infty} \frac{2\pi}{h} f(t) e^{2\pi i/h \Delta E dt} \right|^2.$$

43. The exchange of energy between monatomic gases and solid surfaces. CLARENCE ZENER, (*National Research Fellow*), *Princeton University.*—The calculation of the accommodation coefficient, α, of an inert gas with a metallic surface is intrinsically much simpler in the quantum mechanics than in the classical mechanics. This simplification has been taken advantage of to find α as a function of the physical characteristics of the metal and gas. The dependence of α upon temperature is given primarily by the factor $(U-U_0)/T$, where U is the internal energy of the crystal. This is in agreement with the experiments of Richards on He and W. Two arbitrary parameters have been introduced, one the force constant d in the repulsive potential $V=Ce^{-r/d}$, the other a factor arising in averaging over all angles of incidence. These parameters will, however, be nearly constant for the series He, Ne, A. It is predicted that α will increase, remain constant, or decrease with the series He, Ne, A according as d is less than, equal to, or greater than 10^{-9} cm. Experiments are being carried out at Princeton to determine this force constant.

44. A critique of sp^3 valency. J. H. VAN VLECK, *University of Wisconsin.*—In the April 1932 Phys. Rev., Mulliken shows that by extending to polyatomic molecules the diatomic configuration theory of Mulliken and Hund, it is possible to form a model for valences in complicated molecules apparently without merging the s and p wave functions to yield the so-called sp^3 valences of Slater and Pauling. To study this question further, the secular determinant for CH_4 is now examined. It is found that the sp^3 hybridization is encountered only when the repulsions between the four electrons of the H atoms are included, and the Slater-Pauling form is a good aproximation only when these repulsions are fairly large. The Mulliken model, without the sp^3 combinations, allows eight electrons to "pile up" sometimes on one H atom, just as the Hund two-center model in H_2 allows two electrons sometimes to be on the same H atom. Any attempt to predict tetrahedral properties from the geometry of the sp^3 wave functions without invoking electron repulsions appears somewhat questionable.

45. Multiplet splitting and intensities of intercombination lines. HUGH C. WOLFE, *Fellow of the Lorentz Foundation, University of Utrecht.*—Weyl has shown that many properties of free atoms can be derived on the basis of irreducible representations of rotations in R_3. Kramers has obtained an elegant formulation of Weyl's methods through the use of symbolic representation (theory of invariants) of wave functions and operators. This method is particularly adapted to the problem of multiplets (interactions between two or more "vectors," e.g., orbital angular momenta, spins). Integrations yielding matrix elements are only symbolic and the results, being determined by invariance properties, contain therefore unknown constant factors of the nature of radial integrals. Kramers' method is applied to spectra involving two valence electrons, of which one is in an s state, (singlet and triplet P, D, F, etc.). The constants which represent the interaction energies (1) electrostatic, (2) spin-orbit, (3) spin of one electron-orbit of the other (other types of interaction as yet being neglected) are expressed in terms of the three intervals of the singlet-triplet multiplet. These constants have been determined for many spectra. (3) is most often not negligible. The intensities of singlet-triplet intercombination lines are found in terms of the intervals and compared with observations on Hg.

46. A method for sensitizing photographic plates to the short ultraviolet wave-lengths. A. J. ALLEN AND R. FRANKLIN, *Cancer Research Fund, Graduate School of Medicine, University of Pennsylvania and The Bartol Research Foundation.*—As is well known, the sensitivity of ordinary photographic plates can be increased to wave-lengths below 2400A by coating them with certain fluorescent mineral oils. The desirable oil converts the shorter waves into longer ones which are not absorbed by the gelatin. Oiling the plates, however, has certain disadvantages and uncertainties. The same principle is made use of in the following method of sensitization. Plates of the desired quality, i.e., size of grain and sensitivity, are submersed in a solution of $2\frac{1}{2}$ g. amino G acid (Eastman Kodak Co. T. 477), $2\frac{1}{2}$ g. sodium carbonate in 100 cc of water for a few seconds, the entire surface being lightly rubbed with a piece of absorbent cotton to insure a uniform coating. They are then removed and allowed to dry in a vertical position on an ordinary plate drying rack. The result is a thin, rather durable coat of amino G salt crystals which give a bright blue fluorescence when exposed to ultraviolet radiations (also to x-rays and β and γ-rays). A similar coating of G salt produces a greenish blue fluorescence which is not as effective as a sensitizer. After exposure, and just before developing and fixing in the usual manner, dip the plates in a pan of water, or rinse under the water tap for an instant to insure uniform development. Plates sensitized in this manner are compared with oil sensitized, Eastman ultraviolet sensitized, and plates sensitized with Eastman ultraviolet sensitizing solution.

47. A broad range vacuum spectrograph for the extreme ultra-violet. K. T. COMPTON AND J. C. BOYCE, *Massachusetts Institute of Technology.*—A two-meter focus normal incidence vacuum spectrograph has been constructed to cover with a dispersion of 4.3 A per mm the whole range from the central image up to the first order of λ2500. The body of the spectrograph consists of brass plates screwed and soldered together, the whole exterior being coated with glyptal lacquer. End covers, removable to permit introduction of the photographic plate and the adjustment of the grating, are each attached with two rubber gaskets. An auxiliary pumping system produces a rough vacuum between gaskets and prevents leakage past the inner ones. A Gaede mercury vapor pump with suitable liquid air trap provides an initial vacuum of about 10^{-5} mm. and then maintains in the spectrograph a pressure about one hundredth of that in the discharge tube used as light source. Hilger Schumann plates, 3 by 24 inches, on special thin glass are bent to the focal curve of the grating. A magnetic control provides for moving the plate between successive exposures. Preliminary tests with electrodeless discharge, capillary discharge, and hollow cathode lamp indicate that the instrument is suitable for the investigation of short wave-length spectra from gas discharges. Construction of this spectrograph was made possible by a grant from the Carnegie Institution of Washington.

48. Diffraction experiments with especial reference to the nature of errors of gratings. R. W. WOOD, *Johns Hopkins University.*—During the past two or three years a study had been made of the causes producing the very troublesome, though very faint, spurious lines which appear near the main lines in the case of practically all large gratings. They lie usually much closer to the main line than the first order ghost, and give an appearance of hyperfine structure. Visual and photographic records of the appearance of the grating surface as observed by the light of the spurious lines, (the main line and all but one spurious line being screened off by knife edges) show that narrow vertical elements of the grating conspire in the production of each spurious line. The cause of these non periodic errors of spacing is, without doubt, the variable friction which the grating carrier experiences as it moves along the ways of the ruling engine. Methods of reducing this trouble will be described, and photographs of various mercury lines made with the 40 foot spectrograph since its transfer to Tuxedo will be shown.

49. Quantitative spectrographic analysis. O. S. DUFFENDACK AND R. A. WOLFE, *University of Michigan.*—A method of quantitative spectrographic analysis based upon the relative intensities of selected spectra lines in a single spectrogram has been developed and shown to give as consistent results as quantitative chemical analysis. By determining the relative intensities of a selected pair of lines in a graduated series of specimens like the material under investigation, a working curve can be determined giving the relationship between the relative intensities of the lines and the percentage of the test element. This curve need be determined but once for analyses over a given percentage range. Hansen's step diaphram method of measuring relative

intensities of spectral lines is used. When the test material is an alloy, an arc source is preferred. Investigation revealed that at certain arc currents, the relative intensity of the selected lines varies only slightly with the current. An arc of this current is used for the analysis. A theory of the intensities of spectral lines in an open arc has been developed and accounts for the relations used in the method. This investigation was made possible by support from the A. C. Spark Plug Company.

50. The structure of the ultraviolet absorption spectrum of formaldehyde. G. H. DIEKE, *Johns Hopkins University and* G. B. KISTIAKOWSKY, *Harvard University.*—The ultraviolet absorption bands of CH_2O were photographed in the third order of the 40 foot Tuxedo spectrograph, and until now the bands at 3520, 3430 and 3390A analyzed. Their structure is, both as far as the position and the intensities of the lines are concerned, exactly what has to be expected theoretically for a molecule of this type. The molecule is almost a symmetrical top. The deviations from this shape are felt only for $K<4$, and result in a shift and a doubling of the lines which increases with increasing J. Lines belonging to successive rotations about the CO-axis show intensity alternations as in the hydrogen molecule. The expected combination relations are fulfilled within the limits of experimental errors. The three moments of inertia for the ground level are $A=24.58$, $B=21.63$, and $C=2.951\times10^{-40}$. This gives for the H−H distance 1.88A, and if the angle between the CH bonds is assumed to be the tetrahedron angle, for the C−O distance 1.19 and for the C−H distance 1.15 A. Henry and Schou's previous analysis was not confirmed.

51. A new system of bands in sulphur dioxide. T. C. CHOW, *Princeton University.*—About eighty bands in the region 2000–2400A were recorded from a discharge in sulphur dioxide gas flowing rapidly. No trace of sulphur could be detected in the tube after nine hours exposure. Two thirds of these bands have been arranged in a scheme of levels. Comparisons with the known band spectra of SO, O_2, and O_2^+ show quite definitely that these bands do not belong to any of these known systems. Particularly the known system of bands of SO (2400–3940A) has many different features from these bands. Because of the weakness of the source, rotational structures have not been obtained. It appears that these emission bands may be due to the SO_2 molecule itself. Absorption measurements in SO_2 were therefore undertaken. (In the region 2400–2000A no accurate measurements have ever been published.) About sixty strong absorption bands were recorded and arranged into sequences. Twenty bands which constitute three sequences appear both in emission and absorption. This agreement between absorption and emission gives quite a strong support to the hypothesis that SO_2 is the probable emitter of those emission bands.

52. The near infrared bands of ammonia under high dispersion. J. D. HARDY, *National Research Fellow, University of Michigan.*—The Ammonia bands at 1.5μ, 1.9μ, and 2.2μ have been studied under high dispersion and the fine structure of the first and last of the two bands has been brought out for the first time. From theoretical considerations, supported by the complex character of the band, the 1.5μ band is attributed to the overlapping of several combination bands. The band at 2.2μ is of the perpendicular type as is the band at 1.9μ. Barker, who first resolved the 1.9 μ band, suggested that it might be a fundamental but a further study of this band and the one at 2.2μ seems to indicate that this classification might be wrong. Further investigation of the molecule in the light of present data will be needed to throw light on the perpendicular type of vibration.

53. Vibrational levels in ammonia-like molecules. PHILIP M. MORSE AND N. ROSEN, *Massachusetts Institute of Technology.*—Dennison has shown that the nitrogen atom in the ammonia molecule can vibrate along a line perpendicular to the plane of the hydrogen atoms, and that it has two symmetrically placed points of equilibrium. The nitrogen atom's potential field thus has two minima, separated by a "hill." Quantum mechanics requires that the vibrational levels for such a field be doublets, which has been observed in the ammonia spectrum. The writers have found a form of potential field whose levels could be computed with good accuracy, giving values of the levels and the doublet separations in good agreement with the experimental data of Dennison and Hardy. This field has its two minima 0.73 angstroms apart, separated by a "hill" 1/4 volt high.

54. Predissociation in the spectrum of iodine chloride. WELDON G. BROWN, *National Research Fellow, University of Chicago* AND G. E. GIBSON, *University of California.*—A group of bands lying just beyond the convergence of the ordinary visible absorption bands of iodine chloride have been analyzed and found to consist of P and R branches. The upper state for this system is derived from normal iodine and excited chlorine atoms and is interpreted as the $^3\Pi_{0+}$ state predicted by Mulliken. It is thus analogous to the upper states of the well-known visible bands of the homonuclear halogens. The upper state of the ordinary ICl bands is now known to dissociate into two normal atoms and is classified as the $^3\Pi_1$ member of this multiplet. Above the level $v=3$ of the $^3\Pi_0$ state predissociation sets in, presumably as a result of interaction with a repulsive O^+ state derived from two normal atoms. Apparently the intersection of these curves gives rise to a new state with a minimum at the point of intersection, for at this point a new set of energy levels is observed to begin. In absorption transitions to this state result in sharp lines only if the energy levels coincide at the same rotational quantum number with the levels of the original $^3\Pi_0$ state. Otherwise the lines are diffuse. This is interpreted as due to momentary existence of the molecule in the $^3\Pi_0$ state as an intermediate step in the absorption process, a step which is followed either by predissociation giving normal atoms or by a radiationless transition into the new O^+ state.

55. Infrared spectra of the noble gases. WILLIAM F. MEGGERS AND C. J. HUMPHREYS, *Bureau of Standards.*—The first spectra of He, Ne, A, Kr and Xe have been photographed with complete details from 7600 to 12100A by exploiting two very remarkable emulsions made by the Eastman Kodak Company. These plates have sensitivity maxima at 8600A and at 9600A. The first plate was used for the range 7600–9200A and the second for 8600–12100A. The sources were Geissler tubes operated with uncondensed high voltage a.c. discharges, and the spectrographs were concave gratings of 21 feet radius except for the last 900A which was observed with a Hilger E_2 spectrograph with glass prism. Many new lines have thus been added to the spectroscopic data for each of the noble gases and analysis has resulted in confirmation and extension of the tables of spectral terms. A new band extending from 9100 to 11000A has been observed in He. The resonance lines of He have been measured as 10829.09 (20) and 10830.30 (100). The longest wave-lengths recorded in Ne, A, Kr and Xe are 12066, 11738, 12124, 11134A, respectively. The second spectra are being investigated in the infrared in the same manner.

56. An extension of the Pd I-like isoelectronic sequence to Sb VI and Te VII. G. K. SCHOEPFLE, *Cornell University.* (*Introduced by J. R. Collins.*)—Terms arising from the configuration d^{10}, d^9s, d^9p of Sb VI and Te VII are given along with the wave-lengths and frequencies of the stronger lines. Term separations and a Moseley Diagram are given and the centroids are computed for the entire sequence. The lines for the transitions $^3P\ D\ F$, $^1P\ D\ F$ ($4d^95p$) into ^3D, ^1D ($4d^95s$) fall in the vacuum region between 784A and 1331A, while for the shorter wave-length lines for the transitions $^1P_1$, $^3P_1$, and $^3D_1{}^0$ ($4d^95p$) into $^1S_0(4d^{10})$, the frequencies are obtained by extrapolation of the Moseley Diagram.

57. Hyperfine structure of Ga II and In II. J. S. CAMPBELL, *National Research Fellow, University of Chicago.*—The spectra of ionized gallium and indium, photographed with a 21-foot grating, show wide hyperfine structure. The assumption of $i=3/2$ for gallium best fits the observed separations and estimated intensities; a nuclear moment of 9/2 or 11/2 is indicated for indium. Relative separations of a number of terms agree with the formulae of Goudsmit and Bacher (Phys. Rev. **34**, 1501 (1929) for two-electron configurations involving an s electron. The In I lines classified by Sawyer and Lang (Phys. Rev. **34**, 712 (1929)) as ($4s^24p$) ^2P $-(4s4p^2)$ ^4P show hyperfine structure which is due to the quartet term, and which substantiates their classification.

58. A test of hyperfine structure theory. R. F. BACHER, *Mass. Inst. of Tech.* AND J. S. CAMPBELL, *University of Chicago, National Research Fellows.*—The total hyperfine structure separations of the two members of the doublet arising from the single $5p$ electron have been found from a study of the resonance lines of indium. The values of these separations represent averages of observations with a variety of plate separations with a Fabry-Perot interferometer.

Difficulties due to isotope displacement and the corresponding complication of the patterns are not found in indium as it is a single element. Since it may be shown that the nuclear moment of indium is greater than $1\frac{1}{2}$, the theoretical value as given by Fermi or Racah for the ratio of these separations is independent of the nuclear moment. $\Delta^2P_{\frac{3}{2}}$ is found to be 0.390 cm^{-1} and $\Delta^2P_{1\frac{1}{2}}$ to be 0.133 cm^{-1} giving a ratio 2.9. This is not in agreement with the uncorrected theoretical value 1.67; it is in somewhat better agreement with the value corrected according to Racah, 2.05; and it is in quite reasonable agreement with the value corrected according to Breit, $\backsim 2.7$.

59. Hyperfine structure of the vanadium spectrum. H. E. WHITE, *University of California, Berkeley.*—Our present knowledge concerning the hyperfine structure of spectral lines enables one to predict for vanadium (at. wt. 51, at. no. 23), a finite nuclear spin and a hyperfine structure. Because of the hundreds of lines in the vanadium arc spectrum and the high intensity required for interferometers only a few of the lines are sufficiently isolated for study. The V I lines were excited in an atmosphere of argon by means of a Paschen hollow cathode cooled to liqud air temperatures (a Schuler tube). With a large three prism glass spectrograph in conjunction with Fabry-Perot Etalons a number of the lines have been observed as narrow unresolved hyperfine multiplets. Eight or ten of the wider patterns (total width about 0.1A) have been studied in an effort to determine the nuclear spin. In the quartet system of multiplets, λ4851 ($^4D_{1\frac{1}{2}} - {}^4F_{2\frac{1}{2}}$) reveals four diagonal components. λλ4670 ($^4P_{2\frac{1}{2}} - {}^4D_{3\frac{1}{2}}$) and 5670 ($^4D_{3\frac{1}{2}} - {}^4F_{4\frac{1}{2}}$), although not completely resolved, appear to contain six components. The first three or four diagonal components of these lines are resolved and the remainder of the pattern indicates two more making six in all. With these preliminary results one can say that for the vanadium nucleus $I \geq 5/2$, and that the g-factor is small. The total widths of the unresolved patterns for the multiplet $^6D - {}^6F$ ($3d^34s - 3d^34p$) are in excellent agreement with Goudsmit's equations.

60. The Paschen-Bach effect of hyperfine structure and the polarization of resonance radiation: the *D* lines. L. LARRICK, *State University of Iowa.*—The polarization of sodium resonance radiation has been calculated on the basis of the hyperfine multiplet theory of Goudsmit and Bacher as a function of the hyperfine separation constants of the $1^2S_{1/2}$ and $2^2P_{3/2}$ levels and the intensity of an applied magnetic field for a nuclear moment of one (in units of $h/2\pi$). Comparison with experiment shows good agreement with $A = 0.0012$ cm^{-1} for the $2^2P_{3/2}$ level, except for very small fields (H = 40 gauss) in which the polarization increases less rapidly than the theory demands. This is probably due to the fact that the first approximation used takes no account of the finite breadth of levels.

61. Polarization of sodium resonance radiation and nuclear moment of the sodium atom. N. P. HEYDENBURG, L. LARRICK, AND A. ELLETT, *State University of Iowa.*—The polarization in zero magnetic field of sodium D line resonance radiation is calculated as a function of the nuclear moment I. For plane polarized exciting radiation (D_2 alone) we find

$$P_{D_2} = \frac{16I^6 + 48I^5 + 64I^4 + 48I^3 - 5I^2 - 31I - 18}{112I^6 + 336I^5 + 288I^4 + 16I^3 - 73I^2 - 17I - 6}$$

$$P_{D_1} = 0.$$

From this we calculate the table below:

I	P_{D2}	P_{D2+D1}
0	60	50
1/2	40.54	33.33
1	20.50	16.6
3/2	18.61	15.07
2	17.33	14.02
5/2	16.47	13.32
3	15.91	12.84
7/2	15.54	12.56
4	15.28	12.35
9/2	15.09	12.19
	14.28	11.54
Observed		$16.48 \pm .33$

The polarization was measured by the Cornu method—observations made by four observers showed good agreement giving a mean value of 16.48 ± 0.33 percent. This agrees well with the result calculated for $I=1$ whereas observations on band spectra indicate $I \geq 3/2$ and present ideas of nuclear structure demand $I=$ odd multiple of $\frac{1}{2}(h/2\pi)$.

62. Quenching of mercury resonance radiation by H_2, CO, and N_2. J. S. OWENS AND O. S. DUFFENDACK, *University of Michigan.*—The quenching of mercury resonance radiation by H_2, CO, and N_2, at temperatures from 200°C to 700°C, has been investigated with a two-fold purpose: (1) the determination of the dependence of the quenching upon the temperature, and (2) the determination of the reactions occurring in the quenching process by each gas. Accurate quantitative measurements of the quenching were made possible by improved equipment and technique. Quenching by H_2 was found to be independent of the temperature, and to consist of a two-step process; hence action radii of 2^3P_1 Hg atoms calculated upon the basis of a one-step process have little actual meaning. Quenching by CO and by N_2 was found to decrease with increase in temperature, and the process of quenching to be very complicated. Equations were derived which fit the experimental curves within experimental error (2% for H_2 and CO, 5% for N_2). For CO and N_2 the processes occurring were determined, but not their individual probabilities. In the case of H_2, the probability of each process of the reaction was evaluated.

63. Collisions of the second kind involving ionization and excitation. K. B. THOMSON AND O. S. DUFFENDACK, *University of Michigan.*—A study has been made of the excitation of spark levels in metallic atoms by collisions of the second kind with rare gas ions, as a function of the energy discrepancy. The enhancement of the relative populations of certain levels, with respect to their populations in a "normal" discharge was measured by comparing the relative intensities of lines originating in these levels in the two types of excitation. The relative intensities were measured by a modification of Hansen's step-diaphragm method. A small diaphragm was made, for which the ratio of the widths of successive steps was 1.5. There were 6 steps in all, and the widest was 3 mm. Intensity markers were placed on the plates by replacing the slit of the spectrograph with this diaphragm and photographing the continuous spectrum from a condensed aluminium or magnesium spark in hydrogen. The results show that, while in general the probability of excitation of a level increases as the discrepancy between the level (measured from the normal atom) and the ionization potential of the rare gas atom decreases, there are exceptions to this rule. In certain cases, where a triplet level and a singlet level had about the same discrepancy, the triplet level was distinctly preferred. Anomalous results were also obtained for the $d^9\,6s$ levels of silver.

64. Electron temperatures and the concentration of excited atoms in a caesium positive column. F. L. MOHLER, *Bureau of Standards.*—Probe measurements in the positive column of a caesium discharge give the electron energy, electron concentration, the power input per cm, and the power loss by flow of ions to the walls. The power input under low pressure low current conditions must be largely accounted for by inelastic collisions at the first resonance potential and the measurements give a value of the effective collision area of about 5×10^{-15} cm². With high currents and pressures the power loss by inelastic collision would be many times the power input except for the fact that collisions of the second kind give back the excitation energy to the electrons. The concentration of excited atoms must then be nearly equal to the equilibrium concentration for a temperature equal to the electron temperature. This conclusion has been checked by photographing the spectrum of a strip lamp as viewed through the discharge tube and finding the lamp temperature at which the resonance lines disappear. The lamp temperatures are in general slightly less than the electron temperatures though the difference is scarcely more than the experimental error. This shows that there is nearly an equilibrium between the electrons and the first excited state.

65. The angular distribution of electrons scattered elastically and inelastically in mercury vapor. JOHN T. TATE AND R. RONALD PALMER, *University of Minnesota.*—A long electron gun was mounted to rotate about a well-shielded scattering region from which electrons scattered by gas molecules through a definite angle from a beam of small cross-section were collected, and their velocities determined, by a stationary collector containing an efficient Faraday cage, 6.0

cm in length. Angular distribution curves for electrons scattered elastically, for electrons scattered at excitation of the atom (mainly 6.7 volt energy loss), and for electrons resulting from ionizing impacts are presented for 80, 120, 230, 490, and 700 volt electrons. In general, for a particular group the curves are steeper the higher the velocity of the incident electrons. The curves for the elastic group show a diffraction at large angles, and the positions of the peaks agree well with those found by Arnot. The curves for the excitation group are much steeper than are those for the elastic group, and fall to very small values at large angles. The curves for the ionization group are also steeper but not so steep as the excitation group. The ionization group is divided into sections and further characteristics are observed. Numerical integration of these curves gives the cross-sectional area for collision, the efficiency of ionization, and the efficiency of excitation for electron impact.

66. Polarization of radiation from metals bombarded by slow electrons. C. BOECKNER, *Bureau of Standards.*—A metal electrode in a gas discharge (Cs vapor) when drawing large electron currents has been found to emit radiation having a continuous spectrum throughout the visible and ultraviolet. Since the direction of motion of the bombarding electrons is normal to the surface, one might expect from analogy to continuous x-rays that the radiation should be more intense for oblique angles of emission and should be partially polarized. This was found to be the case for both tungsten and platinum. Light polarized with the electric vector in the plane of emission is about three times more intense when observed at 60° to the normal than when observed in a direction normal to the electrode surface. The intensity with the electric vector perpendicular to the plane of emission was approximately independent of the angle of emission. From measurements made on electrodes heated to incandescence it was found that the intensity of the thermal radiation varied only slowly with angle for both directions of polarization. This latter fact renders it difficult to explain the intensity relations by considerations involving the optical properties of the metal.

67. Influence of the electrical discharge on the secondary emission from the cathode. WILFRID J. JACKSON, *New Jersey College for Women, Rutgers University, New Brunswick, New Jersey.*—Measurements have been made, using the same apparatus as described by Jackson, (Phys. Rev. **30,** 473 (1927)), on the secondary emission from a molybdenum cathode as influenced by the electrical discharge in hydrogen at low pressure. The secondary emission from the Mo target, which had not been heat treated, increased from about 1% at 250 volts to 14% at 750 volts when bombarded by K^+ ions, and showed a marked decrease after a discharge in hydrogen had been passed for 5 minutes using the Mo target as cathode. In the latter case the emission could not be detected for positive ion velocities less than 400 volts and reached a value of about 4% at 750 volts. The gas was pumped out and the pressure reduced to about 10^{-5} mm. of mercury in all cases before measurements were taken. The general aspects of these results are in agreement with results published by Câmpan, (Physik. Zeit. **23,** 593 (1931)). Work is in progress using other targets and gases.

68. Measurement and observation of vacuum conditions in finished (sealed-off) vacuum tubes, incandescent lamps and gas discharge devices. HENRY J. MILLER, *Emporium, Pa.*—Direct current and alternating current measuring methods employing audio and radio frequencies are described which are used to determine the degree of vacuum as well as to study the changes of vacuum occurring in sealed off vacuum and gas filled electrical devices. An attempt is made to show that the type of exhaust and the kind of getter employed to produce the vacuum has a definite influence upon the vacuum characteristics as determined by the methods which are described. Special reference is made to the use of the abnormal shot effect for the purpose of determining vacuum conditions in radio receiving tubes.

69. Effect of a glass target on cold emission. WILLARD H. BENNETT, *Mendenhall Laboratory of Physics, Ohio State University.*—Using the method described previously, (Phys. Rev. **39,** 182 (1932)) emission from a cold cathode was directed at a glass disk in a magnetic field. Behavior of the emission shows that a stream of positives from the glass target follows the electron stream back to the cathode. This stream of positives persists indefinitely and the spot on the glass where the electrons strike deteriorates slowly. The observation regarding the abun-

dance of this supply of positives and its effect on the severity of breakdown confirms the theory of breakdown offered previously. It further shows that in the design of high voltage tubes, it is not sufficient to degas the electrodes but one must give careful consideration to the effect of the possible targets of small emission currents on possible breakdown. A tube intended to be used in investigations on atomic disintegrations is to be built at this laboratory using the principles arrived at in the work on cold emission.

70. The disappearance of gas in discharge tubes. ALBERT W. HULL AND E. E. BURGER, *General Electric Co., Schenectady, N. Y.*—These experiments were undertaken to test the hypothesis, for which there was experimental evidence, that the disappearance of noble gases in an electric discharge is due to penetration of the ions into the cathode surface, whence they diffuse very slowly. An arc plasma was drawn into the annular space between well degassed metal cylinders, one of which was charged to negative voltages up to 1000. The rate of disappearance of gas, at constant pressure and voltage, was found to decrease as the total amount absorbed increased, indicating saturation. Nearly all of this gas could be recovered by heating the electrode, which also restored the initial rate of cleanup. The following evidence, however, indicates that part of the cleanup is of a different nature: 1st. The greater the amount cleaned up, the smaller is the fraction that can be recovered. 2nd. When the two cylinders are heated separately, it is found that the external cylinder, which received the sputtered deposit, also contains absorbed gas, in general more than the negatively charged cylinder. It is concluded that gas disappears both by penetration into the cathode and by adsorption on the sputtered deposit.

71. Measurements of small currents using pliotron tubes. L. R. HAFSTAD, *Johns Hopkins University and Department of Terrestrial Magnetism, Carnegie Institution of Washington. (Introduced by J. A. Bearden.)*—The sensitivity of the single-tube circuit using the FP-54 Pliotron was considerably increased by mounting the tube in a vacuum, keeping the batteries at constant temperature and, following Professor Ruark, operating the tube with the floating control grid initially at its equilibrium potential. The limiting fluctuations apparently inherent in the tube itself were determined by using extreme precautions with the batteries and accessory apparatus and were reported at the Cambridge meeting. For the photographic recording of alpha- and H-particles over long periods of time only moderate sensitivities are required but the steady drift must be made small. A completely new set was assembled for the above purpose in which drifts of less than 10 mm per hour were obtained by means of a loaded counter-cell. With ordinary precautions and with low film speed (20 centimeters per hour) a sensitivity of 400 electrons per millimeter shows small fluctuations of about 2 mm in 30 seconds. Slow deviations as large as 8 mm in three minutes also appear but these cannot be confused with pulses such as are produced by particles when the ionization-chamber is connected. This represents a practical sensitivity which is directly attainable.

72. Evaporation and migration of thorium on tungsten. WALTER H. BRATTAIN, *Bell Telephone Laboratories, Inc.*—The work reported in abstract (Phys. Rev. **35,** 1431 (1930)), was continued. Thorium evaporates from a tungsten surface at an appreciable rate at 2200°K. The evaporation rate depends on the temperature and the fraction of the surface covered (f). Except for small values of $f<.2$ the rate of evaporation is approximately an exponential function of f. The rates of evaporation determined by Langmuir, (Phys. Rev. **22,** 357 (1923)) and Andrews, (Phys. Rev. **33,** 454 (1929)), are comparable with the above results when account is taken of the difference between Langmuir's parameter θ and our f. It was found that thorium could be deposited on one side of a tungsten ribbon and then made to migrate to the other side by flashing the tungsten ribbon at 1535°K. to 1655°K. This could be done without loss of thorium due to evaporation. The thorium lost from the front side Δf_1 was always equal to the amount gained by the back Δf_2. This constitutes a proof that f is proportional to the amount on the surface. The rates of migration were determined at 1535°K. and 1655°K. They depend on the difference in concentration (f_1-f_2) in much the same way as the rate of evaporation depends on f.

73. The emission of positive ions from heated metals. LEROY L. BARNES, *Cornell University.*—Filaments of iron and nickel have been heated in a mass spectrograph, and at temperatures just below their melting points it is found that singly charged atoms of iron and nickel are

emitted. Similar attempts to obtain positive ions of platinum, uranium and thorium have not met with success. Rhodium and columbium ions have been obtained, which is in agreement with the results already reported by H. B. Wahlin.

74. On thermionic currents limited by pure electron space charge. EVERETT W. THATCHER, *Union College, Schenectady, N. Y.*—Work has been continued on the damping of thermionic emission variations with increasing space charge (See Phys. Rev. **39**, 474 (1932)) and subsequent letter to the editor). Further evidence has been obtained that the depression of shot effect in pure electron space charge is given by

$$\frac{\overline{V_s^2}}{\overline{V_i^2}} = f\left(\frac{i_0}{i}\right) = \left(\frac{\partial i_0}{\partial i}\right)^2_{E=\text{const}}$$

where i_0 is the space current collected at the anode and i the total emission current. i_0/i characterizes the space charge situation in the tube. It has been found expedient to represent this ratio by a new tube parameter P for which has been coined the term "*static receptance.*" Similar coefficients may be defined to refer to the limitation of current by space charge at each stage in its passage through the multi-electrode tube. (P_{gf}, the grid filament receptance, being the ratio of the electron current reaching the grid region to that emitted from the filament, etc. A consistent convention has been adopted for the coefficient $\delta i_0/\delta i$; which might be called in conformity with established nomenclature the dynamic (or A.C.) receptance. Data will be presented extending the range of previous measurements on the dependence of the dynamic receptance upon the static receptance. This relation provides the basis for predictions of actual space charge fluctuation levels where experimental difficulties have prevented exact determination. These parameters, incidentally, seem to have some promise of becoming powerful tools in thermionic current analysis. Their properties are under further investigation.

75. Photo electric emission from different metals. H. C. RENTSCHLER, D. E. HENRY AND K. O. SMITH. *Research Laboratory, Westinghouse Lamp Co., Bloomfield, N. J.*—A method was developed for preparing surfaces of any metal from which the photoelectric sensitivity of the metal was measured. The metals tested are Thorium, Uranium, Titanium, Zirconium, Cerium, Tantalum, Tungsten, Copper, Silver, Magnesium, Aluminum, Cadmium, Zinc, Calcium and Barium. For Tungsten and Tantalum the values of the photo electric work function here obtained agree with the values of the Thermionic work function obtained by Dushman. For Thorium, Calcium, Uranium and Zirconium the values of the photoelectric work function are considerably higher than the thermionic values for thin coatings of the corresponding metals on Tungsten. The photoelectric threshold wave-length for Barium metal is considerably shorter than that for Barium oxide coated cathodes commonly used in radio tubes and similar devices

76. Mass spectrograph study of the ionization and dissociation of benzene by electron impact. ERNEST G. LINDER, *Cornell University.*—Benzene (C_6H_6) has been analyzed by a mass spectrograph designed especially for use with large molecules. Ions have been found containing carbon in amounts from C_6 to C_1, with various amounts of hydrogen attached. The principal primary ion for 120-volt electrons appears to be $C_6H_5^+$, this constituting about 50 percent of all the ions. The C_4 group makes up about 20 percent, and the C_3 group about 8 percent. By varying the pressure it has been shown that dissociation by collision with other molecules occurs, H atoms being stripped from the carbon ring. Molecules such as C_6H^+ and C_6^+ are apparently thus produced. No H^+ ions have been detected. The results confirm the stability of the benzene ring found in thermal dissociation studies. The ring does not break up under electron impact as readily as do straight chain molecules such as the *n*-paraffins studied with the mass spectrograph by Stewart and Olson (J.A.C.S., **53**, 1236 (1931)).

77. Probe measurements on arcs at atmospheric pressure. R. C. MASON, *Westinghouse Elec. & Mfg. Co., East Pittsburgh.*—Small probe wires, 5 to 20 mils in diameter, moving at constant velocity, were used to study a low current carbon arc in air at atmospheric pressure; the currents and voltages were recorded by an oscillograph. The arc voltage increased 3 to 12 volts maximum when the probe was in the arc, independent of the potential applied to the

probe. The maximum increase in arc voltage, with probes of different sizes and shapes, did not vary greatly with probe velocity, between 10 and 100 cm/sec., but was an increasing function of the probe perimeter. A dark space, of diameter two to three times that of the probe wire, surrounded the probe, indicating that the state of ionization near the wire was not the same as in adjacent parts of the arc. As the space charge sheaths around the probe are smaller than the dark space, it seems probable that the usual Langmuir probe determination of space potential, ion density, and electron temperature (cf. Nottingham, Jour. Franklin Inst. 206, 43, (1928); 207, 299, (1929); Bramhall, Phil. Mag. 13, 682, (1932)) will not give the characteristics of an arc undisturbed by the measuring probe.

78. The intermediate free path case in the theory of a plasma. LEWI TONKS, *General Electric Co., Schenectady, N. Y.*—A theory of ion motions and potential distribution in the uniform positive column has been developed by Tonks and Langmuir, (Phys. Rev. **34**, 876 (1929)), for both the case where an ion generated in the gas falls without collision to the wall, and for the (Schottky) case where the ion velocity is proportional to field strength. The case of velocity α (field)$^{1/2}$ was touched upon but was thought to be unimportant. It now appears that in a mercury arc this neglected case is of prime importance from 5 to 30 baryes pressure and perhaps higher. From measurements of arc gradient, electron temperature, and positive ion current to the wall in the pressure range cited, values of arc current and electron density have been calculated which check with the more directly observed values in a fairly satisfactory way, and check far better than values calculated on either of the other two bases.

79. Further experimental data on the electrostatic and magnetic components in the electrodeless discharge. CHAS. T. KNIPP AND V. M. SMITH, *University of Illinois.*—About a year ago the senior author published photographs (Phys. Rev. **37**, 6 (1931)) showing the relative intensities of the discharge due to the two fields. These fields acted through the intervening glass walls of the discharge vessel. Since then four discharge tubes have been constructed of 12 liter Pyrex flasks, with *internal* energizing coils of No. 8 Cu wire placed as follows: First with a coil of 14 turns and 11 cm diameter, second with a coil of 7 turns similarly placed, third a coil of 1 turn, and fourth with no internal energizing coil. In addition to the above there was placed on the outside round the equator of each flask, with the plane parallel to the inner coil, an energizing coil of No. 10 flexible copper wire consisting of 3 turns. Switches were provided for making various connections. Thus the gas within a given flask could be excited at will, internally, externally, or with the exciting coils in conjunction, or in opposition. The four flasks were connected through the same manifold to a pressure gauge, and to the exhausting pumps. Liquid air traps were used and provision was made for introducing different gases. With this arrangement numerous photographs of the discharge were made which form the subject of this report.

80. The number of Langevin ions in the free atmosphere at Washington, D. C. G. R. WAIT AND O. W. TORRESON. *Department of Terrestrial Magnetism, Carnegie Institution of Washington.*—An apparatus for continuously recording the number of large ions in the free atmosphere has been in operation near the northern boundary of Rock Creek Park since the beginning of March, 1932. Ions having a mobility between 0.3 and 0.0004 cm/sec/volt/cm have been included in the count, experiment having shown that practically all Langevin ions in this locality have a mobility greater than the lower limit. The results from twelve complete days of observation of positive ions, give an average value of 5000 per cc. The average value for the day varies from about 2000 to 6000 per cc. The largest hourly value obtained since recording began is about 16000 per cc. A definite diurnal variation has been found, with two maxima, one shortly after sunrise and the other about twelve hours later, the average diurnal range being from about 3000 to 6000 per cc.

81. Features of the current-system of the upper atmosphere as revealed by the diurnal magnetic variations at Huancayo, Peru. A. G. MCNISH, *Department of Terrestrial Magnetism, Carnegie Institution.* (*Introduced by G. R. Wait.*)—The solar diurnal magnetic variation (designated by S) as recorded at the Huancayo, Peru, Magnetic Observatory of the Carnegie

Institution of Washington, exhibits a marked difference from that computed for the Observatory from the spherical harmonic coefficients of S as derived by Chapman in 1919. Particularly, the observed north-force component of S exceeds this computed value by a factor of three. Assuming that S is due to currents flowing in the upper atmosphere, this difference is explained on the assumption of a more dense current-flow over the western hemisphere, with a particular crowding of the lines of flow over northern South America as is to be expected because of the southward displacement of the magnetic equator in the western hemisphere. Thus this apparent anomaly is quite consistent with the current-theory. On the other hand, if S is due to diamagnetic effects, as suggested by Gunn, the observed north component of S at Huancayo should exceed that computed from Chapman's coefficients by a factor of less than four-thirds, instead of a factor of three as is observed.

82. Ultraviolet transmission of the atmosphere. R. S. ROCKWOOD, *University of New Mexico* AND R. A. SAWYER, *University of Michigan.*—Using a thermocouple and a silvered corex filter, which transmits a narrow band of radiation near $\lambda 3200$, observations have been made of the intensity of ultra-violet solar radiation reaching the earth. Simultaneous measurements were made on the campus of the University of New Mexico, altitude 5100 feet, and at stations at various altitudes up to 10,300 feet in nearby mountains. Data was taken on clear days in late fall when atmospheric conditions are most stable and the amount of water vapor is small and constant. The atmospheric absorption coefficients calculated for each observation were plotted for each altitude against the quantity of water in the light path, calculated from the observed vapor pressure by Hann's equation. Extrapolation to zero water gave an absorption coefficient for unit air mass which varied but little with altitude and agreed within the experimental accuracy with that calculated from Rayleigh's molecular scattering formula, indicating that in dry, clean air molecular scattering is sufficient to account for the depletion of solar radiation at $\lambda 3200$.

83. Visibility in New York City. MORGAN T. RILEY, *National Conference Board on Sanitation. (Introduced by H. H. Sheldon.)*—As dust increases visibility decreases by the equation $583D^{-1.1963}-V=0$. As relative humidity increases visibility decreases by the equation $102.08-6.81V-H=0$. The joint effect of dust and relative humidity was analyzed into their separate effects. The dust count was held constant and visibility measured at increasing relative humidities. In its turn relative humidity was held constant and visibility measured at increasing dust counts. Along a diagonal drawn through the table visibilities are equal with an addition of 10,000 dust particles per cubic foot and a subtraction of 10% relative humidity Above this diagonal subtraction of 10,000 dust and addition of 10% relative humidity gives a visibility that is better. Here therefore dust was more potent. Below the diagonal addition of 10% relative humidity and subtraction of 10,000 dust particles gave poorer visibilities. The proportion of days above the diagonal when dust was more important was 54.2%, of days below the line when relative humidity was more important was 37.0%, while 8.8% of the days found the addition of 10,000 dust particles per cubic foot and the subtraction of 10% relative humidity of equal effect upon visibility. These values can be made the measure of the success of a smoke campaign.

84. Diffusion technique for the separation of the isotopes of hydrogen. R. M. LANGER, *University of Minnesota.*—It is easy after some experience with the problem to understand why Stern and Volmer (Ann. d. Physik **59,** 225, 1919) failed to find evidence for the isotope of hydrogen recently discovered by Urey, Brickwedde and Murphy. Their technique can be very greatly improved and by a modification of their method it is hoped that an apparatus can be developed which will be more economical and more convenient than the counter-diffusion process favored by U., B. and M.,—at least for small increases in the concentration of the heavier isotope. By far the most promising permeable material is paper. The number κ of molecules of a gas of molecular weight M passing in one second through unit area of a paper sample subject to a pressure difference of 1 dyne/cm^2 can be fairly represented by the sum $\kappa=\alpha/(M)^{1/2}+\lambda$ where α and λ are practically independent of M. The first term is the desirable diffusion component and the second a wasteful leak. At atmospheric pressure in

H_2 a typical bond paper might have a value of $\kappa = 10^{12}$. Of this λ might be about 25%. Other papers have sometimes a hundred times smaller value of κ and nevertheless about the same value of λ/κ. Other substances such as rubber, cellophane, parchment, porcelain are practically hopeless for several reasons, besides being exceedingly slow compared with paper.

85. Helium filled G. M. tube counters. J. A. BEARDEN AND C. L. HAINES, *Johns Hopkins University.*—The operation of the Geiger-Muller tube counter filled with air at a pressure of 3 to 7 cm of mercury is well known. In the present work it has been found that similarly constructed counters filled with helium at pressures from 10 to 76 cm of mercury will operate at slightly higher voltages. The sensitivity of the helium filled counters for gamma-rays appears to be somewhat higher than that of the air filled counters. The principal advantages of the present counters are: first, counters can be constructed using extremely thin windows for recording α and β-rays; second, by using a low helium pressure the counters will operate at a very low voltage; third, the range of the working voltage is greater. Counters have been operated for several weeks without any change in sensitivity or operating voltage. It has also been found that a single stage amplifier connected to a cathode ray tube is a satisfactory method for observing the counts.

86. A cloud expansion chamber for automatically photographing the tracks of corpuscular cosmic rays. THOMAS H. JOHNSON, WILLIS FLEISHER, JR. AND J. C. STREET, *Bartol Research Foundation of the Franklin Institute.*—An expansion chamber of new design, operating continuously, is illuminated by photoflash lamps exploded by the coincident discharge of two Geiger-Mueller counters placed above and below the chamber. (See Abstract No. 87 of this program.) The illumination takes place only if the coincident discharge of the counters occurs during the sensitive interval of the chamber. The circuits are arranged so that the sensitive period as well as the delay of the flash after the coincidence can be varied. A large percentage of the photographs obtained with this apparatus contain straight tracks in the line of the counters. The chamber operates at pressures above atmospheric with controls on both expansion ratio and rate of expansion. The laboratory supply of compressed air with a device for accurately controlling the pressure is used to operate the chamber. Three chambers operating simultaneously are being constructed for studying cosmic ray tracks over extended lengths of their paths.

87. Experiments on the corpuscular cosmic radiation. J. C. STREET AND THOMAS H. JOHNSON, *Bartol Research Foundation of The Franklin Institute.*—A new vacuum-tube circuit for recording coincident discharges of two or more Geiger-Mueller counters has been developed with improvements as regards the sensitivity, resolving time and variability of counting rate. The number of accidental coincidences from two counters having individual counting rates of 90 per minute is 2.5 ± 0.5 per hour, corresponding to a resolving time $\tau = 1.5 \times 10^{-4}$ secs. The number of real coincidences corresponds to 7.3×10^{-3} per cm^2 per unit solid angle per

Cm. of lead	0	1	2	5	8
Coincidences per min.	$1.61 \pm .03$	$1.68 \pm .03$	$1.64 \pm .03$	$1.54 \pm .02$	$1.45 \pm .03$
Percent change due to lead	—	+4.4	+1.5	−4.4	−10

second with uncertainties because of end effects and an unknown but finite recovery time of the counters. This is from two to three times the number reported by former observers and yields the more satisfactory value of 98 ions per centimeter of path when used in conjunction with Millikan's latest value of the ionization in an electroscope. The effect of lead placed above the counters has been measured with the results and probable errors shown in the table. The increase with small thicknesses of lead is in agreement with Schindler. The ratio of coincidences at 45° to those in the vertical direction is 0.41 ± 0.04.

(The authors hope to demonstrate a new portable apparatus making a continuous record of the cosmic radiation throughout the period of the meetings.)

88. The direct detection of individual cosmic rays. W. F. G. SWANN AND J. C. STREET, *Bartol Research Foundation of The Franklin Institute.*—The cosmic-ray ionization current was measured in an iron tube 15 feet long, 6 inches internal diameter, filled with nitrogen to a high pressure, and with suitable devices for compensating potential fluctuations and for balancing out the main part of the ionization current. Data for the ionization by a single cosmic ray vary from 20 to 250 ions per centimeter of path. On the basis of 100 ions per centimeter of path, a cosmic ray, traveling the whole length of the above tube, would produce about 4×10^6 ions, and would result in a spurt of ionization current twenty times that caused by an alpha particle, so that it would be distinguishable unambiguously from such spurts. Data obtained from Geiger counters have indicated that 7×10^{-3} cosmic rays pass through one square centimeter per second, having come within unit solid angle. On this basis, the above tube should show spurts corresponding to cosmic rays traveling the whole length, about 4 times per hour. Spurts have been observed and recorded in about the expected amount and frequency. Associated with them, moreover, are a few spurts of larger amounts, having characteristics suggestive of their source having originated in the gas.

89. Diffraction of low-speed electrons by a gold crystal. H. E. FARNSWORTH, *Brown University.*—A previous investigation of electron diffraction by a silver crystal, for normal incidence on a (100) face (to appear shortly in Phys. Rev.), showed that, in general, each observed diffraction beam, between 0 and 325 volts, is made up of several components of fine structure. As the angle of incidence was changed from normal in small steps, the relative intensities of the components of any one beam changed enormously. The components which are present for normal incidence may disappear and others appear at angles of incidence a few degrees from normal. For each beam there is a certain angle of incidence at which the most intense component attains its maximum value. No exact correspondence between the characteristics of the various beams was found. We are now obtaining similar observations for a gold crystal. A fine structure is also observed for these beams. The intensities of the components are also very sensitive to a change in the angle of incidence, but the particular characteristics of any one beam differ considerably from those of the corresponding beam for silver. This is particularly significant since gold and silver have the same lattice structure and also the same lattice constant to within 0.4 percent.

90. Reflection of molecular beams of the rare gases from alkali halide crystals. R. M. ZABEL, *University of Iowa.*—Evidence of diffraction phenomena has been found in the reflection of helium from sodium chloride crystals in agreement with the results obtained by Estermann and Stern (Zeit. f. Phy. **61,** 95, (1930)). Argon reflected from sodium chloride gives a diffuse reflected beam closer to the normal than the expected position of a specular beam. The results obtained in the reflection of argon from sodium chloride are similar to those obtained for mercury reflected from the same surface by Zahl and Ellett (Phys. Rev. **38,** 977 (1931)). Present evidence indicates that argon incident upon lithium fluoride gives rise to relatively less directed and more diffuse scattering than it does when incident upon sodium chloride.

91. Reflection of mercury atoms from lithium fluoride crystals. R. R. HANCOX AND A. ELLETT, *State University of Iowa.*—The scattering of a molecular beam of mercury by a lithium fluoride crystal is studied as a function of crystal and beam temperature. A quasi-specular beam of the type observed by Zahl (H. A. Zahl, Phys. Rev., pp. 977, Vol. 38 (1931)) for other alkali halide crystals is obtained here, with the same characteristic temperature changes.

92. Reflection of beams of Tl, Sb, and Pb from a sodium chloride crystal.—J. M. B. KELLOGG, *State University of Iowa.*—Directed beams of atoms of Tl, Sb, and Pb reflected from a freshly cleaved crystal surface of Sodium Chloride have been observed. In the case of Tl, Pb, and Sb at small angles of incidence the reflection is specular. For Sb incident at a grazing angle of 50° the reflected beam shows a deviation from the specular path in a direction away from the normal.

93. Mean free paths of gases. JOHN A. ELDRIDGE, *State University of Iowa.*—A molecular beam passes through a chamber enclosing gas at low pressure. The emergent beam is measured on a Pirani gauge. The question has been raised whether a collision in the classical sense has any meaning, without specification of the angle of scattering considered. As a preliminary experiment it was determined that the molecules suffering very small deviations (less than a degree) were negligible in number. The mean free paths of H_2, He, N_2, O_2, molecules have been measured; in each case the values found are smaller (by several fold) than the values determined indirectly from kinetic theory. The difference is probably due to neglect of the persistence of velocity in the kinetic theory.

94. Motion of K^+ ions in mercury vapor. CARL FRISCHE, *State University of Iowa.*—Ionization by positive ion impact was studied in A, Ne, N_2, CO, and He at voltages up to 4000 volts and the results seem to check with those of Sutton, (Phys. Rev., **33,** 363 (1929)) and Beeck (Ann. d. Phys. **6,** 8, 1001, (1930)), where ever a check was possible. When the work was extended to an element heavier than K^+ i.e., mercury, the results are more complicated. The evidence seems to indicate; (a) reflection of K^+ ions at all voltages, (b) an increase in mean free path with increase in voltage, (c) no ionization below 250 volts but above 250–350 volts ionization increases with the voltage.

95. Magnetic units. A. E. KENNELLY, *Harvard University.*—The International Electrotechnical Commission (I.E.C.) through its Advisory Committee on *Nomenclature*, after three years of international discussion over certain perplexing ambiguities, all over the world, in the use of the C.G.S. magnetic unit names, brought in a unanimous report to the I.E.C. Plenary Meeting at Oslo, in 1930, recommending the following names for C.G.S. magnetic units: *gilbert* for magnetomotive force $\mathcal{F}$, *oersted* for magnetizing force H, *maxwell* for flux Φ, and *gauss* for flux density B. The Oslo meeting accepted these recommendations unanimously. At an international committee meeting in London, last September, they were reviewed and reindorsed. It would seem that if these resolutions continue to be generally accepted, the confusion that has existed in C.G.S. magnetic unitology, for over thirty years, should be ended. Practically all magnetic literature, at present, is written in C.G.S. magnetic units, but demands of lesser urgency have been made for completing the practical, or *volt-ampere-ohm* system of units in the magnetic series. This is a matter in which the I.E.C. has expressed a desire that the International Physical Union (I.P.U.) should participate. It is hoped that the American Physical Society may formulate opinions on this difficult question, which can only be finally settled by international agreement. Two outstanding questions seem to stand in the way of assigning further unit magnitudes in the practical magnetic system: (a) Should the system be "subrationalized?" Specifically, should the mmf of a coil of N turns, carrying a steady current of I amperes, be $4\pi NI$, or simply NI? (b) Should the flux density B be referred to the square quadrant, the square meter, or the square centimeter? On both of these questions there is much difference of opinion in all countries. Arguments are presented on both sides.

96. Electromagnetic equations and systems of units. LEIGH PAGE, *Yale University.*—Most of the suggestions for a more convenient system of electrical units have ignored the far more important question of the form of the fundamental equations of electromagnetism. These equations are written in their most general form and the following criteria are proposed: (1) There should be only *one* set of fundamental equations in place of the three or four used at present; (2) There should be two systems of units, one c.g.s. for the physicist and one practical for the engineer, both systems using the *same* set of fundamental equations; (3) The eight internationally recognized units (joule, watt, coulomb, ampere, volt, ohm, farad, henry) should be retained in the practical system; (4) The fundamental equations should be symmetrical in form. It is shown that these criteria can be fulfilled in an infinite variety of ways, of which the simplest is that which employs the Heaviside-Lorentz set of equations. For this set of equations the eight internationally recognized units are retained in the practical system provided $\epsilon^{-4}(10)^{-19}$ gm, $\epsilon^{3}(10)^{13}$ cm, and 1 sec. are chosen as units of mass, length, and time respectively, where $\epsilon \equiv 1.06275$. The system of units proposed by Kennelly (Proc. Nat. Acad. Sci. **17,** 147 (1931)) is shown to lead to a much more complicated set of fundamental equations.

97. A general theory of electric and magnetic units. VLADIMIR KARAPETOFF, *Cornell University.*—The fundamental electric, magnetic, and electromagnetic relationships may be written in a general system of units such that they may be obtained in any existing or future system of units by assigning certain values to five parameters (which have nothing to do with the choice of units of length, mass, or time). These parameters are as follows: (1) The ratio between the actual electrostatic flux and the so-called geometric flux; (2) Same for the magnetic flux; (3) A factor which converts a volume of current into the corresponding m.m.f.; (4) The absolute permittivity of vacuum; (5) The absolute permeability of vacuum. These five parameters must satisfy the condition that the velocity of electromagnetic waves in vacuum is a given quantity. A choice of four parameters fixes a type of system of units; by assigning some definite values to three non-electrical quantities, for example, units of length, time, and mass, a specific system of that type is obtained. A new system of units may be devised out of the general system, to satisfy some given specifications. The complete paper has been accepted for presentation before the American Institute of Electrical Engineers and is to be published in their Transactions.

98. Three superfluous systems of electromagnetic units. GEORGE A. CAMPBELL, *American Telephone and Telegraph Co., New York.*—In Nature, for March 5, a reviewer says: "Future students will apparently have to learn not only the electromagnetic and the electrostatic systems of units, but also the Heaviside-Lorentz system." These three systems are added to the practical system. Would it not be far better for future students to learn that they will need but one system of units for both practical and theoretical work as engineers or scientists; that this universal system includes the meter, second, watt, volt, and other basic units which they have been using as home electricians and radio amateurs; that when they come to read the older electromagnetic literature, it will be unnecessary to learn to use the three obsolete systems of units, because it will be simpler to translate anomalous units into the one comprehensive, coherent system by using a conversion table? Since the answers seem to be emphatically in the affirmative, it follows that international magnetic units should be added to the mechanical and electrical units to form a complete, rational system, coherent with the meter, kilogram, second and international ohm. It would be most unfortunate if transition difficulties, real or imaginary, are allowed to discourage the early formulation of supporting opinion.

99. The mosaic structure in metal crystals. A. GOETZ, *California Institute of Technology.*

100. On newly discovered effects in ferromagnetic crystals. FRANCIS BITTER, *Westinghouse Elec. & Mfg. Co.*

101. Hall effect versus intensity of magnetization. EMERSON M. PUGH AND T. W. LIPPERT, *Carnegie Institute of Technology.*—Previously reported work has shown that in two ferromagnetic materials, the Hall e.m.f. is a linear function of the intensity of magnetization (B-H), rather than of B or H alone. Recent investigations employing much improved apparatus with consequently increased accuracy show that such a linear relationship is definite in four additional materials, whether the specimen was annealed, quenched or baked, both on the virgin curve and on all succeeding hysteresis loops. This relation is particularly striking in the case of a slightly ferromagnetic alloy (Fe 70%, Ni 30%) in which the H was sometimes more than half of B, whereas in other materials H was never more than 5% of B. To obtain the required accuracy it was necessary to employ a new method of determining H.

102. Kerr effect and molecular field in rochelle salt. HANS MÜLLER, *Massachusetts Institute of Technology.*—Measurements of the Kerr effect in rochelle salt between $-20°C$ and $25°C$ give for fields above 200 volt/cm a linear relation between change of double refraction and electric field in the a-direction of the crystal, though reversing the field does not reverse the effect. This behaviour can be explained with help of the electric field of the oriented dipoles which are responsible for the anomalous dielectric properties. With a field of 200 volt/cm the orientation and the molecular field reach saturation. The molecular field is very large compared to the applied fields and since the Kerr effect is proportional to the square of the sum

of both fields the effect appears to be linear with the applied field. From the data we estimate a molecular field of 4–8 million volt/cm and a "true" Kerr constant between 10^{-11} and 2×10^{-11} cm³/erg, both varying with temperature. These values are of a reasonable order of magnitude. The molecular field corresponds to an average distance of 4 A between the dipoles, while the average distance between the water molecules in the crystal is 4.04 A.

103. The variation in the Kerr electro-optical constant of nitrobenzene with temperature near a transition point. (9.6°C.) HERBERT TROTTER, JR., *University of Virginia (Introduced by J. W. Beams).*—Wolfke and Mazur (Nature **127,** 741 (1931); **128,** 584 (1931)) have observed a distinct transition point in liquid nitrobenzene at 9.6°C. They note an abrupt change in refractive index, dielectric constant, and slope of the density curve. G. W. Stewart (Phys. Rev., A, **39,** 176 (1932)) also has noted a change in the x-ray diffraction at about this temperature. The author has found a similar change in the Kerr constant at about this point. The method used was a relative one. Light of a narrow range of wave-length was passed through two Kerr cells at right angles, one of the cells being at a fixed, the other at a variable temperature; and potentials on the cells were adjusted to secure compensation. The square of the potential ratio, assuming Kerr's law, varies inversely as the ratio of the Kerr constants. Impulsive potentials (less than 10^{-4} sec) were used to avoid both heating and possible distortion of the electric field.

104. Magneto-optic rotation by condenser discharge. FRANCIS G. SLACK AND W. M. BREAZEALE, *Vanderbilt University.*—The rotation of the plane of polarization of light produced by a condenser discharge across a spark gap has been measured when the condenser discharges through a coil surrounding various media of comparatively high Verdet Constants. The set up is similar to that used by Dr. Fred Allison (J.A.C.S. 52, 3796 (1930)) except that a Lippich double field polarimeter replaces the crossed nicols. Net rotations, positive and negative, are found depending on the material in the field and on the constants of the discharge circuit. These rotations are not found to depend on the length of the wire path leading to the coil unless this materially changes the resistance in the circuit with resulting change of wave form. Curves are obtained showing the variation in rotation with resistance, capacity, and inductance in the circuit. An unexpected and as yet unexplained phenomenon appears in that with reversal of relative direction of net field and direction of light, all other factors held constant, the rotation in the positive or clockwise direction is greater than that in the opposite direction. Efforts to eliminate this asymmetry have to date been unsuccessful. This effect has been found for all materials used including carbon bisulphide, toluene, chloroform, and water.

105. Nature of the phenomena underlying the magneto-optic method of analysis. FRED ALLISON, J. H. CHRISTENSEN AND GEORGE V. WALDO, *Alabama Polytechnic Institute.*—For several years investigations have been in progress in this laboratory concerning the nature of the physical phenomena which produce the minima of light characteristic of compounds in the magneto-optic method of analysis. (Allison, Ind. Eng. Chem. (Analyt. Ed.), **4,** 9 (1932)). The following theories have been tested experimentally and found inadequate: (a) electrostatic effects; (b) effects due to scattering, absorption, depolarization, etc.; (c) transverse magnetic field effects; (d) effects characteristic of the applied magnetic field itself; (e) poor contacts in trolley system and electrical interference. That the phenomena are to be explained on the basis of a time lag in the Faraday effect seems to be indicated from the results of various experiments, namely: the minima are observed with the Nicols (a) crossed and the magnetic fields opposing in the two liquids; (b) completely uncrossed and the fields assisting; (c) uncrossed at any angle (not approaching $\pm90°$), fields opposing. Maxima are observed with Nicols (d) crossed, fields assisting; (e) completely uncrossed, fields opposing. With fields assisting, when the analyzing Nicol is rotated from the crossed position to angles (f) in the direction of the magnetic rotation, minima are observed; (g) in the direction opposite to the magnetic rotation, maxima are observed. The minima and maxima coincide for any given compound. In uncrossed settings of Nicols, a third Nicol serves to reduce the light to the required intensity.

106. The magnetic qualities of large artificial graphite crystals. ALEXANDER GOETZ AND ALFRED FAESSLER. *California Institute of Technology.*—A process applicable to any crystalline substance showing magnetic anisotropies has been developed. It permits to measure susceptibilities in different directions with regard to the crystallographic axis for crystals down to ultramicroscopic sizes. The process consists of settling the crystal powder of equally sized particles in a liquid gelatine solution within the field of a strong electromagnet. After each particle has oriented itself by turning its most paramagnetic direction parallel to the lines of force, the solution is solidified by cooling and each particle thus is fixed in an isolated but crystallographically parallel position with regard to its neighbor. The diamagnetic properties of graphite powders are investigated and the critical size below which the crystal diamagnetism begins to depend on the size of the individual crystal as well as the dependence of this critical size on the field strength were studied. The magnetic anisotropy of these crystals are approximately 28, i.e., 4–5 times larger than the values obtained from natural graphite single crystals. The experiments seem to give definite proof that the crystal diamagnetism is caused by "free" electrons with large paths.

107. Magnetic discontinuities produced by mechanical deformation. DAVID G. C. LUCK, *Massachusetts Institute of Technology.*—The magnetic discontinuities produced by mechanical deformation of various ferromagnetic materials in small magnetic fields have been studied oscillographically. These discontinuities have been found to be largely unaffected by external magnetic field as long as this is small. Soft substances which have high permeability and positive magnetostriction in general show large discontinuities, the magnitude of which varies little between quite different substances. Substances which are hard or have low permeability or negative magnetostriction in general show no discontinuities. The amplitude of the discontinuities depends mainly on the rate of mechanical deformation, both for tension and for torsion of the sample, and is much greater for the first deformation cycle after annealing than for succeeding deformations. The effect seems to be distinctly an elastic one, vanishing when plastic deformation sets in. It vanishes also if the sample is heated to the Curie temperature. This behavior of ferromagnetic material seems explicable on the basis of the Akulov theory of ferromagnetism.

108. The contribution of free electrons to ferromagnetism. CAROL G. MONTGOMERY, *Sloane Physics Laboratory, Yale University.*—The recent experiments of Dorfmann and others (Zeits. für Physik **70,** 796 (1931)) have again raised the question whether free electrons contribute to ferromagnetism. The specific heat of the free electrons measured by thermoelectric data and the calorimetric specific heat both undergo anomalous variations at the Curie point, but the exact connection is not clearly understood. As first pointed out by Duhem in 1888, if free electrons were directly responsible for ferromagnetism, then when one end of a piece of iron is in a stronger magnetic field than the other, there would be a concentration of electrons in that end. This would produce a difference in potential between the ends given by the relation $V=-W\lambda$ where λ is the electrochemical equivalent and W the difference in energy of magnetization per gram. An attempt made to find such an effect in iron using a sensitive galvanometer and an accurate thermostat showed that the effect was less than 5×10^{-10} volts for a field of 15,900 gauss. The potential difference computed by the above expression is of the order of 10^{-4} volts. This seems to indicate definitely that free electrons are not directly responsible for ferromagnetism. The analogous effect for dia- and paramagnetics is below the limits of these measurements, but as Bitter has pointed out (Phys. Rev. **36,** 978 (1930)) it should be accessible in some cases.

109. Line reversal temperature measurements on an internal combustion engine. A. E. HERSHEY AND R. F. PATON, *University of Illinois.*—Engine flame temperatures have been determined by one of the authors (results to appear in Ind. and Eng. Chem.) from radiation measurements with a thermopile calibrated as a radiation pyrometer and absorption measurements by the method of Schmidt (Ann. der Phys., **29,** 998, (1909)), assuming radiation with, only thermal excitation. Since chemiluminescence makes such an assumption open to question flame temperatures have now been found by line reversal. Other investigators have used this

method for a satisfactory determination of continuous flame temperatures, notably Griffiths and Awberry (Proc. Roy. Soc., **123**, 401, (1929)). Continuous radiation is passed through the flame into which Na has been introduced, the intensity of the continuous radiation being varied until the superimposed *D* line just disappears. The brightness temperature of the source of continuous radiation, found with an optical pyrometer, is, with certain corrections, equal to the flame temperature. A stroboscopic shutter permits comparison during 2½ degrees of crank travel at the same point in successive cycles. Temperatures found by the two methods agree satisfactorily. With theoretical air-fuel ratio the maximum temperature from radiation measurements was 2373°K and from line reversal measurements 2310°K, indicating that the effect of chemiluminescence on radiation temperature measurements is negligible.

110. Development of polar characteristics in insulating oils. W. N. STOOPS, *Westinghouse Elec. & Mfg. Co., East Pittsburgh.*— (*Introduced by Chas. F. Hill.*)—The decomposition of transformer oils may be followed quite closely by measuring the dielectric constants of the oils as they deteriorate in service. The change in dielectric constant of an oil depends both on the length of time it has been in service and on the chemical composition of the oil, so that it is possible to distinguish between the decomposition rates of different oils. These data are compared with those obtained on the same oils decomposed very much more rapidly in laboratory tests. The change in dielectric constant is definitely correlated with the change in chemical characteristics. That the change in dielectric constant of the oils is due to the formation of polar molecules is shown by a study of the variation of the dielectric constant and power factor of the decomposed oils with temperature and frequency.

111. Behavior of the copper-cuprous-oxide rectifier at high frequencies. W. P. PLACE, *Union Switch & Signal Company, Swissvale, Pennsylvania.* (*Introduced by L. O. Grondahl.*)—It has been found experimentally that the copper-cuprous-oxide rectifier, which behaves as an asymmetric resistance at ordinary commercial frequencies, has a considerable capacity at the rectifying boundary which impairs its rectifying properties at higher frequencies. This effect of the capacity on the rectifying properties is due to the fact that its impedance at the high frequencies is low enough to become comparable with the resistances of the rectifying boundary. At high frequencies the capacity impedance may be considerably lower than the reverse current resistance, and at low current densities may even be low compared to the forward resistance. By increasing the voltage across the rectifier, the forward resistance can be lowered to such an extent that even at high frequencies it becomes small compared to the capacitance. When this condition exists, the rectifier functions satisfactorily. An analysis with the help of equivalent circuits is presented to illustrate the effect of the static capacity on the rectifying properties of a bridge-type rectifier circuit. Curves, both calculated and experimental, showing the relation between a-c. and d-c. voltages at different impressed voltages and for different frequencies are given.

112. A method of measuring the short-time D. C. Conductivity of insulating liquids. G. W. GARDINER, JR., *Bureau of Standards, Washington, D. C.*—The method consists in comparing the short-time direct current through a test condenser containing the liquid with that through a guard ring air condenser of negligible conductance. In order to eliminate the displacement current, the comparison is made in a bridge having the two condensers in adjacent arms and resistance in the other two arms. The bridge is first balanced with an alternating current source, which is then replaced by a direct current source controlled by a commutator by means of which the direct current potential may be applied once a second for a time which may be varied from 0.002 to 0.500 seconds. The change in potential per cycle of the midpoint of the two condensers, as determined by a sensitive direct current amplifier measures the average irreversible component of the current through the liquid during the time of application of the field.

113. Conductivity of liquid mercury at high temperatures and pressures. FRANCIS BIRCH, *Jefferson Physical Laboratory, Harvard University.*—The electrical conductivity of liquid mercury has been measured in the region between 0 and 1100 degrees centigrade, and from 1 to 4000 atmospheres. In this region the specific resistance increases with temperature, and de-

creases with rising pressure. Taking the specific resistance at 0 and 1 atm. as 1.00, the resistance at 1100° and 1000 atm. is about 4.5, at 1100° and 4000 atm. about 2.9. Both $1/\rho(\partial\rho/\partial T)_p$ and $1/\rho(\partial\rho/\partial p)_T$ decrease as p increases, and increase as T increases. The boiling curve of mercury has been retraced, by an electrical method, and indications found of the liquid-vapor critical point, at about 1460°C and 1600 atmospheres. The criterion applied was the continuous variation of resistance with increasing temperature, at constant pressure.

114. The electrical conductivity of silicon carbide. R. W. SEARS AND J. A. BECKER, *Bell Telephone Laboratories, Inc.*—By measuring the potential between several metallic point probes with a vacuum tube potentiometer, the conduction in crystals of silicon carbide has been shown to obey Ohm's law. Specific resistance of a black opaque crystal was found to be 2.13 ohm cm while for a semi-transparent green crystal it was 0.41 ohm cm. The resistance is independent of direction of current flow. The rectification and non-linearity exhibited by overall current-voltage curves between two contacts on these crystals resides in the large potential drop at the contact junctions. Exploration of various crystal surfaces with a needle-point contact showed that the resistance of this contact varies greatly from one portion of a surface to another and from crystal to crystal. A 0.002 cm displacement of the point contact on smooth surfaces sometimes caused the resistance to change by factors as large as 10,000 while on others it was fairly uniform over large areas. Momentarily applying a large voltage across the contact greatly reduces its resistance and makes it ohmic for small currents.

115. Potential distributions in large cylindrical disks with partially penetrating electrodes MORRIS MUSKAT, *Gulf Research Laboratory.*—The equivalence of the fluid pressure in a liquid bearing sand to a velocity potential gives practical significance to the potential problem of a conducting electrode partially penetrating a large cylindrical disk. A detailed investigation has been made of the potential distributions in such disks for various degrees of electrode penetration. Separate formulas were derived for studying the potential very near the electrode and at large distances from it. An approximation method was developed for determining the proper flux distribution along the electrode surface so as to make its potential uniform. The resistances of the disk for various electrode penetrations and disk thicknesses were computed and a semi-empirical approximation developed for evaluating the resistance without the necessity of going through the details of the analysis.

116. Some physical properties of compressed hydrogen. W. EDWARDS DEMING AND LOLA E. SHUPE, *Bureau of Chemistry and Soils, Washington, D. C.*—The compressibility data on hydrogen taken at the Reichsanstalt, the Leiden and the Fixed Nitrogen Research Laboratories are smoothed and extrapolated to cover the range −215°C to 500°C, and to 1200 atmospheres pressure. A sensitive graphical method is used for obtaining derivatives, and these with certain thermodynamic relations give physical properties of the gas. The properties so calculated are temperature and pressure expansion coefficients, fugacity, heat capacities at constant pressure and volume and the Joule-Thomson coefficient. It was not possible to extend calculations on heat capacities and the Joule-Thomson coefficient below −75°C. The physical properties that are calculated by this method are listed in a table or shown by graphs. The change in C_p at −75°C amounts to 0.95 cal/mole degree over the 1200 atmosphere pressure range. At higher temperatures, pressure causes a much smaller change; at 500°C, C_p increases only 0.08 as the pressure is increased to 1200 atmospheres. C_v at 25, 50, 75, ···, 800 atmospheres increases rapidly with temperature from −75° to 100° and thereafter increases slower. The Joule-Thomson coefficient is negative from −75° to 500° up to 1200 atmospheres.

117. Wall effects in ionization electroscopes. E. J. WORKMAN, *National Research Fellow, California Institute of Technology.*—Cylindrical ionization chambers with different wall thicknesses of aluminum and iron were used for measuring the ionization produced by gamma-rays from radium. The ionization was measured with a deflecting element of the single fiber type. The chambers contained 630 cc of air at atmospheric pressure. The ionization increased rapidly with increase of wall thickness. With gamma-radiation filtered through 1.27 cm of lead, the ionization with aluminum walls increases by 72 percent at a wall thickness of 0.13 cm, then

falls off rather sharply to 68 percent excess at 0.19 cm. The ionization then decreases gradually until at a wall thickness of 2 cm, although no correction for absorption of the radiation by the walls is made, the ionization is still 50 percent greater than is observed with the thinnest wall. Iron shows a greater effect, the ionization-wall thickness curve showing a sharp maximum, with an increase of 89 percent at 0.38 cm wall, and evidence of another maximum (86 percent at (86 percent) at 0.13 cm. For thicknesses above 0.15 cm the curve falls gradually, showing a 35 percent excess at 1.37 cm wall thickness. The wall effect is increased by increasing the hardness of the radiation. These results show that the ionization produced by the hard gamma-rays in the gas of an ionization chamber is due largely to secondary and tertiary effects originating in the walls of the chamber.

118. Cosmic-ray energies and their bearing on the nature of these rays. ROBERT A. MILLIKAN AND CARL D. ANDERSON, *California Institute of Technology.*—About nine-tenths of cosmic-ray energy tracks fall in the region between 7 and 500 million volt electrons. About one-tenth of the tracks seem to correspond with energies of the order of a billion, 10^9, volts. All the tracks seem to be best interpreted from the standpoint of the photon theory of the nature of the rays. The rays are absorbed primarily by the nucleus, rather than by extranuclear electrons as heretofore supposed, and the fact that the nucleus, a massive object, is disintegrated means that it is able to absorb practically the whole of the incident energy, so that the maximum value of the measured energy may well be approximately the actual energy of the incoming photons.

119. A formal macroscopic approach to quantum phenomena. WM. BENDER, *University of Chicago.*—Employing the transformation of the form

$$\xi_\alpha = n_\alpha B_\alpha + \epsilon_\alpha$$

between coordinate (amorphous) and metered (empirical) space, in which B_α is a quantum relative to a scale; n_α the ordinal number of the last scale mark of the reading; and ϵ_α an estimate made by an observer, a metric for metered space is set up:

$$(nB+\epsilon)^2 = eg_{ij}(n^iB^i+\epsilon^i)\ (n^jB^j+\epsilon^j)$$

This quadratic form in finite differences is taken to be invariant analogous to the invariance of ds in $ds^2 = eg_{ij}dx^idx^j$ of metrical space. For light propagation $nB+\epsilon=0$ and for a geodesic $\delta(nB+\epsilon) = \pm B$. In (2), B is shown to be an *absolute* kinematical quantum, n an absolute quantum number, and ϵ a spacetime uncertainty. The physical interpretation of B is given by consideration of an array of light-connected Michelson octagonal mirror clocks considered synchronized when a steady, sharp, return image is realized by an observer at any clock of the array. It will be found by any observer that all the inter-clock optical paths are an integral multiple of B, which is found to be the smallest inter-clock optical path. This light-velocity effect is generalized leading to a spacetime-matter quantum principle.

120. A method for measuring the power factor of a condenser. ARTHUR W. SMITH, *University of Michigan.*—The power factor of a condenser, C, can be measured directly in terms of a variable self inductance, L, in a parallel circuit. In series with C is a non-inductive resistance R, and in series with L is a resistance S and one coil of a mutual inductance, M. The inductance, L', of the latter coil must be somewhat less than M. These two parallel circuits look somewhat like a Wheatstone bridge, but there is no point on the inductive circuit that separates the resistance from the inductance. Therefore the other coil of the mutual inductance is connected in series with the telephone to introduce an e.m.f. that will just balance the effect of L', and any other constant inductance in this circuit. The power factor of a condenser is conveniently represented in terms of a resistance N in series with the condenser, and this is measured by the relation $N = L\,R/M$. When the ratio R/M is set at 10 or 100 the value of N is read directly on the scale of the inductance L.

121. A proposal to abolish the absolute electrical dimension systems. E. WEBER, *The Polytechnic Institute of Brooklyn. (Introduced by W. L. Severinghaus).*—A physical quantity is given by numerical value and unit. All the possible units of a quantity are defined as its "di-

mension." The physical quantities are involved in theoretical laws and definitions. The proper combination of all known relations permits a reduction of all dimensions used to a set of a few independent dimensions, which is then called a dimension system. In mechanics, three fundamental dimensions are necessary to form a dimension system, whereas in heat, as well as in electromagnetism, four fundamental dimensions are required. The paper proves that the attempt to reduce the four required fundamental dimensions in electromagnetism to only three independent dimensions leads to many contradictions, and even incorrect results. It is, therefore, proposed to *abolish* the absolute dimension systems and to introduce two new dimension systems, based upon the two dimension systems of mechanics, known as the physical and the technical dimension systems. The former consists of the fundamental dimensions of mass, length and time; and latter of force, length and time. Adding electric charge as a new dimension, two dimension systems are obtained, which may be called the electrophysical and electrotechnical, respectively. In the former all the unit names now used in the *absolute* dimension systems are defined on the basis of the four fundamental dimensions. The electrotechnical system uses all the so-called practical units, but again on the basis of the four respective fundamental dimensions. This proposal at once reconciles the inconsistencies which now cause so much trouble.

122. X-ray energy levels by the Fermi-Dirac Theory. R. D. RICHTMYER, *Cornell University.*—Dirac's relativistic wave equation for the electron has been treated in the general case of central symmetry by C. G. Darwin, resulting in the two radial equations

$$\frac{2\pi}{h}\left(\frac{w+eV(r)}{c}+mc\right)F(r)+\frac{dG(r)}{dr}-\frac{k}{r}G(r)=0$$

$$-\frac{2\pi}{h}\left(\frac{W+eV(r)}{c}-mc\right)G(r)+\frac{dF(r)}{dr}+\frac{k+2}{r}F(r)=0$$

These equations have been solved for the K energy level of Cu, using as potential function a modification of the Fermi potential function. The method of solution is one devised by Dr. Louis C. Roess and Professor E. H. Kennard. The value of W which gives F and G integrable quadratically is found to lie between the experimental value and a value 0.35 percent lower.

AUTHOR INDEX TO ABSTRACTS OF WASHINGTON MEETING

Allen, A. J. and R. Franklin—No. 46
Allison, Fred, J. H. Christensen and George V. Waldo—No. 105
Allison, Samuel K.—No. 25
Anderson, Carl D.—see Millikan

Bacher, R. F. and J. S. Campbell—No. 58
Barnes, LeRoy L.—No. 73
Barrett, C. S. and H. F. Kaiser—No. 36
Barth, Tom F. W.—No. 35
——— see Kracek
Bearden, J. A. and C. H. Shaw—No. 24
——— **and C. L. Haines**—No. 85
Becker, J. A.—see Sears
Bender, William—No. 119
Bennett, Willard H.—No. 69
Birch, Francis—No. 113
Bitter, Francis—No. 100
Blackwood, Oswald—No. 32
Boeckner, C.—No. 66
Botset, Holbrook G.—No. 7
——— See Wyckoff
Boyce, J. C.—see Compton
Brattain, Walter H.—No. 72
Breazeale, W. M.—see Slack
Brown, Weldon G. and G. E. Gibson—No. 54
Burger, E. E.—see Hull

Campbell, George A.—No. 98
Campbell, J. S.—No. 57
——— see Bacher
Canfield, R. H.—No. 33
Castleman, R. A., Jr.—No. 1
Chow, T. C.—No. 51
Christensen, J. H.—see Fred Allison
Colwell, R. C.—No. 3
Compton, K. T. and J. C. Boyce—No. 47
Costant, F. W.—No. 9

Darnell, R. C.—No. 6
Deming, W. Edwards and Lola E. Shupe—Nos. 13, 116
Dieke, G. H. and G. B. Kistiakowsky—No. 50
Duffendack, O. S. and R. A. Wolfe—No. 49
——— see Owens
——— see Thomson

Eldridge, John A.—No. 93
Ellett, A.—see Heydenburg
——— see Hancox

Faessler, Alfred—see Goetz
Failla, G.—No. 30
Farnsworth, H. E.—No. 89

Fleisher, Willis, Jr., see Johnson
Ford, O. Rex and C. B. Post—No. 29
Franklin, R.—see Allen
Fricke, Hugo and Martha Washburn—No. 31
Frische, Carl—No. 94

Gallishohat, N.—No. 12
Gardiner, G. W., Jr.—No. 112
Gibson, G. E. —see Brown
Goetz, A.—No. 99
——— **and Alfred Faessler**—No. 106
Groper, L.—see Uhlenbeck
Gunn, Ross—No. 21

Hafstad, L. R.—No. 71
Haines, C. L.—see Bearden
Hanawalt, J. D.—see Morell
Hancox, R. R. and A. Ellett—No. 91
Hardy, J. D.—No. 52
Henry, D. E.—see Rentschler
Hershey, A. E. and R. F. Paton—No. 109
Heydenburg, N. P., L. Larrick and A. Ellett—No. 61
Hirsh, F. R., Jr., and F. K. Richtmyer—No. 28
Hoyt, Archer—No. 23
Hubbard, J. C.—No. 4
Hull, Albert W. and E. E. Burger—No. 70
Humphreys, C. J.—see Meggers

Jackson, Wilfrid J.—No. 67
Johnson, Thomas H., Willis Fleisher, Jr. and J. C. Street—No. 86
——— see Street

Kaiser, H. F.—see Barrett
Karapetoff, Vladimir—No. 97
Kaufman, S. and F. K. Richtmyer—No. 27
Kellogg, J. M. B.—No. 92
Kennelly, A. E.—No. 95
Kinsey, E. L. and O. L. Sponslor—No. 38
Knipp, Chas. T. and V. M. Smith—No. 79
Kracek, F. C., Tom F. W. Barth and C. J. Ksanda—No. 34
Ksanda, C. J.—see Kracek

Langer, R. M.—No. 84
Larrick, L.—No. 60
——— see Heydenburg
Linder, Ernest G.—No. 76
Lippert, T. W.—see Pugh
Luck, David G. C.—No. 107

McLachlan, Dan—No. 20
McNish, A. G.—No. 81
Margenau, Henry—No. 40

Mason, R. C.—No. 77
Meggers, William F. and C. J. Humphreys—No. 55
Miller, Henry J.—No. 68
Millikan, Robert A. and Carl D. Anderson—No. 118
Mohler, F. L.—No. 64
Montgomery, Carol G.—No. 108
Morell, L. G. and J. D. Hanawalt—No. 37
Morse, Philip M. and N. Rosen—No. 53
Morton, G. A.—No. 22
Müller, Hans—No. 102
Muskat, Morris—No. 115
——— see Wyckoff

Onsager, Lars—No. 10
Owens, J. S. and O. S. Duffendack—No. 62

Page, Leigh—No. 96
Palmer, R. Ronald—see Tate
Paton, R. F.—see Hershey
Place, W. P.—No. 111
Plesset, Milton S.—No. 17
Plyler, E. K.—No. 16
Post, C. B.—see Ford
Pugh, Emerson M. and T. W. Lippert—No. 101

Rentschler, H. C., D. E. Henry and K. O. Smith—No. 75
Richtmyer, R. D.—No. 122
Richtmyer, F. K.—see Hirsh
——— see Kaufman
Riley, Morgan T.—No. 83
Rockwood, R. S. and R. A. Sawyer—No. 82
Rosen, N. and C. Zener—No. 42
——— see Morse

Sawyer, R. A.—see Rockwood
Schoepfle, G. K.—No. 56
Sears, R. W. and J. A. Becker—No. 114
Seitz, F.—No. 39
Shaw, C. H.—see Bearden—No. 24
Shortley, George H.—No. 18
Shupe, Lola E.—see Deming
Slack, Francis G. and W. M. Brezeale—No. 104
Smith, Arthur W.—No. 120
Smith, K. O.—see Rentschler
Smith, V. M.—see Knipp
Sponslor, O. L.—see Kinsey
Sterne, T. E.—No. 19
Stoops, W. N.—No. 110
Street, J. C. and Thomas H. Johnson—No. 87
——— see Johnson
——— see Swann
Stueckelberg, E. C. G.—No. 41
Stuhlman, Otto, Jr.—No. 2
Swann, W. F. G. and J. C. Street—No. 88

Tate, John T. and R. Ronald Palmer—No. 65
Thatcher, Everett W.—No. 74
Thomson, K. B. and O. S. Duffendack—No. 63
Tonks, Lewi—No. 78
Torreson, O. W.—see Wait
Tripp, William A.—No. 11
Trotter, Herbert, Jr.—No. 103

Uehling, E. A. and G. E. Uhlenbeck—No. 14
Uhlenbeck, G. E. and L. Gropper—No. 15
——— see Uehling

Van Dyke, K. S.—No. 5
Van Vleck, J. H.—No. 44

Wait, G. R. and O. W. Torreson—No. 80
Waldo, George V.—see Fred Allison
Washburn, Martha—see Fricke
Weber, E.—No. 121
White, H. E.—No. 59
Williams, John H.—No. 26
Wolfe, Hugh C.—No. 45
Wolfe, R. A.—see Duffendack
Wood, R. W.—No. 48
Workman, E. J.—No. 117
Wyckoff, R. D., H. G. Botset, and M. Muskat—No. 8

Zabel, R. M.—No. 90
Zener, Clarence—No. 43
——— see Rosen

AUTHOR INDEX TO VOLUME 40

References with (A) are to abstracts of papers presented at meetings of the Physical Society and references with (L) are to Letters to the Editor.

Adams, Norman I., Jr. (see Kovarik, Alois F.)—718

Alden, Lucas (see DuMond, Jesse W. M.)—165

Allen, A. J. and R. Franklin. Method for sensitizing photographic plates to the short ultraviolet wave-lengths—1038(A)

Allison, Fred, J. H. Christensen, and George V. Waldo. Nature of the phenomena underlying the magneto-optic method of analysis—1052(A)

——— **and John L. Condon.** Experiment in support of the hypothesis of a time lag in the Faraday effect—1021(L)

——— **and Roy Goslin.** Transformation product of potassium—1015(L)

Allison, Samuel K. Reflecting and resolving power of calcite for x-rays from 0.21 to 2.3A—1032(A)

Anderson, Carl D. (see Millikan, Robert A.)—325; 1056(A)

Anderson, Paul A. Molecular process of crystal growth in hexagonal metals. Deposition upon monocrystalline hemispheres of zinc—596

Anslow, Gladys A. Dissociation of the carboxyl group in amino acids and related substances, produced by absorption of ultraviolet light—115(L); erratum—639(L)

Bacher, R. F. and J. S. Campbell. Test of hyperfine structure theory—1040(A)

——— **and John Wulff.** *G*-value of the normal state of Bi I—123(A)

Bäcklin, Erik. Absolute value of x-ray wave-lengths and e/m as calculated from x-ray dispersion measurements—112(L)

Bainbridge, K. T. Mass-spectrograph—130(A)

Barnes, LeRoy L. Emission of positive ions from heated metals—1044(A)

——— **and R. C. Gibbs.** Positive ions of mass 220—318(L)

Barrett, C. S. and H. F. Kaiser. New orientations forming in a crystal of Ag-Cu during precipitation—1035(A)

Barth, Tom F. W. Unit of structure of the minerals of the sodalite family—1034(A)

——— (see Kracek, F. C.)—1034(A)

Bayley, P. L. Dielectric losses in rocksalt—120(A)

Beams, J. W. and M. Podtiaguine. Propagation of luminosity in long discharge tubes—129(A)

Bearden, J. A. Absolute x-ray wave-lengths—471(L)

Bearden, J. A. Precision wave-length measurements with the double crystal x-ray spectrometer—133(A)

——— **and C. L. Haines.** Helium filled G.M. tube counters—1048(A)

——— **and C. H. Shaw.** Refraction of x-rays by calcite crystals—1031(A)

Beck, Carl A. On the radial induced electromotive force discovered by Corbino—607

Becker, J. A. (see Sears, R. W.)—1055(A)

Bender, William. Formal macroscopic approach to quantum phenomena—1056(A)

Bennett, Willard H. Effect of the target on breakdown in cold emission—416; 1043(A)

Benz, Carl (see Poulter, Thos. C.)—872

Birch, Francis. Conductivity of liquid mercury at high temperatures and pressures—1054(A)

Birge, Raymond T. Calculation of errors by the method of least squares—207

——— Probable values of e, h, e/m and α—228; an addition—319(L)

Bishop, Edna R. Copper isotopes—16

Bitter, Francis. Mosaic structure of cobalt crystals—125(A)

——— On newly discovered effects in ferromagnetic crystals—1051(A)

Blackwood, Oswald. Further x-ray evidence as to the size of a gene; and as to the energy of mutation by ultraviolet rays—1034(A)

Bleakney, Walker. Ionization potential of molecular hydrogen—496

——— Isotopes of hydrogen as studied with a mass spectrograph—130(A)

Blodgett, Katharine B. and Irving Langmuir. Accommodation coefficient of hydrogen; a sensitive detector of surface films—78

Bloomenthal, S. Converse piezoelectric effect in mixed crystals isomorphous with Rochelle salt—121(A)

Bock, Charles D. Wide angle magnetic spectrometer—130(A)

Boeckner, C. Polarization of radiation from metals bombarded by slow electrons—1043(A)

——— Radiation from caesium bombarded by slow speed electrons—122(A)

Bonner, T. W. Luminosity of a flame containing sodium vapor—105

Botset, Holbrook G. Radon content of soil gas—1027(A)

Botset, H. G. (see Wyckoff, R. D.)—1027(A)
Boyce, J. C. (see Compton, K. T.)—1038(A)
——— (see Ladenburg, R.)—1018(L)
Bradbury, Norris E. Absolute values of the mobility of gaseous ions in pure gases—508
——— Mobility experiments in gaseous mixtures and aging experiments in pure gases—524
——— Photoelectric currents in gases between parallel plates as a function of the potential difference—980
Bradley, Charles A., Jr. Smekal-Raman spectra of $SiHCl_3$, $CHFCl_2$ and CF_2Cl_2—908
——— **and Harold C. Urey.** Relative abundance of hydrogen isotopes in natural hydrogen—889
Brattain, Walter H. Evaporation and migration of thorium on tungsten—1044(A)
Breazeale, W. M. (see Slack, Francis G.)—1052(A)
Breit, G. Remark on Gamow's treatment of radioactive disintegration—127(A)
Brickwedde, F. G. (see Urey, Harold C.)—1; 464(L)
Briggs, H. B. (see Ives, Herbert E.)—121(A); 802
Brown, Weldon G. and G. E. Gibson. Predissociation in the spectrum of iodine chloride—529; 1040(A)
Broxon, James W. Dependence of the ionization produced by the cosmic penetrating radiation upon pressure and temperature—1022(L)
Burger, E. E. (see Hull, Albert W.)—1044(A)

Campbell, George A. Three superflous systems of electromagnetic units—1051(A)
Campbell, J. S. Hyperfine structure of Ga II and In II—1040(A)
——— (see Bacher, R. F.)—1040(A)
Canfield, R. H. Methods for computing lattice energy constants—1034(A)
Castleman, R. A., Jr. Mechanism of atomization accompanying solid injection—1025(A)
Chow, T. C. New system of bands in sulphur dioxide—1039(A)
Christensen, J. H. (see Allison, Fred)—1052(A)
Clark, G. L. and K. E. Corrigan. Crystal structure of insulin—639(L)
Cohn, Willi M. Some spectrographic studies of negative point discharges at low pressure—122(A)
Cole, Kenneth S. Surface forces of the sea urchin egg—131(A)
Collins, George. Raman spectra of a series of octanols—829
Colwell, R. C. Diagonal symmetry in Chladni plates—1026(A)
——— Mathematical theory of Chladni plates—125(A)
Compton, K. T. and J. C. Boyce. Broad range vacuum spectrograph for the extreme ultraviolet—1038(A)
Condon, John L. (see Allison, Fred)—1021(L)
Constant, F. W. Capillary action at low pressures—1027(A)
Copeland, Paul L. Total secondary emission of electrons from metals as a function of primary energy—122(A)
Corrigan, K. E. (see Clark, G. L.)—639(L)
Croup, A. H. Effect of temperature on the absorption bands of benzene and some of its derivatives at low temperatures—345

Darbyshire, Orrell. Absorption spectrum of iodine monochloride in the near infrared—366
Darnell, R. C. Hydrodynamic characteristics of twelve symmetrical hydrofoils—1027(A)
Davisson, C. J. and L. H. Germer. Diffraction of electrons by metal surfaces—124(A)
Day, Ralph K. Variation of the vapor viscosities of normal and isopentane with pressure by the rotating cylinder method—281
Debye, P. Interferometric measurements on single molecules—124(A)
Dehlinger, W. On the ultra high-frequency oscillation of the magnetostatic vacuum tube—120(A)
Deming, W. Edwards and Lola E. Shupe. Graphical presentation of compressibility data—1028(A)
——— **and Lola E. Shupe.** Some physical properties of compressed gases. III. Hydrogen—848; 1055(A)
Dickinson, T. M. (see Metcalf, G. F.)—134(A)
Dieke, G. H. and G. B. Kistiakowsky. Structure of the ultraviolet absorption spectrum of formaldehyde—1039(A)
——— **and J. W. Mauchly.** Structure of the third positive group of CO-bands—123(A)
Doan, Gilbert E. and J. Leland Myer. Arc discharge not obtained in pure argon gas—36
Duane, William. Examining by a densitometer new lines in *K* series x-ray spectra—132(A)
DuBridge, Lee A. Book review—641
Duffendack, O. S. and R. A. Wolfe. Quantitative spectrographic analysis—1038(A)
——— (see Owens, J. S.)—1042(A)
——— (see Thomson, K. B.)—1042(A)
DuMond, Jesse W. M., Harry A. Kirkpatrick, and Lucas Alden. Search for preferentially directed electron velocities in crystalline graphite with the multicrystal spectrograph—165
Dunham, J. L. New terms in the energy level formula of a rotating vibrator—126(A)

Eldridge, John A. Mean free paths of gases—1050(A)
Ellett, A. Book review—322
——— (see Hancox, R. R.)—1049(A)
——— (see Heydenburg, N. P.)—1041(A)

Failla, G. Comparison of effects produced by 200k.v. x-rays, 700 k.v. x-rays and gamma-rays—1033(A)
Farnsworth, H. E. Diffraction of low-speed electrons by a gold crystal—1049(A)
——— Diffraction of low-speed electrons by single crystals of copper and silver—684
Faessler, Alfred (see Goetz, Alexander)—1053(A)
Feenberg, Eugene. Scattering of slow electrons by neutral atoms—40
Fleischer, Willis, Jr. (see Johnson, Thomas H.)—1048(A)
Ford, O. Rex and C. B. Post. Satellites near the $K\alpha_1$ line—1033(A)
Found, Clifton G. (see Langmuir, Irving)—129(A)
Franklin, R. (see Allen, A. J.)—1038(A)
Frazier, Richard H. Further data of the thermal diffusivity of nickel—592
Fricke, Hugo and Martha Washburn. Reduction by x-rays of aqueous chromic acid solutions and the influence of added organic substances—1033(A)
Frische, Carl. Motion of K^+ ions in mercury vapor—1050(A)

Gallishohat, N. Aberration of the second order in the Michelson-Morley experiment—1028(A)
Gardiner, G. W., Jr. Method of measuring the short-time d.c. conductivity of insulating liquids—1054(A)
Garrett, Paul H. Mean lives of mercury lines λ2537 and λ1849—779
Gehrts, A. Deviation of anode currents in diodes from the three-halves power law—434
Germer, L. H. (see Davisson, C. J.)—124(A)
Gerry, Harold T. and Louis J. Gillespie. Calculation of normal vapor pressures from the data of the gas current method, particularly in the case of iodine—269
Gibbs, R. C. and J. E. Ruedy. Term values in the arc spectrum of selenium—204
——— (see Barnes, LeRoy L.)—318(L)
——— (see Shapiro, C. V.)—354
Gibson, G. E. (see Brown, Weldon G.)—529; 1040(A)
Gillespie, Louis J. (see Gerry, Harold T.)—269
Gleason, Paul R. New method of measuring x-ray intensities employing an electronic photo-cell—134(A)
Glockler, George. Book reviews—321
Goetz, Alexander and Alfred Faessler. Magnetic qualities of large artificial graphite crystals—1053(A)
——— **and Rudolf C. Hergenrother.** X-ray studies of the thermal expansion of bismuth single crystals—643
——— **and Rudolf C. Hergenrother.** X-ray studies on Bi single crystals—137
Goetz, A. Mosaic structure in metal crystals—1051(A)
Gortner, Ross Aiken. Book review—475
Goslin, Roy. (see Allison, Fred)—1015(L)
Grace, Norman S. New effect produced by the action of x-rays on matter—634(L)
Granath, L. P. (see Rose, John L.)—476(L); 760
Green, J. B. and R. A. Loring. Zeeman effect in the spectrum of Pb III—883(L)
Grondahl, L. O. Note on the discovery of the photo-electric effect in a copper-oxide rectifier—635(L)
Gropper, L. (see Uhlenbeck, G. E.)—1029(A)
Gunn, Ross. Principles of a new portable electrometer—307; 1031(A)
——— Book review—642

Hafstad, L. R. Measurements of small currents using pliotron tubes—1044(A)
Haines, C. L. (see Bearden, J. A.)—1048(A)
Halpern, Otto. "Inner force" of Lorentz and the statistical calculation of the dielectric constant and magnetic permeability—134(A)
Hanawalt, J. D. (see Morell, L. G.)—1035(A)
Hancox, R. R. and A. Ellett. Reflection of mercury atoms from lithium floride crystals—1049(A)
Hardy, J. D. Near infrared bands of ammonia under high dispersion—1039(A)
Harvey, G. G. (see Jauncey, G. E. M.)—329
Henry, D. E. (see Rentschler, H. C.)—1045(A)
Hergenrother, Rudolf C. (see Goetz, Alexander)——137; 643
Hershey, A. E. and R. F. Paton. Line reversal temperature measurements on an internal combustion engine—1053(A)
Herzberg, G. Rotational structure and predissociation of the P_2 molecule—313(L)
Herzfeld, K. F. Book review—887
Heydenburg, N. P., L. Larrick, and A. Ellett. Polarization of sodium resonance radiation and nuclear moment of the sodium atom—1041(A)
Hidnert, Peter and H. S. Krider. Thermal expansion of nickel steels—131(A)
Hill, E. L. Book reviews—321; 642
Hirsh, F. R., Jr. Note on the satellites accompanying the x-ray diagram line $K\alpha_1$—151
——— **and F. K. Richtmyer.** Production of the molybdenum $L\alpha$ satellites by fluorescent absorption of silver $L\alpha$ radiation—1033(A)
Hoyt, Archer. Shape of an x-ray line—477; 1031(A)
Hubbard, J. G. Ultrasonic absorption in gases—1026(A)
Hughes, A. L. and J. H. McMillen. Note on electron scattering in argon—469(L)
Hulburt, E. O. Ionization of the upper atmosphere—129(A)

Hull, A. W. Electronic devices as aids to research—131(A)
——— **and E. E. Burger.** Disappearance of gas in discharge tubes—1044(A)
Hull, H. L. Two-crystal analysis of *L*-absorption limits of mercury—132(A); 676
Hultgren, Ralph. Equivalent chemical bonds formed by *s*, *p*, and *d* eigenfunctions—891
Humphreys, C. J. (see Meggers, William F.)—1040(A)
Hutchisson, Elmer and Morris Muskat. Quantum mechanics of lithium hydride—340
——— (see Osgood, T. H.)—129(A)

Ives, Herbert E. and H. B. Briggs. Depth of origin of photoelectrons—121(A); 802

Jackson, Wilfrid. Influence of the electrical discharge on the secondary emission from the cathode—1043(A)
Jauncey, G. E. M. and G. G. Harvey. Temperature and the Compton effect of sylvine—329
Jensen, J. C. Relation of branching of lightning discharges to changes in the electrical field of thunderstorms—1013(L)
Johnson, M. H., Jr. Spin-orbit interaction for many electron configurations—127(A)
——— Theory of complex spectra. Part II. Intensities—133(A)
Johnson, Thomas H. Calculation concerning the nature of the secondary corpuscular cosmic radiation—468(L)
——— **and J. C. Street.** Production of multiple secondaries in lead by cosmic radiation—638(L)
——— **and Willis Fleischer, Jr., and J. C. Street.** Cloud expansion chamber for automatically photographing the tracks of corpuscular cosmic rays—1048(A)
——— (see Street, J. C.)—1048(A)
Jordahl, O. M., W. G. Penney and R. Schlapp. Paramagnetic susceptibilities in crystals—637(L)

Kaiser, H. F. (see Barrett, C. S.)—1035(A)
Karapetoff, Vladimir. General theory of electric and magnetic units—1051(A)
Kassel, Louis S. and Morris Muskat. Surface energy and heat of vaporization of liquids—131(A); 627
Kaufman, Sidney. New forbidden lines in the *L* series—116(L)
——— **and F. K. Richtmyer.** Forbidden x-ray lines in the *L* series—1032(A)
——— (see Richtmyer, F. K.)—132(A)
Kellogg, J. M. B. Reflection of beams of Tl, Sb, and Pb from a sodium chloride crystal—1049(A)
Kennelly, A. E. Magnetic units—1050(A)
Kenty, Carl. Line broadening and the imprisonment of resonance radiation—633(L)
Kernaghan, Marie. Measurements of the height of a large drop of mercury—1020(L)
Kinsey, E. L. and O. L. Sponsler. Molecular structure of ice and water—1035(A)
Kirkpatrick, Harry A. (see DuMond, Jesse W. M.)—165
Kistiakowsky, G. B. (see Vaughan, William E.)—457
——— (see Dieke, G. H.)—1039
Knipp, Chas. T. and V. M. Smith. Further experimental data on the electrostatic and magnetic components in the electrodeless discharge—1046(A)
Kolthoff, I. M. Book reviews—117; 475
Kovarik, Alois F. and Norman I. Adams, Jr. New determination of the disintegration constant of uranium by the method of counting α-particles—718
Kracek, F. C., Tom F. W. Barth, and C. J. Ksanda. Molecular rotation in the solid state and the polymorphic relations of the univalent nitrate—1034(A)
Krider, H. S. (see Hidnert, Peter)—131(A)
Kruger, P. Gerald. Is γ-radiation produced by proton transitions in the nucleus?—318(L)
——— Gamma-radiation and its relation to nuclear structure—727
Ksanda, C. J. (see Kracek, F. C.)—1034(A)
Kunsman, C. H. and R. A. Nelson. Some factors involved in the disappearance of hydrogen in the presence of potassium or lithium ion sources—128(A); 936

Ladenburg, R. and G. Wolfsohn. Dispersion of oxygen in the ultraviolet—123(A)
——— **C. C. Van Voorhis, and J. C. Boyce.** Absorption of oxygen in the region of short wavelengths—1018(L)
Langer, R. M. Diffusion technique for the separation of the isotopes of hydrogen—1047(A)
Langmuir, Irving and Clifton G. Found. New type of electric discharge characterized by electron emission from the walls—129(A)
——— **and John Bradshaw Taylor.** Mobility of caesium atoms adsorbed on tungsten—463(L)
——— (see Blodgett, Katharine B.)—78
Larrick, L. Paschen-Back effect of hyperfine structure and the polarization of resonance radiation: the *D* line—1041(A)
——— (see Heydenburg, N. P.)—1041(A)
Laubengayer, A. W. (see Shapiro, C. V.)—354
Lawrence, Ernest O. and M. Stanley Livingston. Production of high speed light ions without the use of high voltages—19
Li, Ching Hsien. Magnetic properties of magnetic crystals at low temperature—1002

Linder, Ernest G. Mass-spectrograph study of the ionization and dissociation of benzene by electron impact—1045(A)
Lindsay, R. B. and F. E. White. Theory of acoustic filtration in solid rods—125(A)
Lippert, T. W. (see Pugh, Emerson M.)—1051(A)
Livingston, M. Stanley (see Lawrence, Ernest O.)—19
Locher, Gordon L. Attempts to induce temporary radioactivity in matter—884(L)
——— Compounds photoelectric effect of x-rays in light elements—484
Loomis, F. W. and R. E. Nusbaum. Magnetic rotation spectrum and heat of dissociation of the sodium molecule—380
Loring, R. A. (see Green, J. B.)—883(L)
Luck, David G. C. Magnetic discontinuities produced by mechanical deformation—1053(A)
——— Sound velocity in reactive mixtures of real gases—125(A); 440
Lyman, Theodore. Notes on the luminescence of glass and fluorite—122(A); 578

MacColl, L. A. Note on the transmission and reflection of wave packets by potential barriers—621
Margenau, Henry. Pressure shift and broadening of spectral lines—387
——— Quantum analogue of Lorentz broadening of spectral lines—1036(A)
——— Shift of the transmission band of silver by cold working—800
Mason, R. C. Probe measurements on arcs at atmospheric pressure—1045(A)
Matheson, Lorne A. Intensity of infrared absorption bands—813
Mattauch, J. (see Smythe, W. R.)—429
Mauchly, J. W. (see Dieke, G. H.)—123(A)
McLachlan, Dan. Graphical projection method of determining the coordinates of point-groups—1030(A)
McMillen, J. H. (see Hughes, A. L.)—469(L)
McNish, A. G. Features of the current-system of the upper atmosphere as revealed by the diurnal magnetic variations at Huanoayo, Peru—1046(A)
Meggers, William F. and C. J. Humphreys. Infrared spectra of the noble gases—1040(A)
Messenger, Helen A. (see Webb, Harold W.)—466(L)
Metcalf, G. F. Special tubes for the amplification of small voltages—131(A)
——— **and T. M. Dickinson.** New low noise vacuum tube—134(A)
Michels, Walter C. Accommodation coefficients of helium and argon against tungsten—472(L)
Miles, J. B., Jr. and H. P. Robertson. Dielectric behavior of colloidal particles with an electric doublelayer—583
Miller, Henry J. Measurement and observation of vacuum conditions in finished (sealed-off) vacuum tubes, incandescent lamps and gas discharge devices—1043(A)
Miller, L. F. Book review—888
Millikan, Robert A. and Carl D. Anderson. Cosmic-ray energies and their bearing on the photon and neutron hypotheses—325
——— **and Carl D. Anderson.** Cosmic-ray energies and their bearing on the nature of these rays—1056(A)
Mitchell, Allan C. G. Hyperfine structure and the polarization of mercury resonance radiation—964
Mohler, F. L. Electron temperatures and the concentration of excited atoms in a caesium positive column—1042(A)
——— Positive column of a caesium discharge—122(A)
Montgomery, Carol G. Contribution of free electrons to ferromagnetism—1053(A)
Morell, L. G. and J. D. Hanawalt. X-ray study of the plastic working of Mg-alloys—1035(A)
Morse, Philip M. and N. Rosen. Vibrational levels in ammonia-like molecules—1039(A)
Morton, G. A. X-ray scattering curves for NH_4 and I in NH_4 at various temperatures—1031(A)
Müller, Hans. Kerr effect and molecular field in Rochelle salt—1051(A)
Mulliken, R. S. Electronic structures of polyatomic molecules and valence—55
Murphy, G. M. (see Urey, Harold C.)—1; 464(L)
Muskat, Morris. Potential distributions in large cylindrical disk with partially penetrating electrodes—1055(A)
——— (see Hutchisson, Elmer)—340
——— (see Kassel, Louis S.)—131(A);627
——— (see Wyckoff, R. D.)—1027(A)
Myer, J. Leland (see Doan, Gilbert E.)—36

Nelson, R. A. (see Kunsman, C. H.)—128(A); 936
Nielsen, Harald H. Torsion oscillator-rotator in the quantum mechanics—445
Nusbaum, R. E. (see Loomis, F. W.)—380

O'Bryan, H. M. Absorption and dispersion of celluloid between 300A and 1000A—123(A)
Onsager, Lars. Viscosity and particle shape in colloid solutions—1028(A)
Osgood, T. H. and E. Hutchisson. Nature of electrical contact between metals—129(A)
Overback, Wilcox (see Stearns, J. C.)—636(L)
Owens, J. S. and O. S. Duffendack. Quenching of mercury resonance radiation by N_2, CO, and N_2—1042(A)

Page, Leigh. Electromagnetic equations and systems of units—1050(A)
——— (see Zeleny, John)—299
Palmer, R. Ronald (see Tate, John T.)—731; 1042(A)
Parker, Allan E. Attempt to determine the nuclear moment of beryllium—1014(L)
Paton, R. F. (see Hershey, A. E.)—1053(A)
Penney, W. G. (see Jordahl, O. M.)—637(L)
Pike, Eugene W. Efficiency of electron emission by metastable atoms—314(L)
Place, W. P. Behavior of the copper-cuprous-oxide rectifier at high frequencies—1054(A)
Plesset, Milton S. Dirac electron in simple fields—1030(A)
Plyler, E. K. Theory of the atom of energy—1029(A)
Podtiaguine, M. (see Beams, J. W.)—129(A)
Post, C. B. (see Ford, O. Rex)—1033(A)
Potapenko, G. Investigations in the field of the ultra-short electromagnetic waves. III. Electronic oscillations in vacuum tubes and the causes of the generation of the dwarf waves—988
Poulter, Thos. C. Apparatus for optical studies at high pressure—860
——— **and Carl Benz.** Lens effect of pressure windows—872
——— **and Robert O. Wilson.** Permeability of glass and fused quartz to ether, alcohol, and water at high pressure—877
Pugh, Emerson M. and T. W. Lippert. Hall effect versus intensity of magnetization—1051(A)

Race, Hubert H. Dielectric losses in insulating materials—124(A)
Randall, H. M. (see Weber, Louis Russell)—835
Rashevsky, N. Some practical applications of electronic devices—131(A)
——— Some problems of theoretic physics connected with cell physiology—133(A)
——— Spontaneous dispersion of small liquid systems which are the seat of physico-chemical reactions—132(A)
Rentschler, H. C., D. E. Henry, and K. O. Smith. Photoelectric emission from different metals—1045(A)
Reyerson, L. H. Book review—642
Rice, O. K. Exchange of translational and vibrational energy in gas reactions—126(A)
Richtmyer, F. K. and S. Kaufman. Satellites of the x-ray lines $L\alpha_1$ and $L\beta_2$ for the high atomic number elements—132(A)
——— (see Hirsh, F. R., Jr.)—1033(A)
——— (see Kaufman, S.)—1032(A)
Richtmyer, R. D. X-ray energy levels by the Fermi-Dirac theory—1057(A)
Riley, Morgan T. Visibility in New York City—1047(A)
Robertson, H. P. (see Miles, J. B., Jr.)—583
Rockwood, R. S. and R. A. Sawyer. Ultraviolet transmission of the atmosphere—1047(A)
Rodebush, W. H. Entropy of nitrous oxide and carbon dioxide—113(L)
Rose, John L. and L. P. Granath. Hyperfine structure of lead—467(L); 760
Rosen, N. and M. S. Vallarta. Relativity and the uncertainty principle—127(A); 569
——— **and C. Zener.** Double Stern-Gerlach experiment and related collision phenomena—502; 1036(A)
——— (see Morse, Philip M.)—1039(A)
Ruedy, J. E. (see Gibbs, R. C.)—204
Rutledge, George. Reliable method of obtaining the derivative function from smoothed data of observation—262

Samson, E. W. Effects of temperature and nitrogen pressure on the afterglow of mercury resonance radiation—940
Saper, Paul G. Ultraviolet bands of silicon monoxide—465(L)
Sawyer, R. A. (see Rockwood, R. S.)—1047(A)
Schlapp, R. (see Jordahl, O. M.)—637(L)
Schoepfle, G. K. An extension of the Pd I-like isoelectronic sequence to Sb VI and Te VII—1040(A)
Sears, R. W. and J. A. Becker. Electrical conductivity of silicon carbide—1055(A)
Seitz, F. Lorentz double refraction in cubic crystals—1036(A)
Shapiro, C. V., R. C. Gibbs, and A. W. Laubengayer. Absorption band spectra of germanous sulfide: the isotopic constitution of germanium—354
Shaw, C. H. (see Beardean, J. A.)—1031(A)
Shenstone, A. G. Perturbed series in line spectra—123(A)
Shortley, George H. Calculation of first order atomic energies for configurations involving almost closed shells—1030(A)
——— Theory of complex spectra—185
Shupe, Lola E. (see Deming, W. Edwards)—848; 1028(A); 1055(A)
Slack, C. M. Shielding of an electrode from a high potential gradient by means of a charged dielectric—132(A)
Slack, Francis G. and W. M. Breazeale. Magneto-optic rotation by condenser discharges—1052(A)
Slater, J. C. Analytic atomic wave functions—126(A)
Smallwood, Hugh M. Ionization of organic acids—128(A)
Smith, Arthur W. Method for measuring the power factor of a condenser—1056(A)

Smith, K. O. (see Rentschler, H. C.)—1045(A)
Smith, Lloyd P. Comparison of the theoretical results of Sugiura and Sommerfeld on the production of x-rays—885(L)
Smith, P. T. Book reviews—474
Smith, Scott W. Refractive index of liquids for x-rays—156
Smith, V. M. (see Knipp, Chas. T.)—1046(A)
Smyth, C. P. Molecular shape and orientation in liquids—124(A)
Smythe, W. R. and J. Mattauch. New mass-spectrometer—429
Snoddy, L. B. Dark current time in condensed discharges in air at atmospheric pressure—409
Sponsler, O. L. (see Kinsey, E. L.)—1035(A)
Sterns, J. C. and Wilcox Overback. Factors influencing ionization produced by cosmic and gamma-rays—636(L)
Stein, W. S. Emission of negative electricity from nickel whem bombarded by positive lithium ions —425
Sterne, T. E. Mixed crystals in statistical mechanics —133(A)
——— Rigorous treatment of assemblies containing crystals, in quantum and classical statistical mechanics—1030(A)
Stoops, W. N. Development of polar characteristics in insulating oils—1054(A)
Street, J. C. and Thomas H. Johnson. Experiments on the corpuscular cosmic radiation—1048(A)
——— (see Johnson, Thomas H.)—638(L); 1048(A)
——— (see Swann, W. F. G.)—1049(A)
Stueckelberg, E. C. G. Theory of inelastic collisons —1036(A)
Stuhlman, Otto, Jr. Mechanics of effervescence—1026(A)
Swann, W. F. G. and J. C. Street. Direct detection of individual cosmic rays—1049(A)

Tate, John T. and R. Ronald Palmer. Angular distribution of electrons scattered elastically and inelastically in mercury vapor—731; 1042(A)
Taylor, John Bradshaw (see Langmuir, Irving)—463(L)
Thatcher, Everett W. On the reduction of shot effect fluctuations by electron space charge—114(L)
——— On thermionic currents limited by pure electron space charge—1045(A)
——— (see Williams, N. H.)—121(A)
Thomson, K. B. and O. S. Duffendack. Collisions of the second kind involving ionization and excitation—1042(A)
Tonks, Lewi. Intermediate free path case in the theory of a plasma—1046(A)
Torreson, O. W. (see Wait, G. R.)—1046(A)
Townsend, Agnes. Temperature changes accompanying magnetization in nickel—120(A)
Tripp, William A. Relationship of gravitation and electromagnetism—1028(A)
Trotter, Herbert, Jr. Variation in the Kerr electro-optical constant of nitrobenzene with temperature near a transition point (9.6°C)—1052(A)
Tu, Yuching. Precision comparison of calculated and observed grating constants of crystals—662

Uehling, E. A. and G. E. Uhlenbeck. Transport phenomena in Einstein-Bose and Fermi-Dirac gases—1029(A)
Ufford, C. W. Relative intensities of multiplet transition in complex spectra—974
Uhlenbeck, G. E. and L. Gropper. Equation of state of a non-ideal Einstein-Bose or Fermi-Dirac gas—1029(A)
———(see Uehling, E. A.)—1029(A)
Urey, Harold C., F. G. Brickwedde, and G. M. Murphy. Hydrogen isotope of mass 2 and its concentration—1
——— F. G. Brickwedde, and G. M. Murphy. Relative abundance of H^1 and H^2 in natural hydrogen—464(L)
——— (see Bradley, Charles A., Jr.)—889

Valasek, Joseph. Book reviews—117; 474
Vallarta, M. S. (see Rosen, N.)—127(A); 569
Van Dyke, K. S. Electric network equivalent of a piezoelectric resonator—1026(A)
Van Vleck, J. H. Critique of SP^3 valency—1037(A)
——— Theory of the magnetic quenching of iodine fluorescence and of Λ-doubling in $^3\Pi_0$ states—544
——— Book review—322
Van Voorhis, C. C. (see Ladenburg, R.)—1018(L)
Vaughan, William E. and G. B. Kistiakowsky. Heat of sublimation of carbon—457

Wait, G. R. and O. W. Torreson. Number of Langevin ions in the free atmosphere at Washington, D. C.—1046(A)
Waldo, George V. (see Allison, Fred)—1052(A)
Warren, B. E. Crystal structure of the silicates—124(A)
Washburn, Martha (see Fricke, Hugo)—1033(A)
Webb, Harold W. and Helen A. Messenger. Size of the mercury metastable atom—466(L)
Weber, E. Proposal to abolish the absolute electrical dimension systems—1056(A)
Weber, Louis Russell and H. M. Randall. Absorption spectrum of water vapor beyond 10μ—835
Weinstein, D. H. Lower limit for the ground state of the helium atom—797
Welch, George B. Additional experimental verification of Fowler's photoelectric theory—470(L)

Weld, LeRoy D. Analysis of cosmic-ray observations—713
White, F. E. (see Lindsay, R. B.)—125(A)
White, H. E. Plausible explanation of the alkali inverted doublets—316(L)
——— Hyperfine structure of the vanadiam spectrum—1041(A)
Wigner, E. On the quantum correction for thermodynamic equilibrium—749
Wilkins, T. R. Response of various photographic emulsions to alpha-rays—130(A)
Williams, E. J. Loss of energy by fast electric particles—881(L)
Williams, John H. Correction to wave-length measurements with the double-crystal spectrometer—636(L)
——— Wave-lengths of the tungsten *K*-series spectrum with the double spectrometer—791; 1032(A)
Williams, N. H. and E. W. Thatcher. On thermal electronic agitation in conductors—121(A)
Williams, S. R. Joule magnetostrictive effect in a series of cobalt-iron rods—120(A)
Wilson, Robert O. (see Poulter, Thos. C.)—877
Wold, P. I. Reversals of Hall effect in tellurium—128(A)
Wolfe, Hugh C. Multiplet splitting and intensities of intercombination lines—1037
Wolfe, R. A. (see Duffendack, O. S.)—1038(A)
Wolfsohn, G. (see Ladenburg, R.)—123(A)
Wood, Lawrence A. Hall effect with audio-frequency-currents—128(A)
Wood, R. W. Diffraction experiments with especial reference to the nature of errors of gratings—1038(A)
Workman, E. J. Wall effects in ionization electroscopes—1055(A)
Wulff, John (see Bacher, R. F.)—123(A)
Wyckoff, R. D., H. G. Botset, and M. Muskat. Flow of liquids through porous materials under the action of gravity—1027(A)

Yagoda, Herman. Ionization potential of radon—316(L)
——— Ultimate lines of element 87—1017(L)
Young, L. A. Wave functions for many electron atoms—127(A)

Zabel, R. M. Reflection of molecular beams of the rare gases from alkali halide crystals—1049(A)
Zachariasen, W. H. Crystal lattice of germano sulphide, GeS—917
——— Crystal lattice of potassium pyrosulphite, $K_2S_2O_5$, and the structure of the pyrosulphite group—113(L), 923
——— Note on a relation between the atomic arrangement in certain compounds, groups and molecules and the number of valence electrons—914
Zahn, C. T. Dielectric constant of dichlorethane, dibromethane, chlorobromethane, and diacetyl; and the phenomenon of free rotation—291
Zeleny, Anthony. Book review—322
Zeleny, John and Leigh Page. Problem of the rotating magnet—299
Zener, Clarence. Elastic reflection of atoms from crystals–126(A); 178
——— Exchange of energy between monatomic gases and solid surfaces—335; 1037(A)
——— Note on accommodation coefficients—1016(L)
——— (see Rosen, N)—502; 1036 (A)
Zwicky, F. Secondary structure and mosaic structure of crystals—63

ANALYTIC SUBJECT INDEX TO VOLUME 40

References marked (A) are to abstracts of papers presented at meetings of the Physical Society, those marked with (L) are to Letters to the Editor.

Absorption of light (see also **Spectra, absorption**)
In ultraviolet by celluloid, H. M. O'Bryan—123 (A)
Shift of the transmission band of Ag by cold working, H. Margenau—800

Accommodation coefficient
Of H_2, K. Blodgett, I. Langmuir -78
Monatomic gases and solid surfaces, C. Zener—335, 1016(L); W. C. Michels—472(L)

Acoustics
Sound velocity in relative mixtures, D. G. C. Luck—125(A); 440
Theory of Chladni plates, R. C. Colwell—125(A); 1026(A)
Theory of filtration in solid rods, R. B. Lindsay, F. E. White—125(A)
Ultrasonic absorption in gases, J. C. Hubbard—1026(A)

Aerodynamics (see also **Hydrodynamics**)
Characteristics of symmetrical hydrofoils, R. C. Darnell—1027(A)

Alloys
Orientations forming in Ag-Cu during precipitation, C. S. Barrett, H. F. Kaiser—1035(A)
Plastic workings of Mg-alloys, L. G. Morell, J. D Hanawalt—1035(A)

Arcs (see also **Discharge of electricity in gases**)
Discharge not obtained in pure A, G. E. Doan, J. Myer—36
Electron emission by metastable atoms, E. W. Pike—314(L)
Electron temperatures and concentration of excited atoms in a Cs arc, F. L. Mohler—1042(A)
Intermediate free path case in the theory of a plasma, L. Tonks—1046(A)
Probe measurements, R. C. Mason—1045(A)
Radiation from metals bombarded by slow electrons, C. Boeckner—1043(A)
Secondary emission from the cathode, W. Jackson—1043(A)

Atomic and molecular beams
Double Stern-Gerlach experiment, N. Rosen, C. Zener—502; 1036(A)
Reflection of atoms from crystals, C. Zener—126 (A); 178
Reflection of Hg atoms from lithium floride crystals, R. R. Hancox, A. Ellett—1049(A)
Reflection of rare gases from alkali halide crystals, R. M. Zable—1049(A)
Reflection of Tl, Sb, and Pb from a NaCl crystal, J. M. B. Kellogg—1049(A)

Atomic structure (see **Energy states of atoms; Spectra**)

Atomization
Mechanism accompanying solid injection, R. A. Castleman, Jr.—1025(A)

Atmosphere (see **Meterology**)

Atmospheric electricity (see also **Geophysics; Aurora; Meteorology**)
Ionization of the upper atmosphere, E. O. Hulburt—129(A)
Lightning discharges and the electrical field of thunderstorms, J. C. Jensen—1013(L)

Biophysics
Comparison of effects produced by x-rays and gamma-rays, G. Failla—1033(A)
Crystal structure of insulin, G. L. Clark, K. E. Corrigan—639(L)
Dispersion of small liquid systems, N. Rashevsky—132(A)
Reduction by x-rays of aqueous solutions and influence of organic substances, H. Fricke, M. Washburn—1033(A)
Size of gene, energy of mutation, O. Blackwood—1034(A)
Surface forces of the sea urchin egg, K. S. Cole—131(A)
Theoretical physics and cell physiology, N. Rashevsky—133(A)

Book Reviews
Angerer, E. V. Wissenschaftliche Photographie. Eine Einfuehrung in Theorie und Praxis—117
Auerbach, F. and W. Hort. Handbuch der Physikalischen und Technischen Mechanik—887
Berthoud, A. Matiere et Atomes. Second Edition—321
Boutaric, A. Les Colloides et L'Etat Colloidal—475

Book Reviews (continued)
Bruhat, Georges. Le Soleil—642
Fraser, G. J. Molecular Rays—322
Gmelins Handbuch der Anorganischen Chemie. Eighth Edition. System-Nummer 7: Brom.—117
Hobson, E. W. The Theory of Spherical and Ellipsoidal Harmonics—322
Newton, Sir Isaac. Opticks: Or, a Treatise of the Reflections, Refractions, Inflections and Colours of Light—474
Ostwald, W. Kolloidwissenschaft, Elektrotechnik und Heterogene Katalyse—642
Person, Fred G. General Physics for Home Economics Students—322
Rakshit, J. N. Association Theory of Solution and Inadequacy of Dissociation Theory—475
Saha, M. N. and B. N. Srivastava. A Text Book of Heat—888
Shorter, L. R. Introduction to Vector Analysis—474
Simon, H. and R. Suhrmann. Lichtelektrische Zellen und Ihre Anwendung—641
Spinney, L. B. A Text Book of Physics—474
Stark, J. Atomstrukturelle Grundlagen der Stickstoffehemie—321
Stark, J. Fortschritte und Probleme der Atom Forschung—321
Veroffentlichungen den Wissenschaftlichen Zentral Laboratoriums der Photographischen Abteilung AGFA. Band II—117
Weizel, W. Bandenspektren. Band I. Handbuch der Experimentalphysik Erg.—642

Broadening of spectral lines
Imprisonment of resonance radiation, C. Kenty—633(L)
And pressure shift, H. Margenau—387; 1036(A)

Capillary action (see also Surface tension)
At low pressures, F. W. Constant—1027(A)

Chemical reactions
Disappearance of H_2 in the presence of K or Li ion sources, C. H. Kunsman, R. A. Nelson—128(A); 936
Reaction rate from sound velocity measurements, D. G. C. Luck—125(A); 440

Cold emission (see **Discharge of electricity in high vacua; Thermionic emission; High voltage tubes; and Machines**)

Collisions of second kind
Involving ionization and excitation, K. B. Thomson, O. S. Duffendack—1042(A)

Collision phenomena
And double Stern-Gerlach experiment, N. Rosen, C. Zener—502; 1036(A)
Theory of inelastic collisions, E. C. G. Stueckelberg—1036(A)

Colloids
Dielectric behavior, J. B. Miles, Jr., H. P. Robertson—583

Combustion
Temperature measurements on an internal combustion engine, A. E. Hershey, R. F. Paton—1053(A)

Compton effect (see **X-rays, diffraction, scattering etc.**)

Constants, physical
Probable values of e, h, e/m and α, R. T. Birge—228; 319(L)

Cosmic radiation
Analysis of observations, L. D. Weld—713
Coincidence of two G. M. counters, J. C. Street, T. H. Johnson—1048(A)
Dependence of ionization produced upon pressure and temperature, J. W. Broxon—1022(L)
Detection of individual rays, W. F. G. Swann, J. C. Street—1049(A)
Energies and nature of rays, R. A. Millikan, C. D. Anderson—1056(A)

Cosmic radiation (continued)
Factors influencing ionization, J. C. Stearns, W. Overback—636(L)
Loss of energy by fast electric particles, E. J. Williams—881(L)
Multiple secondaries in Pb, T. H. Johnson, J. C. Street—638(L)
Nature of the secondary radiation, T. H. Johnson—468(L)
Photographing tracks of corpuscular rays, T. H. Johnson, W. Fleischer, Jr., J. C. Street—1048(A)
Photon and neutron hypotheses, R. A. Millikan, C. D. Anderson—325
Wall effects in ionization electroscopes, E. J. Workman—1055(A)

Crystals and crystal structure
Atomic arrangement and the number of valence electrons, W. H. Zachariasen—914
Bi crystals grown within and outside a magnetic field, A. Goetz, R. C. Hergenrother—137
Calculated and observed grating constants, Yuching Tu—662

Crystals and crystal structure (continued)
Cold working of Ag, H. Margenau—800
Deposition upon monocrystalline hemispheres of Zn, P. A. Anderson—596
Forms of Te, P. I. Wold—128(A)
Of GeS, W. H. Zachariasen—917
Graphical projection method, D. McLachlan—1030(A)
Of insulin, G. L. Clark, K. E. Corrigan—639(L)
Of $K_2S_2O_8$, W. H. Zachariasen—113(L); 923
Lattice energy constants, R. H. Canfield—1034(A)
Lorentz double refraction, F. Seitz—1036(A)
Minerals of the sodalite family, T. F. W. Barth—1034(A)
Molecular rotation in solid state, F. C. Kracek T. F. W. Barth, C. J. Ksanda—1034(A)
Molecular structure of ice and water, E. L. Kinsey, O. L. Sponslor—1035(A)
Mosaic structure in Co, F. Bitter—125(A)
Mosaic structure of calcite, S. K. Allison—1032(A)
Orientations forming in Ag-Cu during precipitation, C. S. Barrett, H. F. Kaiser—1035(A)
Plastic workings of Mg-alloys, L. G. Morell, J. D. Hanawalt—1035(A)
Secondary and mosaic structure, F. Zwicky—63
Thermal expansion of Bi single crystals, A. Goetz, R. C. Hergenrother—643

Critical potentials (see **Potentials, critical**)

Dielectric constants
Of dichlorethane, dibromethane, chlorobromethane, and diacetyl; free rotation, C. T. Zahn—291
Polar characteristics of insulating oils, W.N. Stoops—1054(A)
Statistical calculation, O. Halpern—134(A)

Dielectrics and dielectric properties
Behavior of colloidal particles with an electric double-layer, J. B. Miles, Jr., H. P. Robertson—583
Losses in insulating materials, H. H. Race—124 (A)
Losses in rocksalt, P. L. Bayley—120(A)

Diffraction of atoms (see **Atomic and molecular beams**)

Diffraction of electrons (see **Electrons, diffraction**)

Diffusion
Mobility of Cs atoms adsorbed on W, I. Langmuir, J. B. Taylor—463(L)
Technique for the separation of the isotopes of hydrogen, R. M. Langer—1047(A)

Dimensions and dimensional analysis
Proposal to abolish the absolute electrical dimension systems, E. Weber—1056(A)

Discharge of electricity in gases (see also **Arcs; Electrons in gases; Electrodeless discharge**)
Dark current time in condensed discharges, L. B. Snoddy—409
Disappearance of gas in discharge tubes, A. W. Hull, E. E. Burger—1044(A)
Discharge characterized by electron emission from the walls, I. Langmuir, C. G. Found—129(A)
Energy distribution in positive column, F. L. Mohler—122(A)
Intermediate free path case in the theory of a plasma, L. Tonks—1046(A)
Propagation of luminosity in discharge tubes, J. W. Beams, M. Podtiaguine—129(A)

Discharge of electricity in high vacua (see also **Thermionic emission; High voltage tubes and Machines**)
Effect of the target on breakdown, W. H. Bennett—416; 1043(A)

Dispersion
Of celluloid between 300A and 1000A, H. M. O'Bryan—123(A)
Of oxygen in the ultraviolet, R. Ladenburg, G. Wolfsohn—123(A)

Dissociation
Heat of Na_2 from magnetic rotation spectrum, F. W. Loomis, R. E. Nusbaum—380
Of the carboxyl group in amino acids, G. A. Anslow—115(L); 639(L)

Dynamics
Motion of Chladni plates, R. C. Colwell—125(A), 1026(A)

Effervescence
Mechanics of effervescence, O. Stuhlman, Jr.—1026(A)

Elasticity
Secondary structure of crystals, F. Zwicky—63

Electrical conductivity and resistance
Of liquid Hg at high temperatures and pressures, F. Birch—1054(A)
Nature of electrical contact between metals, T. H. Osgood, E. Hutchisson—129(A)
Of silicon carbide, R. W. Sears, J. A. Becker—1055(A)

Electrical circuits
Network equivalent of a piezoelectric resonator, K. S. Van Dyke—1026(A)
Principles of a new portable electrometer, R. Gunn—307, 1031(A)

Electrodeless discharge
Electrostatic and magnetic components in the discharge, C. T. Knipp, V. M. Smith—1046(A)

Electromagnetic theory
Torque on magnet carrying current, J. Zeleny, L. Page—299

Electrons
Dirac electron in simple fields, M. S. Plesset—1030(A)

Electron diffraction
Angular distribution of electrons scattered in Hg vapor, J. T. Tate, R. R. Palmer—731; 1042(A)
By a Au crystal, H. E. Farnsworth—1049(A)
By metal surfaces, C. J. Davisson, L. H. Germer—124(A)
By single crystals of Cu and Ag, H. E. Farnsworth—684

Electrons in metals
Thermal agitation, N. H. Williams, E. W. Thatcher—121(A)

Electrons, secondary
As a function of primary energy, P. L. Copeland—122(A)
Influence of the electrical discharge on the secondary emission, W. J. Jackson—1043(A)
From Ni when bombarded by positive Li ions, W. S. Stein—425

Electron tubes (see **Discharge of electricity in high vacua; Vacuum tubes**)

Electro-optical effects (see also **Photoelectric effect and properties**)
Kerr effect and molecular field in Rochelle salt, H. Müller—1051(A)
Variation in the Kerr constant of nitrobenzene with temperature, H. Trotter, Jr.—1052(A)

Electrostatics
Potential distributions in cylindrical disks with penetrating electrodes, M. Muskat—1055(A)

e/m
Probable values of e, h, e/m and α, R. T. Birge—228; 319(L)
From x-ray dispersion measurements, E. Bäcklin—112(L), J. A. Bearden—471(L)

Elements
Positive ions of mass 220, L. L. Barnes, R. C. Gibbs—318(L)

Energy states of atoms (see also **Atomic structure; Spectra, atomic**)
Configurations involving almost closed shells, G. H. Shortley—1030(A)
Lower limit for the ground state of He atom, D. H. Weinstein—797
Theory of the atom of energy, E. K. Plyler—1029(A)

Entropy
Of N_2O and CO_2, W. H. Rodebush—113(L)

Equations of state
Of a nonideal Einstein-Bose or Fermi-Dirac gas, G. E. Uhlenbeck, L. Gropper—1029(A)

Errata
Dissociation of the carboxyl group in amino acids, G. A. Anslow—639(L)
Inelastic and elastic electron scattering in A, A. L. Hughes, J. H. McMillen—469(L)

Evaporation
Of Cs atoms adsorbed on W, I. Langmuir, J. B. Taylor—463(L)
And migration of Th on W, W. H. Brattain—1044(A)
Surface energy and heat of vaporation, L. S. Kassel, M. Muskat—131(A); 627

Excitation of atoms and molecules
Concentration of excited atoms in a Cs arc, F. L. Mohler—1042(A)
Mean lives of Hg lines λ2537 and λ1849, Paul H. Garrett—779

Faraday effect (see **Magneto-optical effects**)

Ferromagnetism (see **Magnetic properties**)

Field currents (see **Discharge of electricity in high vacua**)

Flames
Luminosity with Na vapor, T. W. Bonner—105

Galvanomagnetic effects
Radial induced electromotive force, C. A. Beck—607

Gamma-rays (see also **Radioactivity**)
Comparison of effects produced by x-rays and γ-rays, G. Failla—1033(A)
Of Ga II and In II, J. S. Campbell—1040(A)

Gamma-rays (see also **Radioactivity**) (continued)
Induced temporary radioactivity, G. L. Locher—884(L)
γ-radiation and nuclear structure, P. G. Kruger—318(L)
Wall effects in ionization electroscopes, E. J. Workman—1055(A)

Gases
Accommodation coefficient of H_2, K. B. Blodgett, I. Langmuir—78
Accommodation coefficient of monatomic gases, C. Zener, 335, 1016(L); W. C. Michels—472(L)
Disappearance of H_2 in the presence of K or Li ion sources, C. H. Kunsman, R. A. Nelson—128(A); 936
Equation of state of a nonideal Einstein-Bose or Fermi-Dirac gas, G. E. Uhlenbeck, L. Gropper—1029(A)
Graphical presentation of compressibility data, W. E. Deming, L. E. Shupe—1028(A)
Mean free paths, J. A. Eldridge—1050(A)
Physical properties of compressed gases, hydrogen, W. E. Deming, L. E. Shupe—848; 1055(A)
Transport phenomena in Einstein-Bose and Fermi-Dirac gases, E. A. Uehling, G. E. Uhlenbeck—1029(A)

Gravitation
Relationship to electromagnetism, W. A. Tripp—1028(A)

Hall effect
With audiofrequency currents, L. A. Wood—128(A)
Dependence on intensity of magnetization, E. M. Pugh, T. W. Lippert—1051(A)
In tellurium, P. I. Wold—128(A)

Heat of dissociation (see **Dissociation**)

High pressure phenomena
Apparatus for optical studies, T. C. Poulter—860
Lens effect of pressure windows, T. C. Poulter, C. Benz—872
Permeability of glass and fused quartz to ether, alcohol, and water, T. C. Poulter, R. O. Wilson—877

High voltage tubes and machines
Effect of the target on breakdown, W. H. Bennett—416; 1043(A)

Hydrodynamics
Characteristics of symmetrical hydrofoils, R. C. Darnell—1027(A)
Flow of liquids through porous materials, R. D. Wyckoff, H. G. Botset, M. Muskat—1027(A)

Hyperfine structure
Of λ3067 in Bi arc, R. F. Bacher, J. Wulff—123(A)
Isotope displacements in Pb, J. L. Rose, L. P. Granath—467(L); 760
Nuclear moment of Be, A. E. Parker—1014(L)
Paschen-Back effect, polarization of *D* lines, L. Larrick—1041(A)
And the polarization of Hg resonance radiation, A. C. G. Mitchell—964
Test of theory, R. F. Bacher, J. S. Campbell—1040(A)
Of V I, H. E. White—1041(A)

Indetermination principles (see **Quantum mechanics, general**)

Intensities in spectra (see also **Spectra,** etc.)
Of infrared absorption bands, L. A. Matheson—813
Of intercombination lines, H. C. Wolfe—1037(A)
Ionization and excitation by collisions of second kind, K. B. Thomson, O. S. Duffendack—1042(A)
Multiplet transitions in complex spectra, C. W. Ufford—974
Quantitative spectrographic analysis, O. S. Duffendack, R. A. Wolfe—1038(A)
Theory of complex spectra, M. H. Johnson, Jr.—133(A)

Ionization by impact (see also **Ionization potentials**)
And dissociation of benzene, E. G. Linder—1045(A)
Of Hg by K^+ ions, C. Frische—1050(A)

Ionization by radiation (see **Photoionization**)

Ionization potentials
Of molecular H_2, W. Bleakney—496
Of radon, H. Yagoda—316(L)

Ions, high speed
Loss of energy by fast electric particles, E. J. Williams—881(L)
Production without the use of high voltages, E. O. Lawrence, M. S. Livingston—19

Ions in gases
Motion of K^+ ions in Hg vapor, C. Frische—1050(A)
Number of Langevin ions in the free atmosphere, G. R. Wait, O. W. Torreson—1046(A)
Wall effects in ionization electroscopes, E. J. Workman—1055(A)

Ions, mobility (see also **Ions in gases**)
Absolute values in pure gases, N. E. Bradbury—508
Mobility of Cs atoms adsorbed on W, I. Langmuir, J. B. Taylor—463(L)
Mobility in gaseous mixtures and aging in pure gases, N. E. Bradbury—524
Photoelectric currents in gases between parallel plates, N. E. Bradbury—980

Isotopes
Of Cu, E. R. Bishop—16
Displacements in the hyperfine structure of Pb, J. L. Rose, L. P. Granath—467(L); 760
Of Ge, C. V. Shapiro, R. C. Gibbs, A. W. Laubengayer—354
Of H^2, H. C. Urey, F. G. Brickwedde, G. M. Murphy—1; 464(L)
Of H as studied with a mass-spectrograph, W. Bleakney—130(A)
Relative abundance of isotopes in natural H, C. A. Bradley, Jr., H. C. Urey—889
Technique for the separation of the isotopes of H, R. M. Langer—1047(A)

Kerr effect (see **Electro-optical effects**)

Kinetic theory of gases (see **Gases**)

Light waves
Aberration of the second order, N. Gallishohat—1028(A)

Liquids (see also **Hydrodynamics**)
Dispersion of small liquid systems, N. Rashevsky 132(A)
Ionization of organic acids, H. M. Smallwood—128(A)

Luminescence
Of glass, fluorite and quartz, T. Lyman—122 (A); 578

Magnetic properties
Contribution of free electrons to ferromagnetism, C. G. Montgomery—1053(A)
Discontinuities produced by mechanical deformation, D. G. C. Luck—1053(A)
Of large artificial graphite crystals, A. Goetz, A. Faessler—1053(A)
Of magnetite crystals at low temperature, Ching Hsien Li—1002
Paramagnetic susceptibilities in crystals, O. M. Jordahl, W. G. Penney, R. Schlapp—637(L)
Statistical calculation, O. Halpern—134(A)
Temperature changes accompanying magnetization, A. Townsend—120(A)

Magneto-optical effects
Phenomena underlying the magneto-optic method of analysis, F. Allison, J. H. Christensen, G. V. Waldo—1052(A)
Rotation by condenser discharge, F. G. Slack, W. M. Breazeale—1052(A)
Time lag in the Faraday effect, F. Allison, J. L. Condon—1021(L)
Transformation products of K detected, F. Allison, R. Goslin—1015(L)

Magnetostriction
Joule magnetostrictive effect in Co-Fe, S. R. Williams—120(A)

Mass-spectrographs (see also **Methods and instruments**)
For low pressure measurements, W. Bleakney—496
A new type, W. R. Smythe, J. Mattauch—429
Positive ions of mass 220, L. L. Barnes, R. C. Gibbs—318(L)
Study of ionization and dissociation of benzene by electron impact, E. G. Linder—1045(A)

Mechanics (see **Dynamics**)

Mechanics, quantum—atomic structure and spectra
Atomic energies for configurations involving almost closed shells, G. H. Shortley—1030(A)
Intensities of multiplet transitions in complex spectra, C. W. Ufford—974
Lower limit for the ground state of He atom, D. H. Weinstein—797
Pressure shift and broadening, H. Margenau—387; 1036(A)
Spin-orbit interaction, M. H. Johnson, Jr.—127 (A)
Theory of complex spectra, M. H. Johnson, Jr.—133(A), G. H. Shortley—185
Wave functions, analytic, J. C. Slater—126(A)
Wave functions for many electron atoms, L. A. Young—127(A)
X-ray levels by Fermi-Dirac theory, R. D. Richtmyer—1057(A)

Mechanics, quantum—general
Accommodation coefficient, C. Zener—335; 1016 (L); W. C. Michels—472(L)
Collision phenomena, N. Rosen, C. Zener—502; 1036(A)
Comparison of results of Sugiura and Sommerfeld on the production of x-rays, L. P. Smith—885 (L)
Dirac electron in simple fields, M. S. Plesset——1030(A)

Mechanics, quantum—general (continued)

Exchange of translational and vibrational energy, O. K. Rice—126(A)

Formal macroscopic approach to quantum phenomena, W. Bender—1056(A)

Gamow's treatment of radioactive disintegration, G. Breit—127(A)

Reflection of atoms from crystals, C. Zener—126 (A); 178

Relativity and the uncertainty principle, N. Rosen, M. S. Vallarta—127(A); 569

Scattering of slow electrons, E. Feenberg—40

Torsion oscillator-rotator, H. H. Nielsen—445

Transmission and reflection of wave packets by potential barriers, L. A. MacColl—621

Mechanics, quantum—molecular structure and spectra

Energy level formula of a rotating vibrator, J. L. Dunham—126(A)

Equivalent chemical bonds formed by *s*, *p*, and *d* eigenfunctions, R. Hultgren—891

Of lithium hydride, E. Hutchisson, M. Muskat—340

Mechanics, statistical

Assemblies containing crystals, T. E. Sterne—1030(A)

Mixed crystals, T. E. Sterne—133(A)

Quantum correction for thermodynamic equilibrium, E. Wigner—749

Transport phenomena in Einstein-Bose and Fermi-Dirac gases, E. A. Uehling, G. E. Uhlenbeck—1029(A)

Metastable atoms and molecules

Afterglow of Hg resonance radiation, E. W. Samson—940

Electron emission by metastable atoms, E. W. Pike—314(L)

Size of the Hg atom, H. W. Webb, H. A. Messenger—466(L)

Meteorology

Current-system of the upper atmosphere, A. G. McNish—1046(A)

Ionization of the upper atmosphere, E. O. Hulburt—129(A)

Lightning discharges and the electrical field of thunderstorms, J. C. Jensen—1013(L)

Ultraviolet transmission of the atmosphere, R. S. Rockwood, R. A. Sawyer—1047(A)

Visibility as function of dust and humidity, M. T. Riley—1047(A)

Methods and instruments

Calculation of probable errors, R. T. Birge—207

Computing lattice energy constants, R. H. Canfield—1034(A)

Principles of a new portable electrometer, R. Gunn—307; 1031(A)

Graphical presentation of compressibility data, W. E. Deming, L. E. Shupe—1028(A)

He filled G.M. tube counters, J. A. Bearden, C. L. Haines—1048(A)

Large Geiger counters, W. F. G. Swann, J. C. Street—1049(A)

Least square adjustment of observations, L. D. Weld—713

Lens effect of pressure windows, T. C. Poulter, C. Benz—872

Line reversal temperature measurements, A. E. Hershey, R. F. Paton—1053(A)

Mass-spectrograph, K. T. Bainbridge—130(A)

Measurements of small currents using pliotron tubes, L. R. Hafstad—1044(A)

Measurement of vacuum conditions in finished (sealed-off) vacuum tubes, H. J. Miller—1043(A)

Measurements on height of drop of Hg, M. Kernaghan—1020(L)

Measuring power factor of a condenser, A. W. Smith—1056(A)

Method of determining the coordinates of point-groups, D. McLachlan—1030(A)

Nature of errors of gratings, R. W. Wood—1038(A)

New low noise vacuum tube, G. F. Metcalf, T. M. Dickinson—134(A)

New mass-spectrometer, W. R. Smythe, J. Mattauch—429

Obtaining the derivative function from data of observation, G. Rutledge—262

Optical studies at high pressure, T. C. Poulter—860

Photographing tracks of corpuscular rays. T. H. Johnson, Willis Fleischer, Jr., J. C. Street—1048(A)

Portable cosmic-ray counter, J. C. Street, T. H. Johnson—1048(A)

Probe measurements on arcs, R. C. Mason—1045 (A)

Production of high speed ions, E. O. Lawrence, M. S. Livingston—19

Production of large artificial graphite crystals, A. Goetz, A. Faessler—1053(A)

Quantitative spectrographic analysis, O. S. Duffendack, R. A. Wolfe—1038(A)

Recording spectrometer, range to 30μ, L. R. Weber, H. M. Randall—835

Sensitive detector of surface films, K. B. Blodgett, I. Langmuir—78

Methods and instruments (continued)
Sensitizing photographic plates to the ultraviolet, A. J. Allen, R. Franklin—1038(A)
Shielding from a potential gradient by means of a charged dielectric, C. M. Slack—132(A)
Short-time d.c. conductivity of insulating liquids, G. W. Gardiner, Jr.—1054(A)
Spectrograph for the extreme ultraviolet, K. T. Compton, J. C. Boyce—1038(A)
Technique for the separation of the isotopes of H, R. M. Langer—1057(A)
Ultra-short electromagnetic waves, G. Potapenko—988
Use of a densitometer on x-ray lines, W. Duane—132(A)
Vapor pressures from data of the gas current method, H. T. Gerry, L. J. Gillespie—269
Wide angle magnetic spectrometer, C. D. Bock—130(A)

Mobility of ions (see also **Ions, mobility**)
Number of Langevin ions in the free atmosphere, G. R. Wait, O. W. Torreson—1046(A)

Molecular beams (see **Atomic and molecular beams**)

Molecular structure and constants (see also **Spectra molecular; Raman spectra**)
Electronic structures of polyatomic molecules, R. S. Mulliken—55

Multiplets (see also **Spectra, atomic**)
Multiplet splitting, H. C. Wolfe—1037(A)
Of P^{31} nucleus, G. Herzberg—313(L)

Nuclear spin (see also **Hyperfine structure**)
Moment of Na, N. P. Heydenburg, L. Larrick, A. Ellett—1041(A)

Nucleus
Moment of Be, A. E. Parker—1014(L)
γ-radiation and nuclear structure, P. G. Kruger—318(L)

Neutrons
Hypotheses and cosmic-rays, R. A. Millikan, C. D. Anderson—325

Optical constants and properties
Lorentz double refraction, F. Seitz—1036(A)

Optical instruments (see **Methods and instruments**)

Oscillators (see also **Electrical circuits**)
Generation of the dwarf waves, G. Potapenko—988
Magnetostatic vacuum tube, W. Dehlinger—120(A)
Piezoelectric resonator, K. S. Van Dyke—1026(A)

Paschen-Back effect
Hyperfine structure and polarization of *D* lines, L. Larrick—1041(A)

Photoelectric effect and properties
Compound photoelectric effect of x-rays in light elements, G. L. Locher—484
Depth of origin of photoelectrons, H. E. Ives, H. B. Briggs—121(A), 802
Emission from different metals, H. C. Rentschler, D. E. Henry, K. O. Smith—1045(A)
Verification of Fowler's theory, G. B. Welch—470(L)

Photography
Response of photographic emulsions to α-rays, T. R. Wilkins—130(A)
Sensitizing photographic plates to the ultraviolet, A. J. Allen, R. Franklin—1038(A)

Photoionization
Dependence on pressure and temperature, J. W. Broxon—1022(L)

Plasmoidal discharges (see **Discharge of electricity in gases**)

Piezoelectric effect
Converse piezoelectric effect in mixed crystals, S. Bloomenthal—121(A)

Polarization, electrical (see also **Dielectric constants**)
And electronic structures of polyatomic molecules, R. S. Mulliken—55

Polarization of radiation
Of *D* lines and nuclear moment of the atom, N. P. Heydenburg, L. Larrick, A. Ellett—1041(A)
Of Hg λ2537 and hyperfine structure, A. C. G. Mitchell—964

Potential barriers
Transmission and reflection of wave packets, L. A. MacColl—621

Potentials, critical (see **Ionization potentials**)

Proceedings of the American Physical Society
Cambridge Meeting, February 25–27, 1932—118
Washington Meeting, April 28–30, 1932—1024

Predissociation
Of the P_2 molecule, G. Herzberg—313(L)
In the spectrum of ICl, W. G. Brown, G. E. Gibson—529, 1040(A)
Theory of magnetic quenching of I fluorescence as predissociation, J. H. Van Vleck—544

Quenching of radiation
Of Hg resonance radiation by H_2, CO, and N_2, J. S. Owens, O. S. Duffendack—1042(A)
Theory of magnetic quenching of I fluorescence, J. H. Van Vleck—544

Radiation
From metals bombarded by slow electrons, C. Boeckner—122(A); 1043(A)
From negative point discharges at low pressure, W. M. Cohn—122(A)

Radioactivity
Calculation of radioactive disintegration constant, G. Breit—127(A)
Disintegration constant of U, A. F. Kovarik, N. I. Adams, Jr.—718
Induced temporary radioactivity, N. S. Grace, 634(L) G. L. Locher—884(L)
γ-radiation and nuclear structure, P. G. Kruger—318(L)
Radon content of soil gas, H. G. Botset—1027(A)
Response of photographic emulsions to α-rays, T. R. Wilkins—130(A)
Theory of the atom of energy, E. K. Plyler—1029(A)
Transformation product of K, F. Allison, R. Goslin—1015(L)

Raies Ultimes
Of element 87, H. Yagoda—1017(L)

Raman spectra
Of nineteen octanols, G. Collins—829
Smekal-Raman spectra of $SiHCl_3$, $CHFCl_2$ and CF_2Cl_2, C. A. Bradley, Jr.—908

Reaction rates
Exchange of translational and vibrational energy, O. K. Rice—126(A)

Rectifiers
Conductivity of silicon carbide, R. W. Sears, J. A. Becker—1055(A)
Copper-cuprous-oxide rectifier at high frequencies, W. P. Place—1054(A)
Photoelectric effect in a copper-oxide rectifier, L. O. Grondahl—635(L)

Relativity
Aberration of the second order, N. Gallishohat—1028(A)
Formal macroscopic approach to quantum phenomena, W. Bender—1056(A)

Resistance, electrical (see **Electrical conductivity and resistance**)

Resonance radiation
Afterglow of Hg radiation, temperature and N_2 pressure effects, E. W. Samson—940
And line broadening, C. Kenty—633(L)

Scattering of electrons (see also **Collision diameter; Electrons in gases; Electron diffraction**)
Angular distribution of electrons scattered in Hg vapor, J. T. Tate, R. R. Palmer—731; 1042(A)
In A, A. L. Hughes, J. H. McMillen—469(L)
Slow electrons, E. Feenberg—40

Scattering of light (see also **Raman spectra**)
By the atmosphere for λ3200, R. S. Rockwood, R. A. Sawyer—1047(A)

Shot effect
Reduction by electron space charge, E. W. Thatcher—114(L)

Sound (see **Acoustics**)

Spark discharge
Dark current time, L. B. Snoddy—409

Specific heat
And magnetic properties of magnetite, Ching Hsien Li—1002

Spectra, absorption (see also **Absorption of light**)
Effect of temperature on bands of benzene, A. H. Croup—345
Of Ge S, C. V. Shapiro, R. C. Gibbs, A. W. Laubengayer—354
Of ICl, O. Darbyshire—366
Intensity of infrared bands, Lorne A. Matheson—813
Of O_2 for short wave-lengths, R. Ladenburg, C. C. Van Voorhis, J. C. Boyce—1018(L)
Of O_2 in ultraviolet, R. Ladenburg, G. Wolfsohn—123(A)
Of SO_2, T. C. Chow—1039(A)
Ultraviolet of formaldehyde, G. H. Dieke, G. B. Kistiakowsky—1039(A)
Of water vapor beyond 10μ, L. R. Weber, H. M. Randall—835

Spectra, atomic
Alkali inverted doublets, H. E. White—316(L)
G-value of the normal state of Bi I, R. F. Bacher, J. Wulff—123(A)
Of hydrogen (H^2), H. C. Urey, F. G. Brickwedde, G. M. Murphy—1; 464(L)
Infrared of the noble gases, W. F. Meggers, C. J. Humphreys—1040(A)
Isoelectronic sequence in Sb VI and Te VII, G. K. Schoepfle—1040(A)

Spectra, atomic (continued)
Mean lives of Hg lines λ2537 and λ1849, P. H. Garrett—779
Perturbed series, A. G. Shenstone—123(A)
Pressure shift and broadening, H. Margenau—387; 1036(A)
Term values of Se I, R. C. Gibbs, J. E. Ruedy—204
Theory of complex spectra, M. H. Johnson, Jr.—133(A); G. H. Shortley—185
Ultimate lines of element 87, H. Yagoda—1017(L)

Spectra, general
Vibrational levels in ammonia-like molecules, P. M. Morse, N. Rosen—1039(A)

Spectra, molecular
Of N_2, F. W. Loomis, R. E. Nusbaum—380
Near infrared of ammonia, J. D. Hardy—1039(A)
Of P_2, G. Herzberg—313(L)
Predissociation in ICl, W. G. Brown, G. E. Gibson—529; 1040(A)
Of SO_2, T. C. Chow—1039(A)
Theory of magnetic quenching of iodine fluorescence and of Λ-doubling in $^3\Pi_0$ states, J. H. Van Vleck—544
Third positive group of CO bands, G. H. Dieke, J. W. Mauchly—123(A)
Ultraviolet bands of SiO, P. G. Saper—465(L)

Spectra, x-rays (see **X-ray, spectra**)

Spectroscopy, technique
Infrared of the noble gases, W. F. Meggers, C. J. Humphreys—1040(A)
Measuring x-ray intensities by means of an electronic photo-cell, P. R. Gleason—134(A)
Nature of errors of gratings, R. W. Wood—1038(A)
Quantitative spectrographic analysis, O. S. Duffendack, R. A. Wolfe—1038(A)
Spectrograph for the extreme ultraviolet, K. T. Compton, J. C. Boyce—1038(A)

Statistical mechanics (see **Mechanics, statistical**)

Sublimation
Heat of carbon, W. E. Vaughan, G. B. Kistiakowsky—457

Surface tension (see also **Capillary action**)
Height of a drop of Hg, M. Kernaghan—1020(L)

Terrestrial magnetism
Current-system of the upper atmosphere, A. G. McNish—1046(A)

Thermal conductivity
Thermal diffusivity of Ni, R. H. Frazier—592

Thermal diffusivity (see **Thermal conductivity**)

Thermal expansion
Of Ni steels, P. Hidnert, H. S. Krider—131(A)

Thermionic emission of electrons, emitting surfaces
Deviation of anode currents from the three-halves power law, A. Gehrts—434
Evaporation and migration of Th on W, W. H. Brattain—1044(A)
Limited by electron space charge, E. W. Thatcher—1045(A)

Thermionic emission of positive ions
From heated metals, L. L. Barnes—1044(A)

Thermodynamics
Quantum correction for thermodynamic equilibrium, E. Wigner—749

Uncertainty principle (see **Quantum mechanics, general**)

Units
Electromagnetic equations and systems of units, L. Page—1050(A)
General theory of electric and magnetic units, V. Karapetoff—1051(A)
Magnetic units, A. E. Kennelly—1050(A)
Superfluous systems of electromagnetic units, G. A. Campbell—1051(A)

Vacuum tubes
Deviation of anode currents from the three-halves power law, A. Gehrts—434
Measurement of vacuum conditions in finished (sealed-off) vacuum tubes, H. J. Miller—1043(A)
New low noise vacuum tube, G. F. Metcalf, T. M. Dickinson—134(A)

Valence
Bonds formed by *s*, *p*, and *d* eigenfunctions, R. Hultgren—891
sp^3 valency, J. H. Van Vleck—1037(A)

Vaporization (see **Evaporation**)

Vapor pressure
Of I_2, gas current method, H. T. Gerry, L. J. Gillespie—269

Viscosity
Of normal and isopentane, variation with pressure, R. K. Day—281
Particle shape in colloid solutions, L. Onsager—1028(A)

Visibility
As function of dust and humidity, M. T. Riley—1047(A)

Work function (see **Electrons, thermionic; Photoelectric effect**)

X-rays, absorption

Action of x-rays on matter, N. S. Grace—634(L) G. L. Locher—884(L)
Comparison of effects produced by x-rays and γ-rays, G. Failla—1033(A)
Compound photoelectric effect of x-rays in light elements, G. L. Locher—484
L-absorption limits of Hg, H. L. Hull—132(A), 676
Reduction by x-rays of aqueous solutions and influence of organic substances, H. Fricke, M. Washburn—1033(A)

X-rays, diffraction scattering, reflection and refraction

Breadth of Compton line from crystalline graphite, J. W. M. DuMond, H. A. Kirkpatrick, L. Alden—165
Reflecting and resolving power of calcite, S. K. Allison—1032(A)
Refraction by calcite crystals, J. A. Bearden, C. H. Shaw—1031(A)
Refractive index of liquids, S. W. Smith—156
Scattering curves for NH_4 and I in NH_4I at various temperatures, G. A. Morton—1031(A)
Temperature and the Compton effect, G. E. M. Jauncey, G. G. Harvey—329

X-rays, emission

Comparison of results of Sugiura and Sommerfeld on the production of x-rays, L. P. Smith—885 (L)
Energy levels by Fermi-Dirac theory, R. D. Richtmyer—1057(A)
Production of satellites by fluorescent absorption, F. R. Hirsch, Jr., F. K. Richtmyer—1033(A)
Satellites near the $K\beta_1$ line, O. R. Ford, C. B. Post—1033(A)
Shape of an x-ray line, A. Hoyt—477; 1031(A)

X-rays, spectra and spectroscopy, wave-length measurements

Absolute value of wave-lengths, E. Bäcklin—112 (L); J. A. Bearden—471(L)
Forbidden lines in the L series, S. Kaufman, F. K. Richtmyer—1032(A); S. Kaufman—116(L)
Grating constants of crystals, Yuching Tu—662
Precision wave-length measurements, J. A. Bearden—133(A)
Satellites accompanying the x-ray diagram line $K\beta_1$, F. R. Hirsh—151
Satellites of the x-ray lines $L\alpha_1$ and $L\beta_2$, F. K. Richtmyer, S. Kaufman—132(A)
Shapes and widths of L-absorption limits of Hg, H. L. Hull—132(A); 676
Wave-lengths with the double spectrometer, J. H. Williams—636(L); 791; 1032(A)

X-rays, tubes, apparatus

Measuring x-ray intensities by means of an electronic photo-cell, P. R. Gleason—134(A)
Precision wave-length measurements, J. A. Bearden—133(A)
Shielding by means of a charged dielectric, C. M. Slack—132(A)
Use of densitometer on x-ray lines, W. Duane—132(A)

Zeeman effect

Of Pb III, J. B. Green, R. A. Loring—883(L)

CURRENT LITERATURE OF PHYSICS

Extracts from the Tables of Contents of Some of our Contemporaries

PROCEEDINGS OF THE ROYAL SOCIETY

SERIES A. VOL. 136, NO. A829 MAY 2, 1932

On the Influence of Hydrogen on the Pyrolysis of Ethane and Ethylene near 600° Part I. By **M. W. Travers and L. E. Hockin** 1
Band Spectrum of Nitrogen Sulphide. By **A. Fowler and C. J. Baker** 28
Notes on the Theory of Radiation. By **C. G. Darwin** 36
Phenomena of Superconductivity with Alternating Currents of High-Frequency. By **J. C. McLennan, A. C. Burton, A. Pitt and J. O. Wilhelm** 52
Determination of the Heat of Dissociation of Fluorine and of the Latent Heat of Vaporization of Lithium. By **M. S. Desar** 76
On the Torsion of Cylinders of Symmetrical Section. By **W. J. Duncan** 95
Quantum Analysis of the Rotational Structure of the First Positive Bands of Nitrogen (N_2). By **S. M. Naudé** 114
Motility of Positive Alkali Ions in Argon, Neon and Helium. By **A. M. Tyndall and C. F. Powell** 145
On a Determination of the Pitot-Static Tube Factor at Low Reynolds Numbers with the Special Reference to the Measurement of Low Air Speeds. By **E. Ower and F. C. Johansen** 153
Some Special Solutions of the Equations of Axially Symmetric Gravilational Fields. By **T. Lewis** 176
On the Action of Tuned Rectangular Frame Aerials when Receiving Short Waves. By **L. S. Palmer** 193
On the Nature of X-rays. By **J. A. Wasastjerna** 233
Atomic Heat of Bismuth at Higher Temperatures. By **L. G. Carpenter and T. F. Harle** 243
Dipole Moments and Molecular Structure. Part I. A Simple Resonance Method for the Measurement of Dielectric Constants. By **J. W. Smith** 251
Dipole Moments and Molecular Structure. Part II. The Trichlorides of the Elements of Group V. By **J. W. Smith** 256
Theoretical Intensities in the Spectrum of H_2. By **W. C. Price** 264
Atomic Scattering Power of Iron for Various X-ray Wave-lengths. By **A. J. Bradley and R. A. H. Hope** 272
Collision of Slow Electrons with Atoms. I. General Theory and Elastic Collisions. By **H. S. W. Massey and C. B. O. Mohr** 289
Thyratron "Scale of Two" Automatic Counter. By **C. E. Wynn-Williams** 312
Investigations with a Wilson Chamber I—on the Photography of Artificial Disintegration Collisions. By **P. M. S. Blackett and D. S. Lees** 325
Further Investigation with a Wilson Chamber. III. Accuracy of the Angle Determination. By **P. M. S. Blackett and D. S. Lees** 338
Ranges of the α-Particles from the Radioactive Emanations and "A" Products and from Polonium. By **W. B. Lewis and C. W. Wynn-Williams** 349
Quantum Mechanics of Electrochemistry. II. By **R. W. Gurney** 378
Association of γ-Rays with the α-Particle groups of Thorium C. By **C. D. Ellis** 396
The γ-Rays from Actinium Emanation and their Origin. By **Lord Rutherford and B. V. Bowden** 407
Artificial Production of Nuclear γ-Radiation. By **H. C. Webster** 428
Relativistic Quantum Mechanics. By **P. A. M. Dirac** 453

PHILOSOPHICAL MAGAZINE AND JOURNAL OF SCIENCE

VOL. 13, NO. 87 MAY, 1932

Collisional Friction on Electrons moving in Gases. By **E. C. Childs** 873
Theory of Heat Conduction and Convection from a Low Hot Vertical Plate. By **W. S. Kimball and W. J. King** 888
Preliminary Report of the Anomalous Variation of the Electrical Conductivity of Quartz with Temperature. By **Sadakichi Shimizu** 907
Decay of Torsional Oscillation of an Iron Wire Effect of Variation of Period. By **F. W. Alexander** 934
Certain Variations in the Optical Constants of Copper. By **H. Lowery and R. L. Moore** .. 938
Measurement of Current in Electrodeless Discharges by means of Frequency Variations. By **J. Tykocinski-Tykociner** 953
Theory of Electromagnetic and Electrostatic Induction in Electrodeless Discharges. By **Jakob Kunz** 964
Effect of Spatial Induction on the Discrimination of Differences in Brightness. By **James F. Shearer** 975
Dielectric Constant and Power Factor of some Solid Dielectrics at Radio-Frequencies. By **W. Anderson** 986
Light Absorption, the Raman Effect, and the Motions of Electrons in Gases. By **V. A. Bailey** 993
Transient Phenomena at the Breaking of an Inductive Circuit. By **J. A. Wilcken** 1001
Simple Method for the Numerical Solution of Differential Equations. By **W. G. Bickley** . 1006
Rates of Condensation and Evaporation in Intensively Dried Systems. The Effect of Intensive Drying on the Accommodation Coefficient of Liquid and Solid Surfaces for Molecules of their own Vapours. By **F. J. Wilkins** 1014
Precision Measurements of the Crystal Parameters of some of the Elements. By **E. A. Owen and John Iball** 1020
X-Ray Investigation of the Bismuth-Antimony Alloys. By **E. G. Bowen and W. Morris Jones** 1029
Operational Calculus. Part I. Definition of an Operational Representation of a Function and some Properties of the Operator Derived from this Definition. By **H. V. Lowry** .. 1033
Electromagnetic Waves and Pulses. By **W. E. Sumpner** 1049

NATURE

VOL. 129, NO. 3263 MAY 14, 1932

Physics and Chemistry of the Soil. By **H. A. D. Neville** 706
Vortex Motion in Vibrating Columns of Air 711
Letters to the Editor:
Modification of Light Quanta by Elastic Heat Oscillations in Scattering Media. By **E. Gross** 722
Isotopic Displacement and Hyperfine Structure. By **Giulio Racah** 723
Electric Arc between Carbon and Substances which are Insulators at Ordinary Temperatures. By **Mariano Pierucci** 724
Electrical Potential Differences across Onion Epidermis. By **A. C. Giese, R. I. Giese, and S. C. Brooks** 724
Photomicrographic Method for Magnification and Recording in High Speed Pressure Indicators. By **James Taylor and Robert Wark** 725
Temperatures of the Wolf-Rayet Stars. By **V. Ambarzumian** 725
Acoustic and Telephone Measurements 731

NATURE

VOL. 129, NO. 3264 MAY 21, 1932

Letters to the Editor:
Suggested Wireless Observations during the Solar Eclipse of August 31, 1932. By **E. V. Appleton and S. Chapman** 757

Stark Effect for Argon. By **Nils Ryde** 758
Auroral Spectrum in the Infrared. By **W. Jevons** 759
Sound-change and Indeterminism. By **Alan S. C. Ross** 760
Crystal Lattice Distortion in Stretched Wire. By **W. A. Wood** 760
True Weight of Benzopurpurin 4*B*, and the Electrical Conductivity of its Aqueous Solutions. By **S. M. Neale and J. Hanson** 761
Winter in the Ionosphere. By **R. A. Watson Watt** 761

ZEITSCHRIFT FÜR PHYSIK

VOL. 75, NOS. 9 AND 10 — APRIL 29, 1932

Hyperfine Structure of Lead Lines in the Wave-length Region from λ5000 to λ8000. Detection of the Lead Isotope 204. By **H. Schüler and E. G. Jones** 563
Variation with Temperature of the Ionization Produced by γ-Rays. By **Kurt Wolff** 570
Visual Spectroscopy Method for Heterochromatic Photometry. By **L. S. Ornstein, J. G. Eymers and D. Vermeulen** 575
Optical Study of the Accommodation Coefficient of Molecular Rotations in a Gas. By **W. R. van Wijk** 584
Strengthening of the Interference Colors of Thin Oxide Films. By **A. Güntherschulze and F. Keller** 597
Rotation-Vibration Spectrum of Ammonia. By **P. Lueg and K. Hedfeld** 599
Conductivity of Oils at Low Temperatures. By **A. Gemant** 613
Configuration Space and Second Quantization. By **V. Fock** 622
On the Method of Second Quantization. By **P. Jordan** 648
Study of the Glow Discharge in Pure MercuryVapor. By **Fritz Köppen** 654
Problem of the Dissociation Produced by Positive Ion Impact. By **A. Schechter** 671
Hyperfine Structure and Selective Absorption. By **B. Venkatesachar** 676
Change of the Electrical Conductivity of Fluid Metals in a Magnetic Field. By **Ibrahim Fakidow and I. Kikoin** 679
On the Electrical Diffusion of Ions of One Sign in a Gas. By **N. Wolodkewitsch** 680

ZEITSCHRIFT FÜR PHYSIK

VOL. 75, NOS. 11 AND 12 — MAY 6, 1932

Modified Reststrahl Method for the Visible and Ultraviolet Regions of the Spectrum. By **Cl. Schaefer** 687
Spectra of the Inert Gases. By **Ebbe Rasmussen** 695
On the Scattering of Short γ-Radiation by Heavy Elements. By **Lise Meitner and H. H. Hupfeld** 705
Anomalies in Cathode Sputtering. By **Cl. Münster** 716
Infrared Characteristic Frequencies of Alkali Halide Crystals. By **R. Bowling Barnes** 723
Piezoelectric Determination of the Breaking Strength of Thin Metal, Glass and Quartz Fibers. By **F. Seidl** 735
M Series in the Ultra-soft X-ray Region. By **J. A. Prins and A. J. Takens** 741
Derivation of the Brown Surface Formula. By **E. M. Brumberg and S. I. Wawilow** 746
Grating Energy of the Alkaline Earth Oxides and Sulphides and the Electron Affinity of Oxygen and Sulphur. By **Joseph E. Mayer and Margaret McC. Maltbie** 748
Resonance Penetration of α-Particles into the Aluminum Nucleus. By **K. Dieber and H. Pose** 753
Temperature Dependence of the Plasticity and Stretch Rigidity of Rocksalt Crystals. By **Walter Theile** 763
Tempering of Salt Crystals. By **Ernst Rexer** 777
Electron Diffraction by Single Crystals. By **J. J. Trillat and Th. v. Hirsch** 784
Measurement of Flame Velocities. By **A. Becker and K. Vogt** 804
Magnetism of Free Electrons. By **L. Posener** 809
Production of Rays of High Speed Molecules at the Cathode of an Arc. By **R. Risch and F. Lüdi** 812
Theory of the Glow Discharge and of the Low Voltage Arc. By **H. A. Schwab** 823
Theory of the Arc Discharge. By **H. A. Schwab** 829

ZEITSCHRIFT FÜR PHYSIK

VOL. 76, NOS. 1 AND 2 — MAY 12, 1932

Law of Cathode Fall. By **A. v. Hippel** 1

On the Isotope Displacement Effect for Mercury, Thallium and Lead. By **H. Schüler and E. G. Jones** 14

Anisotropic Fluids in Electrical Fields. II. By **W. Kast** 19

Measurements with the Photoelectric Relay. By **R. Bowling Barnes and F. Matossi** 24

On the Absorption Spectrum of Mercury Vapor. By **Heinrich Kuhn and Kurt Freudenberg** 38

Raman Spectrum of Water Solutions of Sodium and Potassium Hydroxide. By **J. Rud Nielsen** 55

On the Dissociation of Molecule Ions by Collision. By **E. Friedländer, H. Kallmann, W. Lasareff and B. Rosen** 60

On the Impacts of Slow Electrons in Gases. III. By **E. Friedländer, H. Kallmann, W. Lasareff and B. Rosen** 70

Theory of the Change in the Electrical Resistance of Metals Produced by Hydrostatic Pressure. By **Kôtarô Honda, Tamotu Nishina and Tokutarô Hirone** 80

Photoelectric Cells with Cathode of Thin Alkali Films. By **Rudolf Sewig** 91

Ultraviolet Absorption of Nitrates and Chromates at 20°K. By **Hildegard Schaumann** 106

On the Intensity Drop in Forbidden Series. By **S. Sambursky** 132

DIE NATURWISSENSCHAFTEN

VOL. 20, NO. 20 — MAY 13, 1932

Short Original Communications:

γ-Radiation from Boron and Beryllium. By **H. Becker and W. Bothe** 349

Nature of the Penetrating Beryllium Radiation. By **F. Rasetti** 350

DIE NATURWISSENSCHAFTEN

VOL. 20, NO. 21 — MAY 20, 1932

Electron Optics and the Electron Microscope. By **E. Brüche and H. Johannson** 353

Short Original Communications:

Discovery and Isolation of Element 91. By **Aristid v. Grosse** 362

Remarks on the Foregoing. By **Otto Hahn and Lise Meitner** 363

Blocking Layer (Sperrschicht) in the Case of Lead Sulphide. By **F. Heineck** 365

Raman Effect of Molecules of the Type XY_6 and XY_8. By **Otto Redlich** 365

Disintegration Process Produced by Cosmic Radiation. By **W. Heisenberg** 365

Selection Rule for Nuclear γ-Radiation. By **K. Bechert** 366

ANNALEN DER PHYSIK

VOL. 13, NO. 2 — APRIL 8, 1932

Radiation Produced by the Retardation of Protons and Fast Electrons. By **Otto Scherzer** 137

Continuous and Continuous-Discreet X-ray Spectrum According to the Theory of Kramers and According to the Wave Mechanics. By **A. W. Maue** 161

Studies of Ultrashort-wave Tubes. By **H. Collenbusch** 191

Acoustical Filters. By **E. Waetzmann and F. Noether** 212

Theory of the Secondary Electron Emission from Metals. By **Herbert Fröhlich** 229

ANNALEN DER PHYSIK

VOL. 13, NO. 3 — APRIL 20, 1932

Analysis of the Ultraviolet Emission from the Earth Alkali Phosphors. By **Otmar Schellenberg** 249

Variability of the Magnetic Ion Moments of Some Elements of the Iron Series. By **Hermann Fahlenbrach** 265

Transmission of Thin Platinum Films in the Wave-length Region from 0.25 to 2.5μ. By **Erich Schuch** 297

Energy Balance of the Positive Columns in Inert Gases. By **K. Sommermeyer** 315

Strong Excitation of Spectra in the Electric Vacuum Furnace by Electron Impacts of Small Energy. By **Rudolf Ritschl** 337
Characteristic Electric Vibrations of Conducting Rods. By **Karl F. Lindman** 358
Neutralization Cross Section of Hydrogen Molecules with Respect to Slow Protons. By **Heinrich Bartels** 373

PHYSICA

VOL. 12, NO. 5 MAY, 1932
Relativistic Theory of the Interaction of Two Charged Particles. By **A. D. Fokker** 145
Temperature Radiation from Flames and from Discharges in Gases. By **M. J. Druyvesteyn and W. de Groot** 153
Temperature Coefficient of Resistance. By **P. Clausing** 167
(Kanntteekeniegen). By **L. Hamburger** 169

COMPTES RENDUS

VOL. 194, NO. 16 APRIL 18, 1932
On the Stationary Cavitations in a Fluid in Irrotational Motion. by **Henri Poncin** 1312
Electrical Analogies in Hydrodynamics. By **J. Pérès and L. Malavard** 1314
On the Zeros of the Velocities in the Problem of Three Bodies. By **Kivelisvitch** 1317
Photoelectric Photometer with Amplification for the Measurement of Feeble Illumination. By **G. Rougier** 1319
On the Origin and the Evolution of Stars and Amorphous Nebulosities According to the Dualistic Cosmogeny. By **Émile Belot** 1321
On the Unit of Length Used in the First Measurements of the Circumference of the Earth. By **André Berthelot** 1323
On the Oscillations of a Tube Adjusted Near the Limit of Maintenance. By **Y. Rocard** ... 1325
Magnetization of Ferromagnetic Powders in Weak Fields. By **R. Chevallier** 1327
Free Electrons in Ionized Gases in a Magnetic Field. By **Th. V. Ionescu and C. Mihul** 1330
Constitution of the Oxide of Rectifiers and of Copper Oxide Photoelectric Cells. By **Léon Dubar** 1332
New Method of Measurement of Very Small Angles of Rotation. By **G. Siadbei** 1334
Raman Effect in Salt Solutions. By **A. Silveira** 1336
Antistokes Terms in the Fluorescent Spectrum of I_2. By **J.-J. Agarbiceanu** 1338
On an Example of the Mobility of Radioactive Atoms on the Surface of Solid Bodies. By **H. Jedrzejowski** 1340
Existence of Neutrons and the Constitution of the Nuclei of Light Atoms. By **Francis Perrin** 1343
On the Radioactivity of Potassium. By **Pierre Auger** 1346

COMPTES RENDUS

VOL. 194, NO. 17 APRIL 25, 1932
New Algebraic Representation of Alternating Currents and of All Other Oscillatory Phenomena. By **André Blondel** 1413
From the Elastic Figure to the Fundamental Equations for the Strength of Materials. By **Louis Roy** 1418
Letters:
On the Problem of Torsion of an Elastic Beam. By **N. Mouskhelichvili** 1435
On the Problem of Elastic Vibrations. By **V. Smirnoff and S. Soboloff** 1437
On the Equilibrium of a Thick Circular Plate and of a Plate in the Form of a Circular Sector. By **B. Galerkin** 1440
On the Stability of the Couette Movement of a Viscous Liquid. By **Alfred Rosenblatt** 1443
Rational Theory of Belts. By **R. Swyngedauw** 1445
Extension of Stokes' Theorem Relative to Fluid Stars. By **R. Wavre** 1447
On the Radius of Convergence of a Series in the Problem of Two Bodies. By **D. Belorizky** 1449
Solution of the Dynamic Problem of Elasticity. By **Ch. H. Müntz** 1456
High Precision Method of Measuring Length and Thickness. By **Marcel Mennesson** 1459

Measurement of the Thermal Conductivity of Insulators: Calorimetric Method. By **Pierre Vernotte** 1462
Electrical Conductivity of Black Paper: Applications. By **Léon Grillet** 1464
Electrostriction of Benzene. By **M. Pauthenier and P. Delahaye** 1465
Method of Measuring High Intensities in Continuous Currents. By **Charles Dietsch** 1466
Magnetization of Macroscopic Powders in Weak Fields. By **R. Chevallier** 1468
Absorption Spectra of the Derivatives of Ethylene and Benzene in the Infrared. By **R. Freymann** 1471
Rotatory Dispersion of Benzene Solutions of Dextro-α-Pinene and Levo-β-Pinene. By **J. Rabinovitch** 1474
Contribution to the Study of the Raman Spectrum of Water. By **Horia Hulubei** 1474
Spectroscopy of X-rays by the Transmission of a Non-collima Beam across a Curved Crystal. By **Y. Cauchois** 1479
Composition of Atomic Nuclei. By **Georges Fournier** 1482
Rational Utilization of Solar Heat. By **H. Barjot** 1484
γ-Ray Spectrum of the Derivatives or Radiothorium. By **D. Skobelzyn.** 1486
Centrifuging of Alkaline Solutions of Polonium. By **C. Chamié and A. Korvezee** 1488
Formation of Acetylene from Methane Under the Influence of a Condensed Spark at Low Pressure. By **Pierre Montagne** 1490
Comparison of Electrolytic Deposts of Zinc and of Cadmium from the Point of View of the Protection of Steel Against Corrosion. By **H. Figour and P. Jacquet** 1493
Effect of Substitutions on the Characteristic Frequencies of Organic Bodies. By **Georges Allard** 1495

COMPTES RENDUS

VOL. 194, NO. 18 — MAY 2, 1932

On Rolling Without Sliding of a Solid Body on a Deformable Surface. By **Constantin Woronetz** 1555
Elastic and Plastic State of a Body Infinite in Two Dimensions Pierced by a Circular Hole. By **M. Davin** 1557
Trace of the Lines of Flow in the Fluid Motion of Oseen Around a Circle. By **J. Pérès and L. Malavard** 1560
Multipoint Movement Corresponding to the Equation of Jacobi for the Case of a Single Point. By **M. A. Buhl** 1562
Maintenance of Oscillations in the Most General Passive Network. By **Ph. Le Corbeiller** 1564
Phosphorescent Sulphides: Intervention of Impacts of the Second Kind. By **Maurice Curie** 1566
On the Degree of Homogeneity of Filtered γ-Rays from Th C'' and the Verification of the Klein-Nishina Formula. By **D. Skobelzyn** 1568
Quantity of Actinium in Uranium Minerals. By **Ellen Gleditsch and M. Ernst Foyn** 1571
Raman Spectrum of Some Cyclic Hydrocarbons. By **Etienne Canals, Marcel Godchot and Germaine Cauquil** 1574

COMPTES RENDUS

VOL. 194, NO. 19 — MAY 9, 1932

Dispersion of Neutrons from Beryllium and the Existence of Recoil Nuclei Produced by Excited Lithium. By **M. de Broglie and L. Leprince-Ringuet** 1616
Gravity Measurements with the Apparatus of Holweck-Lejay. By **P. Lejay and R. Goudey** 1632
Investigation of a New Ray as a Standard of Wave-length. By **Albert Pérard** 1633
Elastic Limit of Extra Soft Steel Drawn through a Draw Plate. By **Jean Galibourg** 1635
On a Vacuum Contact Interrupter for High Tension Currents. By **Georges Vaudet** 1637
Direct Reading Electrical Chronograph which Permits the Precise Measurement of Very Short Intervals of Time. By **Raymond Dubois and Louis Laboureur** 1639
Variation with Thickness of Magneto Optic Effects by Transmission through Thin Films of Iron. By **Marcel Cau** 1642
Photographic Effect of Pressure. By **Ny Tsi-Ze and Chien Ling-Chao** 1644
Penetrating Power of Radiation (Neutrons) Excited in Beryllium by α-Rays. By **Jean Thibaud and F. Dupré La Tour** 1647

LE JOURNAL DE PHYSIQUE

VOL. 3, NO. 4, SERIES VII — APRIL, 1932

Method of Determining the Ozone Content of the Atmosphere. By **H. Mineur** 145
On the Periodic Properties of Atomic Nuclei. By **G. I. Pokrowski** 150
Characteristic Oscillations of an Ionized Gas According to the Wave Mechanics. By **J. J. Placinteanu** 155
Magnetic Properties of Manganese and Chromium in Solid Solution. By **M. L. Neel** 160
Some Observations Concerning an Article Entitled "On the Dirac Equation." By **Al. Proca** 172

HELVETICA PHYSICA ACTA

VOL. V, NO. 1

Measurements in the Vicinity of a Broadcasting Station. By **Hans Zickendraht** 3
New Method for the Measurement and Registration of Photoelectrical Active and Ionizing Radiations. By **A. Stäger** 26
Application of the Optics of Turbid Media to the Light of the Atmosphere. I. The Lighting of an Ideal Atmosphere at Sunset and during Twilight. By **P. Gruner** 31
On the Properties of Ferromagnetic Substances in Sheets and Wires. By **Albert Perrier** 59

HELVETICA PHYSICA ACTA

VOL. V, NO. 2

Attempt at a Theory of the Emission of β-Rays by Radioactive Nuclei. By **A. Schidlof and H. Saini** 73
Investigation of the Change Produced by Ultraviolet Radiation on the Transmission of Glasses for Ultraviolet Light. By **R. Lassé** 92
Visibility of Ultraviolet Radiations and the Absorption of the Human Eye. By **Paul Bächtiger** 103
Translational Electron Groups at the Cathode of a Self-Sustaining Arc Discharge. By **M. Wehrli and P. Bächtiger** 107
On Dielectric Constant Resistance and Phase Angle of Ice. By **H. Wintsch** 127

THE JOURNAL OF THE ACOUSTICAL SOCIETY OF AMERICA

VOL. III, NO. 4 — APRIL, 1932

Noise Specifications for Large Reduction Gears in Terms of Physical Units. By **E. J. Abbott** 445
On Sound Diffraction Caused by Rigid Circular Plate, Square Plate and Semi-Infinite Screen. By **L. J. Sivian and H. T. O'Neil** 483
Loudness and Intensity Relations. By **Lloyd B. Ham and John S. Parkinson** 511
Effect of Position on the Absorption of Materials for the Case of a Cubical Room. By **C. A. Andree** 535
Comments on the Theory of Horns. By **William M. Hall** 552
Interference Elimination with the Warble Tone. By **W. L. Barrow** 562
Investigation of Gamma in a Mixture of Gases. By **Garnet F. Barnes** 579
Mathematical Theory of Vibrating Membranes and Plates. By **R. C. Colwell and J. K. Stewart** 591

PROCEEDINGS OF THE NATIONAL ACADEMY OF SCIENCES

VOL. 18, NO. 5 — MAY, 1932

Application of Photoelectric Cells Sensitive in the Infrared to Stellar Photometry. By **John S. Hall** 365
Rotational Structure of the Ultraviolet Absorption Bands of Formaldehyde. By **G. H. Dieke and G. B. Kistiakowsky** 367
Combination of Carbon Monoxide and Oxygen Under the Influence of Radon. By **S. C. Lind and Charles Rosenblum** 374

BUREAU OF STANDARDS JOURNAL OF RESEARCH

VOL. 9, NO. 1 — JULY, 1932

Use of α-Benzoinoxime in the Determination of Molybdenum. By **H. B. Knowles** 453
Effect of Zinc Coatings on the Endurance Properties of Steel. By **W. H. Swanger and R. D. France** 454
Power Input and Dissipation in the Positive Column of Caesium Discharge. By **F. L. Mohler** 455
Thermal Expansion of Some Silicates of Elements in Group II of the Periodic System. By **R. F. Geller and Herbert Insley** 456
Automatic Reverberation Meter for the Measurement of Sound Absorption. By **W. F. Snyder** 457
Note on the Probable Presence of 2, 2-Dimethylpentane in a Midcontinent Petroleum. By **Johannes H. Brunn and Mildred M. Hicks-Bruun** 458
Notes on the Orifice Meter: The Expansion Factor for Gases. By **Edgar Buckingham** 459
Theory of Voltage, Dividers and their use with Cathode Ray Oscillographs. By **Melville M. Peters, George F. Blackburn, and Paul T. Hannem** 460

JOURNAL OF THE FRANKLIN INSTITUTE

VOL. 213, NO. 6 — JUNE, 1932

Research and Development in Metallurgy. By **C. E. MacQuigg** 483
Amplifiers for Precise Oscillographic Measurements. By **Sigmund K. Waldorf** 605
Tungsten Lamp. By **W. E. Forsythe and E. M. Watson** 623
On the Evolutionary Origin of the Solar System. By **Ross Gunn** 639
Hatchet Planimeter. By **Robert Sparks** 661

JOURNAL OF THE OPTICAL SOCIETY OF AMERICA

VOL. 22, NO. 6 — JUNE, 1932

Plane Waves of Light III. Absorption by Metals. By **Thornton C. Fry** 307
Retinal Chromatic Fields as a Function of Wave-length. By **Charles A. Rinde** 333
Relation Between Certain Types of Luminescence. By **E. L. Nichols and Frances G. Wick** 357
Trichromatic Functions of the Average Eye. By **W. F. Hamilton and Ellis Freeman** 369

REVIEW OF SCIENTIFIC INSTRUMENTS

VOL. 3, NO. 6 — JUNE, 1932

Improved Form of Electrocardiograph. By **S. H. Caldwell, C. B. Oler and J. C. Peters, Jr.** 277
Mechanical Analogy for Coupled Electrical Circuits. By **Herbert J. Reich** 287
Automatic Safety Device for Water Cooled X-ray Tubes. By **Graham W. Marks and J. Grebmeier** 294
Chart of Some Electromagnetic Relations. By **W. Edwards Deming and F. G. Cottrell** 296
Notes on the Evaporation of Ag, Be, Cr, and Si. By **C. Hawley Cartwright** 298
Lecture-Demonstration Oscillograph. By **Wm. W. Hansen** 305
Time-Pressure Characteristics of Various Diffusion and Molecular Pumps. By **Peter J. Mills** 309
Projection Galvanometer. By **Richard H. Howe** 323

PHYSICS

VOL. 2, NO. 6 — JUNE, 1932

Electronic Devices as Aids to Research. By **A. W. Hull** 409
On the Ultra High-Frequency Oscillation of the Magnetostatic Vacuum Tube. By **Walter Dehlinger** 432
Experimental Study of Parallel-Cut Piezoelectric Quartz Plates. By **Gerald W. Fox and W. G. Hutton** 443
Electrostatic Alternator. By **Charles A. Culver** 448
Mechanics of Effervescence. By **Otto Stuhlman, Jr.** 457
Size and Size Distribution of Fog Particles. By **H. G. Houghton** 466